Anthropogenic impacts on shallow lake ecosystems in the middle Yangtze floodplain since the 19th century

Linghan Zeng, MSc., BSc.

Thesis submitted to the University of Nottingham
for the degree of Doctor of Philosophy
September 2020

Abstract

The Yangtze floodplain lakes, which are important water resources in China, have been reported to suffer from eutrophication and water quality degradation. Palaeolimnological proxies including chlorophyll and carotenoid pigments, chironomids and stable carbon and nitrogen isotopes in dated sediment cores from six lakes with distinct catchment characteristics were analysed to investigate the influence of anthropogenic activities (agriculture, industry/urbanization, dam construction) and climate on algal community and lake ecosystems for sustainable development and water management purposes.

Sedimentary TN and TP flux indicated increased nutrient loadings into the middle Yangtze floodplain lakes with the intensification of agricultural and industrial/urban activities in the catchments. Regression analysis showed that agricultural activities were the main source of N loading into the lakes, whereas large quantities of P were from urban/industrial point source. Mann-Kendall coefficients suggested an overall increase in algal production in these Yangtze floodplain lakes over the last two centuries. However, the timing and main driver of algal production increase were different. Generalized additive models (GAMs) and regression analysis showed that increasing N loading from agricultural activities was the main driver of the increases in algal production after ~ the 1940s CE in Honghu and Futou Lakes which are dominant in agricultural activities in the catchments. For Luhu and Wanghu Lakes where industrial and urban activities are dominant in the catchments, major increases in algal production started from ~ the 1980s CE due to the increasing nutrient (mainly P)

loading with the intensification of urbanization/industrialization. With the intensification of human activities, algal production also increased in Dongting and Poyang Lakes since ~ the 1980s CE. However, the free hydrological condition concealed the influence of nutrient loading in these two lakes. After ~ 2000 CE, the disproportional increase of P relative to N from industrial and urban point sources resulted in the low sedimentary N: P ratios (< 10) and hence the increase in N_2-fixing cyanobacteria (indicated by aphanizophyll) in Dongting, Poyang, Luhu and Wanghu Lakes. In contrast, the consistent N loading from agricultural activities led to the high sedimentary N: P ratios (> 15), and hence N_2-fixing cyanobacteria were rare in Honghu and Futou Lakes. In the four lakes with potential HABs, concentrations and sedimentation rates of pigments were low in the large and open Dongting and Poyang Lakes than Luhu and Wanghu Lakes, resulting from the flush of nutrients and algae out of the lakes.

Results of the UVR index showed that free hydrological connection with the Yangtze River, which leads to extensive water level fluctuations and high concentrations of suspended particle concentrations, resulted in low underwater light condition in the Yangtze floodplain lakes. Local dam construction which hydrologically isolated the lakes from the Yangtze River promoted the underwater light conditions in the Yangtze floodplain lakes, stimulating benthic communities as indicated by the increased abundance of macrophyte-related chironomids. Since the 1990s CE, underwater light condition deteriorated in the lakes with the increase in algal production due to the intensification of human activities in the catchments. For severely polluted lakes with potential HABs, local dam construction amplified the symptoms of eutrophication (Luhu and Wanghu Lakes), resulting in the shift from macrophyte-dominated state to algal dominated state as indicated by the transition in chironomid communities and the decrease in $\delta^{13}C$. In contrast, the free hydrological connection with the Yangtze River may alleviate the eutrophication in Dongting and Poyang Lake as suggested by moderate abundance of macrophyte-related chironomids. For less polluted lakes (Honghu and Futou), the increase of macrophytes after local dam construction may buffer against eutrophication, maintaining the lakes in a macrophyte-dominate state as indicated by the high abundance of macrophyte-related chironomids and high values of $\delta^{13}C$.

This study demonstrates that nutrients from catchment anthropogenic activities are the fundamental factor influencing ecosystem structures in floodplain lakes, followed by hydrological modification caused by local dam construction. Compared with agricultural activities, urbanization and industrial activities are more likely to cause eutrophication and HABs. Free hydrological connection with the main channel is efficient at relieving the symptoms of eutrophication resulted from anthropogenic disturbance in floodplain lakes by flushing nutrients and algae out of the lake.

Acknowledgements

I would like to thank my supervisors Suzanne McGowan and George Swann for their endless encouragement, inspirational ideas, and always giving priority to our meetings. Suzanne encouraged me to get involved in the School activities and to attend international conferences to build academic networks. George has always been there when I got stuck with the statistical analysis and had problems with interpreting the isotopes. A big thank you also goes to Xu Chen from China University of Geosciences (Wuhan), who encouraged me to apply for the PhD and provided enormous help during field, laboratory work and data analysis. It would have been impossible to finish this PhD without your help and support.

I would also like to thank the people who helped me with the laboratory work. An enormous thank you goes to Teresa Needham who has always been there setting up all the equipments, microscopes and workbenches I needed, and fixing all the problems I had. I am grateful to Melanie Leng, Jack Lacy, Andi Smith and Chris Kendrick from NIGL at the British Geological Survey for providing help with analysing the isotopes. I also want to thank Yanmin Cao from South-Central University of Nationalities and Stefan Engels who is now at Birkbeck, University of London for the help in chironomid analysis, and for their suggestions on the identification and interpretation of chironomids.

A huge thank you to the students of Xu Chen from China University of Geosciences (Wuhan), Chunling Huang, Qianglong Qiao, Xue Bai, Jia Liang and Jia Peng, for their help in field work and collecting the historical archives. Thank you to Jing Ji for supplying the total phosphorus data for Dongting, Honghu, Luhu, Wanghu and Poyang Lakes.

I am really grateful to a number of previous and current PhD students in the School of Geography, including Charlotte Briddon, Jessica Zhang, Haydar Martinez-Dyrzo, Luis Fernando Legarda Garzón, Ahmad AlShdaifat and Marzhan Baigaliyeva. I would especially like to thank Charlotte Briddon for the help with HPLC, visa application, language checking, statistical analysis and kindly providing information when I had problems in accessing it during the pandemic. A special thank you goes to Mark Stevenson who generously guided me and gave me a home when I first came to Nottingham.

Thank you to my friends Benjamin Chambers, Simon Robinson, Tim Whiteley, and Naomi Bond for the talks, games, sports and food. Your guidance, kindness and generosity have made my life, as a foreigner, to know, to enjoy, and to adapt to this country much easier and smoother. I would also like to thank my friends from China, some of these include Qi Zeng, Rebecca Tong, Brian Liao, Kevin Li, Ligang Xu and Vera Liu. Your company, and the food we cooked and shared together have always been the best medicine to drive my homesick away.

Last but not least, I am indebted to my families who have always been there encouraging, supporting, and clapping for me.

I am lucky to have been funded by the Vice-Chancellor's Scholarship for Research Excellence (International) from the University of Nottingham and the School of Geography. This opportunity has opened the gate to an entirely new academic world to a student from rural China. Isotopes in this thesis were funded by the NERC Isotope Geosciences Facilities Steering Committee (IP-1727-0517).

CONTENTS

LIST OF FIGURES

LIST OF TABLES

LIST OF ABBREVIATIONS

HB….Hubei

HN….Hunan

JX….Jiangxi

DT….Dongtin Lake

HH….Honghu Lake

FT….Futou Lake

LH….Luhu Lake

WH….Wanghu Lake

PY….Poyang Lake

ANOVA….Analysis of variance

ATTZ….Aquatic/terrestrial transition zone

ATP….Adenosine triphosphate

CAM….Crassulacean acid metabolism

CFCS….Constant flux constant sedimentation

Chl….Chlorophyll

CIC….Constant initial concentration

CNY….Chinese Yuan Renminbi

CO_2….Carbon dioxide

CRS….Constant rate of supply

DCA….Detrended correspondence analysis

DMAR….Dry mass accumulation rate

DNA….Deoxyribonucleic acid

DIN….Dissolved inorganic nitrogen

E*m* flux….Energy – mass flux

FPC….Flood-pulse concept

GAMs….Generalized additive models

HCO_3^-….Bicarbonate

HPLC….High performance liquid chromatography

HABs….Harmful algal blooms

IUCN….International Union for Conservation of Nature

KOH….Potassium hydroxide

LD….Local dam

LUCC….Land use and cover change

MK….Mann-Kendall

N….Nitrogen

NBSC….National Bureau of Statistics of China

NH_4^+….Ammonium

NO_2^-….Nitrite

NO_3^-….Nitrate

P….Phosphorus

PCA….Principal component analysis

PDA….Photodiode array

PDB….Pee Dee Belemnite

PEG….Plankton Ecology Group

PEP….Phosphoenol pyruvate

R….Total annual rainfall

RBP….Ribulose-diphosphate

RCC….River-continuum concept

RNA….Ribonucleic acid

Rubisco….Ribulose 1,5-bisphosphate carboxylase-oxygenase

SD….Standard deviation units

Si….Silica

SRP….Soluble reactive phosphorus

T….mean annual temperature

TGD….Three Gorges Dams

TN….Total nitrogen

TP….Total phosphorus

TSS….Total suspended solids

UVR…. Ultraviolet radiation

WRT….Water retention times

Z_A….Z-scores of agricultural proxies

Z_U…. Z-scores of urban/industrial proxies

CHAPTER 1 INTRODUCTION

1.1 Introduction

Freshwater, one of the Earth's most valuable resources, is essential for human life (UN-Water, 2020). Although more than 70% of the Earth's surface is covered with water, drinkable freshwater accounts for less than 3.5% of the total water volume (Shiklomanov, 1993). With climate change, the continuous growth of population, social-economic development and water pollution, water shortages have occurred since the 19th century (UN-Water, 2020). In the early 2000s CE, more than one billion people suffered from water crises worldwide (Aldhous, 2003).

The situation is more serious in China, which has ca. one fifth of the world's total population but less than 7% of global freshwater resources (Qiu, 2010). Per capita water resources are 2,100 m^3 in China, less than a quarter of the world average (Zhang et al., 2005). With the expansion and intensification of agricultural and industrial activities and urbanization since the 1980s CE, China has been plagued by an increasingly severe water crisis (Jiang, 2009). It has been reported that ca. 80% of the lakes are suffering from eutrophication and that ca. 300 million people in rural areas lack access to safe drinking water (Liu and Yang, 2012).

The Yangtze River, known as the "mother river of China", has thousands of lakes in its basin and is one of the most important water resources in China, accounting for more than 35% of the country's water resources (Liu et al., 2016). More than 400 million people live in the Yangtze Basin with industries and farming in the basin making up ca. 40% of the nation's economy (WWF, 2012). With the development of agriculture (including processes such as land reclamation and fertilizer application) in the basin since the 1950s CE and the intensification of urbanization and industrialization after the 1980s CE, water storage capacity markedly shrank (decreased by ~ 50 billion m^3 between 1950 CE and 2010 CE) (WWF, 2012) and large quantities of nutrients from human sources were transported into the aquatic system. In combination with the rising temperature in recent decades which increased internal nutrient releasing from the sediments and favored the growth of cyanobacteria, water quality degradation and cultural eutrophication have been widely reported in this area (Guo, 2007; Chen et al., 2013). Such pressures have accelerated and amplified the water crisis in China (Yang et al., 2008; Liu et al., 2016; Yu et al., 2019).

Apart from the increasing nutrient loading from human perturbation, hydrological modification caused by the installation and construction of dams has raised ecological and biological concerns (Maavara et al., 2020). Since the 1950s CE, more than 50,000 dams have been built in the Yangtze Basin for social-economic benefits (Yang et al., 2011). The construction of the world's largest hydropower station, the Three Gorges Dam (TGD) (constructed between 1994 CE and 2006 CE), has severely modified the natural hydrological setting of the Basin. As the TGD traps ~ 39 km^3 water in its reservoir (Milliman and Farnsworth, 2011), downstream lakes have been experiencing dramatic and prolonged recession in water storage, resulting in a decline in water surface area and loss of ecosystem functions (Figure 1.1) (Mei et al., 2015; Liu et al., 2016). In the largest freshwater lake (Poyang, 2933 km^2) in China, more than 55% of the recession was attributed to the installation of TGD (Mei et al., 2015). As a result, another dam, at the confluence of Poyang Lake and the Yangtze River, has been proposed to maintain water areas and ecosystem function of the lake. However, this idea of resolving the problems caused by dam installation by installing more dams is highly debated (Li, 2009).

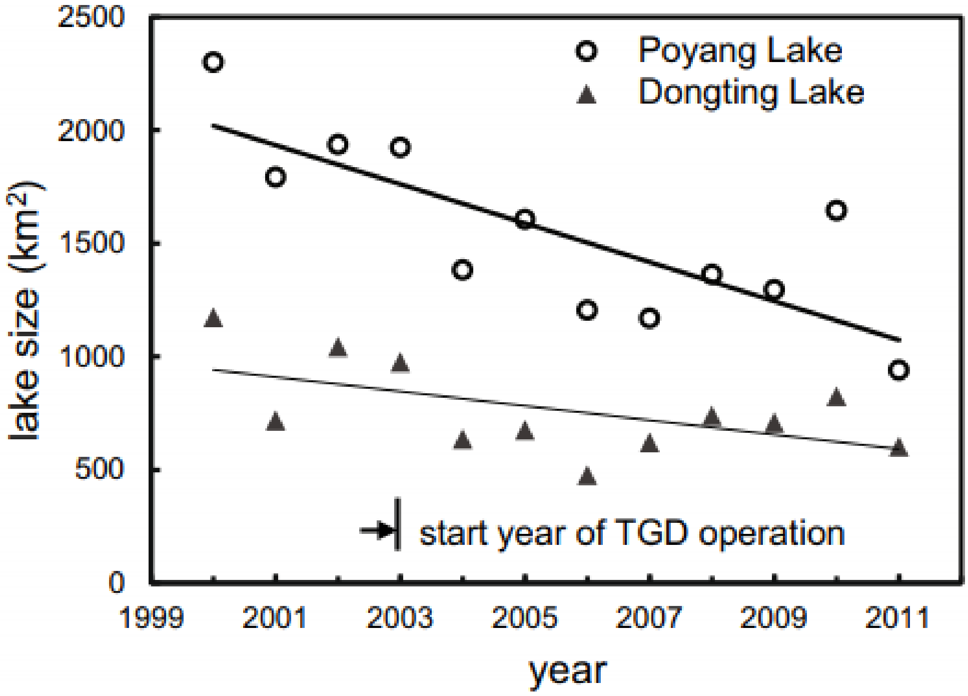

Figure 1.1 Variation of the lake size of the largest and second largest freshwater lakes in China between 2000 CE and 2011 CE (from Liu et al., 2016).

With the combined effects of anthropogenic perturbations and hydrological modification as well as climate change, shallow lake ecosystems in the Yangtze floodplain are suffering from various problems such as lake area shrinkage, eutrophication and water quality degradation (Yang et al., 2008; Du et al., 2011; Yu et al., 2019). However, the lack of long-term water monitoring over the period of lake ecosystems change means that it is hard to focus management priorities. For the purpose of water quality management and sustainable development of the freshwater lakes in the Yangtze floodplain, this thesis aims to extricate the effects of multiple stressors on shallow freshwater ecosystems (focusing on primary producer communities) in the middle Yangtze Basin using multi-decadal palaeolimnological comparisons of lakes across a range of perturbations including hydrological alteration, agricultural development and urban/industrial expansion.

1.2 Thesis outline

This thesis is composed of 9 chapters. The first chapter gives an overall introduction to the thesis. In the second chapter, the potential role of multiple stressors including nutrients, underwater light penetration and hydrology in influencing floodplain freshwater ecosystems is reviewed. Chapter 3 gives a detailed review of the recent history of social-economic development in the middle Yangtze floodplain and the problems that lakes in the region are facing, with an introduction to each individual study lake. In Chapter 4, the capabilities of the proxies used in this study are reviewed, followed by a description of the laboratory methods and the statistical analyses. Chapter 5 presents and describes the preliminary results of the proxies collected from each individual lake. Chapter 6 links sedimentary pigments with historical archives and examines the potential drivers of algal production and community compositional change in the middle Yangtze floodplain lakes (Objective 1). Chapter 7 synthesises the sedimentary pigments and chironomid datasets focused on Objective 2 to investigate the influence of hydrological modification and increasing nutrients on the underwater light conditions and how it may affect lake ecosystems. Chapter 8 reconstructs the history of long term organic matter cycling, investigating sediment core and modern allochthonous and autochthonous sources using geochemical proxies including C/N ratios, $\delta^{13}C$ of organic matter and bulk nitrogen isotopes (Objective 3). Chapter 9 summaries the main findings and addresses the hypotheses posed, followed by recommendations for water quality management of floodplain lakes in areas similar to the Yangtze floodplain.

CHAPTER 2 LITERATURE REVIEW

This chapter provides a literature review of the background of river-floodplain systems and the key ecosystem processes in floodplain lakes.

2.1 Floodplain and floodplain lakes

Floodplains are the relatively flat areas adjacent to a river, which are inundated with water when overtopping of the main channel occurs (Loos and Shader, 2016). Floodplains are highly dynamic and variable systems which experience periodic floods, accompanied by the re-flushing of water and the erosion and deposition of sediments and nutrients, which create habitats for a variety of vegetation, fish and other animals (Junk et al., 1989). Globally, the estimated area of floodplains related to rivers and lakes is 0.8 - 2.2 million km^2 (Mitsch and Gosselink, 2000; Entwistle et al., 2019).

Large river-floodplain ecosystems are important for human beings (Tockner et al., 2010; Palmer and Ruhi, 2019), providing various hydrological, biological and societal benefits (Junk et al., 1989; Johnson et al., 1995; Tockner and Stanford, 2002) (Figure 2.1). Hydrologically, floodplains can store and convey floodwaters, reduce flood velocities and peaks, promote infiltration, groundwater and aquifer recharge, and maintain sediment budgets. In terms of biological benefits, floodplains which act as habitats for fish, waterfowl, and other rare, threatened and endangered species are rich in biodiversity. It is estimated that floodplain areas contribute up to ca. 25 % of the total land based ecosystem services in the world (Mitsch and Gosselink, 2000). From a social-economic perspective, floodplains provide fertile lands and water for agriculture, forestry, industry and aquaculture, as well as recreational activities. These benefits make floodplains appealing and productive for humans to inhabit. As a consequence, floodplains are normally some of the most densely-populated and intensively developed areas on Earth (Tockner et al., 2010). More than 80%, 45% and 10% of the floodplains across Europe, North America (without northern Canada and Alaska) and Africa have been cultivated, respectively (Tockner and Stanford, 2002). More than 50% of the population of Japan inhabits floodplain areas (Nakamura et al., 2006). The middle and lower Yangtze floodplain in China is a habitat for more than a quarter of the nation's population (NBSC, National Bureau of Statistics of China).

Figure 2.1 Sketch showing the various hydrological, and socio-economic benefits of river-floodplain systems (image from The Nature Conservancy, https://www.nature.org/en-us/what-we-do/our-priorities/protect-water-and-land/land-and-water-stories/benefits-of-healthy-floodplains/**)**

Studies on large river-floodplain systems have aimed to understand and effectively steward these important zones (Vannote et al., 1980; Junk et al., 1989; Johnson et al., 1995; Tockner and Stanford, 2002). For example, Vannote et al. (1980) proposed the river-continuum concept (RCC) to study river floodplain ecosystems based on their studies on stable, undisturbed streams in north temperate, forested river systems. However, the RCC mainly focuses on longitudinal processes within the main channel, with little consideration of the complex and dynamic interaction between the river and its lateral floodplain area (Vannote et al., 1980). In fact, river-floodplain systems are composed of complex inter-connected systems including shallow lakes (Palmer and Ruhi, 2019). This has led to efforts to investigate how the main channel interacts with its lateral floodplain area to influence the biotic and abiotic processes in floodplain lakes. The flood-pulse concept (FPC) and the ideal of the flow-biota-ecosystem process nexus attempt to better encompass such ideas (Junk et al., 1989; Johnson et al., 1995; Bayley, 1995; Palmer and Ruhi, 2019).

According to the FPC (Junk et al., 1989) and the flow-biota-ecosystem process nexus (Palmer and Ruhi, 2019), the river and its floodplain are an inseparable unit in terms of water, sediment, and organisms. In a river-floodplain system, the main channel provides water, sediments and nutrients to the lateral floodplain, which may influence the organic and inorganic processes in the floodplain (Junk et al., 1989; Bayley, 1995; Palmer and Ruhi, 2019). Conversely, abiotic and biotic processes in the floodplain may considerably alter the nutrient status and attributes of the main channel as well (Junk et al., 1989; Palmer and Ruhi, 2019). The flood pulse causes a dynamic boundary, also known as the aquatic/terrestrial transition zone (ATTZ), between the main channel and the floodplain. The flooding and drawdown of the main channel are the main driving forces that produce, maintain, and affect the adaptations of biota that have evolved in the river-floodplain ecosystem (Bayley, 1995). Thus, the natural hydrological connection between the main channel and its lateral floodplain plays an important role in maintaining the wellbeing of river-floodplain ecosystems (Junk et al., 1989; Palmer and Ruhi, 2019).

2.2 Hydrological modification in floodplains

With social-economic development over the last several decades, extensive and intensive human perturbations have exerted substantial negative effects on Earth, causing problems such as climate warming, ozone depletion, and air and water pollution (Waters et al., 2016). For example, the total area of eutrophic waterbodies experienced a more than 60-fold increase from less than 150 km^2 to more than 8,500 km^2 between the 1970s CE and the 2010s CE in China (Shen et al., 2020). As one of the most densely populated and severely developed areas, floodplains are one of the landscapes most threatened by anthropogenic activity, especially floodplain lakes (Scheffer et al., 1993; Yang et al., 2008; Tockner et al., 2010; Heathcote and Downing, 2012; Dong et al., 2012).

Apart from suffering from eutrophication, hydrological modification is another stressor that threatens floodplains (Yang et al., 2011). Although periodic flooding acts as the lifeblood which maintains the dynamics and functions of floodplains and the biota therein (Junk et al., 1989; Palmer and Ruhi, 2019), it is one of the most costly, damaging and life-threatening natural hazards from a human perspective (Miller et al., 2008). For instance, more than 118 million people are affected by flooding and waterlogging in China each year, with an annual economic cost of more than 201.3 billion Chinese Yuan Renminbi (CNY) between 2006 CE and 2017 CE (Shao et al., 2018). In response, hydrological infrastructures such as levees and dams are often built for flood-risk management purposes (Johnson et al., 2020), as well as for hydropower, irrigation, navigation and other social-economic benefits, altering the natural hydrological setting of large river-floodplain systems across the world (Johnson et al., 1995; Tockner et al., 2010; Moran et al., 2018; Palmer and Ruhi, 2019). For example, there are more than 16 million dams all over the world and 45 thousand of them have an elevation higher than 15 m (Millian and Farnsworth, 2011). Globally, the gross storage capacity of dams and reservoirs experienced a more than 15-fold increase from less than 0.4×10^{12} m^3 to more than 6×10^{12} m^3 between 1940 CE and 2010 CE (Walling, 2012). In Asia and North America, there are 201 and 175 reservoirs respectively with a storage larger than 0.5 km^3 (Millian and Farnsworth, 2011). In the Amazon Basin, there are 100 dams in operation and 137 planned dams (Tundisi et al., 2014).

The impoundment and construction of dams and reservoirs have extensively and intensively modified the flow-biota-ecosystem processes nexus, causing severe ecological side-effects, either directly by cutting off the migration route or indirectly by changing the distribution and biochemical cycles of sediments and nutrients (Johnson et al., 1995; Timpe and Kaplan, 2017; Palmer and Ruhi, 2019). For example, certain types of fish move from one section (e.g., estuary) of a river to another (e.g., the upstream) on a regular basis for breeding and spawning (Secor and Kerr, 2009; Stone, 2016). Anadromous species (e.g., salmon, striped bass and sea lamprey) spawn in the upper stream of a river and live in the sea, whereas catadromous species such as eels live in the rivers and migrate to the sea for spawning and breeding. With dam construction the migration routes of these species are disrupted, resulting in a reduction in biodiversity or even species extinction (Secor and Kerr, 2009; Stone, 2016). For instance, the construction of Don Sahong Dam on the Mekong River has cut off the migration routine of the anadromous pa nyawn catfish which moves upstream to spawn, resulting in a decline in the local fishing industry (Stone, 2016).

Indirectly, dam and reservoir impoundment modifies the river-floodplain ecosystems by altering the natural distribution of sediments and nutrients (Syvitski et al., 2005; Syvitski et al., 2009; Palmer and Ruhi, 2019). In a natural, undisturbed river-floodplain system, the main channel acts as a pipeline, which transports water, sediments, and nutrients from terrestrial to coastal areas (Jansson and Leonardson, 1994; Chen et al., 2020). Over the last 50 years, sediments transported into coastal regions has decreased by more than 10×10^{11} metric tons globally, due to sediment trapping by reservoir impoundment, of which ca. 0.1-0.3 $\times 10^{11}$ metric tons was carbon (Syvitski et al., 2005). Combined with other factors such as climate-related sea level rise, the reduction in sediment load caused by dam construction has accelerated coastal recession, resulting in the sinking of deltas, and the loss of coastal biodiversity (Syvitski et al., 2009; Ezcurra et al., 2019). In the Mexico's Pacific coast, dam construction on the Fuerte River and the Santiago River has recessed the coasts by 7.9 ha and 21.5 ha each year, respectively (Ezcurra et al., 2019).

Concurrent with the reduction in sediment flux, the global distribution of nutrients (e.g., silicon, nitrogen, phosphorus) has also been modified by hydrological modifications (Maavara et al., 2014; Maavara et al., 2015). Studies on river-floodplain systems worldwide show that dam and reservoir construction on the main channel have severely decreased nutrient concentrations and modified downstream nutrient ratios, decreasing primary production and modifying algal communities (Gong et al., 2006; Maavara et al., 2014; Maavara et al., 2015). In 2000 CE, ca. 42 Gmol phosphorus (P) were retained in reservoirs globally, accounting for more than 10% of the total riverine phosphorus loading, which was twice that in 1970 CE (Maavara et al., 2015). Models suggest that dam construction and reservoir impoundment have trapped 5.3% of the reactive silica (Si) in rivers (ca. 372 Gmol silica each year), in which dissolved and particulate forms account for 43.8% and 56.2%, respectively (Maavara et al., 2014).

However, a recent study on the Mekong River shows that cascade dams and reservoirs only retain and trap nutrients bound on sediments, but increase the fluxes of nitrogen and phosphorus in bioavailable forms (Chen et al., 2020) (Figure 2.2). In general, dam construction may prolong water retention times (WRT), elevate water depth and decrease water mixing in cascade reservoirs, which results in elevated organic matter accumulation in the reservoirs (Chen et al., 2020). The decomposition of organic matter consumes oxygen which, combined with the elevated water level and decreased water mixing which limit the supply of atmospheric oxygen, results in a hypoxic environment at the bottom of the reservoir. The reduced condition may stimulate the release of phosphorus from the sediments and transform the calcium-bound phosphorus to iron-bound phosphorus which is bioavailable. Similarly, nitrogen is transformed into the ammonium forms. Therefore, downstream waters are constantly supplied with hypoxic waters from the base of the cascade reservoir that are rich in dissolved inorganic nitrogen (DIN) and bioavailable phosphorus.

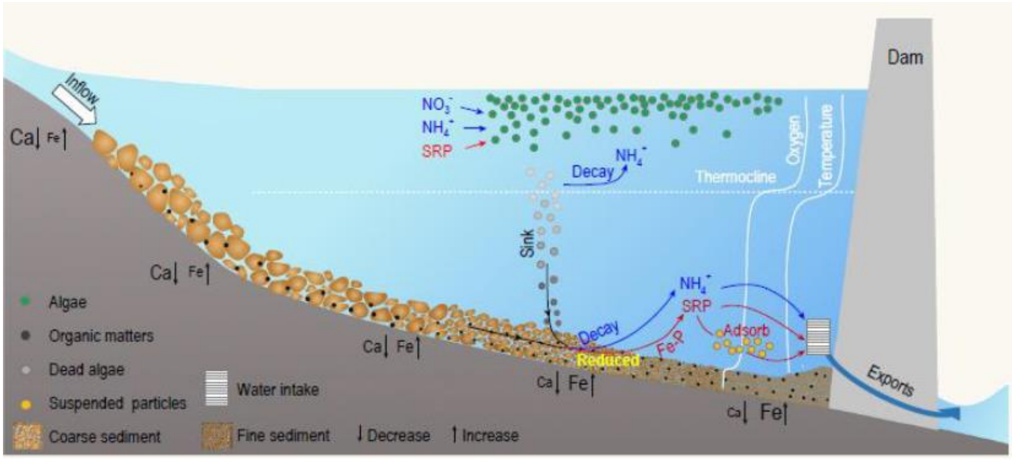

Figure 2.2 Conceptual mechanisms of the biogeochemical transformations of nitrogen and phosphorus in cascade reservoir in floodplain area (from Chen et al., 2020).

Dam construction also plays an important role in regulating the global carbon cycle (Downing et al., 2008; Syvitski et al., 2009; Mendonça et al., 2012; Maavara et al., 2017). However, the effects of dam construction on the global carbon cycle are complex. On one hand, dam construction and reservoir impoundment may stimulate carbon release (Barros et al., 2011; Catalán et al., 2016; Maavara et al., 2017). Firstly, the prolonged water retention times caused by dam construction may accelerate the decay of organic carbon, enhancing the emission of carbon dioxide (CO_2) (Catalán et al., 2016). Moreover, the expansion of the inundated area after dam construction and reservoir impoundment may promote the aerobic mineralization of organic matter and the emission of CO_2 and methane (Barros et al., 2011; Catalán et al., 2016). Coastal recession after dam construction makes a contribution to the carbon emission in coastal areas as well (Syvitski et al., 2009).

On the other hand, dam construction and reservoir impoundment have been regarded as important carbon sinks, promoting global carbon burial (Mendonça et al., 2012). Firstly, dam construction and reservoir impoundment retain nutrients in the river-floodplain systems, enhancing primary production, which fixes CO_2 into organic form by photosynthesis (Mulholland and Elwood, 1982). Secondly, the prolonged water retention times after dam construction and reservoir impoundment promote the deposition and sedimentation of autochthonous and allochthonous carbon (Downing et al., 2008; Maavara et al., 2017). Taken together, Maavara et al.'s (2017) study showed that dam construction has an overall effect of promoting carbon emissions. In the early 21st century, ca. 4.0 Tmol carbon were emitted by dam construction and reservoir impoundment, with the value projected to increase to ca. 6.9 Tmol by 2030 CE with future dam construction (Maavara et al., 2017).

In consideration of the value and merits, as well as the fragility and vulnerability, it is important to balance the costs and benefits of hydrological modification for sustainable development of floodplains, especially in developing countries, as the world's hydropower industry gradually moves towards building dams in developing areas (Moran et al., 2018). The situation is more serious in the middle and lower Yangtze floodplain in the largest developing country, China. In the Yangtze Basin, more than 50,000 dams have been built, including the Three Gorges Dam (TGD) which is the largest dam in the world (Yang et al., 2011) (Figure 2.3). After the construction of the TGD, 44 of the 162 endemic fish species inhabiting the Yangtze main channel are at threat from global extinction (Park et al., 2003). Mean primary production in the East China Sea has decreased more than 85% due to the reduction in nutrients impounded of the TGD (Gong et al., 2006). As large amounts of silicon were trapped in the reservoir, Si: N ratios decreased from 1.5 to 0.4 in the East China Sea, shifting the dominant phytoplankton species from bacillariophytes to prymnesiophytes, cryptophytes and chrysophytes (Gong et al., 2006). There are more than 1,000 lakes distributed in the middle and lower Yangtze floodplain, with a total water surface area of ca. 15,770 km^2 (Wang et al., 2016). Combined with social-economic development, it seems likely that such shifts in nutrient stoichiometry caused by hydrological modification could influence floodplain lakes as well. Therefore, understanding localised impacts on floodplain lake ecosystems helps to constrain the broader patterns of dam construction and provides information for the sustainable development of floodplains.

Figure 2.3 The Three Gorges Dam in the Yangtze River (photo by X. Chen).

2.3 Primary production in lakes

Phototrophic primary production, which is the transformation of solar energy into organic matter, is important in the mass and energy circulation and hence is important in regulating the structure and wellbeing of lake ecosystems (Pierson, 2012). First developed on deep, stratifying lake ecosystems in temperate regions, the Plankton Ecology Group (PEG) model provides a conceptual understanding of the seasonal variation in primary production under the control of resources (e.g., light, nutrients) and biological interactions such as competition, predation and grazing (Sommer et al., 1986; Sommer et al., 2012). The PEG-model is consist of 24 statements which describe the step by step seasonal succession of plankton in an idealised deep and stratified lake rich in nutrients on an annual basis (Sommer et al., 1986) (Figure 2.4).

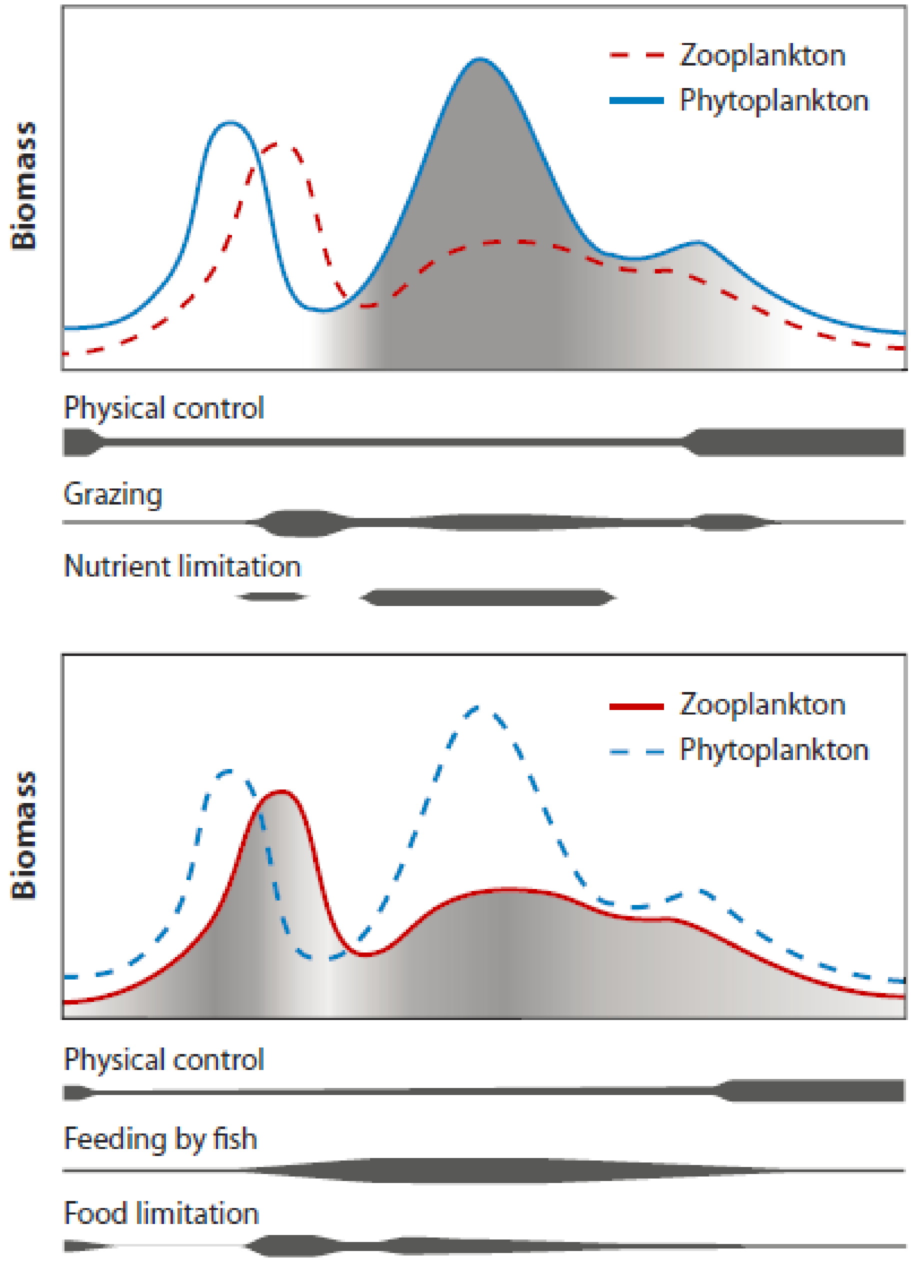

Figure 2.4 The seasonal succession of the phytoplankton (top) (dark shading, inedible for zooplankton; light shading, edible for zooplankton) and zooplankton (bottom) (dark shading, small herbivores; light shading, large herbivores) in an idealized stratifying lake rich in nutrients. The thickness of the horizontal bars indicates the seasonal change in relative importance of physical factors, grazing, nutrient limitation, fish predation, and food limitation (cited from Sommer et al., 2012).

The thaw of ice cover and water turn over with temperature increases in late winter and early spring result in increases in nutrients and light availability, promoting the growth of small, fasting growing algae such as small centric diatoms and cryptophytes. Herbivorous zooplankton which feed on small algae increase due to increases in food availability as well as hatching from the resting stage. As the predation rate on phytoplankton by herbivorous zooplankton exceeds the reproduction rate of phytoplankton, the phytoplankton biomass sharply decreases, resulting in a clear water phase with low phytoplankton production.

With the development of autogenic succession, a complex phytoplankton community starts to develop due to reduced grazing pressure and improved nutrient availability in summer. Firstly, cryptophytes and chlorophytes dominate in the phytoplankton community, taking up soluble reactive phosphorus (SRP), and resulting in a phosphorus-limited environment which prevents the blooming of algae. Competition for phosphorus leads to the replacement of chlorophytes by bacillariophytes. With the growth of silica-shelled bacillariophytes, the lake becomes silica depleted, shifting the dominant species from bacillariophytes to dinoflagellates and/ or cyanobacteria. The growth of dinoflagellates and/ or cyanobacteria, gradually depleted the nitrogen, favouring the growth of N_2-fixing cyanobacteria.

The period of autogenic (internally-driven) succession is terminated by factors related to physical changes which include increased mixing depth resulting in nutrient replenishment to the epilimnion and a deterioration of the effective underwater light climate. After a minor reduction of algal biomass, an algal community develops which is adapted to being mixed. Large unicellular or filamentous algal forms appear. Among them, bacillariophytes become increasingly important as autumn progresses. This association of poorly-ingestible algae is accompanied by a variable biomass of small, edible algae. A reduction of light energy input results in a low or negative net primary production and an imbalance with algal losses which causes a decline of algal biomass to the winter minimum.

The PEG model provides a standard template to describe the seasonal succession of primary production in primarily deep, stratifying temperate lake ecosystems (Sommer et al., 1986), but this basic successional sequence is observed in many lake typologies with the changes in nutrient condition according to the resource competition theory (Reynolds, 1998). The situation is more complicated in shallow lakes where macrophytes and benthic communities are usually important in guiding nutrient cycling and seasonal succession of phytoplankton (Scheffer et al., 1993; Jeppesen et al., 1997; Sayer et al., 2010). Macrophytes are important in providing refuge for zooplankton grazers, which may potentially control phytoplankton production via food-web processes (Jeppeseen et al., 2003). Moreover, shallow lakes rarely stratify and have shorter water retention times and so are less controlled by vertical structuring in the water column and are more susceptible to processes such as algae wash out through flushing, especially in floodplain areas (Scheffer et al., 1993; Tockner et al., 1999). These lead to less predictable phytoplankton responses to stressors than may be expected in deeper lakes (Scheffer et al., 1993). In recent years, excessive nutrient loading from human activities has modified the response of primary producers in freshwater lakes.

2.4 Eutrophication of inland waters

After being introduced by Weber (1907) to describe the nutrient status of mires, the terms eutrophic and oligotrophic have been adopted by limnologists and palaeolimnologists to distinguish waterbodies with different trophic levels and phytoplankton productivity (Thienemann, 1918; Naumann, 1919). Oligotrophic waterbodies are nutrient-poor. Eutrophication arises from the extravagant availability of growth-limiting nutrients which control the production of autotroph biomass (Chislock et al., 2013). With nutrient enrichment, lakes gradually change from an oligotrophic to eutrophic state (Battarbee et al., 2005). Under natural circumstances, lakes are hypothesized to go through an auto-eutrophic trajectory with the gradual infill of nutrients and sediments from the catchment over hundreds to thousands of years (Battarbee et al., 2005), although it is now known that earlier stages of lake evolution involve oligotrophication stages (Engstrom et al., 2000). This is known as ontogeny or natural lake evolution.

Over recent decades, human activities have left a distinct footprint on the Earth, leading to the recognition of a new geologic epoch – the Anthropocene (Waters et al., 2016). In this new epoch, intensive and extensive anthropogenic perturbations have substantially modified the biogeochemical cycles of nitrogen (N) and phosphorus (P) (Liu et al., 2016; Waters et al., 2016; Yu et al., 2019). With population growth and social-economic development, the application of fertilization to increase food production and municipal and industrial wastewater discharge have profoundly increased the amount of N and P entering the environment (Galloway et al., 2008; Conley et al., 2009). Chemical synthesis of reactive N has experienced a more than 12-fold increase from ~15 million metric tons (Mt) in 1860 CE to 187 Mt in 2005 CE, which was far beyond the planetary boundaries (Galloway et al., 2008; Yu et al., 2019). Globally, human perturbations have amplified the cycles of N and P by ca. 100% and 400% over the last two centuries, respectively (Falkowski et al., 2000). N and P, which are essential elements for the synthesis of functional groups such as protein and deoxyribonucleic acid (DNA), ribonucleic acid (RNA) and adenosine triphosphate (ATP), respectively, are key limiting nutrients in aquatic ecosystems (Conley et al., 2009). Large influxes of nitrogen and phosphorus from anthropogenic sources in a short period of time have caused the cultural eutrophication of lakes (Battarbee et al., 2005; Smith and Schindler, 2009; Yu et al., 2019).

Cultural eutrophication, caused by excessive nutrient loading from anthropogenic activities, has severely degraded water quality worldwide, resulting in serious ecological consequences in freshwater and costal marine ecosystems (Schindler et al., 2008; Conley et al., 2009; Smith and Schindler, 2009), including the excessive growth of aquatic plants and blooms of algae and cyanobacteria. Bloom is a term used in phytoplankton ecology and limnology to describe a phenomenon when the biomass of one species is significantly higher than the lake's average (Vincent, 2009). Blooms occur when environmental conditions meet the resource requirements of certain species (Vincent, 2009). The proliferation of species which are buoyant and motile under appropriate conditions may cause surface blooms and form a scum at the water surface (Vincent, 2009). The over growth of certain cyanobacteria (e.g., *Anabaena minutissima*, *Oscillatoria agardhii*, *Microcystis aeruginosa*) may result in harmful algal blooms (HABs) and a series of 'side-effects', such as hypolimnetic oxygen depletion and decreasing water transparency (Schindler, 2006; Chislock et al., 2013). HABs may generate toxins that cause health problems to the liver, intestines and nervous system, alongside other economic disadvantages such as taste and odour problems, impairing water treatment processes, and increasing disinfection costs and accelerating the “death” of water bodies (Vincent, 2009). For example, the cyanobacteria blooms in Taihu Lake in the Yangtze floodplain in 2007 CE contaminated the water supply for more than 2 million people in its catchment (Guo, 2007).

Anthropogenic nutrient loading may cause eutrophication and HABs by increasing the amount of phosphorus, nitrogen or both being discharged into waterbodies (Schindler et al., 2008; Conley et al., 2009; Taranu et al., 2015). This process is exacerbated by anthropogenic climate change, increasing nutrient loading (N and P) resulting in the acceleration of cyanobacteria dominance in freshwaters of the north temperate-subarctic regions (Taranu et al., 2015). However, there is debate over which nutrients cause eutrophication and HABs in freshwater ecosystems (Schindler et al., 1977; Downing et al., 2001; Schindler et al., 2008; Burson et al., 2018). Some studies have revealed that cyanobacteria blooms show a strong correlation with the absolute concentrations of nutrients (Downing et al., 2001; McCarthy et al., 2009), drawing forth the argument that the absolute concentration of nutrients is the fundamental factor regulating eutrophication and HABs in freshwater ecosystems (Downing et al., 2001; McCarthy et al., 2009). However, others have emphasized the role of nutrient ratios in regulating the succession of algal communities and HABs according to the resource competition theory (Schindler 1977; Tilman, 1985; Schindler et al., 2008; Burson et al., 2018). For example, low N: P ratios lead to the dominance of cyanobacteria, whereas chlorophytes are more abundant under higher N: P ratio conditions (Schindler 1977; Smith, 1983).

Empirical studies suggested that phosphorus is the key element regulating eutrophication (Schindler 1977; Schindler et al., 2008), leading to a focus on phosphorus rather than nitrogen being managed to control eutrophication (Schindler et al., 2008). Studies based in the Experimental Lakes Area in North America showed that a reduction in nitrogen inputs did not alleviate eutrophication (Schindler et al., 2008) and that low N: P ratios favoured the growth and dominance of N_2-fixing cyanobacteria, which are able to compensate the nitrogen deficiency by fixing N_2 from atmosphere (Schindler 1977; Schindler et al., 2008). In recent decades the utilization of P-containing pesticides and detergents, as well as industrial and urban sewage, have resulted in a faster accumulation of phosphorus than nitrogen in human-impacted freshwater ecosystems (Elser et al., 2007; Yan et al., 2016). In China, there is a disproportionate increase of phosphorus relative to nitrogen due to the increased proportion of phosphorus fertilizers (Yan et al., 2016), which may induce serious eutrophication and HABs.

However, there is increasing evidence that shows that nitrogen plays a key role in regulating water quality and algal production as lakes become phosphorus sufficient (low N: P ratios) (Leavitt et al., 2006; Bunting et al., 2007). The correlation between cyanobacteria abundance in Lough Neagh (Northern Ireland) and agricultural nitrogen input to the catchment indicates that nitrogen may also trigger eutrophication and HABs (Bunting et al., 2007). In Lake Winnipeg, Canada, nitrogen from agricultural activities in the catchment enhanced algal production by three to five times (Bunting et al., 2016), whilst nitrogen from urban sources caused water quality degradation in the Qu'Appelle River catchment in North America (Leavitt et al., 2006). Furthermore, evidence suggests that algal community composition in freshwater systems is not only influenced by the amount, but also the chemical forms of nitrogen (reduced or oxidative) (Donald et al., 2011; Glibert et al., 2016). The established paradigm is that algae preferentially uptake reduced N (ammonium, NH_4^+) rather than oxidative N (nitrate, NO_3^-) as NH_4^+ is more easily transported across the cell membrane and the uptake and assimilation of NH_4^+ are energy saving (Glibert et al., 2016). Different chemical forms of nitrogen may modify the phytoplankton community composition due to the different metabolism pathways of NH_4^+ and NO_3^- (Blomqvist et al., 1994; Donald et al., 2011; Glibert et al., 2016). Oxidative (NO_3^-) and reduced (NH_4^+) N are transported through the cell membrane by different transporters. After being transported into the cells by transporters, NO_3^- is firstly being reduced to nitrite (NO_2^-) and then NH_4^+ by nitrate reductase. Nitrate reductase is more easily and efficiently generated in eukaryotes (Blomqvist et al., 1994; Glibert et al., 2016). Therefore, diatoms are more capable in utilizing nitrogen in oxidised forms (Blomqvist et al., 1994), whereas the prokaryote species such as cyanobacteria, dinoflagellates and many other species forming HABs favour reduced forms of nitrogen (Glibert et al., 2006; McCarthy et al., 2009). Chlorophytes, which generate transporters for both reduced and oxidative nitrogen, can adapt to conditions with different nitrogen forms (Fernandez and Galvan, 2007). The implication of this is that freshwater management should not only focus on the absolute concentrations of nitrogen and phosphorus, but also on N: P ratios as well as the different chemical forms of nutrients.

2.5 Light availability for aquatic primary production

Due to a focus on deep, stratified and temperate lakes, the classic PEG model is mainly based on studies of phytoplankton which are physically advantaged in obtaining enough light irradiation. It does not consider the fact that benthic communities (benthic algae, macrophytes) account for a large proportion of primary production in nutrient-poor clear shallow lakes (Vadeboncoeur et al., 2003; Karlsson et al., 2009). Primary production is the synthesis of organic materials from inorganic compounds (e.g., CO_2, water) by primary producers through biochemical processes including photosynthesis and chemosynthesis (Falkowski and Raven, 2013). Photosynthesis transforms CO_2 and water into organic matter under light irradiation (Bryant and Frigaard, 2006). Hence, light availability is an important factor regulating primary production (Karlsson et al., 2009; Leavitt et al., 2009).

For benthic and planktonic communities where habitats may be located in layers beneath the photic zone at certain times of the year, photosynthetic production is fundamentally limited by light availability (Vadeboncoeur et al., 2003). Shallow freshwater lakes are highly dynamic and the three primary zones (littoral, photic and aphotic) of a lake may change from one to another with water level fluctuation (Figure 2.5). Light must therefore be considered as a key variable in shaping the structure and production of primary producers, especially the benthic communities, in shallow freshwater ecosystems (Karlsson et al., 2009; McGowan et al., 2018).

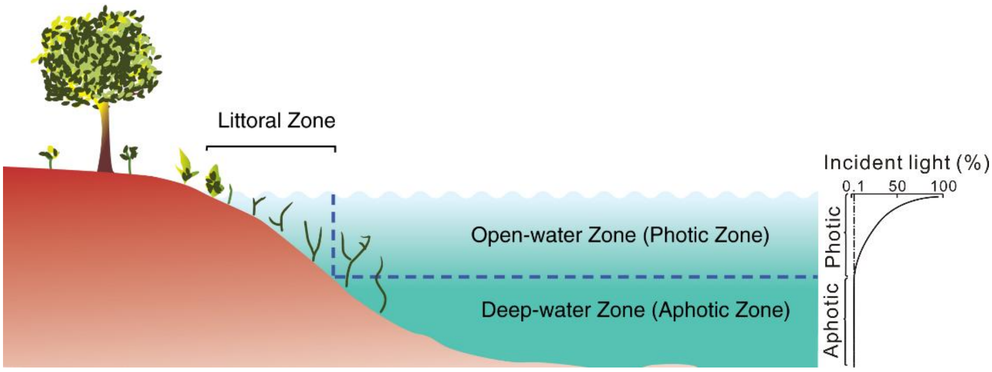

Figure 2.5 The three primary zones (littoral, photic and aphotic) of a lake and the vertical decline of light in water column (modified from Desonie, Earth's Fresh Water).

Except for a small amount being reflected into the atmosphere, most solar radiation reaching a lake penetrates into the water column and is scattered, absorbed as heat or transformed into other forms through biochemical processes (e.g., photosynthesis) (Lampert and Sommer, 2007), resulting in an exponential vertical decline in light radiation with depth (Scheffer et al., 1997) (Figure 2.5). The degree of light attenuation is represented by the vertical attenuation coefficient (k_d) (Scheffer et al., 1997). In shallow freshwater lakes, light is predominantly absorbed and scattered by dissolved organic matter (DOM) and undissolved particulate matter such as algae, detritus and suspended sediment particles (Scheffer et al., 1997). The vertical attenuation coefficient and the related light transmission are determined by a combination of various dissolved or undissolved, organic or inorganic materials (Scheffer et al., 1997; Karlsson et al., 2009).

Among all these substances, total suspended solids (TSS) is of particular importance in influencing light availability and therefore primary production (Scheffer et al., 1997; Swift et al., 2006), especially in tropical and temperate floodplain systems which receive large quantities of riverine sediments (Wu et al., 2010; Duong et al., 2019). For instance, the increase of TSS-induced turbidity during the dry to wet transition resulted in a decrease in phytoplankton concentration in the Red River (Duong et al., 2019). Empirical evidence indicates that light attenuation shows a negative relationship with TSS concentrations (Scheffer 1997; Swift et al., 2006; Hannouche et al., 2011). Waterbodies with high TSS concentrations are characterized by high turbidity and low light conditions, whereas low TSS concentration waters have high light penetration deeper into the water column and low light attenuation (Scheffer 1997; Swift et al., 2006).

Generally, TSS is composed of inorganic and organic matter (e.g., algae, detritus), with individual fractions having different impacts on turbidity (Scheffer, 1997; Swift et al., 2006). A study on five Dutch lakes showed that phytoplankton contributed most to the turbidity (Scheffer, 1997). Based on a model, a separate study revealed that more than 50% of the turbidity was caused by inorganic suspended matter in Lake Tahoe, with algae contributing a further 20% (Swift et al., 2006). The grain size of particles can also influence light transmission (Scheffer, 1997). Lakes with easily resuspendable particles (e.g., clay) are normally characterized by high turbidity and hence low algal production, whereas waterbodies with coarser particles (e.g., sand, gravel) which are more easily deposited experience optimal light conditions and hence high algal production (Scheffer, 1997).

Apart from light limitation caused by detritus and suspended organic (algae and other microbiota) and inorganic particles, increasing number of studies have revealed that water level fluctuation is a major factor explaining the variability in light penetration, ultraviolet (UV) damage and algal production and composition among and within certain lake types (Coops et al., 2003; Cantonati et al., 2014). On the one hand, radiation is essential for primary production, but over exposure to certain wavelengths of radiation causes damaging effects (Cantonati et al., 2014; McGowan et al., 2018). For instance, over exposure to UV-B damages the DNA, lipids, membranes and genomes of organisms (Bell et al., 2018). Empirical study of a deep mountain lake shows that water level fluctuation induced light gradient has favoured distinct benthic cyanobacteria and algae communities along the water depth gradient (Cantonati et al., 2014). The shallow littoral areas where the effects of water level fluctuation were most pronounced were periodically over exposed to UV radiation, and its associated damaging effects on phyto-biota. Therefore, pseudaerial cyanobacteria and UV-resisting phenoecodemes with yellow-brown scytonemin-rich sheaths which provide protection against UV radiation were dominant. In contrast, the deep zones were light limited and algal communities were characterized by low light adapted species with colorless sheaths or pink-red-violet cell contents.

2.6 Primary production in floodplain lakes

Studies on primary production in floodplain lakes are more complex due to several reasons (Junk et al., 1989; Tockner et al., 2002; McGowan et al., 2011; Zeng et al., 2018). First, floodplain lakes are shallow lakes in which benthic production (i.e., benthic algae, macrophytes) makes a large contribution to the primary production in addition to phytoplankton (Karlsson et al., 2009). Second, the main channel and the floodplain lakes are inseparable components in a river-floodplain system according to the flood-pulse concept (Junk et al., 1989). Flow regime, biota and ecosystem processes interact and interplay with each other under the flow-biota-ecosystem processes nexus framework (Palmer and Ruhi, 2019). In a river-floodplain system, the periodic flood pulse which transports water, nutrients, sediments and biota across the aquatic/terrestrial transition zone results in seasonal variation in light (through influencing water level fluctuation and TSS) and nutrient conditions in floodplain lakes (Junk et al., 1989; Bayley, 1995). Thus, the natural hydrological connection between the main channel and its lateral floodplain plays an important role in regulating the primary production in floodplain lake ecosystems (Junk et al., 1989; Johnson et al., 1995; Palmer and Ruhi, 2019).

Natural hydrological connectivity can influence the biota and ecosystem processes in floodplain lakes through immediate flushing (Palmer and Ruhi, 2019). A study in the lower Danube floodplain shows that algal production in floodplain lakes reached a peak during phases with intermediate connections with the main channel (Heiler et al., 1995). The low algal concentration during the surface connection phase was attributed to the direct export (flushing/removal) of algal biomass. Apart from the direct effects, hydrological connectivity may influence the biota and ecosystems in floodplain areas through indirect processes such as nutrient and sediment transportation, and species interactions (Junk et al., 1989; Palmer and Ruhi, 2019). Studies on large river-floodplain systems over different climate and geographical areas show that hydrological connectivity which maintains the energy and mass interaction between the main channel and the floodplain lakes plays an important role in regulating the light and nutrient conditions and hence primary production in floodplain lakes (Junk et al., 1989; Van den Brink et al., 1992; Tockner et al., 1999; Squires and Lesack, 2003; Wiklund, 2012).

Primary production in floodplain lakes responds to hydrology in different ways, depending on the relative difference in nutrient concentrations between the rivers and lakes. In a river-floodplain system with nutrient-rich rivers, the main channel acts as the major source of both allochthonous nutrients and suspended particles of lateral floodplain lakes (Junk et al., 1989; Squires et al., 2002). Here, algal production responds to hydrology in a unimodal way (Squires et al., 2002, McGowan et al., 2011) (Figure 2.6a). Open-drainage lakes which are freely connected with the main channel receive more nutrients than closed-drainage basins which are isolated from the main channel (Van den Brink et al., 1992; Van den Brink, 1994; Knowlton and Jones, 1997; Tockner et al., 1999; Squires et al., 2002; Wiklund, 2012) (Figure 2.6a). Meanwhile, more suspended particles from the main channel are transported into open lakes relative to closed drainage lakes as well, which promotes the absorption and scatter of light. As a result, light radiation in closed lakes is higher than that in open lakes (Figure 2.6a). Algal production in open-drainage lakes which benefits from high nutrient inputs is limited by poor light conditions due to the high concentrations of suspended particles, whereas in closed-drainage lakes which are relatively transparent algal production is restricted by low nutrient availability (Figure 2.6a). Lakes with an intermediate hydrological connection with the main channel have optimal conditions of both light and nutrients (which may be delivered periodically rather than continuously), hence the highest primary production (Knowlton and Jones, 1997; Squires and Lesack, 2003; Wiklund, 2012). Therefore, primary production shows a theoretical unimodal response to hydrological connectivity due to the trade-off between light and nutrient availability (Figure 2.6a) (Knowlton and Jones, 1997; Squires and Lesack, 2003; McGowan et al., 2011; Wiklund, 2012).

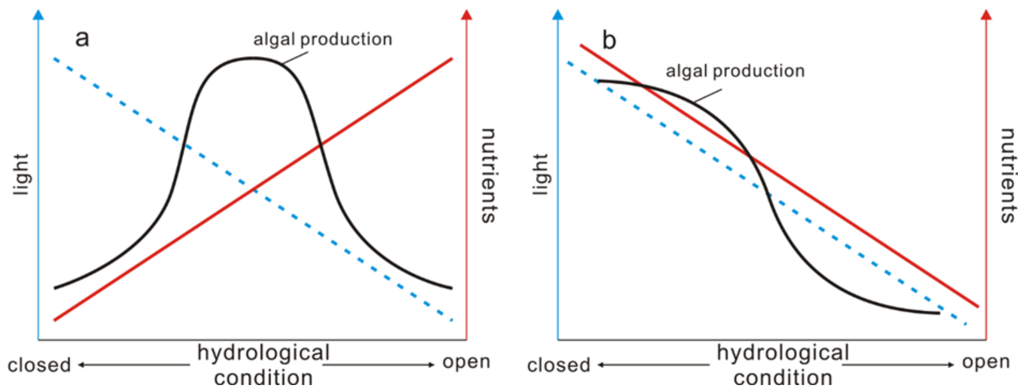

Figure 2.6 Conceptual diagram showing the theoretical responses of light, nutrients and algal production of floodplain lakes along a gradient of hydrological connectivity in river-floodplain systems where nutrient concentrations are river > lake (a) and river < lake (b). The red solid line indicates nutrients; the blue dashed line indicates light condition; the black solid line indicates algal production.

In river-floodplain systems where nutrient concentrations in rivers are lower than those in floodplain lakes or river-floodplain systems experiencing strong evaporation, algal production shows a monotonic decreasing trend with enhanced hydrological connectivity with the main channel (Figure 2.6b) (Sokal et al., 2008; Wikland, 2012). Free hydrological connection which transports nutrient-poor main channel water into open drainage lakes dilutes the nutrient concentration in the floodplain lakes. As a result, nutrient concentrations in open-drainage lakes are lower than in closed basin lakes due to the dilution by ‘clean’ main channel water (Sokal et al., 2008) (Figure 2.6b). Combined with the poorer light conditions in open-drainage lakes due to the high influxes of suspended particles from the main channel (Wikland, 2012), primary production shows a monotonic downward trend along the closed to open hydrological gradient (Sokal et al., 2008; Sokal et al., 2010) (Figure 2.6b). In this situation, which is observed in remote subarctic and relatively “pristine” systems, hydrologically closed lakes have higher primary production due to good light conditions and higher nutrient concentrations which may be cycled from lake sediments, while primary production in open drainage lakes is limited by poor light conditions and low nutrients.

Apart from influencing the overall primary production, hydrological connectivity with the main channel may influence the algal community composition as well (Van den Brink et al., 1992; Peršić and Horvatić, 2011). In recent decades, increasing nutrient loadings from human activities including agricultural and industrial development and urbanization have substantially increased nutrient influxes into river floodplain systems, resulting in eutrophication and the modification of algal communities in floodplain lakes (Galloway et al., 2008; Conley et al., 2009). In the lower Rhine river-floodplain system, the severely polluted Rhine River exported large amounts of nutrients (mainly phosphorus and nitrogen) into hydrologically open lakes (Van den Brink et al., 1992), resulting in phytoplankton communities dominated by cyanobacteria and chlorophytes which favour low Si: N and Si: P conditions (Van den Brink, 1994). In contrast, planktonic communities in closed-drainage lakes were characterized by bacillariophytes which grow in conditions of relatively high Si availability (Van den Brink, 1994). In the North-Eastern Croatia stretch of the Danube, as the main channel provides large amounts of nitrogen to the lateral floodplain, algal communities in lakes with strong hydrological connection with the main channel were characterized by chlorophytes which favour high N: P ratios, while lakes that were hydrologically isolated from the main channel were abundant in cyanobacteria (Peršić and Horvatić, 2011).

2.7 Aquatic stable state transitions

The classic eutrophication paradigm mainly focuses on algal production and community succession in the water column (Leavitt et al., 2006; Schindler et al., 2008; Donald et al., 2011). Predicting the ecosystem response to eutrophication in shallow lakes is complicated, as the benthic communities interact with phytoplankton communities through the control of resources (e.g., light, nutrients) and biological interactions (i.e., predation, competition) are also important components of the ecosystem (Scheffer et al., 1993; McGowan et al., 2005). Both empirical and theoretical evidence suggests that shallow freshwater lakes respond to nutrients in a bistable pathway where ecosystems have two alternative stable states dominated by either algae or macrophytes (Scheffer et al., 1993; Scheffer et al., 2001). In shallow aquatic ecosystems, the two important primary producer communities (algae and macrophytes) are dominant under different limnological conditions. In the clear water state, shallow lakes are usually dominated by macrophytes, whereas the turbid-water state has high phytoplankton biomass (Scheffer et al., 1993; McGowan et al., 2005). Therefore, the conceptual model of alternative stable states is considered a more comprehensive way of summarizing the effects of eutrophication on shallow freshwater ecosystems (Scheffer et al., 1993).

Alternative stable states theory suggests that under low nutrient conditions, the clear water macrophyte-dominated state is most common (Scheffer et al., 1993; Blindow et al., 1993). Under high nutrient conditions the algal-dominated turbid state with poor light conditions is prevalent (Scheffer et al., 1993; Burson et al., 2018). Under intermediate nutrient conditions, a lake may exist in either of the two alternative stable states, and external perturbations (e.g., bio-manipulation, hydrology) may switch it from one to another (Scheffer et al., 1993; Blindow et al., 1993). The presence of macrophytes is considered a key regulator and feature of ecosystem structure, and hence ecosystem state (Scheffer et al., 1993). In each state, positive feedback mechanisms may pose a ‘basin of attraction’ where buffer mechanisms exist to keep the lake in that state (Scheffer et al., 1993; Blindow et al., 1993) (Figure 2.7). Increasing nutrient loadings may disrupt buffers and decrease the resilience of a macrophyte-dominated ecosystem to increase the likelihood of passing into another ‘attraction basin’ of the algal-dominated ecosystem (Scheffer et al., 1993).

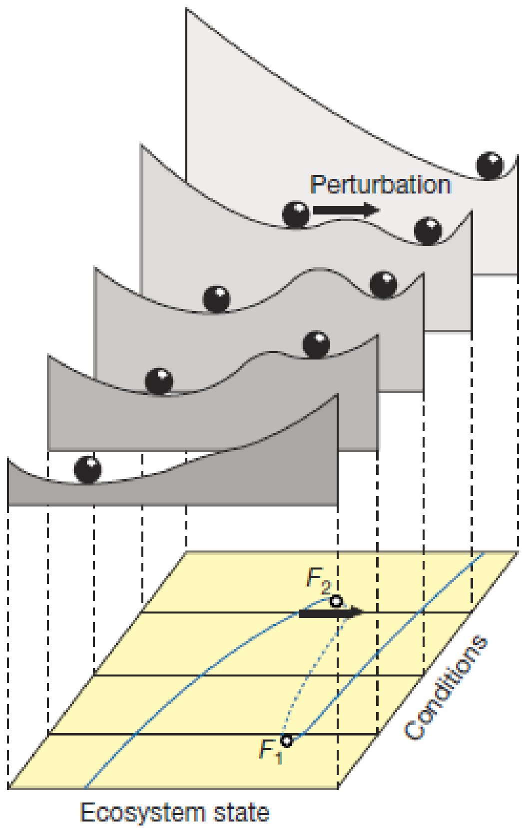

Figure 2.7 External conditions affect the resilience of multi-stable ecosystems to perturbation. The bottom plane shows the equilibrium curve. The stability landscapes depict the equilibria and their basins of attraction at five different conditions. Stable equilibria correspond to valleys; the unstable middle section of the folded equilibrium curve corresponds to a hill. If the size of the attraction basin is small, resilience is small and even a moderate perturbation may bring the system into the alternative basin of attraction. (from Scheffer et al., 2001)

Feedback loops and mechanisms involved in the aquatic stable state transitions are complex and diverse (Scheffer et al., 1993; Jeppesen et al., 1997). Nutrient mediated "bottom-up" processes are a cornerstone for aquatic stable state transition (Scheffer et al., 2003; Jeppesen et al., 2003; McGowan et al., 2005). Under low nutrient conditions, phytoplankton biomass and production are low. Low phytoplankton production results in high light penetration, favouring the growth of macrophytes. The "top-down" theory which links benthic and planktonic species through a series of food-web processes is important to feedback loops in aquatic stable states as well (Jeppesen et al., 2003). In shallow freshwater lakes, phytoplankton biomass is influenced by top predators through food web interactions as described by the fish-invertebrate-periphyton cascade (Jones and Sayer, 2003). High abundance of planktivorous fish would limit the growth and biomass of zooplankton feeding on phytoplankton. Conversely, the absence of planktivorous fish stimulates the growth of zooplankton, which restricts the growth of phytoplankton (Jeppesen et al., 1997; Jeppesen et al., 2003). The growth of macrophytes make the limnological conditions more suitable for sustaining macrophyte dominance through a series of positive feedbacks, including prohibiting the resuspension of sediments, providing refuges for zooplankton which control phytoplankton production and promoting nutrients sequestration in water column (Scheffer et al., 1993; McGowan et al., 2005). The positive feedback enforces the clear water state dominated by macrophytes. Increasing nutrients promote phytoplankton production, including some bloom-forming cyanobacteria (Schindler et al., 2008; Parel et al., 2011). The high phytoplankton production results in enhanced algae induced turbidity, promoting the scattering and absorbing of light, which may shade out the benthic competitors including macrophytes (Schindler et al., 2008; Conley et al., 2009; Smith and Schindler, 2009; Burson et al., 2018). Therefore, increasing nutrients would decrease the resilience and reduces the buffers of the macrophyte-related clear water state. Efforts to return the lake to the clear water state through nutrient reduction are resisted by the buffer mechanisms of the turbid state; hence showing hysteresis to nutrient reduction (Scheffer et al., 1993).

Studies in recent years show that aquatic stable state transitions are much complex and elaborated than the simple original model which describes the shifts between the macrophyte-dominated clear water sates to the algal dominated turbid states (Scheffer and van Nes, 2007). Evidence of the long-term variation in macrophytes and phytoplankton during the aquatic stable state transition is contentious and not clear on all lakes (Sayer et al., 2010). This is because both macrophytes (e.g., submerged, floating) and algae (e.g., benthic, planktonic) contain different groups and the change between groups (e.g, benthic algae to planktonic algae) may also indicate aquatic stable state transiton (Scheffer van Nes, 2007). For example, evidence from two Danish lakes showed that there was a shift from benthic algae to planktonic species with no increase in total algal production during aquatic stable state transition (McGowan et al., 2005).

2.8 Palaeolimnology

Forecasting the future dynamics for effective management of lake ecosystems requires knowledge and deep understanding of how environmental perturbations (measured as E and *m* influxes) have affected ecosystems in the past (Battarbee et al., 2005; Battarbee et al., 2012). Limnology normally focuses on relatively short time scales (days, years) using methods such as lake experiments, monitoring surveys or nutrient addition bioassays (Schindler et al., 2008; Paerl et al., 2011), but such approaches are unable to capture natural variability in energy and mass influx such as variation in solar radiation, vegetation succession in the catchment and longer-term shifts in hydrology (Leavitt et al., 2009). Restoration or rehabilitation of damaged lakes in social and biological critical zones requires knowledge of the degree to which present day conditions deviate from those expected in the absence of significant anthropogenic regulation (i.e. reference conditions) (Bennion et al., 2011). Some ecosystem changes are expressed at temporal scales that are inadequately captured by available monitoring datasets of aquatic communities (Sayer et al., 2010). In contrast, palaeolimnology (lake sediment core analysis) can provide an integrated record of lake history (Battarbee et al., 2005). Information on how lakes respond to the energy and mass influxes are being synthesised and preserved in the lakes in the form of mass (lake sediments) (Leavitt et al., 2009). According to the law of superposition, lake sediments are deposited in order, meaning sediment age increases with the burial depth. By analysing the physical, chemical and biological proxies preserved in dated sediment cores, information on the historical evolution of lake ecosystems and the long-term variation in energy and mass influxes caused by climate, catchment processes and anthropogenic perturbation can be extracted (Battarbee et al., 2005; Leavitt et al., 2009; Bennion et al., 2011).

In combination with monitoring data, palaeolimnology offers the best opportunity of generating data sets of sufficient length and quality to address these questions of ecosystem change in lakes (Bennion et al., 2005; Stevenson et al., 2015; Moorhouse et al., 2018) and fluvial landscapes (McGowan et al., 2011; Dong et al., 2016; Foster and Greenwood, 2016). For example, Stevenson et al. (2016) found that forestry plantation and deforesting of the catchment have increased algal production, especially from cryptophytes and colonial cyanobacteria, in upland lakes in north-west Ireland by studying the pigment biomarkers and carbon isotopes preserved in dated lake sediments. Combined with surface sediment surveys, McGowan et al. (2011) found that low flood frequency increases algal production in floodplain lakes by studying algal remains preserved in sediment cores. Comparisons of diatom assemblages in modern samples with those before the 1850s CE showed that lakes in the Yangtze floodplain are suffering from nutrient enrichment caused by human activities (Dong et al., 2016). With the development of statistical analysis, palaeolimnology has made it possible to quantify historical water quality such as the nutrient concentrations (e.g., TP) (Bennion et al., 1996; Yang et al., 2008), salinity (Fritz et al., 1991) and pH (Battarbee et al., 2005) by applying transfer functions calibrated using spatial limnological surveys.

Over the last 30 years, the development of palaeolimnological proxies such as diatoms (Battarbee et al., 2001), pigments (Leavitt and Hodgson, 2001), macrofossils (Birks, 2001; Sayer et al., 2010), pollen (Burden et al., 1986) and cladocera (Jeppesen et al., 2003; Davidson et al., 2011) have provided fruitful information on the historical variation of different trophic levels in freshwater ecosystems. In combination with the application of transfer functions which makes it possible to reconstruct the past nutrient conditions of lakes (Bennion, 1996; Yang et al., 2008), more knowledge has been gained regarding the mechanisms of aquatic stable state transitions in palaeolimnology (McGowan et al., 2005; Wang et al., 2012; Seddon et al., 2014; Randsalu-Wendrup et al., 2016).

For instance, McGowan et al. (2005) revealed that food chain processes-oriented "top-down" effects made a great contribution during the transition from a macrophyte-dominated clear water state to the algal dominated state in two Danish Lakes, based on multiple sedimentary proxies analysis, and nutrient states were also important in combination with the food chain processes but were less important alone.

Light conditions are important in regulating shallow freshwater ecosystems (Karlsson et al., 2009; section 2.5). In aquatic stable state transitions, light/water clarity is implicit and changes synchronously with food web interactions and others processes (Scheffer et al., 1993; Scheffer et al., 1997). However, most of the palaeolimnological studies considering aquatic stable state transitions are based on lakes without major external sources of TSS, and therefore, nutrients and food web processes are the main focus (Scheffer et al., 1993; Jeppesen et al., 2003; McGowan et al., 2005; Wang et al., 2012). In floodplain lakes, allochthonous TSS is an important factor influencing turbidity and hence, potentially, ecosystem states (Scheffer et al., 1997). Over the last few decades, advances in sedimentary pigment analyses have provided new insights in allowing the reconstruction of past light conditions in lakes (Leavitt et al., 1997; McGowan et al., 2012; McGowan et al., 2018). As mentioned in section 2.5, over exposure to UVR causes damage to organisms and influences the photosynthesis processes (Leavitt et al., 1997; Blokker et al., 2005; McGowan et al., 2018). Hence, photosynthesic organisms have developed several protective repair and defence mechanisms for the purpose of survival under UV exposure (Leavitt et al., 1997; Blokker et al., 2005; McGowan et al., 2018). In freshwater ecosystems, benthic algae generates UV-radiation-absorbing pigments (UVR-absorbing pigments) to protect themselves from UV radiation (Leavitt et al., 1997). Leavitt et al.'s (1997) study on alpine lakes showed that the UVR index derived from UVR-absorbing pigments was correlated with the intensity of UV radiation within the lakes. Therefore, the application of UVR pigments is able to provide more sedimentary evidence of the conditions surrounding aquatic stable state transitions from a palaeolimnological perspective.

2.9 Research gap: floodplain lake ecosystem functioning

In recent decades, increasing nutrient loadings from human activities, including agricultural and industrial development and urbanization have substantially increased nutrient fluxes into river floodplain systems, resulting in eutrophication and increases in overall primary production in floodplain lakes (Yang et al., 2008; Galloway et al., 2008; Conley et al., 2009). Concurrently, anthropogenic hydrological alteration (e.g., dam construction, reservoir impoundment) has substantially modified the natural hydrological setting of river floodplain systems, turning hydrologically open lakes into closed lakes (Yang and Lu, 2014; Zeng et al., 2018). As a result, the natural water, nutrient and sediment interaction between rivers and floodplain lakes has been transformed, which may influence primary production and algal community composition in floodplain lakes (Cross et al., 2014; Chen et al., 2016). With the ongoing development of agriculture, industry and urbanization as well as dam and reservoir construction, understanding the long term dynamic of lake ecosystem evolution in large river-floodplain systems affected by hydrology and pollution is of critical value for sustainable development. Although increased efforts has been dedicated to the study of floodplain lakes, the influence of hydrological modification on floodplain lake ecosystem is unresolved and knowledge gaps remain (Vannote et al., 1980; Junk et al., 1989).

On one hand, there is evidence that hydrologically closed lakes tend to develop more phytoplankton, especially bloom-forming cyanobacteria, which may shade out the benthic communities and turn the lakes into an algal dominated turbid state through several mechanisms (Scheffer et al., 1993; Tockner et al., 1999; Liu et al., 2017). Water exchange ratios and water retention times are important factors controlling nutrient cycling and phytoplankton biomass in floodplain lakes (Chen et al., 2016). Local dam construction which isolates lakes from rivers stabilizes the hydrological condition of floodplain lakes, prolonging WRT and decreasing flushing rates. The physiological advantages of cyanobacteria (e.g., high mobility, buoyant) makes them more competitive in lentic waters over bacillariophytes which compete well in turbulent and well mixed waterbodies (Elliott, 2010). Alternatively, in areas with high nutrient loading, prolonged water retention times and reduced flushing rate resulting from local dam construction may reduce the flushing of nutrients (e.g., TP) out of lakes and exacerbate nutrient enrichment. As a consequence, bacillariophytes could be outcompeted by potentially toxic and bloom-forming cyanobacteria which prefer higher phosphorus concentrations and long water retention times (Cross et al., 2014). More directly, local dam construction is efficient at promoting the biomass accumulation of phytoplankton, whereas free hydrological conditions in floodplain lakes may flush phytoplankton out of the lakes (Tockner et al., 1999). Overall, local dam construction which blocks the hydrological connection with the main channel could potentially exacerbate the symptoms of eutrophication caused by increasing nutrient loading in river floodplain systems. In this situation, dam construction turns lakes into an algal-dominated turbid state under eutrophication (Ibáñez and Peñuelas, 2019). On the other hand, local dam construction which turns lotic floodplain lakes into closed systems may stabilize the water level and block the transport of suspended particles into floodplain lakes, improving the light conditions and stimulating benthic communities (e.g., macrophytes) (McGowan et al., 2011; Zeng et al., 2018). The growth and development of macrophytes may buffer against the effects of nutrients, sustaining the lakes in a clear water state (Scheffer et al., 1993; Scheffer et al., 2001).

For open lakes, free hydrological connectivity may alleviate the symptoms of eutrophication as floodplain lakes which are freely connected with the main channel have high water turnover rates and hence are insensitive to nutrient enrichment because of high rates of nutrients and phytoplankton wash-out (Squires et al., 2002; Sokal et al., 2008; Wiklund, 2012). However, the highly variable water level fluctuations and high TSS concentrations in open lakes may result in high water turbidity, suppressing the growth and development of benthic communities (Scheffer et al., 1993; Scheffer et al., 2001).

In the past, most of the classic theories in palaeolimnology such as nutrient limitation of productivity, aquatic stable state transitions and the bottom-up effects have been based on lentic lakes (Schindler et al., 1977; Scheffer et al., 1993; Karlsson et al., 2009). The hydrological condition of floodplain lakes are inherently variable, being strongly lotic during flooding seasons and lentic during the non-flood seasons. Few palaeolimnological studies have tested the capability of these classical theories developed on lentic lakes in floodplain areas.

Past studies on floodplain lakes have also often focused on single drivers. For example, based on the relatively less human disturbed Mackenzie Delta and the Peace-Athabasca Delta in North America, efforts have been paid to figure out the role of natural hydrological variation (flooding caused by precipitation) on the ecosystem of floodplain lakes (Squires et al., 2002; Sokal et al., 2008; Wiklund, 2012). In the intensively and extensively human influenced Yangtze floodplain, previous studies have mainly focused on nutrients (Yang et al., 2008; Dong et al., 2012), whereas knowledge about hydrology has only been increasing in recent years and are currently not clear (Chen et al., 2016; Xu et al., 2017). However, concurrent with the increasing nutrient influxes from human sources, the natural hydrological setting of floodplain lakes has been modified by human perturbation such as dam construction and land reclamation as well. Therefore, it is important to simultaneously investigate the relative importance of multiple stressors (nutrients, hydrology) on floodplain lake ecosystems.

CHAPTER 3 SITE DESCRIPTION AND ENVIRONMENTAL HISTORY OF THE MIDDLE YANGTZE BASIN, CHINA

This chapter gives a detailed review of the recent history of social economic development in the middle Yangtze floodplain and the problems that lakes in the region are facing, with an introduction to each individual study lake.

3.1 The Yangtze Basin

The Yangtze River, formed by the uplifting of Tibetan Plateau and the strengthening of Asian summer monsoon, has a total length of ca. 6,300 km (Zheng, 2015). The Yangtze River is the longest river in China and Asia, and the third longest river in the world (Milliman and Farnsworth, 2011). It ranks fourth and fifth in the world in terms of sediment load (ca. 470 million metric tons (Mt) per year before the 1980s CE) and water discharge (ca. 900 km^3 per year), respectively (Milliman and Farnsworth, 2011). The Yangtze River has a basin area of about 1.8×10^6 km^2, which covers about one fifth of China (Figure 3.1).

Originating from the Tibetan Plateau in Western China, the Yangtze River flows through the deep rocky canyons in the upper reaches. After passing through the Three Gorges area, the Yangtze River meanders along the vast plain in the middle and lower reaches before entering the East China Sea (Figure 3.1). The Yangtze Basin supports more than 400 million of the population in China (Zong and Chen, 2000). In terms of biodiversity, the Yangtze floodplain is one of the most diverse and dynamic areas in China. It is the habitat for ca. 400 species of hydrophytes and hygrophytes and more than 167 mollusc species (Wang et al., 2016). As a major fishery, this area has more than 200 fish species with an additional ca. 50 reptile species, 300 waterfowl species and, over winter, hosts most of the world's Siberian crane (*Grus leucogeranus*) (Wang et al., 2016).

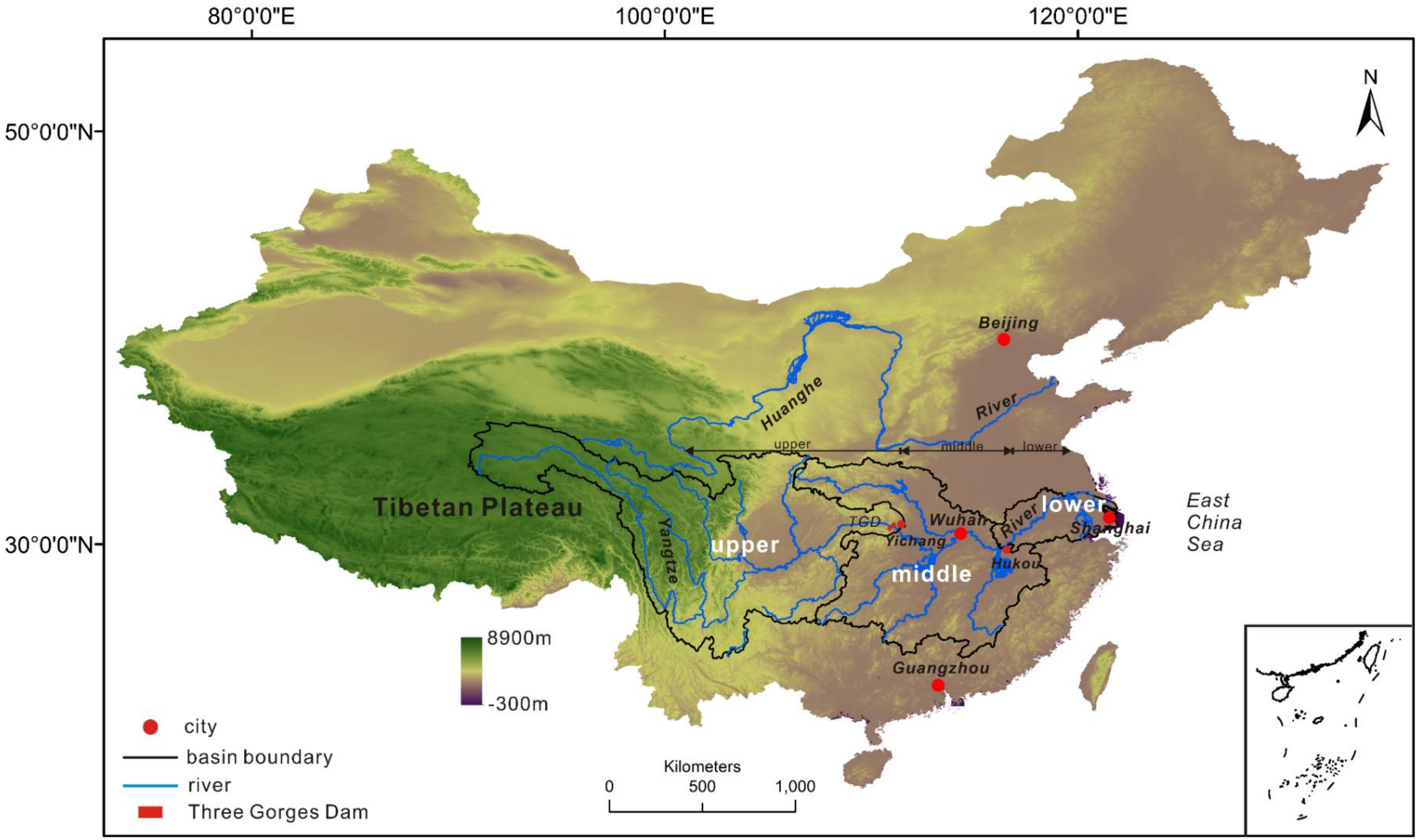

Figure 3.1 Elevation map showing the location and basin of the Yangtze River.

The Yangtze River is divided into the upper, middle and lower reaches by the two prefectures, Yichang and Hukou (Figure 3.1) (Zheng, 2015), and each reach has different geological, geomorphological and climatic characteristics (Chen et al., 2001). The upper Yangtze is the section between the source in the Tibetan Plateau and Yichang (Figure 3.1), with a length of more than 4,300 km and a drainage area of ca. 1.0×10^6 km^2. The geology is characterized by Triassic-Jurassic shallow-marine carbonate, basaltic, Triassic turbiditic rocks, volcanics, shales and sandstones. The geomorphology comprises a V-shaped valley with deep and steep rocky canyons (slopes vary between 10×10^{-5} and 40×10^{-5}), where the main channels are about 0.5 - 1.5 km in width and 5 - 20 m in depth (Chen et al., 2001) (Figure 3.2). Precipitation in the upper Yangtze Basin mainly comes from the Indian summer monsoon (Saito et al., 2017).

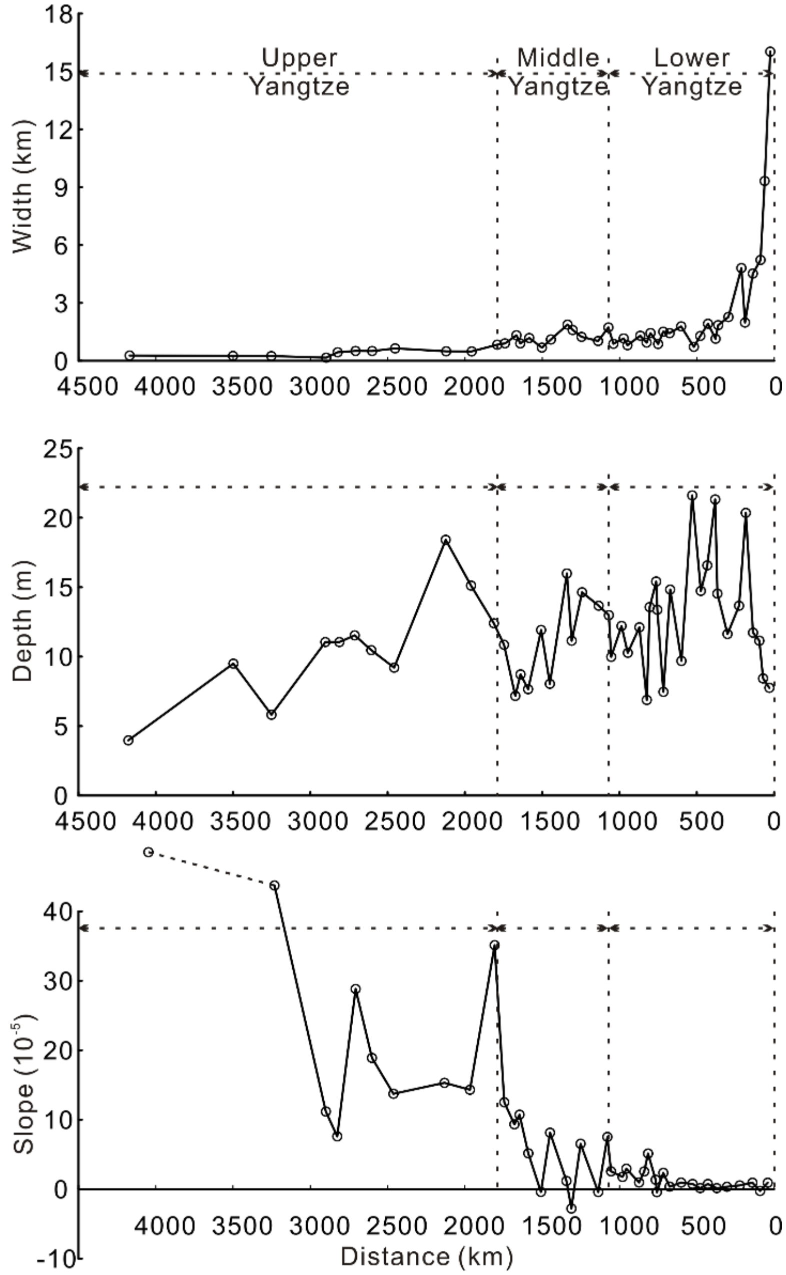

Figure 3.2 Width (upper) and depth (middle) of the Yangtze River and the slope (lower) of the Yangtze valley along the distance to the river mouth (modified from Chen et al., 2001).

The middle Yangtze, defined as the section between Yichang and Hukou, has a length of ca. 950 km and a drainage area of ca. 6.8×10^5 km^2 (Figure 3.1). The middle Yangtze Basin is mainly composed of three provinces, Hubei, Hunan and Jiangxi (Figure 3.3). The geomorphology and geology are distinctly different from the upper Yangtze (Figure 3.2). The middle Yangtze Basin is characterized by a floodplain landscape with lower riverbed slopes (mean = 2.5×10^{-5}), a mean channel width of about 1 – 2 km and an average depth of about 10 m. The floodplain in the middle Yangtze has a sub-tropical monsoon climate, with a mean annual temperature of 13 – 20 °C, and annual precipitation of 800 – 1,600 mm (Wang et al., 2016). The geomorphological setting and seasonally variable monsoonal climate combine to make this area susceptible to floods (Chen et al., 2001). The flooding season is from May to October and the non-flooding season is from November to April in the middle and lower Yangtze floodplain. As a result, the middle Yangtze Basin is characterized by Quaternary fluvial sediments transported by the Yangtze River. Flooding and meandering of the Yangtze River has formed thousands of lakes in this area, including the largest (Poyang) and second largest (Dongting) freshwater lakes in China by area.

The Lower Yangtze is the section between Hukou and the estuary (Figure 3.1). The lower Yangtze has a length of ca. 930 km and a drainage area of about 1.2×10^5 km^2. Geologically, the lower Yangtze Basin is characterized by Quaternary fluvial sediments (Saito et al., 2017) and a floodplain geomorphology with a riverbed slope of about 1.0×10^{-5}. The mean water depth and the width of the lower Yangtze are about 15 m and 15 km, respectively (Figure 2.2) (Chen et al., 2001). Similar to the middle Yangtze floodplain, the lower Yangtze is characterized by a sub-tropical monsoon climate.

3.2 Social-economic development in the middle Yangtze floodplain

China has experienced rapid social-economic development and population growth over the last seventy years (Yang, 2013; Yu et al., 2019). For example, grain production experienced a 5-fold increase from 113.18 Mt in 1949 CE to 657.89 Mt in 2018 CE (NBSC). The economy in China is divided into two stages of development, the "Planned Economy" before 1979 CE and the "Opening up and Economy Reforms" period starting from 1979 CE (Morrison, 2013). During the "Planned Economy" period, China's economy developed at a relatively slow speed, with an average annual economic growth rate of 6.7% between 1953 CE and 1978 CE (NBSC). The economic structure during this period, historically known as the cultivation culture, was characterized by an agriculture based-economy (Morrison, 2013). Since the introduction of the "Opening up and Economy Reforms", China's economy drastically increased, experiencing an annual average growth rate of 9.5% between 1979 CE and 2018 CE (Morrison, 2013). At the same time, the economic structure transformed from a previously agriculture-based economy towards the development of industry and urbanization (Yang, 2013; Morrison, 2013; Zhang et al., 2018). As a result, the urbanization rate in China increased from 19.4% in 1980 CE to 52.6% in 2016 CE (Yang, 2013).

The floodplain area in the middle and lower Yangtze Basin is one of the most densely-populated (Figure 3.3) and well-developed areas in China due to the various social-economic benefits it provides (e.g., water, nutrients, irrigation, transportation, recreation) (Tockner et al., 2010; Dong et al., 2012). With less than 9% of the nation's area, the middle and lower Yangtze is inhabited by about one quarter of the nation's population (ca. 338 million), and generated about a quarter of the nation's agricultural production in 2011 CE (Dong et al., 2012). Population density in the three provinces (Hubei, Hunan and Jiangxi) in the middle Yangtze floodplain is ca. 309 per km^2 in 2017 CE (NBSC).

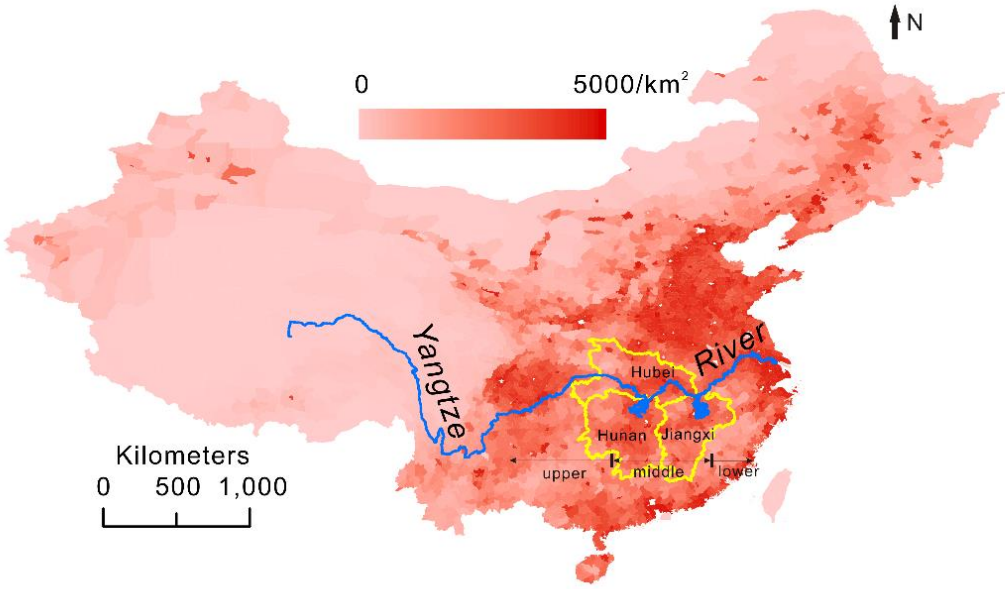

Figure 3.3 Map showing the population density in mainland China based on the population survey in 2010 (data source: NBSC).

3.2.1 Population booming

Over the last century, population in the middle Yangtze Basin has sharply increased, especially after the foundation of the People's Republic of China in 1949 CE (Figure 3.4). Before the 1930s CE, there were about 70 million people in the middle Yangtze Basin (ca. 30 million, 25 million and 15 million in Hubei, Hunan and Jiangxi, respectively) (Figure 3.4). During the tumultuous war period between the 1930s CE and 1950 CE, the population in the middle Yangtze slightly decreased, followed by a substantial increase. In 2016 CE, ca. 180 million inhabited the middle Yangtze Basin. More specifically, the population in Hubei, Hunan and Jiangxi experienced a 1.34-fold increase from 26.34 million to 61.57 million, a 1.38-fold increase from 30.74 million to 73.19 million and a 1.93-fold increase from 15.68 million to 45.92 million, respectively, between 1950 CE and 2016 CE.

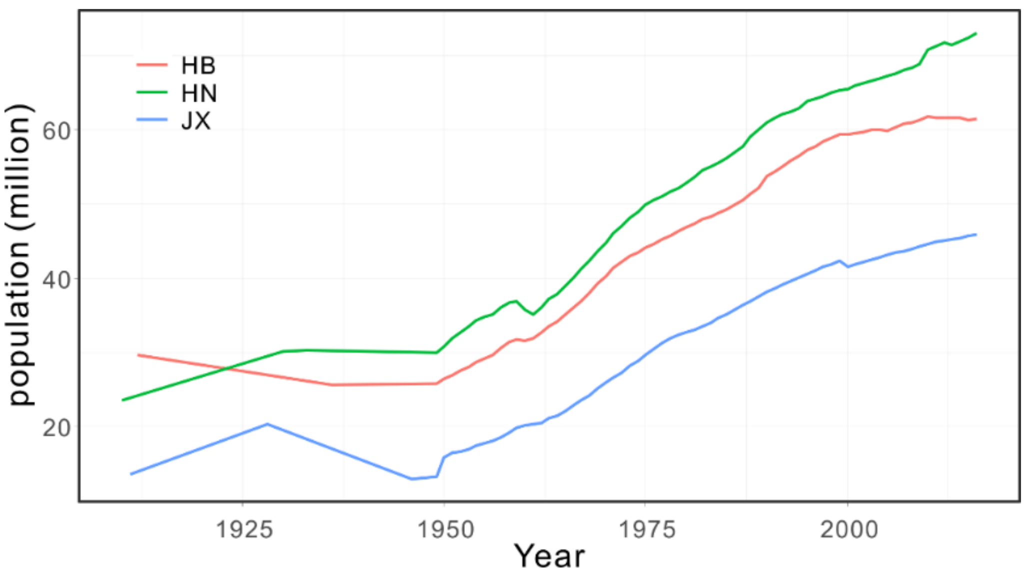

Figure 3.4 Historical changes of population in the three provinces (HB, HN and JX are short for Hubei, Hunan and Jiangxi, respectively) in the middle Yangtze floodplain over the last 100 years (data source: NBSC).

3.2.2 Agriculture development

The Yangtze floodplain is known as a region where rice is cultivated and fish can breed. This area has a long history of agriculture, which goes back to the Neolithic (Long et al., 2016). Most of the land in the middle Yangtze floodplain is used for agriculture. Land use and cover change (LUCC) shows that arable land, forestry and grass land in total accounted for about 80% of the land in Hunan, Hubei and Jiangxi between 1980 CE and 2018 CE (Figure 3.6). Over the last 70 years, grain production has increased markedly in the middle Yangtze in order to meet the food demands of the increasing population, especially between 1949 CE and the early 1980s CE (Figure 3.5a). In 1949 CE, grain production was 640×10^4, 578×10^4 and 388×10^4 metric tons in Hunan, Hubei and Jiangxi, respectively. Since then, grain production sharply increased, reaching about $2{,}650 \times 10^4$ metric tons in Hunan, $2{,}000 \times 10^4$ metric tons in Hubei and $1{,}500 \times 10^4$ metric tons in Jiangxi in the early 1980s CE. After that, grain production gradually increased, reaching $2{,}953 \times 10^4$, $2{,}554 \times 10^4$ and $2{,}138 \times 10^4$ tons in

Hunan, Hubei and Jiangxi in 2016 CE, respectively. Corresponding with the increase in grain production, fertilizer usage has sharply increased in the middle Yangtze Basin over the last 70 years (Figure 3.5b and c). In the early 1950s CE about 0.030×10^4, 0.015×10^4 and 0.061×10^4 metric tons of nitrogen fertilizers were applied in Hunan, Hubei and Jiangxi, respectively. Since then, the utilization of nitrogen fertilizers has shown a continuous increasing trend, reaching a peak at ca. 135×10^4, 190×10^4, 60×10^4 metric tons in the early 2010s CE in Hunan, Hubei and Jiangxi, respectively, followed by a slight decrease. Similar to nitrogen fertilizers, phosphorus fertilizer use increased in the three provinces of the middle Yangtze Basin as well (Figure 3.5c). Between the early 1950s CE and the early 2010s CE, the utilization of phosphorus fertilizers increased from 0.009×10^4, 0.005×10^4 and 0.03×10^4 metric tons to more than 50×10^4, 90×10^4 and 40×10^4 metric tons in Hunan, Hubei and Jiangxi, respectively.

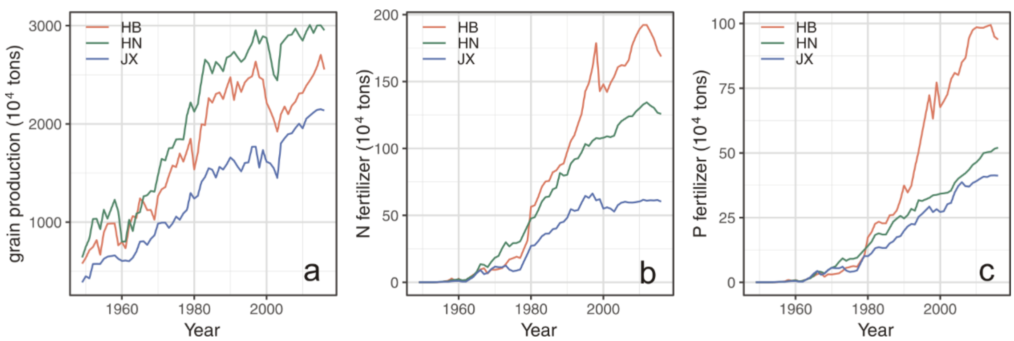

Figure 3.5 Grain production (a) and nitrogen (b) and phosphorus (c) usage in the three provinces (HB, HN and JX are short for Hubei, Hunan and Jiangxi, respectively) in the middle Yangtze floodplain between 1949 CE and 2016 CE.

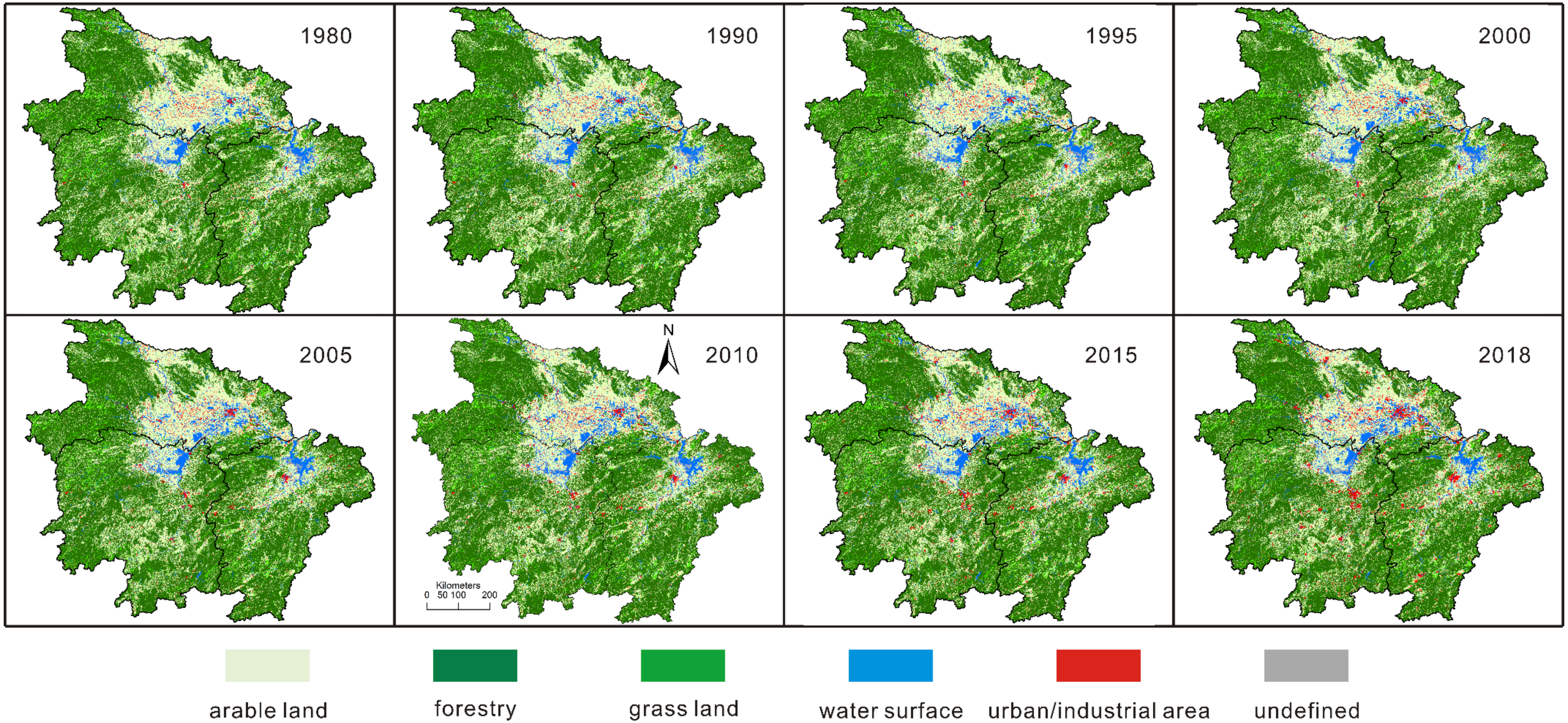

Figure 3.6 Land use and cover change (LUCC) in the three provinces (Hubei, Hunan and Jiangxi) in the middle Yangtze floodplain between the 1980s CE and 2018 CE (arable land is dominated by C_3 plants, i.e., rice) (original data download from Resource and Environment Science and Data Centre).

3.2.3 Urbanization and industrialization

Concurrent with the boom in population and agricultural development, the middle Yangtze Basin experienced rapid urbanization and industrialization over the last several decades, especially since the release of the "Opening and Reform" policy in the late 1970s CE. LUCC shows that urbanization and industrialization steadily increased between 1980 CE and 2000 CE (Figure 3.6). During this period, land used for industrial and urban activities increased from 2.36% to 2.67% in Hubei, from 1.15 to 1.32% in Hunan and from 1.52% to 1.67% in Jiangxi (Figure 3.7). Since 2000 CE, human activities are more intensive in the middle Yangtze floodplain. Land used for industry and urban areas almost doubled, reaching 4.68%, 2.72% and 3.30% in Hubei, Hunan and Jiangxi, respectively.

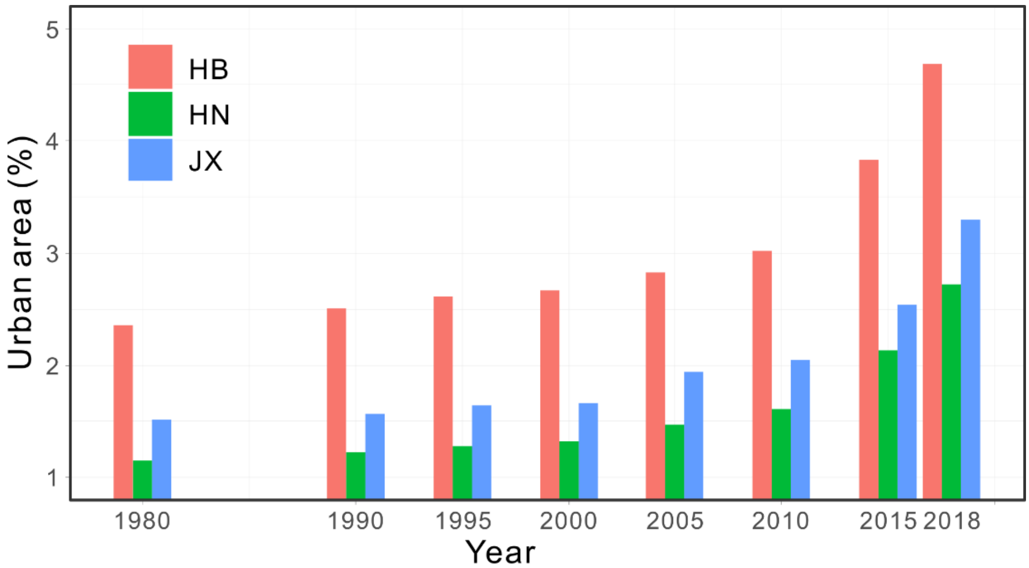

Figure 3.7 Bar chart showing the percentages of urban area in the three provinces (HB, HN and JX are short for Hubei, Hunan and Jiangxi, respectively) in the middle Yangtze floodplain from 1980 CE to 2018 CE (original data download from Resource and Environment Science and Data Centre).

3.2.4 Hydrological modification

Many dams and reservoirs were built in China over the last several decades for a variety of social-economic benefits, such as water supply, hydropower generation, flood control, irrigation, transportation, and recreation (Yang and Lu, 2014) (Figure 3.8). The number of reservoirs in China was less than 72,500 in the early 1970s CE before increasing to ca. 87,500 in the early 1980s CE (Figure 3.8). Due to the abandonment and discarding of some old and poor quality reservoirs, the number slightly decreased in the mid-1980s CE, followed by a gradual increase since 1990 CE. Capacity of the reservoirs gradually increased from ca. 350 km^3 in the early 1970s CE to ca. 500 km^3 in 2000 CE, followed by an exponential increase to more than 700 km^3 in the early 2010 CE with the construction and impoundment of large hydropower dams, such as the TGD, which is the largest dam in the world. In the frequently-flooded Yangtze Basin, there are more than 50 thousand dams and reservoirs (Yang et al., 2011), including the TGD.

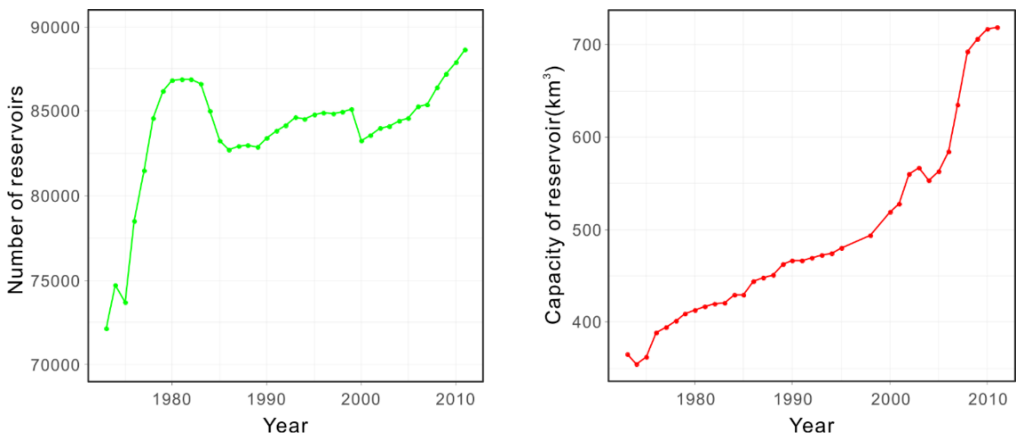

Figure 3.8 Number of reservoirs (or dams) (left) and the capacity of reservoirs (right) in China (redrawn from Yang and Lu, 2014).

3.3 Environmental issues in the middle Yangtze floodplain

There are more than 650 lakes with a water surface area >1 km^2 in the Yangtze floodplain, including the largest (Poyang Lake) and second largest (Dongting Lake) freshwater lakes in China (Dong et al., 2012). With social-economic development, anthropogenic perturbations resulting from agricultural and industrial development and urbanization, including hydrological modifications (e.g., dam construction, reservoir impoundment, embankment) and increasing nutrient loading, have generated profound negative effects on these shallow freshwater ecosystems in the Yangtze floodplain during the Anthropocene (Yang et al., 2008; Yang et al., 2011; Dong et al., 2012; Yu et al., 2019). Lakes in the Yangtze floodplain are suffering from various environmental problems, such as lake area shrinkage, water quality deterioration and declines in biodiversity (Fang et al., 2006; Yang et al., 2008; Yu et al., 2019).

3.3.1 Lake area shrinkage

As population growth and social-economic development progress, more resources and arable land are needed to meet the increasing demand for food, habitats and other living facilities in the Yangtze floodplain. Therefore, land reclamation from lakes for cultivation has become commonplace in this region (Fang et al., 2006). As a result, lake area shrinkage is the most visible threat that Yangtze floodplain lakes are suffering from (Du et al., 2011; Xie et al., 2017). Between 1975 CE and 2015 CE, human activities have transformed 13.8 ± 1.4% (2,132 ± 220 km^2) of the water surface into cropland, fish ponds, built-up areas, vegetation and bare land in the middle and lower Yangtze floodplain (Xie et al., 2017). In the Jianghan Plain (a part of the middle Yangtze floodplain), there were 1,106 freshwater lakes with a total area larger than 7,141 km^2 in the 1950s CE (Fang et al., 2006). More than 410 of these lakes had a water surface area larger than 1 km^2 at this time. However, there were only 958 lakes remaining, of which the total area shrank to less than 2,500 km^2 by the end of the 20th century due to land reclamation (Figure 3.9) (Fang et al., 2006; Du et al., 2011). Wuhan, a prefecture in the middle reaches of the Yangtze floodplain, used to have more than 120 freshwater lakes, but less than 40 of them were remaining by 2016 CE (China Daily, 2016). A study in Dongting Lake (the second largest freshwater lake in China) revealed that the mean water surface area decreased ca. 50% from 4,955 km^2 in the 1930s CE to 2,500 km^2 in the 1990s CE (Dai et al., 2005). Apart from land reclamation and cultivation, sedimentation (natural silt deposition), climate change (e.g. annual rainfall variations) and dam and reservoir impoundment are other potential reasons for lake area shrinkage (Fang et al., 2006; Feng et al., 2013; Xie et al., 2017).

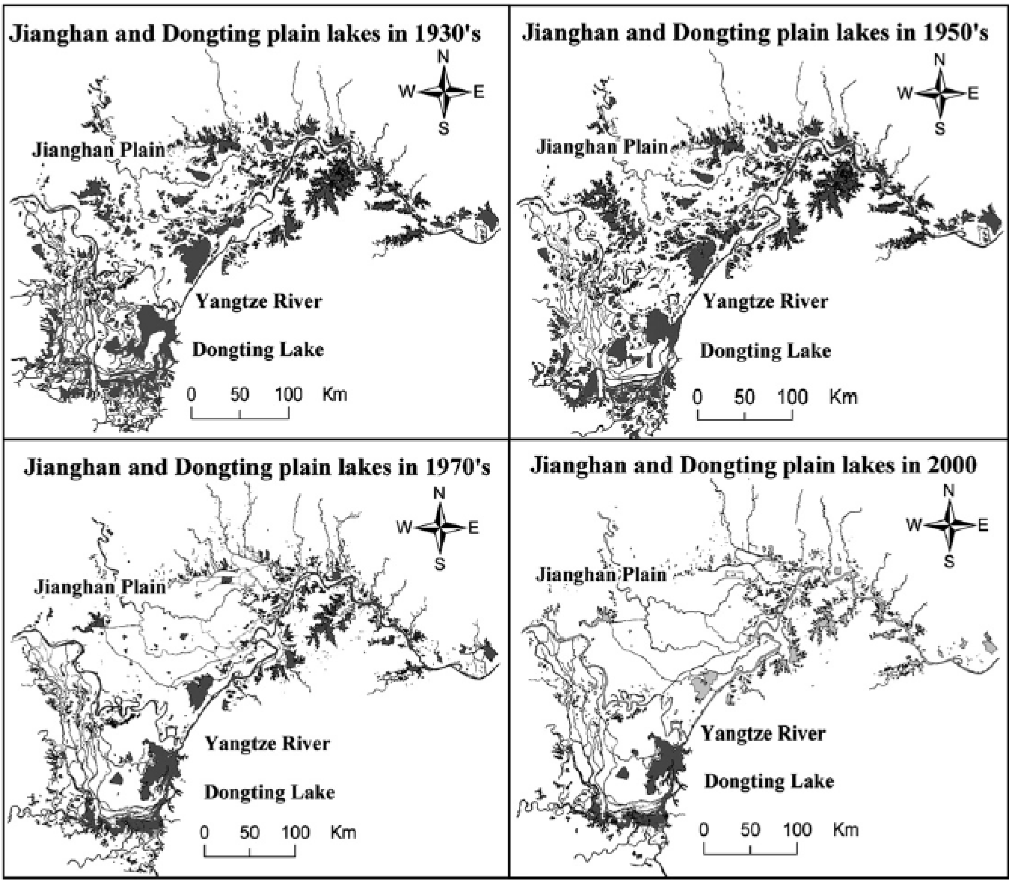

Figure 3.9 Maps showing the water surface area in the Jianghan Plain (a part of the middle Yangtze Basin) in the 1930s CE, 1950s CE, 1970s CE and 2000 CE based on historical relief maps, irrigation maps, Landsat images, historical literature and field investigation (from Du et al., 2011).

3.3.2 Eutrophication

Apart from lake area shrinkage, rapid expansion in population and industrial and agricultural activities are accompanied by excessive loading of nutrients (mainly phosphorus and nitrogen) (Fang et al., 2006; Yang et al., 2008). For example, the usage of fertilizer increased more than 10-fold from the 1950s CE to 2005 CE in China (Gao and Zhang, 2010). At the same time, the urbanization rate in China increased from 19.4% in 1980 CE to 52.6% in 2016 CE (Yang, 2013). In combination, these changes have exerted a heavy N and P burden on the environment, especially freshwater ecosystems (Conley et al., 2009; Smith and Schindler, 2009; Liu et al., 2016; Yu et al., 2019). N discharge to freshwaters increased from about 1 Mt N yr^{-1} in the mid-1950s CE to 14.5 Mt N yr^{-1} in 2014 CE (Yu et al., 2019) and P discharge increased three-fold from ca. 0.5 Tg P yr^{-1} in the 1950s CE to ca. 1.5 Tg P yr^{-1} in the 2000s CE (Liu et al., 2016).

Water quality degradation caused by increasing nutrient loading has become a severe problem in China, resulting in strongly negative ecosystem consequences (Guo 2007; Yu et al., 2019). Problems are more serious in the most densely populated and developed Yangtze Basin. In the middle and lower Yangtze Basin, many freshwater lakes are suffering from eutrophication due to the expansion of agricultural and industrial activities since the 1950s CE, especially after the 1980s CE (Liu et al., 2012). A study in the middle and lower Yangtze Basin reveals that 48 of the 49 studied lakes and reservoirs are in a eutrophic or hyper-eutrophic state (Yang et al., 2008). In Taihu Lake (lower Yangtze) nutrient-rich sewage and agricultural runoff caused HABs including *Microcystis* spp. which generates toxins harmful to the liver, intestines and nervous system, resulting in water deficiency for more than 2 million people in the catchment in 2007 CE

(Guo, 2007). In Chaohu Lake (lower Yangtze) deforestation and reclamation in the catchment, especially increasing loading of nutrients from industrial, agricultural and domestic sewage, has resulted in eutrophication since the 1950s CE (Chen et al., 2011).

In the Yangtze floodplain, total phosphorus (TP) has been proposed to be the most important factor influencing the biota of aquatic ecosystems (Yang et al., 2008; Cao et al., 2014; Dong et al., 2016). These relationships have led to the development of diatom-based (Yang et al., 2008) and chironomid-based (Zhang et al., 2006) TP transfer functions. Using these quantitative methods of reconstruction suggest that Taibai Lake (in the lower Yangtze) has experienced rapid eutrophication since the 1950s CE due to land reclamation, fish aquaculture and the utilization of chemical fertilizers (Yang et al., 2008; Cao et al., 2014). Diatom based TP reconstructions showed that TP in Taibai Lake has increased from less than 50 $\mu g\ L^{-1}$ before the 1920s CE to more than 150 $\mu g\ L^{-1}$ after 2000 CE (Yang et al., 2008). Similar trends were derived from chironomid-TP transfer function, where TP in Taibai Lake increased from ca. 50 $\mu g\ L^{-1}$ in the 1980s CE to ca. 140 $\mu g\ L^{-1}$ in 2006 CE (Cao et al., 2014). By using a 'top-bottom' sediment core approach, Dong et al. (2016) compared diatom species before the 1850s CE with those after 2000 CE in 10 lakes in the middle and lower Yangtze floodplain (Figure 3.10). Diatoms were characterized by non-plankton species before the 1850s CE, while species which can tolerate high nutrient concentrations were more abundant after 2000 CE (Dong et al., 2016). Some lakes have undergone a change from the macrophyte-dominated state to the algal dominated state. *Aulacoseira granulata*, a species which survives in turbulent water, was abundant in samples before the 1850s CE but sparse in samples after 2000 CE. Shifts in diatom species have been attributed to the increasing nutrient loading from human activities in the catchments and hydrological modification (Dong et al., 2016).

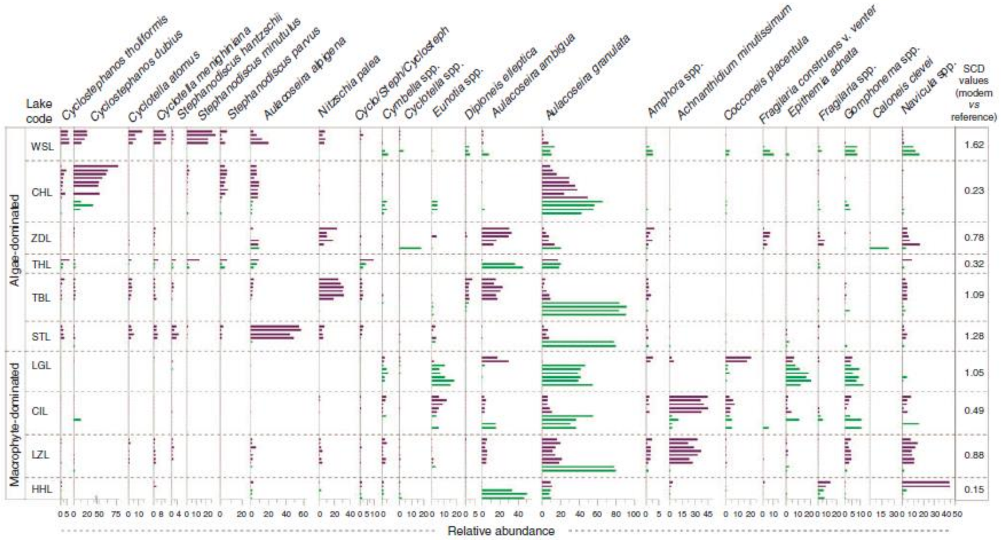

Figure 3.10 Summary diagram of the key diatom taxa in the reference samples (green bars, samples in early parts of the sediment core with dating between 1800s CE and 1850s CE) and modern samples (purple bars, samples in late parts of the sediment core with dating after 2000 CE) of 10 lakes (% relative abundance). The numbers in the right column are the squared chord distance between the averaged reference and modern sample in each lake (cited from Dong et al., 2016).

3.3.3 Hydrological modification

The Yangtze main channel meanders and carries large amounts of water and sediments from the upper reaches into the middle and lower Yangtze floodplain (Wang et al., 2008). The Hankou Hydrological Station which was established in 1865 CE in Wuhan provides long-term instrumental measurements of water discharge in the middle Yangtze River. Annual water discharge in the middle reaches of the Yangtze River fluctuated at ca. 7.5×10^{11} m^3 over the last century, varying from a minimum of 4.5×10^{11} to a maximum of 9.5×10^{11} m^3 per year between 1865 CE and 2017 CE (Wang et al., 2008; Bulletin of the Yangtze River sediments, 2006-2017) (Figure 3.11). Since the 1950s CE, sediment load has also been measured. Wang et al. (2008) used the established relationship between annual water discharge and sediment load between the 1950s CE and 2005 CE to reconstruct the sediment load of the middle Yangtze River prior to the 1950s CE. The result shows that annual sediment load in the middle Yangtze remained relatively stable before the 1960s CE, fluctuating at around ca. 450 Mt. Since the 1960s CE, due to the construction of dams and reservoirs, large quantities of sediments were retained in the upper reaches. For example, the TGD trapped more than 150 Mt sediments in the reservoir each year after impoundment in 2003 CE (Yang et al., 2007). Consequently, waters released from the TGD are sediment starved. The main channel between the TGD and Wuhan changed from a net deposition zone between 1956 CE and 2000 CE (+ 78 Mt per year) to an erosion zone after 2003 CE (− 47 Mt per year) (Yang et al., 2011). As a result, annual sediment load in the middle reaches (in Hankou Hydrological Station) has decreased by more than 60%, from ca. 450 Mt in the 1960s CE to ca. 200 Mt at around 2000 CE (Figure 3.11) (Chen et al., 2001; Wang et al., 2008; Yang et al., 2011). After 2000 CE, the annual sediment load further decreased, hovering at around 100 Mt after 2005 CE.

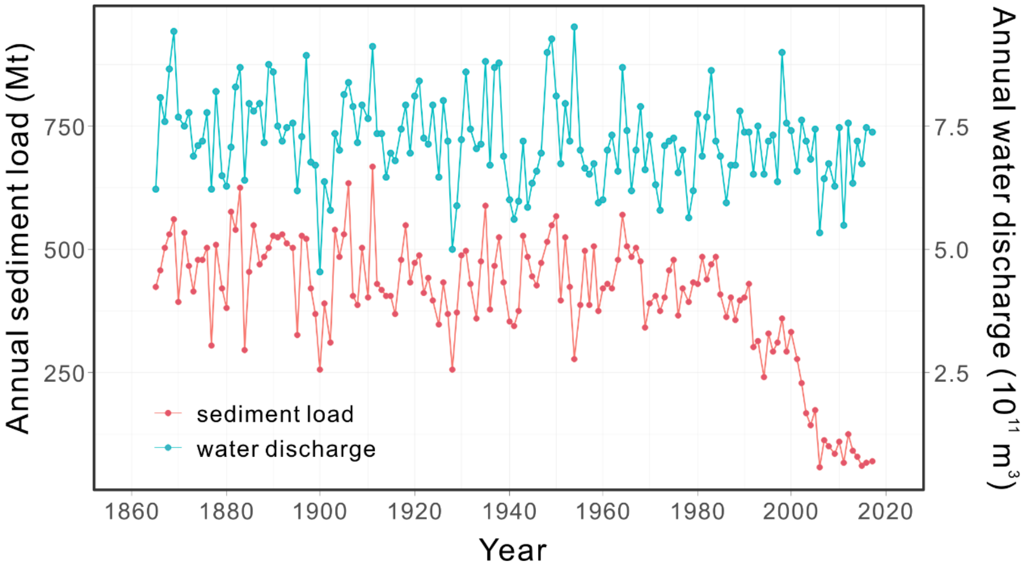

Figure 3.11 Annual sediment load (red) and annual water discharge (blue) in middle reaches of the Yangtze River (Hankou station station) (the red lines indicate five year running average) (data between 1865 CE and 2005 CE were from Wang et al., 2008, data after 2005 CE were cited from Changjiang Water Resources Commission of the Ministry of Water Resources, 2006 – 2017).

3.4 PhD site description

This study focuses on six large (ca. 40 - 3000 km^2) freshwater lakes spanning the whole middle Yangtze Basin (Figure 3.12), aiming to provide a regional understanding of aquatic environmental change. These lakes are important water resources for local residents and they possess high ecological value. Three of the lakes (Dongting Lake, Honghu Lake and Poyang Lake) have been assigned as Ramsar wetlands for their ecological significance.

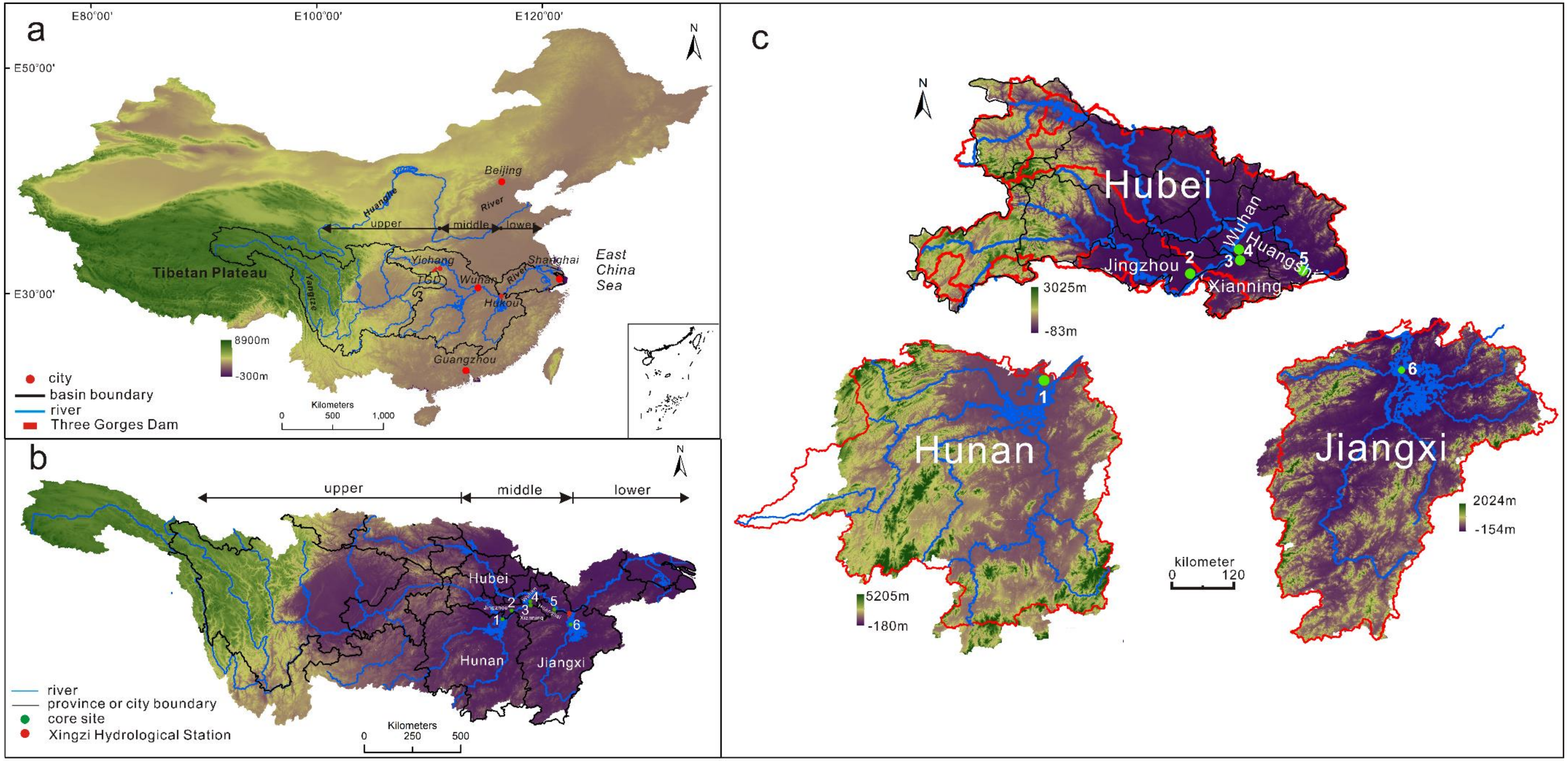

Figure 3.12 Location of the Yangtze Basin (a) in China with insets showing the location of the lakes (indicated by number) in the each administrative area (b, c) (1=Dongting Lake, 2=Honghu Lake, 3=Futou Lake, 4=Luhu Lake, 5=Wanghu Lake, 6=Poyang Lake).

Table 3.1 Location and water chemistry of the study lakes.

Site	1 Dongting	2 Honghu	3 Futou	4 Luhu	5 Wanghu	6 Poyang
Latitude (N)	28°44'-29°35'	29°38'-29°59'	29°55'-30°07'	30°12'-30°17'	29°51'-29°54'	28°24'-29°46'
Longitude (E)	111°53'-113°05'	113°11'-113°28'	114°09'-114°20'	114°9.5'-114°15'	115°20'-115°25'	115°49'-116°46'
Administrative location	Hunan	Jingzhou	Wuhan/Xianning	Wuhan	Huangshi	Jiangxi
Administrative area (km^2)	211855	14069	9178	8494	4583	166900
Mean lake depth (m)	6.4	1.9	2.9	2.7	3.6	5.1
Lake area (km^2)	2500	344	115	40	42	2933
Hydrology	open	dammed	dammed	dammed	dammed	open
Ramsar site	Yes	Yes	No	No	No	Yes
TP (mg/L)	0.054	0.008	0.037	0.068	0.22	0.027
TN (mg/L)	0.17	0.17	0.20	0.33	0.44	0.29
Atomic TN/TP	7.02	47.05	11.84	10.71	4.36	23.61
Dominant phytoplankton	Bacillariophytes ~50% [1]	Bacillariophytes 93.72% [2]	Cyanophytes34.1% Bacillariophytes31.6% Euglenophytes21.6% [3]	Chlorophytes43.5% Cyanophytes41.8% [4]	Cyanophytes 39.67% Bacillariophytes 23.6% Chlorophytes 20.5% [5]	Bacillariophytes >50% [1]

Water samples for TN and TP were collected and analysed in June 2017. Latitude and longitude of lakes are from Google Earth. Dominant phytoplankton groups summarized based on [1] Liu et al., 2017; [2] Deng et al., 2010; [3] Gong et al., 2009; [4] Rao et al., 2018; and [5] Hubei Wildlife Trust, 2005.

3.4.1 Dongting Lake

Dongting Lake (28°44’-29°35’N, 111°53’-113°05’E), located in Hunan Province, is the second largest freshwater lake in China (Figure 3.13). It has a mean water surface area of ca. 2,500 km^2 and a mean water depth of 6.4 m (Wang and Dou, 1998). Dongting Lake provides water resources for more than 6 million people in the catchment. The Dongting watershed has been assigned as Ramsar wetlands due to its critical ecological functions and its unique biodiversity (Ramsar Convention, 2020). The Dongting Lake area harbours approximately 1,400 plant species, 115 fish species and 220 bird species including some endangered species (Xie et al., 2015). Dongting Lake is an important habitat for the endangered Yangtze River Dolphin (*Lipotes vexillifer*) and the endangered Oriental Stork (*Ciconia boyciana*), Siberian Crane (*Grus leucogeranus*) and Chinese sturgeon (*Acipenser sinensis*) (Xie et al., 2015).

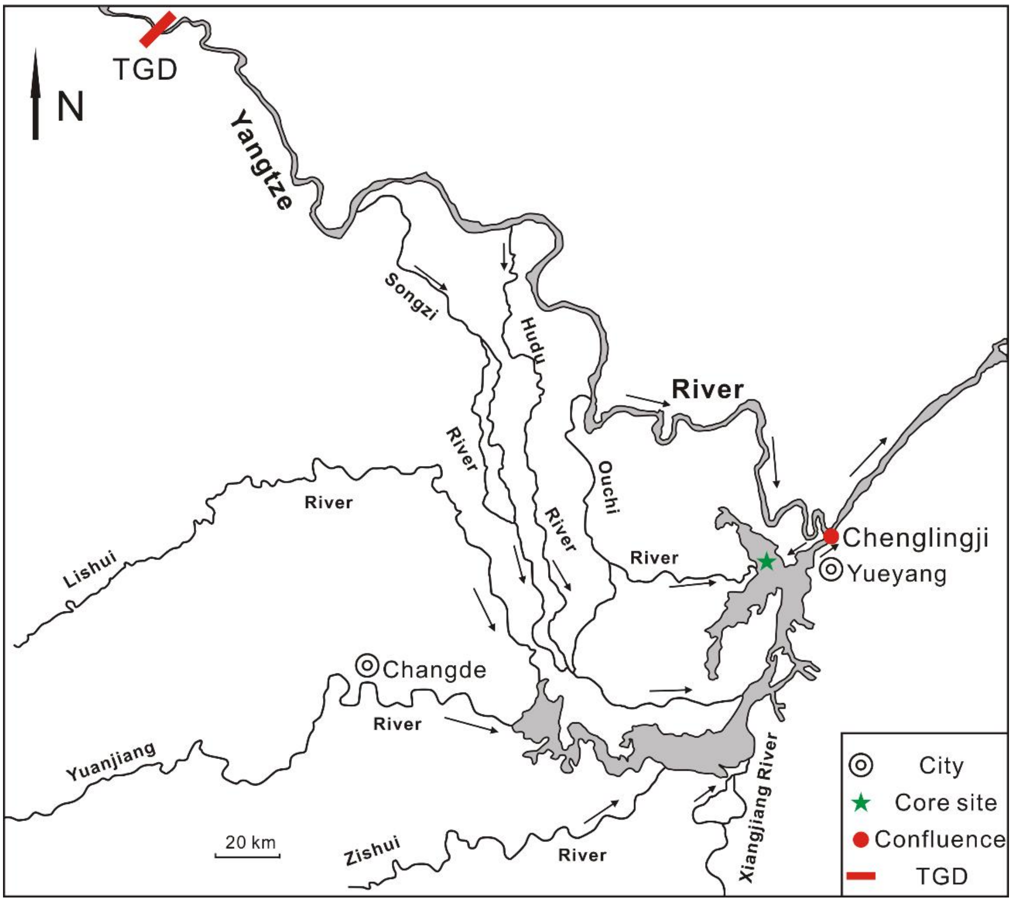

Figure 3.13 Photo of Dongting Lake (upper) (photo by S. McGowan) and sketch map (lower) showing the hydrological setting of the Dongting Lake (the red bar indicates the TGD, the red dot indicates the confluence area of Dongting Lake and the Yangtze River, the green star indicates the core site, the black arrows indicate flow direction).

Dongting Lake is a hydrologically free lake connected with the Yangtze River. The water flowing into Dongting Lake mainly comes from the Yangtze River (which accounts for ca. 30%) and from four tributaries at the south and the west (Xiangjiang River, Zhishui River, Yuanjiang River, Lishui River) (Figure 3.13). Water flows out at Chenglingji where the lake and the Yangtze River converge in the northeast (Chen et al., 2016). Flooding of Dongting Lake from the Yangtze River varies on an annual cycle. The annual difference in water level between the flooding (May-October) and drought (November to April) periods is more than 12 m (Xie et al., 2015). The annual water surface area fluctuation between the flooding and drought season is more than 1,200 km^2 (Ke et al., 2017). A large amount of sediment from the Yangtze River is transported into Dongting Lake each year. The Yangtze main channel contributes more than 80% of the total sediments brought into the lake (Chen et al., 2016). After the impoundment of TGD sediment influx from the Yangtze River into the lake decreased and the the WRTs increased more than 50% from ~18 days to more than 27 days (Chen et al., 2016).

Water quality monitoring shows that TN and TP concentrations have increased over the last twenty years in Dongting Lake. TN and TP increased from ca. 1.0 mg L^{-1} and ca. 0.025 mg L^{-1} in the early 1990s CE to ca. 2.0 mg L^{-1} and ca. 0.15 mg L^{-1} at around 2010 CE (Figure 3.14). N: P ratios have declined from more than 60 in the early 1990s CE to ca. 30 in the late 1990s CE, and fluctuated at around 30 thereafter (Figure 3.14). Chl *a* was low in Dongting Lake, and fluctuated at ca. 1.5 $\mu g \cdot L^{-1}$ before 2005 CE before increasing to ca. 4.5 $\mu g \cdot L^{-1}$ in the early 2010s CE (Figure 3.14). In 2017 CE, TP and TN concentrations in the water column at the core site were 0.054 mg L^{-1} and 0.17 mg L^{-1}, respectively (measured in this study) (Table 3.1). Summer phytoplankton in Dongting Lake was dominated by bacillariophytes (diatoms), which accounted for ca. 50% of the biomass between 2011 CE and 2014 CE (Liu et al., 2017). Of the bacillariophytes, more than 80% was *Aulacoseira spp*. which is abundant in turbulent water bodies (Liu et al., 2017).

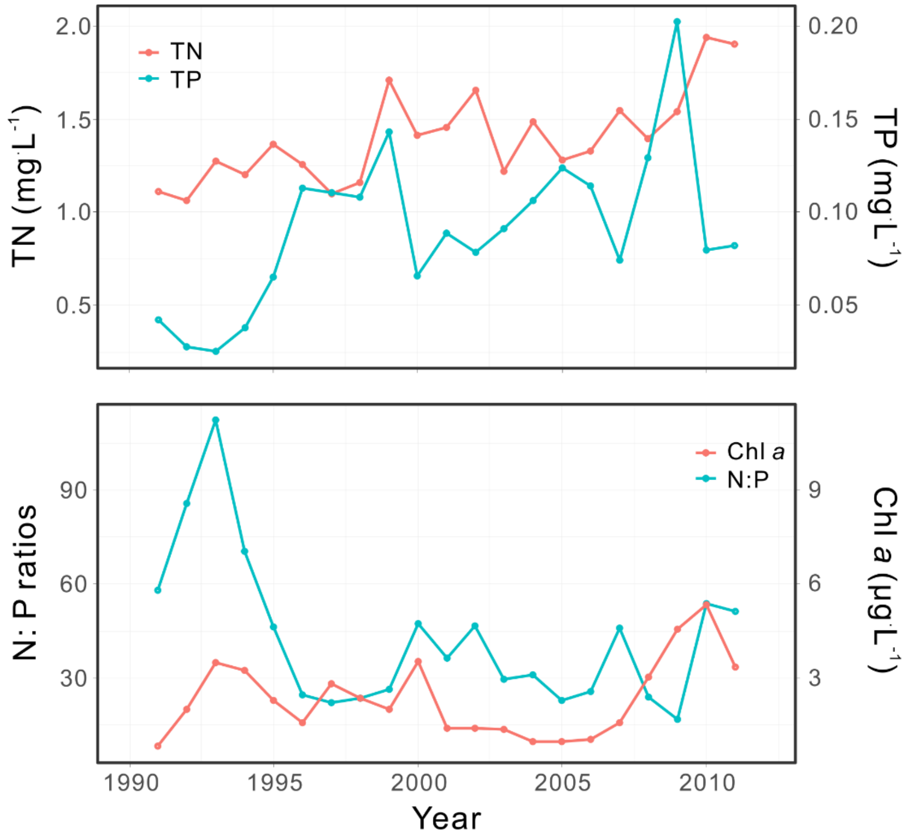

Figure 3.14 Water quality data (annual means) of Dongting Lake between 1991 CE and 2011 CE (cited from Huang et al., 2013).

3.4.2 Honghu Lake

Honghu Lake (29°38'~29°59'N, 113°11'~113°28'E), located in Jingzhou, has a water surface area of 344 km^2 and a mean water depth of 1.9 m (Wang and Dou, 1998) (Figure 3.15). It is an important Ramsar wetland in China due to its position in the East Asian-Australasian Flyway. The favourable environmental conditions of the Honghu Wetland include extensively developed aquatic vegetation, which attracts more than 130 bird, 62 fish, 6 amphibian, 12 reptile, 13 mammal, 379 zooplankton, and 280 phytoplankton species with some listed by the International Union for Conservation of Nature (IUCN) as “threatened” (Ramsar Convention, 2020).

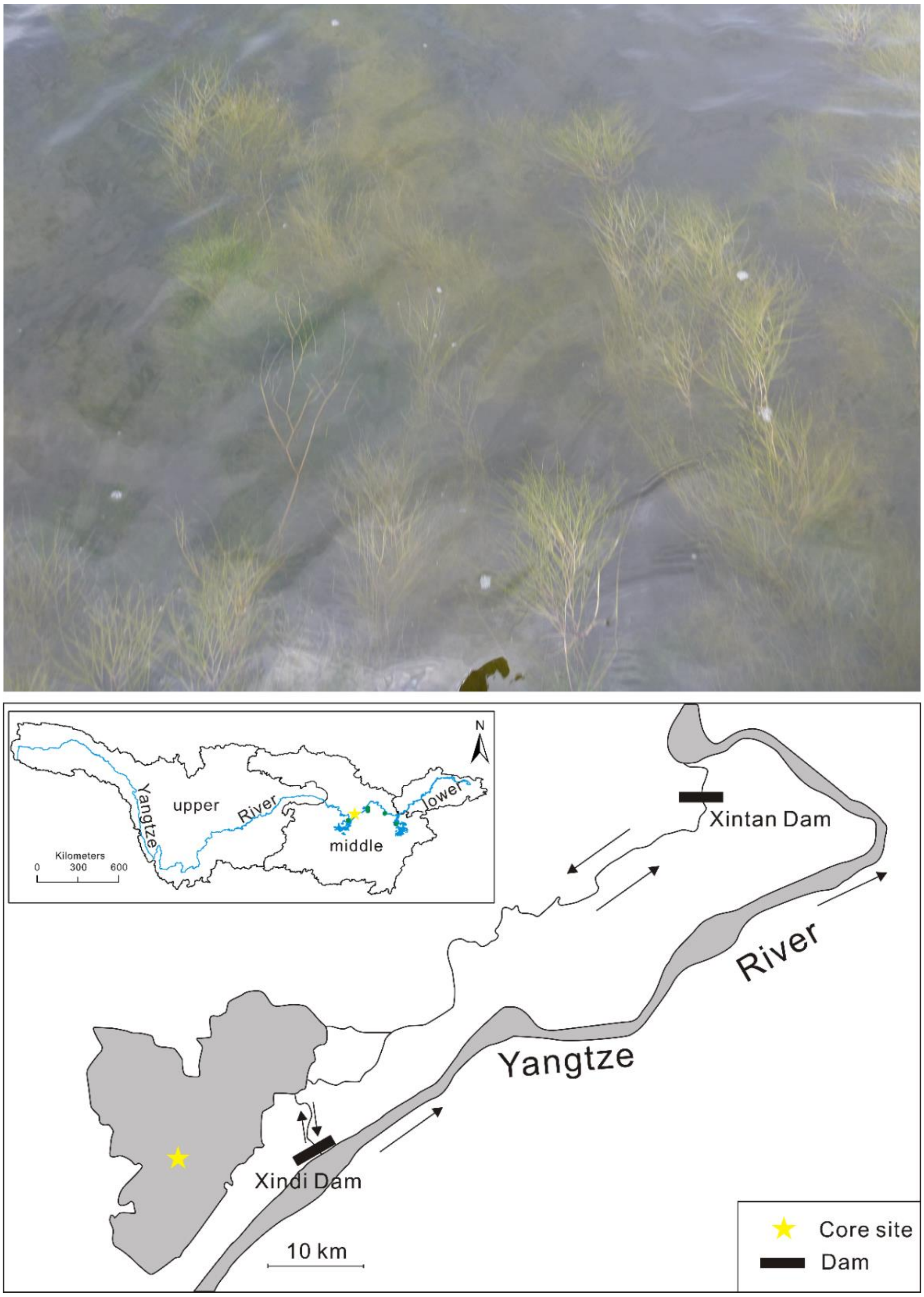

Figure 3.15 Photo of submerged macrophytes (upper) (photo by S. McGowan) and sketch map showing the hydrological setting of the Honghu Lake (the black bar indicates the local dam, the yellow star indicates the core site, the black arrows indicate flow direction).

Before the 1950s CE, Honghu Lake was an open lake, freely connected with the Yangtze River through rivers located at the east of the lake (Figure 3.15). Water flowed into Honghu Lake during flood seasons and out when water level in the Yangtze River was low through these rivers (Zhang et al., 2017). For the benefits of flood control, the natural hydrological linkages between Honghu Lake and the Yangtze River were modified by the establishment of the Xintan Dam in 1959 CE at the northeast. After the impoundment of Xidi Dam at the east in 1971 CE, hydrological connections between Honghu Lake and the Yangtze River were further reduced.

Water quality monitoring shows that TN and TP in Honghu Lake was 0.22 mg L^{-1} and 0.03 mg L^{-1} in 2000 CE, respectively (Jiang et al., 2012) (Figure 3.16). After that, TN sharply increased to ca. more than 1.4 mg L^{-1} in the middle 2000s CE and fluctuated at around 1.2 mg L^{-1} thereafter. TP increased to ca. 0.08 mg L^{-1} in around 2005 CE and fluctuated thereafter. N: P ratios increased from less than 25 in 2000 CE to 125 in 2002 CE and stabilized at ca. 45 between 2004 CE and 2010 CE (Jiang et al., 2012) (Figure 3.16). In 2017 CE, TN and TP concentration in the lake was 0.17 mg L^{-1} and 0.008 mg L^{-1}, respectively (Table 3.1). Honghu Lake is in a clear water state dominated by submerged macrophytes (Figure 3.15), with *Myriophyllum spicatum*, *Potamogeton maackianus*, *Ceratophyllum demersum* and *Hydrilla verticillata* being the dominant species (Song et al., 2016). Phytoplankton in Honghu Lake is dominated by bacillariophytes (93.72%) (Deng et al., 2010).

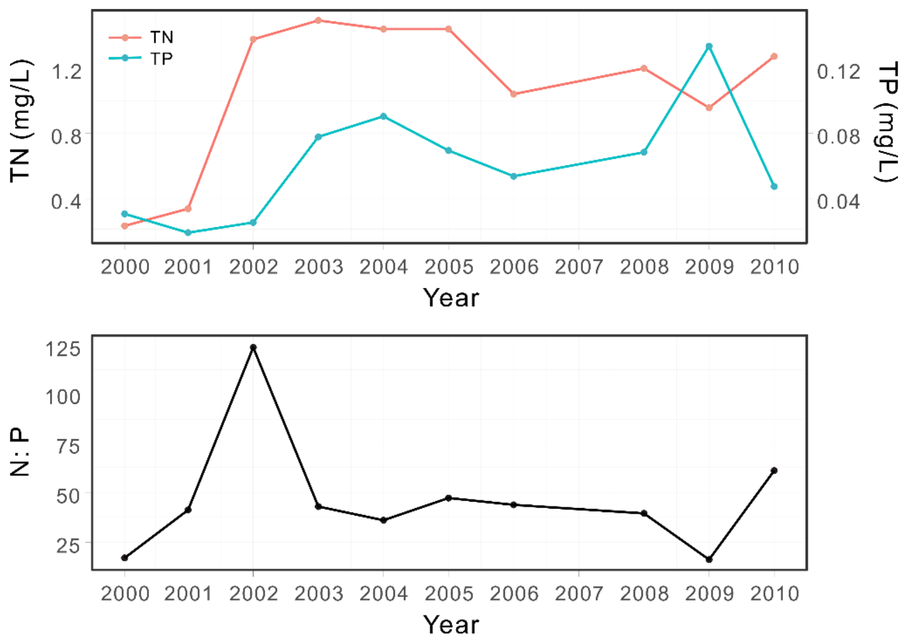

Figure 3.16 Water quality data (annual means) of Honghu Lake between 2000 CE and 2010 CE (cited from Jiang et al., 2012).

3.4.3 Futou Lake

The site description of Futou Lake has been adapted from Zeng (2016) and Zeng et al., (2018).

Futou Lake (29°55'-30°07'N, 114°09'-114°20'E) is located at the edge of Wuhan and Xianning and has a mean water surface area of 126 km^2 and a mean water depth of 2.9 m (Wang and Dou, 1998). Before 1935 CE, Futou Lake was freely connected with the Yangtze River through the Jinshui River (Figure 3.17). Water flows into Futou Lake through the Jinshui River during the flood season when water level in the Yangtze River is higher than the lake, and flows back into the Yangtze River during the dry season. In 1935 CE, a local dam named Jinshui was established at the confluence of the Jinshui River and the Yangtze River for flood control. Since then the lake has changed into a restricted drainage basin. In 1973 CE, another dam (Xinhe Dam) was impounded at the confluence of Jinshui River and Futou Lake.

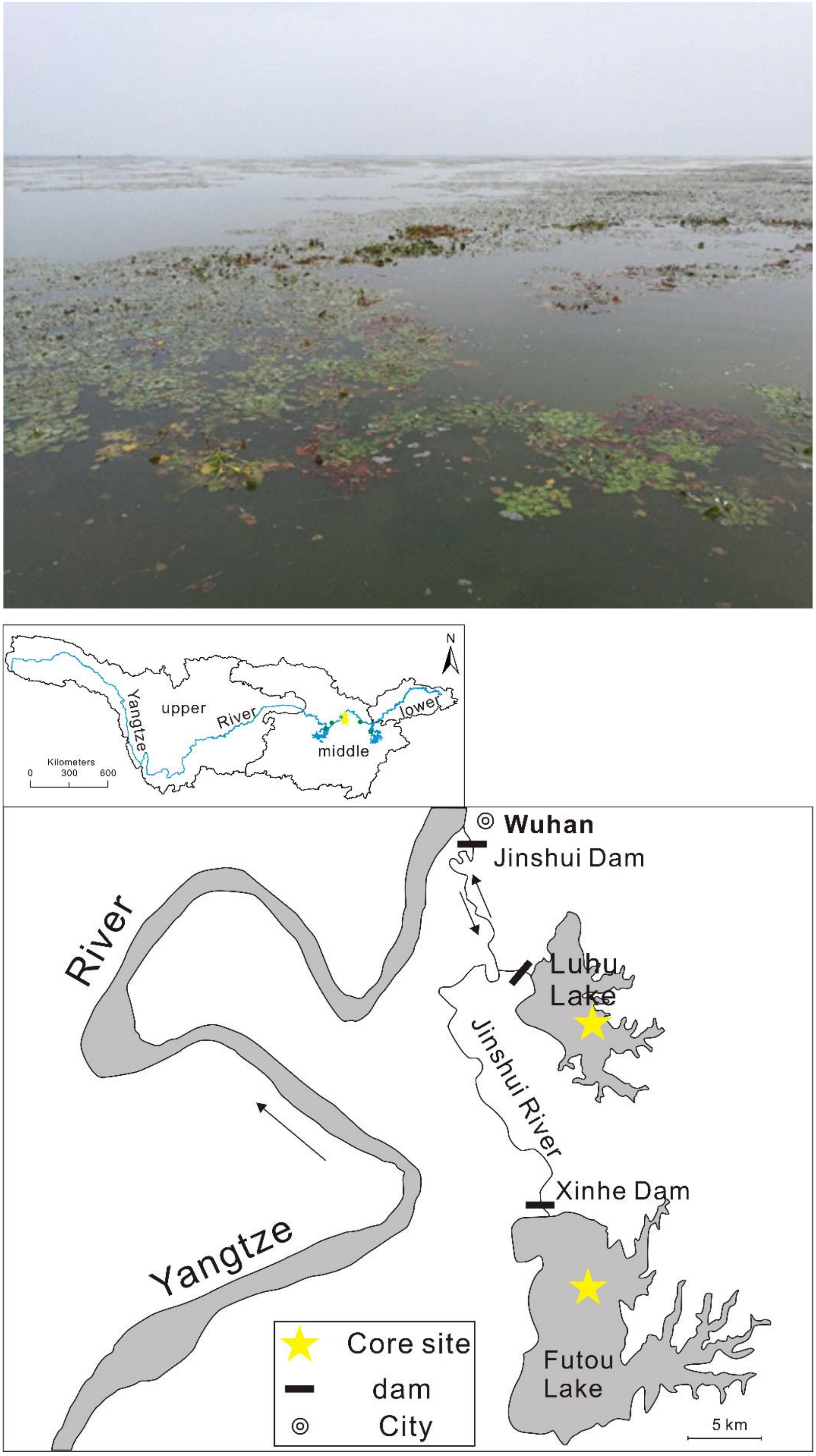

Figure 3.17 Photo of aquatic plants (*Trapa natans*) in Futou Lake (upper) (photo by J. Liang) and sketch map showing the hydrological setting of Futou and Luhu Lakes (the black bar indicates the location of the local dam, the yellow star indicates the core site, the black arrows indicate flow direction).

Observations by locals suggest that Futou Lake had abundant aquatic plants including free-floating (e.g., *Pistia stratiotes*) and submerged (e.g., *Vallisneria natans*, *Potamogeton crispus*, *Ceratophyllum demersum*) plants between the 1970s CE and the early 1990s CE (Hai Zeng, fisherman on Futou Lake, personal communication, July 30, 2017). Declines in aquatic plant abundance have been noted and *Trapa natans* is abundant in recent years (Figure 3.17). After 2000 CE, more than 70% of the water area of Futou Lake was being used as enclosure pens for aquaculture (e.g., *Ctenopharyngodon idella*, *Carassius auratus*, *Parabramis pekinensis*). Each year more than 930 metric tons of total phosphorus and 2,800 metric tons of total nitrogen were supplied to the lake to support aquaculture (Committee for Lake Records Compilation of Hubei Province, 2014). Aquaculture production in Futou Lake increased from less than 10 million Yuan (RMB) in the early 1990s CE to ca. 60 million Yuan (RMB) in 2008 CE (Committee for Lake Records Compilation of Hubei Province, 2014). Water-quality monitoring data revealed that TP in Futou Lake increased from 0.027 mg L^{-1} in the 1990s CE (Wang and Dou, 1998) to 0.04 mg L^{-1} in 2014 CE (Wu et al., 2017) and slightly decreased to 0.037 mg L^{-1} in 2017 CE. Chl *a* sharply increased from 4.27 to 23.47 μg L^{-1} between the early 2000s CE and 2014 CE (Yang et al., 2008; Wu et al., 2017), followed by a slight decrease to 20.58 μg L^{-1} in 2017 CE. Phytoplankton in Futou Lake was dominated by cyanophytes, bacillariophytes and euglenophytes in 2007 CE, which accounted for 34.1% 31.6% and 21.6%, respectively (Gong et al., 2009) (Table 3.1).

3.4.4 Luhu Lake

Luhu Lake (30°12’-30°17’N, 114°9.5’-114°15’E), the smallest of all the study lakes, is located in Wuhan. The mean water depth and water surface area of Luhu

Lake is 2.7 m and 40 km^2, respectively. Luhu Lake was freely connected with the Yangtze River before 1935 CE through the Jinshui River at the west of the catchment (Figure 3.17). Due to the impoundment of Jinshui Dam at the confluence of the Yangtze River and the Jinshui River in 1935 CE and the establishment of Luhu Dam at where Jinshui River enters Luhu Lake in 1967 CE, Luhu Lake has changed into a hydrologically restricted lake.

Due to intensive human disturbance in the catchment, Luhu is in a turbid state with high algal production (Figure 3.18). In 2017 CE, TP and TN concentrations in the water column at the core site were 0.068 mg·L^{-1} and 0.33 mg·L^{-1}, respectively. Phytoplankton in Luhu Lake are dominated by chlorophytes and cyanophytes, which make up 43.5% and 41.8% of the biomass, respectively (Rao et al., 2018).

Figure 3.18 Photo of the confluence of Luhu Lake and Jinshui River (photo by J. Liang).

3.4.5 Wanghu Lake

Wanghu Lake (29°51’-29°54’N, 115°20’-115°25’E), located in Huangshi (Figure 3.19), has a mean water surface area of 42.3 km^2 and a mean water depth of 3.7 m (Wang and Dou, 1998). The Wanghu Lake catchment is of great biological value, and harbours 46 phytoplankton, 34 zooplankton, 7 fish and 152 bird species (Hubei Wildlife Trust, 2005). Before 1965 CE, Wanghu Lake was freely connected with the Yangtze River. During periods when water levels in the Yangtze River were higher than the lake, water flowed into the lake through the Fushui River which is located at the west of Wanghu, while water flowed out of the lake and entered the Yangtze River at Fuchi which is at the confluence of the outflow and the Yangtze River during the dry season (Figure 3.19). Water level fluctuations between the flooding and dry season were about 3 m (Hubei Wildlife Trust, 2005). However, after the establishment of the Fuchi Dam at the confluence of Fuchi River and the Yangtze River in 1965 CE, the lake became hydrologically restricted.

In 2017 CE, TP and TN concentrations in the water column at the core site were 0.22 $mg \cdot L^{-1}$ and 0.44 $mg \cdot L^{-1}$, respectively, which were higher than other lakes. Wanghu Lake is in a eutrophic state and regularly suffers from HABs (Figure 3.19). Macrophytes are rarely developed in Wanghu Lake. Phytoplankton in Wanghu Lake is co-dominated by cyanobacteria, bacillariophytes and chlorophytes, which accounted for 39.67%, 23.6%, and 20.5% of the total biomass, respectively in 2004 CE (Hubei Wildlife Trust, 2004).

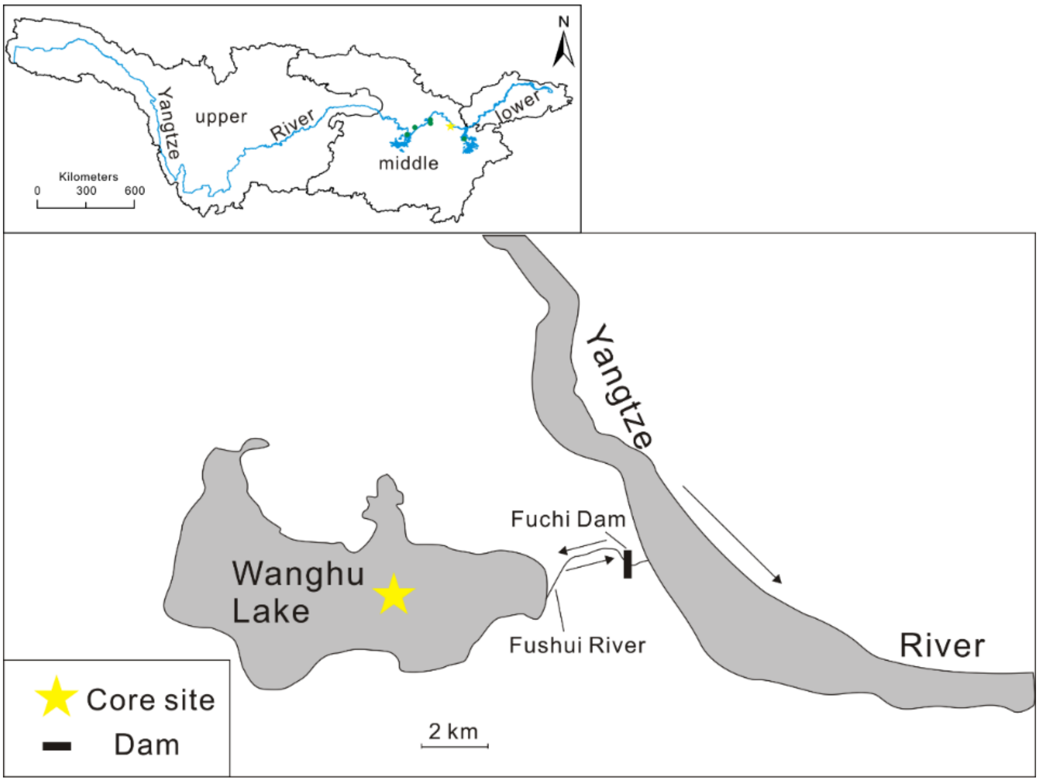

Figure 3.19 Photo of HABs (upper) (photo by author) and sketch map showing the hydrological setting of the Wanghu Lake (the black bar indicates the local dam, the yellow star indicates the core site, the black arrows indicate flow direction).

3.4.6 Poyang Lake

Poyang Lake (28°24'-29°46'E, 115°49'-116°46'E), located in the lower end of the middle reaches of the Yangtze River (Figure 3.20), is the largest freshwater lake in China by area. Poyang Lake is "pan-shaped" and receives inflowing waters from five tributaries (the Ganjiang, Fuhe, Xinjiang, Raohe and Xiushui) (Figure 3.20). The Ganjiang River, Fuhe River and Xinjiang River contribute approximately 89% of the lake's inflow and the Raohe River and Xiushui River account for the remaining 11% (Gao et al., 2014). Water flows into the Yangtze River through a narrow channel at Hukou. Poyang Lake has a complex and dynamic hydrological connection with the Yangtze River. The water exchange rate of Poyang Lake is about 30 days (Wang and Dou, 1998). Lake level fluctuates between flooding and dry seasons by more than 10 m (Harris, 2017). During the flood season (May to October) when the Yangtze water flows back into the lake, the lake water surface area is more than 4000 km^2. However, most of the lake is shallow and dries out during the dry season between November and April, with water depth ranging between more than 100 cm to less than 15 cm (Harris, 2017). The Poyang Lake catchment is important for industrial operations, agricultural activities, drinking water, biodiversity protection and the regulation of environmental functions as well as supporting cultural and recreational functions for approximately 12.4 million residents. Poyang Lake provides habitat for numerous species of plankton, molluscs, fish, birds and mammals and is a Ramsar designated site (Ramsar Convention, 2020).

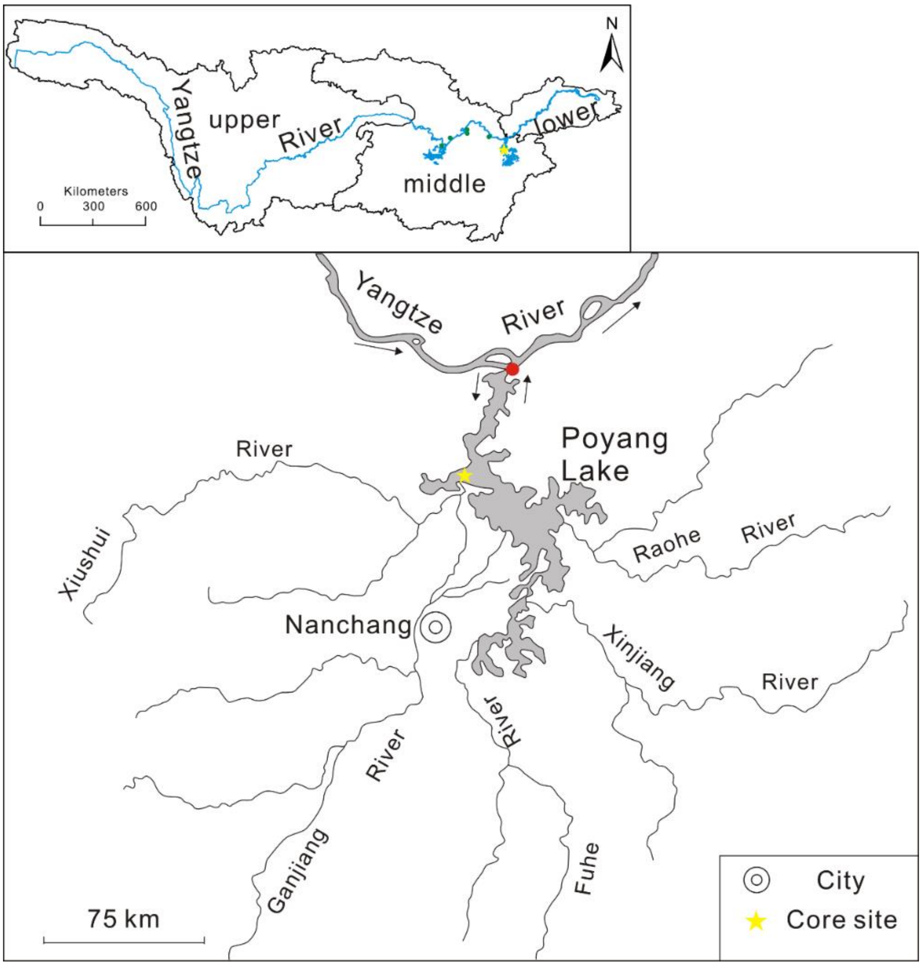

Figure 3.20 Photo of western littoral area (upper) (photo by J. Liang) and sketch map showing the hydrological setting of Poyang Lake (the yellow star indicates the core site, the black arrows indicate flow direction).

Before the 1980s CE, Poyang Lake was in an oligotrophic state. TN in Poyang Lake was 0.05 mg·L^{-1} (Wang et al., 2011) (Figure 3.21). With population growth and social-economic development in the catchment over the last several decades, the water quality of the lake has degraded and the lake has changed into a eutrophic state. Between the 1980s CE and 2006 CE, TN and TP in Poyang Lake fluctuated around ca. 1.0 mg·L^{-1} and 0.08 mg·L^{-1}, respectively. N: P ratios fluctuated between 20 and 55 in Poyang Lake between the 1980s CE and 2006 CE (Wang et al., 2011) (Figure 3.21). In 2017 CE, TP and TN concentrations in Poyang Lake at the core site were 0.03 mg·L^{-1} and 0.29 mg·L^{-1}, respectively. Bacillariophytes make up more than 50% of the summer phytoplankton biomass in Poyang Lake, and *Aulacoseira* sp. (ca. 50%) which is abundant in turbulent water bodies was the dominant bacillariophyte species in the summer (Liu et al., 2017).

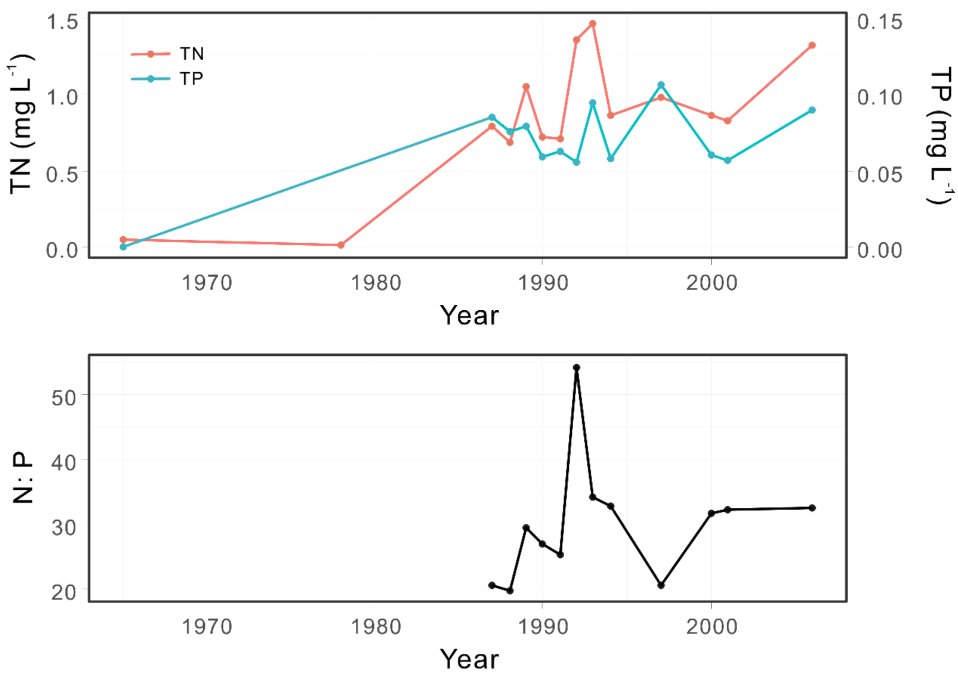

Figure 3.21 Water quality data of Poyang Lake between 1965 CE and 2006 CE (cited from Wang et al., 2011).

3.4.7 Summary of the study sites

In summary, these lakes can be divided into two hydrological categories according to their connection with the Yangtze River. Two of them (the largest lakes) are freely connected with the Yangtze River (Dongting Lake and Poyang Lake) and the other four are hydrologically restricted by local dam constructions (Honghu Lake, Futou Lake, Luhu Lake and Wanghu Lake) (Figure 3.22). The two hydrological open lakes are turbulent, rapidly flushed and have high water level fluctuations. In these two lakes diatoms are the dominant phytoplankton in summer and macrophyte abundance is at moderate level. The four lakes with local dams are characterized by different ecological features (Figure 3.22). Honghu and Futou Lakes are in a clear water state dominated by macrophytes, whereas Luhu and Wanghu Lakes are dominated by plankton including HABs in the summer, with sparse macrophytes.

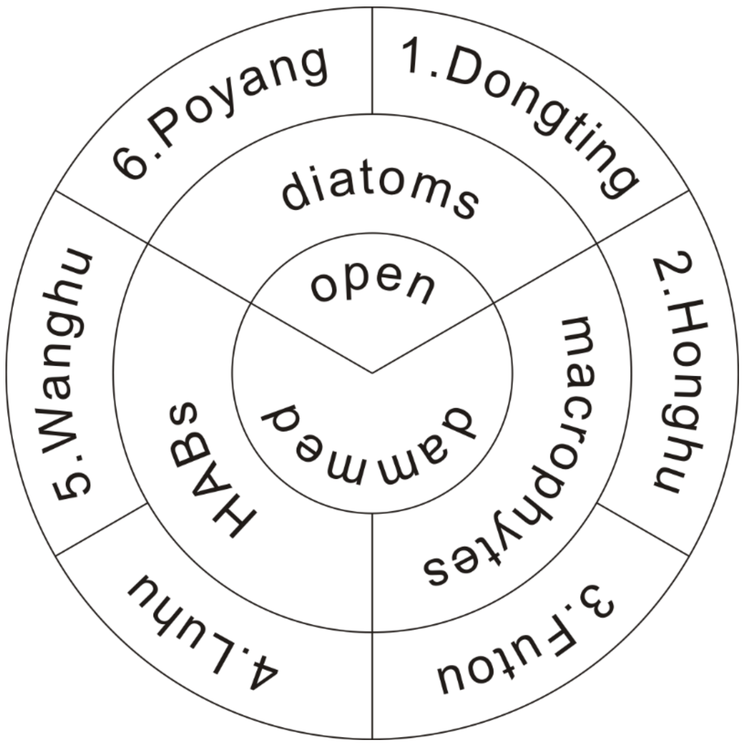

Figure 3.22 Summary of the hydrological conditions and ecological features of the study lakes. Information about phytoplankton are summarized from Table 3.1.

3.5 Research questions and hypotheses

3.5.1 Research questions

This thesis will use these hydrologically and ecologically different lakes to investigate the responses of biotic communities (algae, macrophytes) and organic matter to eutrophication and hydrology in shallow freshwater ecosystems in the Yangtze floodplain area. The aim of this thesis is to:

1. Investigate how and whether algae and macrophytes have responded to the intensification of agricultural and industrial/urban activities in the catchments and changes in hydrological connectivity in the middle Yangtze floodplain lakes (Chapter 6).

2. Explore how hydrological modification caused by local dam construction and anthropogenic disturbance have influenced light penetration and ecosystem structure in the Yangtze floodplain lakes (Chapter 7).

3. Understand long term (~ 200 years) dynamics of organic matter cycling in large river-floodplain systems undergoing hydrological modification and receiving human emitted pollutants.

3.5.2 Hypotheses

The following hypothesises will be tested in this thesis:

1. Chapter 6

- Agricultural activities will increase N loading, and urbanization and industrialization will increase P loading into the middle Yangtze lakes.
- The increase in nutrient loadings from human activities will increase algal production and HABs in these middle Yangtze floodplain lakes.

High P loading from urbanization/industrialization will result in N limitation, promoting N_2-fixing cyanobacteria.

- Connectivity with the Yangtze River will alleviate algal blooms and HABs caused by increasing nutrients due to the high water flushing rates.

2. Chapter 7

- Water level fluctuations will influence underwater light conditions in these Yangtze floodplain lakes, especially in the two large, hydrologically open lakes (Poyang and Dongting) which experience high water level fluctuations during the flooding and non-flooding seasons.
- Local dam construction will improve water clarity in lakes, by impeding the transport of suspended particles from the Yangtze main channel and stabilizing water level fluctuations.
- Anthropogenic nutrient loading from agricultural, industrial and urban development in the catchment will stimulate algal production, resulting in algae-induced turbidity.
- Improved light conditions and stable water levels due to local dam construction will stimulate the growth and development of benthic communities.
- Local dams will amplify the symptoms of eutrophication by increasing water retention times and stimulate the growth of eutrophic species, whereas free hydrological connection with the Yangtze River will alleviate the negative effects caused by nutrients.

3. Chapter 8

- Increases in productivity of algae and HABs caused by enhanced nutrient loadings from agricultural and industrial activities and urbanization in the catchments will increase δ13C in the sediments.
- The growth and development of macrophytes after local dam construction will leave a sedimentary isotopic signature similar to that of submerged macrophytes.

CHAPTER 4 MATERIALS AND METHODS

This chapter describes the process of sample collection, laboratory analysis and statistical analysis.

4.1 Sample collection

4.1.1 Sediment coring

Sediment cores were collected using a gravity corer from each individual lake between 2014 CE and 2017 CE (Table 4.1). The water-sediment interface was well maintained in all of the collected cores. The sediment cores were sectioned at 1-cm intervals in the field after sampling. Subsamples were stored in sealed bags. Subsamples for pigment analysis were stored at −20°C. Subsamples for chironomids, C and N mass and isotopes and chronology were stored at 4°C.

Table 4.1 Location of the sediment cores and the time of sampling.

Site	Latitude (N)	Longitude (E)	Core length	Water depth	Sampling date
Dongting	29°25.08′	112°53.95′	66 cm	3.8 m	July 2017
Honghu	29°49.17′	113°19.60′	87 cm	1.9 m	October, 2015
*Futou	30°03.28′	114°12.41′	87 cm	2.9 m	April, 2014
Luhu	30°14.42′	114°11.41′	101 cm	2.7 m	April, 2016
Wanghu	29°52.32′	115°18.64′	99 cm	3.6 m	May, 2016
Poyang	29°10.15′	116°04.66′	61 cm	5.1 m	October, 2015

* Collected as part of the MSc thesis of Zeng, 2016

4.1.2 Surface sediments and plants in the catchments

Samples from catchment soils, terrestrial plants and aquatic plants in the middle Yangtze floodplain were collected in July 2017 CE and analysed for C/N ratios and stable carbon and nitrogen isotopes to facilitate the interpretation of down core changes. In total, 23 aquatic plant samples, 12 catchment plant samples and 5 catchment soil samples were analysed. The 23 aquatic plant samples included 6 emergent plant samples (*Phragmites adans* × 2, *Nelumbo nucifera* × 3, *Phragmites communis* × 1), 10 floating leaved plant samples (*Eichhornia crassipes* × 4, *Trapa* spp. × 3, *Nuphar* spp. × 1, *Salvinia* spp. × 1 and floating seed × 1) and 7 submerged macrophytes (*Vallisneria natans* × 3, *Potamogeton* × 2, *Ceratophyllum demersum* × 1, *Myriophyllum verticillatum* × 1). The 12 catchment land plants included *Oryza sativa* × 3, *Zea mays* × 2, *Artemisia selengensis* × 2, *Carex* × 1, *Graminae* × 1, *Pinaceae* × 1 and two unidentified catchment plants. Five catchment soil samples were collected from paddy soils. In Honghu, Futou, Luhu, Wanghu and Poyang Lakes, one surface sediment sample was analysed from the cores collected from each lake. In Dongting Lake, 11 surface sediments were collected (Figure 4.1).

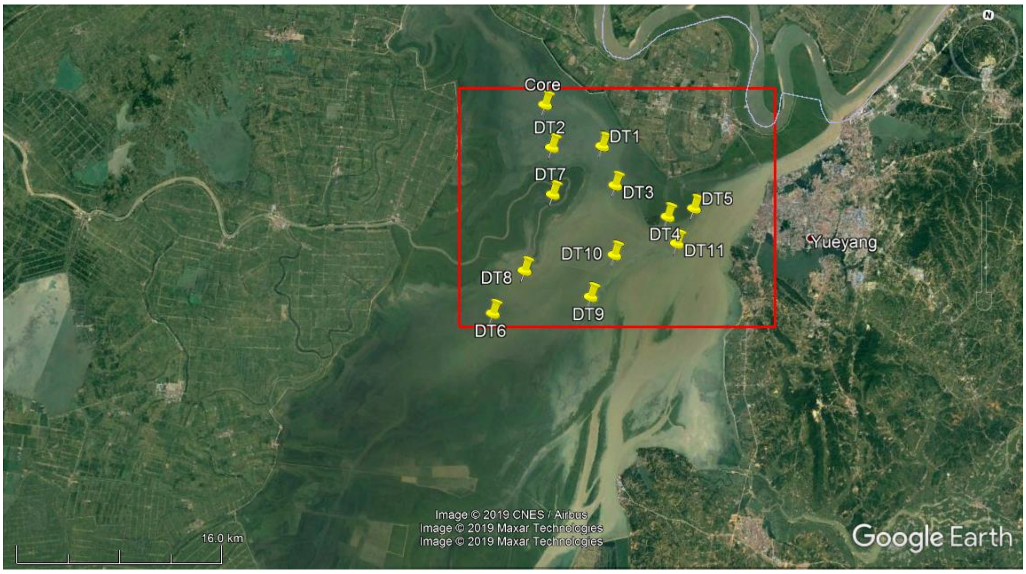

Figure 4.1 Sampling sites of surface sediment in Dongting Lake.

4.2 Laboratory analysis

4.2.1 ^{210}Pb and ^{137}Cs dating

^{210}Pb, which has a half-life of 22.26 years, is the most commonly used method for dating sediment cores spanning the last 150 years (Appleby, 2001; Chen et al., 2019). The principle underlying ^{210}Pb dating is the constant radioactive decay of ^{210}Pb, a process whereby half of the ^{210}Pb is converted to its daughter isotope every 22.26 years. (Appleby, 2001; Chen et al., 2019). ^{210}Pb detected in lake sediments (total ^{210}Pb) is composed of supported ^{210}Pb ($^{210}Pb_{supported}$) generated in-situ by the decay of ^{226}Ra in the lake, and excess ^{210}Pb ($^{210}Pb_{excess}$) derived from the atmosphere through dry and wet deposition which is produced by the decay of ^{222}Rn (Appleby, 2001). The chronology of sediment cores can be established based on the $^{210}Pb_{excess}$ activity profiles in the sediment core and the half-life of ^{210}Pb.

Under a theoretical scenario where the flux and sediment accumulation rate of $^{210}Pb_{excess}$ are constant, known as the constant flux constant sedimentation (CFCS) model, the profile of $^{210}Pb_{excess}$ from the top to the bottom of the sediment core follows an exponential curve (Krishnaswamy et al., 1971). However, the flux and the sedimentation rate of $^{210}Pb_{excess}$ may change due to various factors such as anthropogenic perturbations and climate change (Appleby, 2001; Chen et al., 2019). Therefore, different models are used to date cores deposited with variable sedimentation conditions and in different environments. For example, the constant initial concentration (CIC) model assumes that the initial ^{210}Pb concentration is constant regardless of the changes in sedimentation rate (Robbins and Edgington, 1975; Pennington et al., 1976). The constant rate of supply (CRS) model assumes that the ^{210}Pb flux to sediment is constant over time, which means the initial ^{210}Pb concentration is inversely proportional to the sedimentation rate (Appleby and Oldfield, 1978; Oldfield et al., 1978).

^{137}Cs which has a half-life of 30.17 years is an artificial radioactive isotope of caesium which derives solely from nuclear fission (Krishnaswamy et al., 1971; Ritchie and McHenry, 1990). Since 1952 ± 2 CE, the beginning of nuclear weapons testing worldwide emitted large quantities of ^{137}Cs into the atmosphere. After 1963 CE, worldwide nuclear weapon testing sharply decreased with the introduction of the Treaty Banning Nuclear Weapon Tests in the Atmosphere, in Outer Space and Under Water (Partial Test Ban Treaty, PTBT), which has left a distinct peak at 1963 CE in lake sediments in most geographic areas (Ritchie et al., 1973). Therefore, the 1963 CE ^{137}Cs peak is widely used as a single event chronological marker to date sediment cores (Krishnaswamy et al., 1971; Ritchie and McHenry, 1990; Chen et al., 2019). In 1986 CE, the accident at the Chernobyl Nuclear Power Plant in Ukraine released considerable amounts of ^{137}Cs into the atmosphere (Ritchie and McHenry, 1990; Chen et al., 2019). The 1986 CE ^{137}Cs peak is used as another chronological marker, in particular to verify ^{210}Pb dating of sediment cores from European lakes such as those from Scandinavia and the Baltic region. This peak is less distinct in sediment cores from South and East Asia (Chen et al., 2019).

In this study, the results of $^{210}Pb_{excess}$ in the sediment cores from Honghu, Luhu, Wanghu and Poyang have been published in Chen et al., (2019). $^{210}Pb_{excess}$ in the sediment core from Futou Lake have been published in the thesis of Zeng (2016). For Dongting Lake sediment core, ^{210}Pb and ^{137}Cs were analysed at 2-cm intervals in the State Key Laboratory of Lake Science and Environment, Nanjing

Institute of Geography and Limnology with a gamma spectrometer (Ortec HPGe GWL). Chronologies of the sediment cores were established using the CRS model which applies to circumstances with variable initial concentrations and sedimentation rates of $^{210}Pb_{excess}$ (Appleby, 2001). For sediment cores which extend beyond the ^{210}Pb dating limit, dates before ~ 1850 CE were linearly extrapolated with the lower few samples with measurable $^{210}Pb_{excess}$.

4.2.2 Sedimentary chlorophyll and carotenoid pigments

4.2.2.1 General knowledge about pigments

Sedimentary pigments of photosynthetic organisms including chlorophylls, carotenoids, photoprotective compounds and their derivatives are widely distributed in lakes (Leavitt and Hodgson, 2001; McGowan et al., 2007; Stevenson et al., 2015; Taranu et al., 2015). Sedimentary pigments are widely used in palaeolimnology due to their wide distribution and taxonomic specificity, which means they are not only useful in providing information on primary production but also have advantages in studying algal or bacterial community changes (Leavitt and Hodgson, 2001; McGowan, 2007).

Generally, the basic chemical structure of chlorophylls (Chls) is composed of a phytol chain and a magnesium (Mg) co-ordinated chlorin-ring which is consists of four pyrrole units and an isocyclin-ring (Figure 4.2a) (McGowan, 2007). The degradation of chlorophylls under oxidative conditions generates a series of derivatives. For instance, loss of Mg leads to the generation of pheophytins; loss of the phytol chain transforms chlorophylls into chlorophyllide; pheophorbides are generated when both the Mg and the phytol chain are degraded. The chemical structure of carotenoids includes a chromophore chain composed of eight isoprene (C_5H_8) units and the functional groups on the two ends which defines the differences among different carotenoids (McGowan, 2007) (Figure 4.2b). For example, in *β*-carotene the groups on both ends of the chromophore chain are beta-rings. In *α*-carotene the functional groups on the two ends of the chromophore chain are the alpha-ring and beta-ring, respectively. The chemical structure of scytonemin, one kind of UVR-absorbing compound, includes two identical condensation products of tryptophanyl- and tyrosyl-derived subunits which is linked by a carbon-carbon bond (Figure 4.2c).

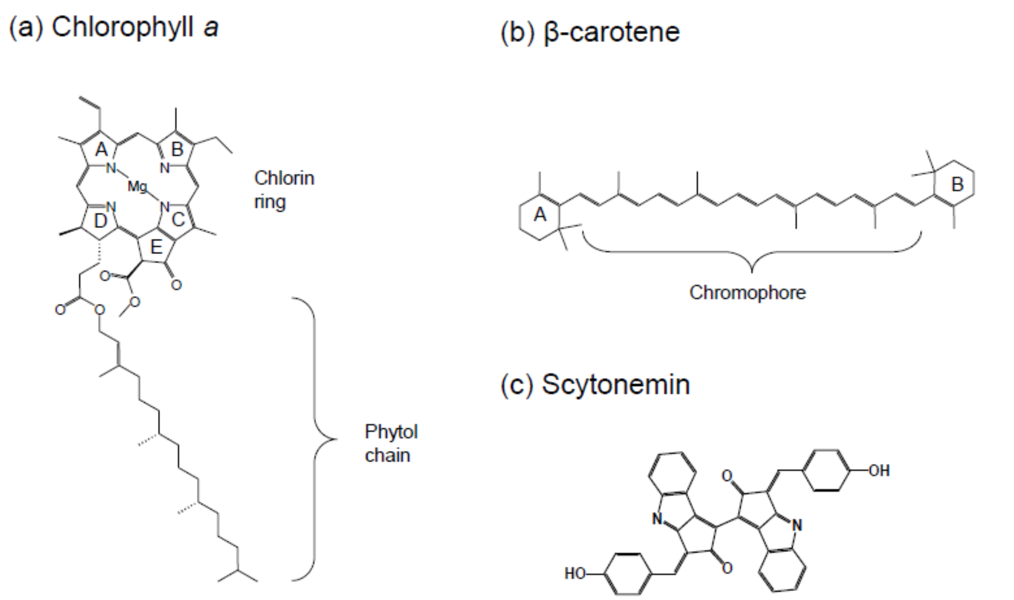

Figure 4.2 Chemical structures of Chl *a* (a), *β*-carotene (b) and scytonemin (c) (from McGowan, 2007).

Many pigments are taxonomically specific to the photosynthetic organisms they originate from (Leavitt and Hodgson, 2001). Alloxanthin is a unique pigment biomarker generated by cryptophytes. Canthaxanthin indicates colonial cyanobacteria, but is also found in herbivore tissues (e.g., crustacean zooplankton). Aphanizophyll is an indicator of filamentous N_2-fixing cyanobacteria and zeaxanthin is a general indicator of cyanobacteria. Diatoxanthin is the proxy pigment for diatoms (bacillariophytes), but can indicate dinophytes and chrysophytes as well. Lutein, Chl *b* and its derivatives (pheophytin *b*, pheophytin *b*') can indicate chlorophytes, euglenophytes and plantae. The UVR-absorbing compound is produced mainly by cyanobacteria as a photo-protectant from UVR damage. But some pigments such as Chl *a*, Chl *a* derivatives (pheophytin *a*, phaeophorbide *a*, pyropheophytin *a*) and *β*-carotene are found in all algal groups, cyanobacteria, macrophytes and higher plants (Table 4.2) (Leavitt and Hodgson, 2001; McGowan et al., 2007).

Table 4.2 Affinity and estimated stability of pigments detected in this study (cited from Leavitt and Hodgson, 2001).

Pigment	Affinity	Stability
alloxanthin	cryptophytes	1
diatoxanthin	bacillariophytes, dinophytes, chrysophytes	2
canthaxanthin	colonial cyanobacteria, herbivore tissues	1
aphanizophyll	N_2-fixing cyanobacteria	2
lutein	chlorophytes, euglenophytes, plantae	1
zeaxanthin	cyanobacteria	1
β-carotene	plantae, algae, some phototrophic bacteria	1
chlorophyll *a*	plantae, algae	3
chlorophyll *b*	chlorophytes, euglenophytes, plantae	2
pheophytin *a*	Chl *a* derivative	1
pheophytin *b*	Chl *b* derivative	2
[1]pheophytin *b'*	Chl *b* derivative	
pheophorbide *a*	Chl *a* derivative	3
pyropheophytin *a*	derivatives of *a*-phorbins	2
UVR-absorbing compound	Photo-protective cyanobacteria	-

[1] not a recognised pigment, a derivate of Chl *b*.

Although widely used in palaeolimnology and palaeoecology as proxies of past primary production and algal community composition, the pigments preserved in sediments do not necessarily reflect the original amount generated by the photosynthetic organisms in lakes (Leavitt and Hodgson, 2001; McGowan et al., 2007). Pigments are decomposed with the influence of factors such as oxygen, heat and light (Leavitt, 1993). During the sinking period, pigments may be chemically and microbially oxidized or be grazed by invertebrates (Leavitt and Hodgson, 2001). More than 95% of pigments are degraded in the water column during sinking (Figure 4.3) (Leavitt and Hodgson, 2001; McGowan, 2007). Therefore, pigments preserved in lake sediments are highly dependent on lake morphology such as water depth which influences the length of sinking period, light penetration and oxygen content (Leavitt and Hodgson, 2001). After being buried, pigments may undergo further degradation. Although pigment degradation during sedimentation is lower compared to that during sinking, it may be influenced by conditions at the sediment-water interface (Leavitt and Hodgson, 2001; McGowan et al., 2007).

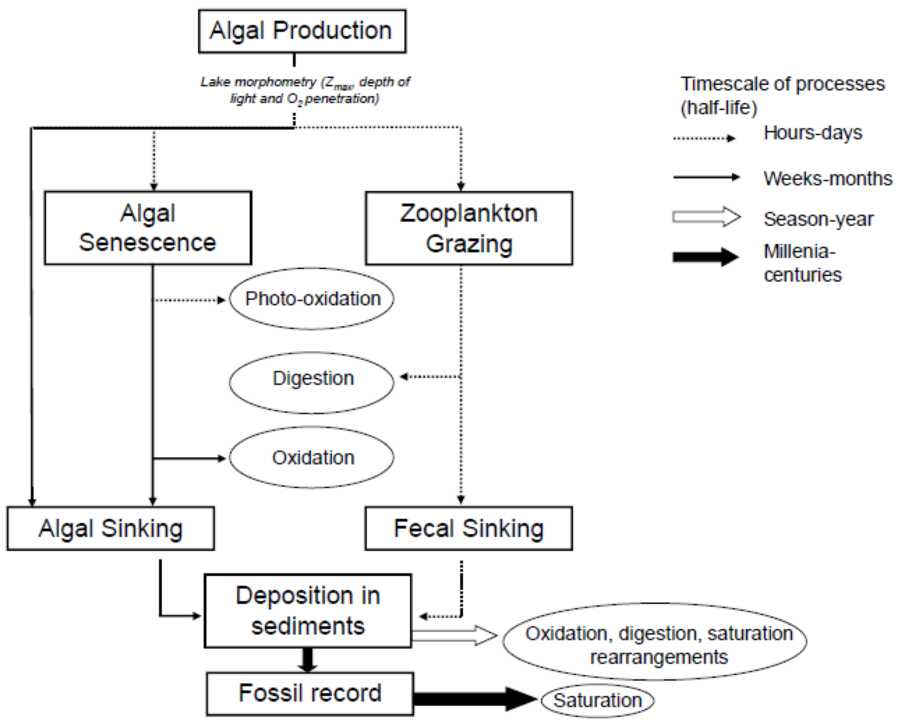

Figure 4.3 Sketch showing the pathways and rate of pigment degradation, sinking and sedimentation (from McGowan (2007)).

4.2.2.2 Application of pigments in palaeolimnology

Eutrophication, caused by excessive nutrient loading, often results in increases in algal production (Schindler et al., 2008; Conley et al., 2009; Smith and Schindler, 2009). Chlorophyll and carotenoid pigments have been widely used in palaeolimnology and palaeoecology to investigate changes in algal production and community change during eutrophication (Leavitt and Hodgson, 2001; McGowan et al., 2007). For example, sedimentary pigments from cyanobacteria (myxoxanthophyll) recorded the disproportional increases in cyanobacteria relative to other phytoplankton in lakes in the north temperate-subarctic regions associated with nutrient enrichment, along with other factors include temperature and max depth (Taranu et al., 2015). Increasing nutrient loading from point sources in the catchments was the main predictor of the increase in sedimentary pigments (e.g., canthaxanthin, β-carotene) in lowland lakes (< 100 m. a. s. l.) of the English Lake district (Moorhouse et al., 2018). In combination with hydrological modification, eutrophication in Dongting Lake (middle Yangtze floodplain) has resulted in the increases in algal production as estimated by the increase in sedimentary pigments such as alloxanthin, diatoxanthin, canthaxanthin, Chl *a* and β-carotene (Chen et al., 2016). In shallow freshwater ecosystems, eutrophication often leads to a shift from the macrophyte-dominated clear water state to the algal dominated turbid state (Scheffer et al., 1993; Scheffer et al., 1997; Dong et al., 2016). By using sedimentary pigments, McGowan et al. (2005) proposed that the shifts from clear to turbid water state in two Danish lakes were accompanied by a shift in algae habitat change from benthic to pelagic production with no increases in total algal production.

Apart from being used to investigate the consequences of eutrophication caused by direct nutrient inputs, sedimentary pigments have been used to study the influence of hydrology on primary production in floodplain lakes (McGowan et al., 2011; Chen et al., 2016). In floodplain lakes in the Peace-Athabasca Delta changes in sedimentary pigments were found to correspond to hydrological conditions (McGowan et al., 2011). Flooding which dilutes nutrient concentration and decreases the abundance of macrophytes (which provide habitat for algae) leads to lower algal production, but algal production increase during periods of reduced flood frequency (McGowan et al., 2011). In Dongting Lake in the Yangtze floodplain, sedimentary pigments revealed the increase in algal production (higher sedimentary pigment concentrations) after the construction of the TGD which prolonged the WRT and decreased the water exchange ratios in the lake (Chen et al., 2016).

4.2.2.3 Routines and principle of pigment analysis using HPLC

Chlorophyll and carotenoid pigments in this study were analysed using an Agilent 1200 series high performance liquid chromatography (HPLC) separation module with quaternary pump, autosampler, ODS Hypersil column (250 × 4.6 mm; 5 μm particle size) and photodiode array (PDA) detector. The analysis of sedimentary pigments using HPLC includes 3 steps: extraction pigments from sediments; separation of pigments using HPLC; pigment identification and quantification (Leavitt and Hodgson, 2001).

Extraction pigments from sediments - Pigments in the sediments are usually extracted using acetone based solvents. Freeze-dried sedimentary samples are weighted and soaked in extraction solvent at −4 ºC under low light condition. After 12h, the samples are filtered and dried under N_2.

Separation of pigments using HPLC - After being extracted and dried, pigments are dissolved in injection solvent and then injected into the HPLC for separation. The principal of pigment separation in the HPLC is "like dissolves like" (Leavitt and Hodgson, 2001). In the HPLC, pigments are carried through a column of packing material consisting of small particles (the stationary phase) which are non-polar by a stream of solvents (the mobile phase) under pressure (>2,000 kPa). In reversed-phase separations, the initial solvent passing through the column is polar (i.e., more similar to water) and by changing the composition of the solvent the polarity gradually decreases with time to end the run with a non-polar solvent mix. Therefore, pigments with higher polarity (e.g., fucoxanthin) which have higher affinity to the mobile phase than the packing material are separated and eluted earlier, followed by less polar pigments (e.g., β-carotene) as the polarity of the solvent declines.

Pigment identification and quantification - After passing through the separation column the eluent is scanned with a PDA detector which scans at multiple wavelengths to produce absorbance spectra of the eluting pigments. A chromatogram may be produced by scanning the eluent at a single wavelength of maximal pigment absorbance to indicate absorbance peaks through time. Individual pigment can be identified by comparing the retention time on the chromatogram under defined separation conditions with known commercial pigment standards separated under the same conditions. The quantification of pigment concentrations is based on the Beer-Lambert law. Known quantities of each pigment commercial standard are converted to the peak areas to produce a calibration curve. Then, the quantity of pigments in the sediment samples are calculated by the established calibration curve and the peak area of pigments, in combination with the amount of sediments and injection solvent used.

4.2.2.4 Pigment analysis procedure in this study

Sedimentary pigments were analysed at the School of Geography in the University of Nottingham. Pigments in the Futou sediment core was analysed by Zeng (2016) as part of an MSc study using the same methods. For sediment cores from Dongting, Honghu, Luhu, Wanghu and Poyang Lakes, pigments were analysed at 1-cm intervals. Firstly, freeze-dried sediments were weighed into vials for extraction. As pigment concentrations were low, ~ 0.2 g dry sediment were used in the top 20 cm; ~ 1.0 g dry sediment were used below 20 cm in this study. Then 5 ml extraction solvent (acetone: methanol: deionised water 80: 15: 5) was added into the vials to extract the pigments. During extraction, the vials were kept in freezer at −4°C for 12 hours. After that, the samples were filtered through a 0.22 μm PTFE syringe filter, followed by drying down under N_2 gas. Subsequently, the samples were dissolved in injection solvent, a mixture of acetone (70%), ion-pairing reagent (25%) and methanol (5%). Samples were transferred into HPLC vials and set up for running in the HPLC. In this study, the solvent streams (the mobile phase) passing through the separation column were a modified version of Chen et al. (2001), where the composition of Solvent A (80% methanol: 20% 0.5 M ammonium acetate), Solvent B (90% acetonitrile: 10% de-ionised water) and Solvent C (100% HPLC-grade ethyl acetate) are changed with time over a 52 minute sequence (Table 4.3). After separation, pigments were identified and the concentrations were calibrated with that of authentic standards obtained from DHI Water and Environment, Denmark with the aid of the absorbance spectrum generated by the PDA detector.

Concentrations of sediment pigments were calculated based on the Beer-Lambert law with the area of pigment peaks, TOC and the amount of injection solvent used. Sedimentary pigments are expressed in n moles pigments g^{-1} total organic carbon (noml g^{-1} TOC) to eliminate the difference in pigment molecular weights and the dilution by minerogenic materials (see section 4.2.4 for details of TOC analysis) (McGowan, 2013).

Table 4.3 HPLC separation conditions for pigment analysis based on a modified version of Chen et al. (2001).

Time (mins)	% Solvent A	% Solvent B	% Solvent C	Flow (ml min^{-1})
0	100	0	0	1
4	0	100	0	1
38	0	25	75	1
39	0	25	75	1
43	100	0	0	1
52	100	0	0	1

4.2.3 Chironomids

4.2.3.1 Chironomids as a proxy in palaeolimnology

Chironomids, also known as “non-biting midges”, are one kind of two-winged flies that feed on non-blood materials such as pollen, honeydew or nectar (Armitage, 1997). In total, there are more than 15,000 chironomid species across the world, and about one third of them have been described (Cranston, 1995). Chironomids are widely distributed in almost all aquatic biotopes (Brooks et al., 2007). Chironomid head capsules are well preserved in lake sediments, and normally, chironomid taxonomy and identification of these remains is based on the shape of the head capsules, mandibles and ventromental plates. Chironomids have been widely used in palaeolimnology due to their wide distribution, environmental sensitivity and ease of identification (Brooks et al., 2007).

Chironomids are sensitive to various environmental factors such as temperature, pH, substrate morphology, water depth, food and oxygen availability, and salinity (Brodersen and Quinlan, 2006) (Figure 4.4). Temperature is regarded as the main factor controlling the abundance and distribution of chironomids worldwide (Brooks et al., 2007). Directly, temperature may govern the birth, hatch and growth of chironomids (Mackey, 1977; Pinder, 1986; Armitage, 1997). Besides, the effects of temperature may also be indirect by mediating the thermal distribution in the lake, or through catchment process and the resulted variation of limnological conditions such as water clarity, food and oxygen availability (Eggermont and Heiri, 2012) (Figure 4.4). Chironomid-temperature transfer functions have been established to reconstruct past temperature in Europe (Oliver et al., 2011), Canada (Walker et al., 1991) and the Tibetan Plateau (Zhang et al., 2017).

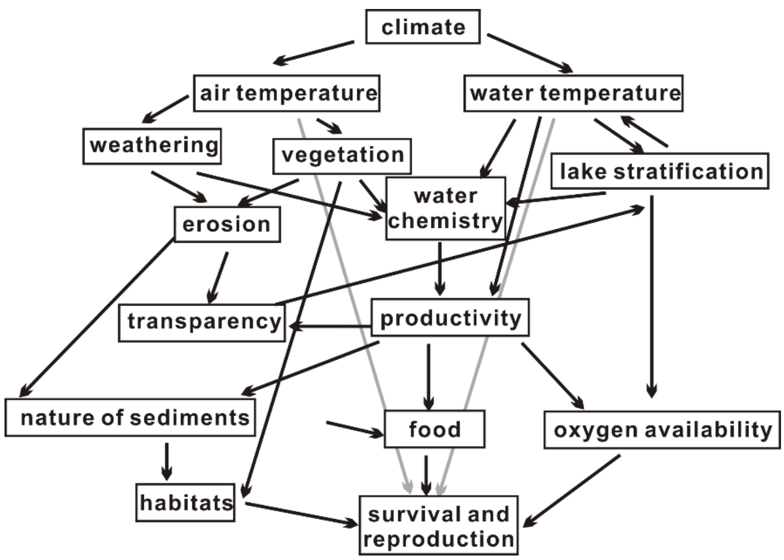

Figure 4.4 Sketch map showing the relationships between chironomids and environmental factors (grey line indicates indirect effects and black line indicates direct effects) (modified from Eggermont and Heiri, 2012).

Water depth also plays an important role in regulating the distribution and community composition of chironomids (Little and Smol, 2001; Engels and Cwynar, 2011). Generally, the diversity of the chironomid community gradually decreases with water depth (Brooks et al., 2007). However, water depth does not shape the chironomid community directly, but by regulating conditions such as oxygen availability, macrophyte growth, stratification and food availability (Engels and Cwynar, 2011). For instance, *Chironomus* and *Tanytarsus* which possess haemoglobin have a high tolerance of depleted oxygen conditions in deep waters, whereas Orthocladiinae are widely distributed in littoral areas where oxygen is abundant (Little and Smol, 2001). Moreover, the littoral areas are often rich in macrophytes (Little and Smol, 2001) and so species such as *Glyptotendipes*, *Polypedilum* and *Dictrotendipes* which inhabit or feed on macrophytes are more abundant in littoral areas (Landgon et al., 2010; Cao et al., 2014).

Food sources of chironomids mainly include microorganisms, algae, detritus of aquatic plants and invertebrates (Armitage, 1997). Food quality and quantity are important for the growth and distribution of chironomids (Ward and Cummins, 1979). For example, waterbodies with high algal productivity have high food availability, hence are more favourable for Chironomini and Tanpodinae. In contrast, Orthocladiinae and *Tanytarsini* which have low food requirements are widely distributed in lakes with low productivity (Armitage, 1997).

Substrates may influence chironomid community composition as well (Pinder, 1980). For example, Diamesinae and Orthocladiinae have a preference for solid rocky substrates (Thienemann, 1954). *Chironomus plumosus*-type and *Procladius* are abundant in soft substrates which are rich in humic materials

(McGarrigle, 1980; Francis and Kane, 1995). Substrates formed by fine particles such as silt and sand are favourable for Chironomiane (Maitland, 1979; Pinder, 1980).

In shallow lakes, the growth of macrophytes may influence chironomid community composition (Brodersen et al., 2001; Langdon et al., 2010; Cao et al., 2014). First, macrophytes may provide refuges for chironomids, protecting them from predators (Taniguchi et al., 2003). Second, periphyton such as bacteria and algae attached to macrophytes serve as important food sources for chironomids (Papas, 2007). Third, macrophytes can modify the light and nutrient conditions of freshwater lakes. Certain species of submerged macrophytes (e.g., *Potamogeton* spp.) are important hosts for periphyton and so *Cricotopus* is widely distributed in waterbodies with a high abundance of *Potamogeton* spp. (Brodersen et al., 2001).

Nutrients are another important factor regulating the distribution and abundance of the chironomid community (Zhang et al., 2006; Brooks et al., 2007). Based on the dominant chironomid species, Thienemann (1918, 1921) classified lakes into oligotrophic *Tanytarsus* lakes and eutrophic *Chironomus* lakes. Nutrients may trigger aquatic stable state transitions between algal dominated clear water and macrophyte-related clear water states, which may influence the food sources and habitat for chironomids (Scheffer et al., 1993; Scheffer et al., 2001). Moreover, phytoplankton blooms caused by increasing nutrients may result in oxygen depletion in the bottom of lakes (Downing et al., 2001; McCarthy et al., 2009).

4.2.3.2 Chironomid preparation and analyses in this study

Chironomid samples were prepared and analysed following the methods of Brooks et al., (2007). Chironomids in the Futou sediment core was analysed by Zeng (2016) as part of an MSc study using the same methods. According to previous studies in the Yangtze region, the concentration of chironomid head capsules in lake sediments is low (Cao et al., 2014), so ca. 10 g of wet sediment was used for each sample. After weighing, the sediments were transferred into beakers and deflocculated using 10% potassium hydroxide (KOH) in a 75 °C water bath for about 15 minutes. Then, sediments were gently washed through 212 μm and 90 μm sieves with water with the remains transferred into a sorting tray. Chironomid head capsules were picked out individually using fine forceps under a dissecting microscope. Afterwards, the head capsules were directly placed onto cover slips and mounted using both Euparal and Hydromatrix. For those mounted using Euparal, the cover slips were left over-night (12 hours) for air drying before being mounted. For those mounted by Hydromatrix, the head capsules were mounted immediately. Slides are placed horizontally for drying after mounting. The chironomid head capsules were identified using a microscope at ×100/×400 magnification. Chironomid taxonomy mainly followed Wiederholm (1983), Oliver and Roussel (1983); Rieradevall and Brooks (2001) and Brooks et al. (2007). At least 50 head capsules were picked out from each sample to make the results and interpretations statistically robust.

4.2.4 Carbon and nitrogen mass and isotopes

Organic matter in lake sediments mainly comes from allochthonous (terrestrial organic matter from the catchments) or autochthonous (e.g., algae, macrophytes) sources. Quantifying and identifying the sources of organic matter is important in palaeolimnology and palaeoclimate studies. Carbon and nitrogen content and their stable isotopes can provide fruitful information about the amount and source of organic matter in lake sediments (Meyers and Teranes, 2001; Leng et al., 2006).

4.2.4.1 Total organic matter and C/N ratios

Identifying the origins of organic matter (allochthonous or autochthonous) in lake sediments can provide information about limnological and environmental conditions including, by inference, climate in the past. Total organic carbon (TOC) which is the amount of organic carbon in the sediments provides information about the production of organic matter and subsequent degradation processes (Meyers and Teranes, 2001). The relative quantities of TOC to total nitrogen (TN) (C/N atomic ratios), which can roughly distinguish algae from higher plants, is widely used in palaeolimnology and palaeoclimate studies to distinguish whether organic matter predominantly derives from aquatic relative to land sources (Meyers and Teranes, 2001) (Figure 4.5). Algae which have a relatively high protein content are characterized by a low C/N ratios (4 – 10), whereas vascular plants, which are rich in cellulose, have high C/N ratios (> 20). C/N ratios between 10 and 20 indicate a mixture of organic matter from algae and vascular land plants, and is common in most lakes (Meyers and Teaners, 2001). Hence, an increase in C/N ratios usually indicates an increase in the relative contribution of terrestrial organic matter, whereas lower C/N ratios are usually interpreted as increased contributions of algae to organic matter in lake sediments (Kaushal and Binford, 1999). In Windermere, an increase in C/N ratios between the 1870s CE and 1890 CE was related to increased influxes of terrestrial organic matter due to urbanization and tourism development

(McGowan et al., 2012). The decrease in C/N ratios since the 1890 CE was attributed to the contribution of organic matter from algae with eutrophication (McGowan et al., 2012). In Lake Pleasant, Massachusetts, the increase in C/N ratios at around 1780 CE was attributed to the increasing loading of terrestrial organic matter after deforestation (Kaushal and Binford, 1999). In upland lakes from north-west Ireland, the increase in algal production after tree planting resulted in decreases in sedimentary C/N ratios (Stevenson et al., 2015).

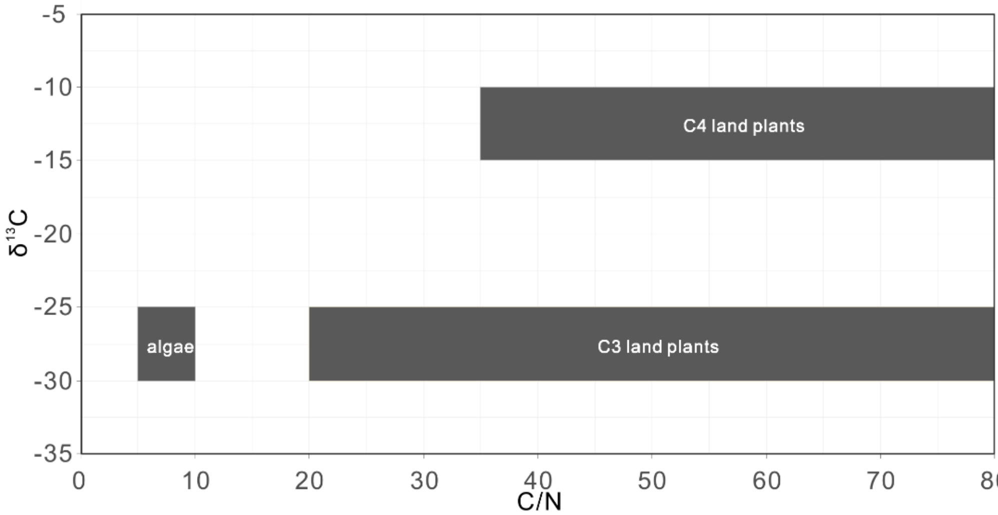

Figure 4.5 Characteristics of C/N ratios and $\delta^{13}C$ of organic matter derived from lacustrine algae, C_3 and C_4 land plants use CO_2 as the source of carbon during photosynthesis (modified from Meyers and Teranes, 2001).

Importantly, the selective degradation of organic matter during sedimentation and early diagenesis may modify the C/N ratios (Meyers and Teranes, 2001). A study based on Nylandssjön Lake in Sweden revealed that ~ 20% of the carbon and ~ 30% of the nitrogen were lost within the first five years after deposition, and the lesser loss of carbon relative to nitrogen caused an increase in C/N ratios (Gälman et al., 2008). However, in most cases the effects of partial degradation on C/N ratios are not large enough to offset the significant C/N ratios differences between algae and vascular land plants, with most of the loss of carbon and nitrogen occurring within five years of deposition, which makes C/N ratios a solid proxy (Meyers, 1997).

4.2.4.2 Carbon isotopes

The difference in the ratio of ^{13}C to ^{12}C isotopes between organic matter and standards (Pee Dee Belemnite (PDB)) is known as $\delta^{13}C$ and is a useful proxy recording the history of carbon cycling in the lake and its catchment (Leng et al., 2006). $\delta^{13}C$ can provide information on within-lake processes such as the way organisms photosynthesize and lake productivity as well as the source of organic matter, catchment land use changes and local/regional climate change (Meyers and Teranes, 2001; Leng et al., 2006) (Table 4.4). In general, organic matter deposited in a lake has two potential sources: allochthonous organic matter from the catchment and autochthonous production within the lake. Photosynthetic organisms in the catchment and within the lake use different sources of carbon (respectively, atmospheric carbon dioxide (CO_2) or aqueous CO_2 and bicarbonate (HCO_3^-)) and have different pathways for photosynthesis. The initial isotopic characteristics of carbon from each source is different, and the different photosynthesis pathways have various fractional effects on the isotopes (Meyers and Teranes, 2001). Consequently, organic matter from different sources have different isotopic signatures (Table 4.4) (Meyers and Teranes, 2001; Leng et al., 2006).

Table 4.4 Lists of the characteristics of $\delta^{13}C$ from different sources and factors may influence the $\delta^{13}C$ of lake sediments (synthetic from Meyers and Teranes, 2001).

Enrichment of $\delta^{13}C$	Depletion of $\delta^{13}C$	Sources
C_4 plants	C_3 land plants	allochthonous
Benthic community	Planktonic community	autochthonous
(Submerged macrophytes)	(phytoplankton)	
Increasing productivity	Decreasing productivity	autochthonous
Increasing pH	Decreasing pH	autochthonous
Increasing temperature	Decreasing temperature	autochthonous
	Suess effect	autochthonous

Terrestrial plants directly utilize atmospheric carbon dioxide (CO_2) which has a carbon isotope discrimination of −7‰ for photosynthesis (Meyers and Teranes, 2001). C_3 and C_4 plants use different pathways in photosynthesis to transform atmospheric CO_2 into organic matter (Hassan et al., 1997; Meyers and Lallier-vergés, 1998). C_3 plants (e.g., wheat, rye, oats, rice, cotton), which use the Calvin photosynthetic pathway in photosynthesis, preferentially take up ^{12}C directly from the atmosphere through ribulose-diphosphate (RBP) carboxylase, resulting in an average isotopic discrimination of −20‰ from the ratio of the inorganic carbon source (Hassan et al., 1997; Meyers and Lallier-Vergés, 1998). Therefore, organic matter produced by C_3 plants is characterized by a $\delta^{13}C$-value (PDB) of about −27‰. In contrast, C_4 plants (e.g., corn), which use the Hatch-Slack pathway in photosynthesis, fix CO_2 after diffusion into the leaf using phosphoenol pyruvate (PEP). The discriminatory power against ^{13}C of PEP in C_4 plants (−4 to −6‰) is lower than that of RBP (−20‰) in C_3 plants (Smith and Samuel, 1971; O'Leary, 1981). Hence, organic matter generated by C_4 plants is less depleted in ^{13}C compared to that synthesized by C_3 plants, characterized by an average value $\delta^{13}C$-value (PDB) of about −14‰ (Smith and Samuel, 1971; O'Leary, 1981; Hassan et al., 1997; Meyers and Lallier-vergés, 1998). Different from the C_3 and C_4 plants, most desert plants and succulents uses the crassulacean acid metabolism (CAM) pathway for photosynthesis (O'Learv, 1988). The isotope discrimination in the CAM pathway varies between −4 and −20‰, hence the $\delta^{13}C$ of organic matter generated by the desert plants varies from −11 to −27‰ (O'Learv, 1988). This variance in $\delta^{13}C$ has been used to study terrestrial shifts between C_3 and C_4 plants in palaeoclimatology (Meyers and Lallier-Vergés, 1998). On the Chinese Loess Plateau, peaks of $\delta^{13}C$ in the palaeosols have been attributed to the development of C_4 vegetation (Vidic and Montañez, 2004).

For autochthonous organic matter synthesised within a lake, $\delta^{13}C$ is mainly influenced by the source of carbon used for photosynthesis (Hassan et al., 1997; Meyers and Lallier-Vergés, 1998). Empirical evidence based on deep lakes where algae is the main source of autochthonous organic matter suggests that primary productivity plays an important role in influencing the $\delta^{13}C$ (Meyers and Teranes, 2001). Algae preferentially assimilate the lighter carbon (^{12}C) for photosynthesis, resulting in the enrichment of ^{13}C in the remaining inorganic carbon pool and newly generated organic matter (Meyers and Teranes, 2001). Thus, lakes experiencing increasing productivity are often accompanied by an enrichment of $\delta^{13}C$ (Meyers and Teranes, 2001). Moreover, when primary productivity increases to a level at which aqueous CO_2 is insufficient, aquatic plants use HCO_3^- as the carbon source, resulting in the enrichment of $\delta^{13}C$ as bicarbonate ($\delta^{13}C$ = 1‰) are more rich in ^{13}C than CO_2 ($\delta^{13}C$ = −7‰). In Lake

Erie, less depletion in sedimentary $\delta^{13}C$ in the late 19th century was attributed to the increase in primary production resulting from increasing phosphorus loading due to early settlement and deforestation in the catchment (Schelske and Hodell, 1995). Primary production decreased in the lake since ca. 1975 CE with the introduction of water management policies which limited P emission, resulting in the depletion in sedimentary $\delta^{13}C$ (Schelske and Hodell, 1995).

For shallow lakes, autochthonous organic matter includes phytoplankton and benthic communities (i.e., benthic algae, submerged macrophytes). $\delta^{13}C$ of organic matter in lake sediments may be altered by the relative abundance of phytoplankton to macrophytes in shallow lakes (Goericke et al., 1994; Wu et al., 2007). Phytoplankton communities which live in the lake surface fix aqueous CO_2 in isotopic equilibrium with atmospheric CO_2 ($\delta^{13}C$ = −7‰) and have a similar $\delta^{13}C$ as C_3 land plants (Hassan et al., 1997; Meyers and Lallier-Vergés, 1998), whereas benthic algal communities and submerged macrophytes generally utilize HCO_3^- (average $\delta^{13}C$ is ~ 1‰) for photosynthesis. Besides, inorganic carbon is fixed under the incentive of the enzyme ribulose 1,5-bisphosphate carboxylase-oxygenase (Rubisco) during photosynthesis (Goericke et al., 1994). Due to the difference in the substrate affinities and specificity factors for Rubisco between submerged plants and cyanobacteria, the isotopic fractionation of macrophytes for Rubisco is 10‰ higher than that of photosynthetic bacteria (Goericke et al., 1994). Therefore, organic matter generated by submerged macrophytes is less depleted in $\delta^{13}C$ than that of phytoplankton (Hassan et al., 1997; Meyers and Lallier-vergés, 1998). In contrast to deep lakes, eutrophication induced increases in algal production is usually accompanied by the decrease of submerged macrophytes in shallow freshwater lakes based on the aquatic stable state transition, and hence the shift from macrophyte-related clear water to the algal-dominated turbid state may result in the decrease of ^{13}C. In Taihu Lake, the depletion of ^{13}C in lake sediments since the 1990s CE has been attributed to the replacement of macrophytes, which have an average $\delta^{13}C$ of about −15.4‰, by cyanobacteria have a $\delta^{13}C$ of about −21.1‰ (Wu et al., 2007).

The equilibrium of the hydration process of CO_2 is determined by various factors such as pH and temperature (Hassan et al., 1997; Meyers and Lallier-Vergés, 1998). High temperature and high pH (alkaline) conditions promote the hydration of CO_2, resulting in elevated ratio of HCO_3^- relative to CO_2. Under alkaline conditions where pH > 8.3, HCO_3^- makes up more than 99 % of the total dissolved inorganic carbon (Hassan et al., 1997). Apart from the generation processes, the decomposition of organic matter during early diagenesis may modify the bulk $\delta^{13}C$ signal as well (Meyers and Lallier-Vergés, 1998). A study in Lake Michigan showed that $\delta^{13}C$ varied in organic matter from different water depths and the surface sediment, implying that early diageneses changes the bulk $\delta^{13}C$ signal (Meyers and Lallier-Vergés, 1998). However, the change in isotope composition during early diagenesis is minimal compared to the discrimination during photosynthesis, which makes $\delta^{13}C$ a solid proxy to detect the source of organic matter in palaeolimnology. Besides, the release of isotopically-light carbon into the atmosphere due to the combustion of fossil fuels has diluted the atmospheric CO_2 pool, resulting in the depletion of $\delta^{13}C$ in organic matter since the 1950s, which is known as the Suess effect (Keeling, 1979).

Although useful in providing information on the source of organic matter, either C/N ratios or $\delta^{13}C$ have limits when applied individually. For instance, $\delta^{13}C$ of phytoplankton utilizing atmospheric CO_2 for photosynthesis has an overlap with that of C_3 land plants (Hassan et al., 1997; Meyers and Lallier-Vergés, 1998). C/N ratios cannot distinguish organic matter generated through the C_3 pathway from that of C_4 plants. Hence, C/N ratios and $\delta^{13}C$ are normally used in combination with each other, and with other proxies in palaeolimnology and palaeoclimatology (Figure 4.5) (Krishnamurthy et al., 1986; Meyers and Lallier-Vergés, 1998; Meyers and Teranes, 2001; Leng et al., 2006; Chen et al., 2017).

4.2.4.3 Nitrogen isotopes

Nitrogen isotopes ($\delta^{15}N$) which is the difference in the ratio of ^{15}N to ^{14}N between samples and standards (atmospheric N_2) can provide information on the source and cycling of organic matter, although they are not widely used in palaeolimnology due to the complexity of interpretation and analytical difficulties (Meyers and Teranes, 2001; Leng et al., 2006). The difference in $\delta^{15}N$ characteristics between allochthonous organic matter from the catchment and autochthonous organic matter generated within a lake originates from the differences in isotopic content of the inorganic nitrogen reservoirs (Hassan et al., 1997; Meyers and Lallier-Vergés, 1998). Land plants which utilize atmospheric N have an average $\delta^{15}N$ of about 0‰ (Peters et al., 1978). Dissolved nitrate is enriched in heavy nitrogen, characterized by an average $\delta^{15}N$ of about 7 to 10‰. Therefore, $\delta^{15}N$ of organic matter from aquatic algae or macrophytes which use dissolved nitrate is ca. 8‰ (Meyers and Lallier-Vergés, 1998). Apart from the difference in isotopic characteristics of nitrogen sources, the dynamics of nitrogen cycling and the discrimination of isotopes during the biogeochemical process and early diagenesis may modify the $\delta^{15}N$ in bulk sediments (Meyers and Lallier-Vergés, 1998; Meyers and Teranes, 2001; Leng et al., 2006).

Therefore, factors such as the characteristics of N pools, N_2-fixing bacteria which are able to use N_2 directly from atmosphere, denitrification which transforms nitrate to N_2 and ammonia volatilization which transforms ammonium to NH_3 should be considered when interpreting the variations in nitrogen isotopes (Meyers and Teranes, 2001; Leng et al., 2006).

Cultural eutrophication has a complex influence on the $\delta^{15}N$ of bulk sediments (Meyers and Teranes, 2001; Leng et al., 2006; Xu et al., 2006; Woodward et al., 2012; Chen et al., 2017). Firstly, eutrophication promotes primary production in aquatic ecosystems (Schindler et al., 2008; Conley et al., 2009; Smith and Schindler, 2009). Primary productivity has the same effects on the discrimination of nitrogen as that of carbon (Meyers and Teranes, 2001; Leng et al., 2006). Similar to that of carbon, lighter nitrogen (^{14}N) is preferentially taken up by organisms, resulting in organic matter generated afterwards that is progressively enriched in ^{15}N (Meyers and Teranes, 2001). Secondly, nitrogen from agricultural and urban sewage are isotopically rich in nitrogen ($\delta^{15}N$ = 10 - 25‰), thus sediments in lakes fertilized by sewage from urban and agricultural sources are rich in $\delta^{15}N$ (Leavitt et al., 2006; McGowan et al., 2012; Moorhouse et al., 2014). In Windermere and Blelham Tarn from the English Lake District, the increase in sedimentary $\delta^{15}N$ was linked with the influx of sewage from agriculture and urbanization (McGowan et al., 2012; Moorhouse et al., 2014). A study in western Ireland showed that lakes located in relatively pristine catchments were characterized by a more depleted sedimentary $\delta^{15}N$ signal compared to lakes in agricultural catchments which integrated organic matter from fertilizers and cattle manure (Woodward et al., 2012). On the other hand, phosphorus induced eutrophication may stimulate the growth of N_2-fixing cyanobacteria which can utilize atmospheric N_2 ($\delta^{15}N$ = 0‰ by definition), resulting in the depletion of $\delta^{15}N$ (Schindler et al., 2008; McGowan et al., 2012; Chen et al., 2017). In Windermere, the decline in sedimentary $\delta^{15}N$ was partly related to growth of N_2-fixing cyanobacteria due to eutrophication (McGowan et al., 2012). Besides, synthetic nitrogen fertilizer, produced via industrial atmospheric N_2 fixation, is depleted in $\delta^{15}N$ (Chen et al., 2017). Therefore, eutrophication caused by the direct import of nitrogen fertilizer leads to the depletion of $\delta^{15}N$ in sediments.

4.2.4.4 C and N mass and isotope analytical procedures

C and N mass and isotopes were analysed at the Natural Environmental Research Council (NERC) Isotope Geoscience Laboratory at the British Geological Survey, after preliminary treatment in the School of Geography at the University of Nottingham. For carbon isotope pre-treatment, freeze-dried samples were soaked in HCl (5%) to ensure that all carbonates were removed, and then washed with deionised water three times to eliminate the extra acid before being dried at 40°C. After that, the dry samples were ground and weighed into tin capsules for analysis. $\delta^{13}C$, TOC and TN content were analysed using Costech Elemental Analyser (EA) and on-line VG TripleTrap and Optima dual-inlet mass spectrometer. TOC and TN content were calibrated using the acetanilide standard. C/N ratios of sediments were calculated by dividing the atomic number of TOC (%TOC/12 g mol^{-1}) by the atomic number of %TN (%TN/14 g mol^{-1}). $\delta^{13}C$ was calibrated to the Vienna VPDB using laboratory standards which were calibrated against NBS-18, NBS-19 and NBS-22 with the following equation:

$$\delta^{13}C = \left(\frac{\left(\frac{13C}{12_C}\right)_{sample}}{\left(\frac{13_C}{12_C}\right)_{standard}} - 1 \right) \times 1000‰$$

Raw samples were freeze-dried and ground for nitrogen isotope analysis. $\delta^{15}N$ was analysed using the Thermo Finnigan DeltaplusXL with oxidative and reductive elemental analysers. $\delta^{15}N$ was calibrated to the standard of atmospheric N_2 using within-run laboratory standards calibrated against NBS-18, NBS-19 and NBS-22 with the following equation:

$$\delta^{15}N = \left(\frac{\left(\frac{15_N}{14_N}\right)_{sample}}{\left(\frac{15_N}{14_N}\right)_{standard}} - 1 \right) \times 1000‰$$

4.3 Historical and instrumental data collection

In order to investigate the potential drivers of algal production and community change, historical and instrumental data from each individual lake were collected and compared with sedimentary pigments in each corresponding lake.

4.3.1 Historical archives of agricultural development and industrialization/urbanization

The administrative divisions of China include five levels: provincial, prefecture, county, township, and village. Historical archives are systematically and methodically compiled at provincial and prefectural levels. Thus, the catchment boundaries were compared with the administrative boundaries of province and prefecture to choose the appropriate level of administration to represent changes within each lake catchment. As the drainage area of Dongting Lake and Poyang Lake is approximately the same as the area of Hunan (provincial level) and Jiangxi (provincial level) (Figure 4.6), respectively, historical archives in Hunan and Jiangxi (provincial level) were collected for the Dongting and Poyang Lake catchments, respectively (Figure 4.6). For the four smaller lakes (Honghu, Futou, Luhu and Wanghu), historical archives were collected at prefecture level. As data before the foundation of People's Republic of China were rarely recorded and poorly preserved, only historical archives between 1949 CE and 2016 CE were collected. Ten historical archival datasets representing a range of human activities including rural and urban population, grain production, aquaculture production, nitrogen and phosphorus fertilizer, concrete and electricity production, the total length of roads and the number of vehicles were collected as proxies of agricultural and industrial development and urbanization in the catchments (Table 4.5).

Table 4.5 Historical archives collected as urban/industrial and agricultural proxies.

Urban/industrial	Agricultural
Urban population (unit: million)	Rural population (unit: million)
Concrete production (unit: Mt)	Grain production (unit: Mt)
Electricity production (unit: billion kw h)	Nitrogen fertilizer (N) (unit: 10^4 metric tons)
Length of roads (10^4 km)	Phosphorus fertilizer (P_2O_5) (unit: 10^4 metric tons)
Number of vehicles (unit: million)	Aquaculture production (unit: 10^4 metric tons)

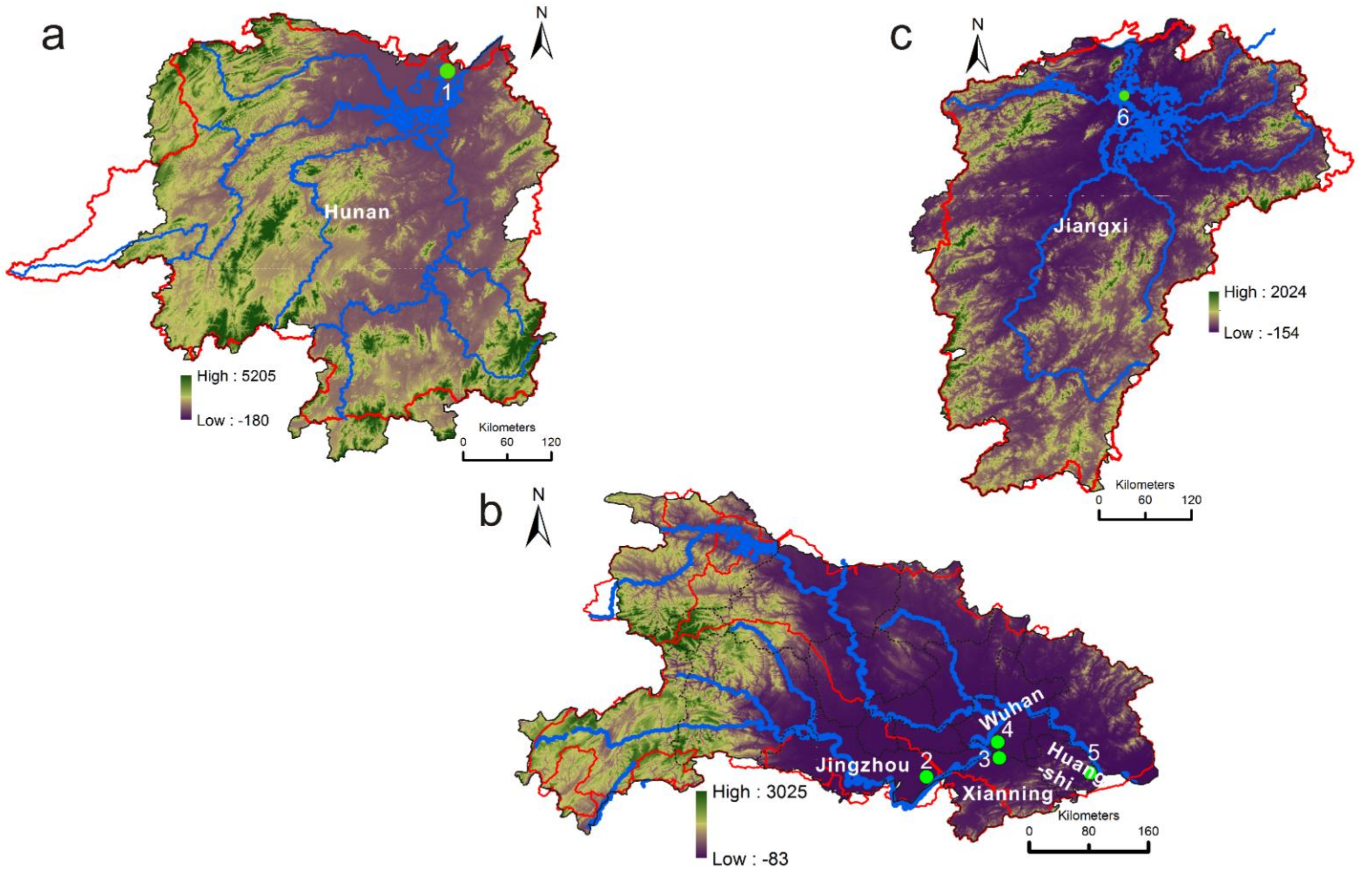

Figure 4.6 Map showing the administrative boundaries (black solid line: provincial level; black solid line: prefecture level) and the drainage boundaries (red solid line) (a. Hunan; b. Hubei; c. Jiangxi) (1=Dongting Lake, 2=Honghu Lake, 3=Futou Lake, 4=Luhu Lake, 5=Wanghu Lake, 6=Poyang Lake).

Fertilizer data was recorded in different forms at different times in each site, from practical weight of all fertilizers (e.g., urea, NH_4Cl, $Ca(H_2PO_4)_2$) in early years to pure weight of all fertilizer ($N + P_2O_5 + K_2O$) and pure weight of each individual fertilizer (N, P_2O_5, K_2O) in recent years (Figure 4.7). In this study, the weights of different fertilizers were transformed to the weights of N and P_2O_5 to unify the dataset and for comparison. For data recorded in practical weight, the practical weight of all fertilizer was firstly converted to the pure weight of all fertilizer. Then, the pure weight of all fertilizer was transformed to the weight of N and P_2O_5 (Figure 4.7). Fertilizers used in China include nitrogen fertilizer, phosphorus fertilizer and compound fertilizer. Compound fertilizer provides nitrogen (N), phosphorus (P) and potassium (K) to the farmland. The mass of compound fertilizers were split their components of N, P_2O_5 and K_2O by using a ratio of 1:1:1 to calculate the total nitrogen and P_2O_5 applied to the farmland (Zhu et al., 2018). So total nitrogen used is the sum of nitrogen fertilizer and one third of the compound fertilizer and P_2O_5 used is the sum of phosphorus fertilizer and one third of the compound fertilizer (Zhu et al., 2018).

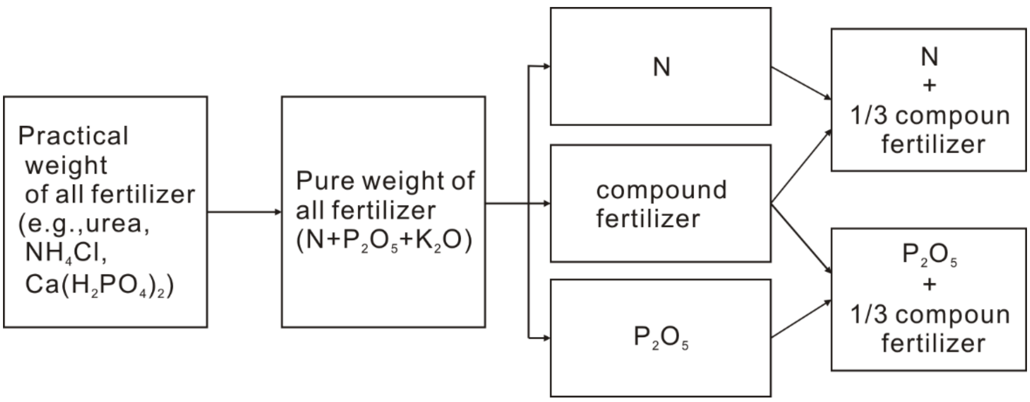

Figure 4.7 Different forms of fertilizers recorded in the archives.

Dongting Lake: For Hunan Province, historical data on electricity production, concrete production, number of vehicles, length of roads, grain production, aquaculture products, rural and urban populations between 1949 CE and 2008

CE were collected from China Compendium of Statistics 1949-2008. Data after 2008 CE were collected from Hunan Statistical Yearbook 2017 and National Bureau of Statistics of China (NBSC) (http://data.stats.gov.cn/). Fertilizer data was recorded as the practical weight of all fertilizer (e.g., urea+NH_4Cl+…) before 1990 CE and the pure weight of all fertilizer (N+P_2O_5+K_2O) since 1990 CE in the China Compendium of Statistics 1949-2008 (Figure 4.8). On the NBSC website and in Zhu et al.'s (2018) study, the fertilizer data was only available since 1980 CE and was recorded as the pure weight of all fertilizer and the weight of each fertilizer (N, P_2O_5, K_2O, respectively). So the pure weight of all fertilizer before 1980 CE was calculated by multiplying the practical weight of all fertilizer before 1980 CE by the average ratio of the pure to practical weight of all fertilizers between 1980 CE and 1989 CE. And then the weight of N and P_2O_5 before 1980 CE was calculated by multiplying the pure weight of all fertilizers before 1980 CE by the average proportion of N and P_2O_5 in the pure weight of all fertilizer between 1980 CE and 1989 CE, respectively.

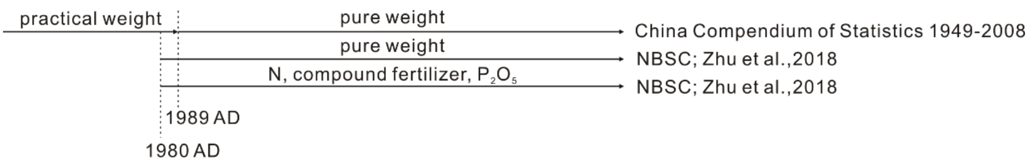

Figure 4.8 Sketch showing the way fertilizer data was recorded and the procedure of collecting N and P (P_2O_5) fertilizer data.

Honghu Lake is located in Jingzhou (prefecture level), Hubei Province (Figure 4.6). Historical archives for Jingzhou were collected for the Honghu Lake catchment. Grain and aquaculture production in Jingzhou were collected from Jingzhou Statistical Yearbook 2017. The other records were poorly recorded in this area. However, data were available for Hubei (provincial level) and the other two prefecture administration (Wuhan and Huangshi, not in the lake catchment) within Hubei (Figure 4.6). So electricity production, concrete production, nitrogen and phosphorus fertilizers, rural and urban population, the number of vehicles and the length of roads were calculated as follows:

$$\text{Data}_{(Jingzhou)} = (\text{Data}_{(Hubei)} - \text{Data}_{(Wuhan)} - \text{Data}_{(Huangshi)}) \times \text{Area}_{(Jingzhou)} / (\text{Area}_{(Hubei)} - \text{Area}_{(Wuhan)} - \text{Area}_{(Huangshi)})$$

where $\text{Data}_{(Hubei)}$, $\text{Data}_{(Jingzhou)}$, $\text{Data}_{(Wuhan)}$, $\text{Data}_{(Huangshi)}$ are the value of archives in Hubei, Jinghou, Wuhan and Huangshi, respectively; $\text{Area}_{(Hubei)}$, $\text{Area}_{(Jingzhou)}$, $\text{Area}_{(Wuhan)}$, $\text{Area}_{(Huangshi)}$ are the administration area of Hubei, Jingzhou, Wuhan and Huangshi, respectively.

Historical archives in Hubei Province were collected from China Compendium of Statistics 1949-2008, Hubei Statistical Yearbook 2017 and NBSC (http://data.stats.gov.cn/). Data on electricity production, concrete production, urban and rural population were continuously recorded at one year scale between 1949 CE and 2016 CE in Hubei. Data on the number of vehicles and length of roads were recorded annually after 1980 CE but at three or four year resolution between 1949 CE and 1979 CE so data for missing years were calculated using linear interpolation. Fertilizer data were converted to the weight of N and P_2O_5 using the method described in Hunan (Dongting catchment). The data sources for Wuhan and Huangshi are explained below.

Futou Lake: As it is located at the edge of Wuhan and Xianning, historical archives for the Futou Lake catchment were estimated to be half of the total of Wuhan and Xianning. Historical archives of Wuhan were collected from Wuhan during the Past Fifty Years, Wuhan Statistical Yearbook 2017 and Hubei Rural Statistical Yearbook 2017. Data on the number of vehicles were only available from 1985 CE, and so data before 1985 CE were calculated using an exponential extrapolation. Historical archives in Xianning were poorly preserved, so historical archives in Xianning were calculated following the method used in Jingzhou, using data from Hubei, Wuhan and Huangshi.

Luhu Lake is located in Wuhan (prefecture level), Hubei (provincial level). Historical archives from Wuhan were collected for the Luhu Lake catchment.

Wanghu Lake is located in Huangshi (prefecture level). Historical archives in the Wanghu Lake catchment are represented by data from Huangshi. Data on rural and urban population, electricity and concrete production, grain production, aquaculture products, the number of vehicles and the length of roads were collected from Huangshi Statistical Yearbook 2017. Fertilizer data were converted to the weight of N and P_2O_5 using the method described in Hunan (Dongting catchment).

Poyang Lake is located in Jiangxi (provincial level). The drainage area of Poyang Lake is approximately the same as the area of Jiangxi Province (Figure 4.6), so historical archives of Jiangxi were collected from the China Compendium of Statistics 1949-2008 and Jiangxi Statistical Yearbook 2017. The division of urban and rural population was only available since 1978 CE. Urban population before 1978 CE was calculated using an exponential extrapolation. Since total population was recorded, rural population before 1978 CE was the difference between total population and urban population. Data on the number of vehicles were available since 1978 CE, and before this time data were calculated by exponential extrapolation. Fertilizer data were converted to the weight of N and P_2O_5 using the method described in Hunan (Dongting catchment).

4.3.2 Climate data

Climate variables between 1900 CE and 2016 CE were collected from the Climatic Research Unit dataset of the University of East Anglia (https://crudata.uea.ac.uk/cru/data/hrg/cru_ts_4.02/ge/) (Harris et al., 2014). In this dataset, global climate datasets are constructed at 0.5° latitude/longitude resolution based on monthly observations at meteorological stations across the world. Lakes in this study are located in the middle Yangtze floodplain, showing similar climatic characteristics. In this study, mean annual temperature and total annual rainfall in each catchment were collected at the nearest grid (Figure 4.9).

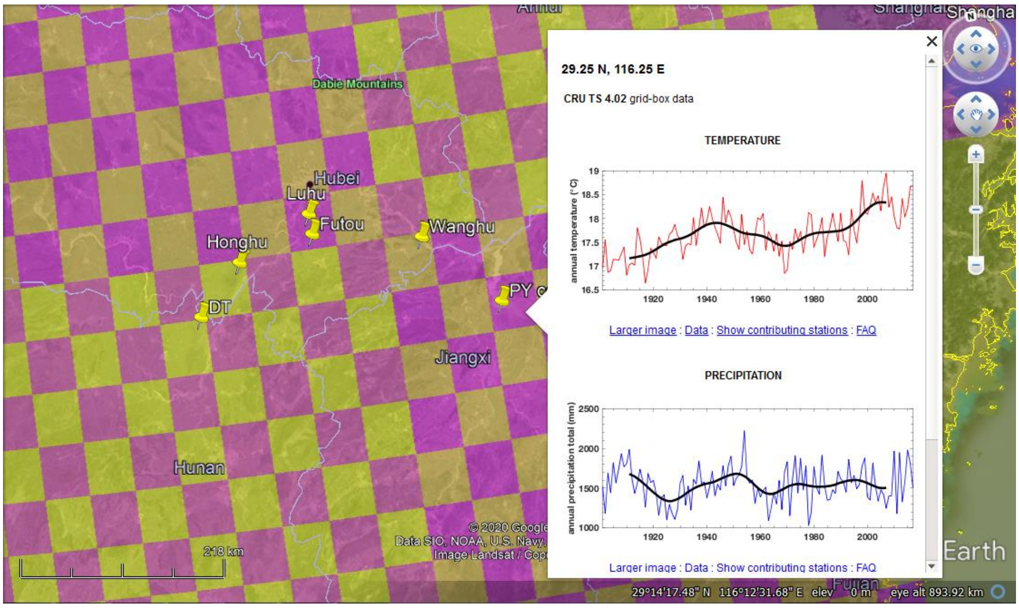

Figure 4.9 Map showing the grid where the climate data collected for each lake catchment. The green and purple blocks represent the 0.5° latitude/longitude resolution grids.

4.4 Numerical analysis

4.4.1 Standardizing data using z-scores

Z-scores can be used to compare temporal changes in parameters which may be measured in different numbers or units (e.g., kg, m). Z-scores measure the standard deviations away from the mean, and are a numerical measurement of a value's deviation from the mean of a group of values in statistics (DeVore, 2017). A z-score of 0 means the data is identical to the mean and a z-score of 1 indicates a value that is one standard deviation from the mean.

Z-scores are calculated using the following formula:

$$z = \frac{(x - \mu)}{\sigma}$$

where μ is the average and σ is the standard deviation.

In this study, Z-scores were used to standardize historical archives to eliminate differences in units or scales of measurements. The 10 historical datasets were standardized using z-scores and then the 5 indicators of agriculture (Z-agriculture) and 5 urban and industrialization archives (Z-urban) were each summed to be used as summary proxies for agricultural and urban/industrial development in the generalized additive model to link algal production with potential drivers (see section 4.4.3). Z-scores were calculated using the *scale()* function in RStudio (version 1.2.1335) (R Core Team, 2020).

4.4.2 Ordination analysis

In palaeolimnology and palaeoecology, each observation normally contains multi-dimensional descriptors. For instance, diatom datasets in palaeolimnology normally includes more than 20 diatom species (Smol et al., 2012). In order to visualise the dataset, approaches trying to plot all the descriptors in a coordinate with as many axes as the number of descriptors or all the possible pairs of descriptors is complicated and impractical (Legendre and Legendre, 2012). For instance, for a diatom dataset with 10 species, it is impossible to visualize a matrix in a coordinate with 10 axes. Similarly, investigating relationships among 45 possible parameter pairs would be tedious or inefficient. Instead, ordination analysis is efficient and useful at uncovering the underlying structure of multivariate datasets in a simplified way (Borcard et al., 2018). In ordination analysis, observations are projected into a new coordinate where the new axes represent the largest possible fraction of the variability of the observations (Borcard et al., 2018).

The principal of ordination is to present the dataset in a transformed coordinate with reduced dimensions while maintaining the main trends and characteristics (Legendre and Legendre, 2012). Observations can be represented as a cluster of points in a coordinate which has the same number of axes as the number of variables. Normally, the cluster has an ellipsoidal shape which is elongated in some directions and flattened in others (Legendre and Legendre, 2012). These directions are not necessarily aligned with a single dimension (= a single variable) of the multidimensional space (Legendre and Legendre, 2012). In ordination analysis, the direction where the cluster is most elongated corresponds to the direction of largest variance of the cluster, which is the first axis (axis 1) that an ordination will extract. The second axis (axis 2) to be extracted is the second most important in variance, provided that it is orthogonal (linearly independent, uncorrelated) to the first one. The process continues until all axes have been computed. Theoretically, the number of axes extracted by ordination can be as many as the number of the variables in the dataset, provided that variables are not correlated with each other (Legendre and Legendre, 2012). Normally, only the first and the second axes are presented for visualization purposes.

Ordination methods include a range of different techniques such as principal component analysis (PCA), correspondence analysis (CA), nonmetric multidimensional scaling (nMDS) (Legendre and Legendre, 2012). Each has their own domain of application. For example, PCA is useful for quantitative data with a linear relationship between the abundance value of species and the environmental variable. CA is suitable for datasets with a unimodal relationship between the abundance value of species and the environmental variable (Borcard et al., 2018). Thus, the distribution (linear or unimodal) of the dataset should be tested before choosing the right ordination methods. Practically, this is achieved using a detrended correspondence analysis (DCA). A gradient length less than 2 standard deviation units (SD) implies a linear model, hence PCA should be used. When the gradient length is larger than 2 SD, CA or DCA should be used as the dataset reveals a unimodal response model. Before ordination analysis, the dataset should be square root (percentage data) - or log (x+1) (abundance data)-transformed to stabilise the variance and dampen the effects of abundant data.

In this study, ordination analysis was applied to extract major trends in the pigment assemblages of all six lakes and chironomid datasets in Futou, Luhu, Wanghu and Poyang Lakes. The pigment dataset was log-transformed and the chironomid dataset was square root-transformed before ordination analysis. DCA was applied to study the distribution of the dataset before choosing the right technique (PCA or DCA/CA). Ordination analysis was conducted using

RStudio (version 1.2.1335) (R Core Team, 2020) with the "*vegan*" (version 2.5-6) package (Oksanen et al., 2019).

4.4.3 Mann-Kendall analysis

The observed time series dataset can be considered to consist of a periodic signal including a trend and a noise component (Shumway and Stoffer, 2017). The fundamental interest in studying time series dataset is to investigate the trend which would normally be masked and complicated by the noise and the periodic signal (Shumway and Stoffer, 2017). In palaeolimnology, it is often useful to investigate if there is a monotonic upward or downward trend in sedimentary proxies over time (Mann, 1945; Gilbert, 1987). Mann-Kendall (MK) coefficient values can give such information. The MK coefficient compares older observations with randomly selected younger observations in a time series. Based on the differences between the younger and older observations, an indicator function taking on the values 1 (if younger > older), 0 (if younger = older) or –1 (if younger < older) is derived (Gilbert, 1987). The sum of the results of the indicator function and the variance of the sum can statistically determine if there is an upward or downward trend in the dataset.

The output of the Mann-Kendall trend analysis is the MK coefficient values (tau) with a *p* value. A *p* value >0.05 indicates there is no trend in the dataset. If the *p* value falls in the cut-off range (normally <0.05), it means there is a monotonic trend in the dataset. A tau ranging between 0 and +1 indicates there is an upward trend in the dataset and a negative tau (between –1 and 0) means the observation decreases over time.

In this study, the MK trend test was applied to sedimentary pigment data (pigment PCA axis 1), C/N ratios and $\delta^{13}C$ in sediment cores to investigate trends in algal production, C/N ratios and carbon isotopes over the last two centuries. The MK trend test was conducted using the *MannKendall()* function in RStudio (version 1.2.1335) (R Core Team, 2020) with the "*Kendall"* (version 2.2) package (McLeod, 2011).

4.4.4 Regression analysis

In recent decades, palaeolimnology and palaeoecology have advanced from previously descriptive disciplines to become increasingly quantitative as numerical and statistical approaches have developed (Smol et al., 2012). Regression analysis can be used to identify relationships between the 'response' or 'dependent' variable and one or more 'explanatory' or 'independent' variables (Chatterjee and Hadi, 2006). Mathematically, the relationship between dependent variable Y and the set of independent variables $X_1, X_2, \ldots, X_p$, can be approximated by the regression model

$$Y = f\,(X_1, X_2, \ldots, X_p) + \varepsilon$$

where the function $f\,(X_1, X_2, \ldots, X_p)$ describes the relationship between Y and $X_1, X_2, \ldots, X_p$ and ε is assumed to be a random error representing the discrepancy in the approximation which accounts for the failure of the model to fit the data exactly (Chatterjee and Hadi, 2006).

In linear regression, the dependant or responsible variable is related with predictor or explanatory variables in a linear way. Hence, the linear regression can be expressed as

$$Y = \beta_0 + \beta_1 X_1 + \beta_2 X_2 + \cdots + \beta_p X_p + \varepsilon$$

where $\beta_0, \beta_1, \beta_2, \cdots, \beta_p$ are constants called the regression coefficients (Chatterjee and Hadi, 2006).

A simple linear regression with one response variable $Y = \{y_1, y_2, \ldots, y_i\}$, and one explanatory variable $X = \{x_1, x_2, \ldots, x_i\}$ can be modelled as

$$Y = \beta_0 + \beta_1 X + \varepsilon$$

In this model, β_1 is the slope of the fitted line, β_0 is the intercept on y axis (Figure 4.10) (Chatterjee and Hadi, 2006). ε measures the discrepancy in the approximation and so is the error of the regression model (Chatterjee and Hadi, 2006).

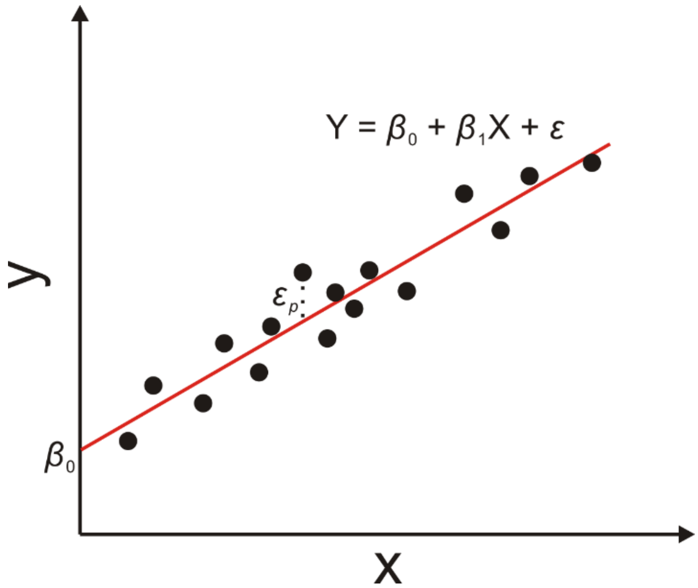

Figure 4.10 Conceptual model of simple linear regression.

There are different criteria to choose the best model in simple linear regression. The commonly used model is the least squares regression (Chatterjee and Hadi, 2006). In the simple linear regression, each observation has a discrepancy, which is the difference between the observed value and the fitted value (the residual). For instance in Figure 4.9, the pth observation has a discrepancy ε_p $(= y_p - \beta_0 -$

$\beta_1 x_p$), which is the vertical distances from the point to the line. In a dataset with n observations, the sum of squares of these distances is

$$\sum_{i=1}^{n} \varepsilon_i^2 = \sum_{i=1}^{n} (y_i - \beta_0 - \beta_1 x_i)^2$$

The least square regression fit is the model with the smallest sum of squares of error. Under the least square criteria,

$$\beta_1 = \frac{\Sigma(y_i - \bar{y})(x_i - \bar{x})}{\Sigma(x_i - \bar{x})^2}; \beta_0 = \bar{y} - \beta_1 * \bar{x}$$

After fitting the model, the effectiveness of using X as a predictor of Y is evaluated by the characteristics of β_1. If β_1 is not significantly different from 0, it means there is no linear relationship between Y and X. If β_1 is significantly larger than 0 ($p < 0.05$), it indicates there is a positive linear relationship between Y and X, meaning one unit increase in X results in β_1 increase in Y. If β_1 is significantly smaller than 0 ($p < 0.05$), it indicates there is a negative linear relationship between Y and X, meaning one unit increase in X results in β_1 decrease in Y (Chatterjee and Hadi, 2006).

In Chapter 6, simple linear regression was used to model the relationship between algal production (response variable, measured by the first pigment PCA axis) and sedimentary TN or TP flux (explanatory variable) since ~ 1850 CE. In Chapter 8, simple linear regression was used to investigate the relationship between $\delta^{13}C$ or C/N ratios (response variable) in surface sediments and water depth (explanatory variable) in Dongting Lake. Linear regression was performed using the *lm()* function in RStudio (version 1.2.1335) (R Core Team, 2020).

4.4.5 Generalized additive models (GAMs)

A major drawback of regression analysis approaches (such as linear regression and logistic regression) is that a prescribed functional form between the response variable and the explanatory variables is assigned (Wood 2017; Simpson, 2018). In contrast, generalized additive models (GAMs) allow the relationship between the response and explanatory variables to be determined from the data themselves (Simpson and Anderson, 2009; Wood, 2017; Simpson, 2018).

Generalized additive models are analogous to an extended version of a generalized linear model, in which the parametric assumption is relaxed and the parametric terms are replaced by smooth functions of the covariates (Wood, 2017; Simpson, 2018). Generally, the relationships between the response variable $Y = \{y_1, y_2, \ldots, y_i\}$ and the explanatory variable $X = \{ x_1, x_2, \ldots, x_i\}$ can be mathematically modelled as:

$$y_i \sim \mathrm{EF}(\mu_i, \Theta)$$

$$g\,(\mu_i) = \beta_0 + f\,(x_i)$$

$$\mu_i = g^{-1}\,(\beta_0 + f\,(x_i))$$

where μ_i (e.g., the mean count or the probability of occurrence) is the expected value of the response variable y_i ($\mu_i \equiv \mathrm{E}(Y_i)$); f is the smooth function of the covariate; g is the link function and g^{-1} is its inverse (Simpson, 2018). The link function maps values from the response scale on to the scale of the linear predictor. The link function depends on the distribution of the response variable (Table 4.6).

Table 4.6 Distribution of response variable and link function (adapted from Ouyang and Ge, 2013).

Family of response variable	Link functions
Normal distribution	Identity link: $g(x) = x$
Binomial distribution	Logit link: $g = \log(x/(1-x))$
Poisson distribution	Log link: $g(x) = \log(x)$
Gamma distribution	Log link: $g(x) = \log(x)$
Negative binomial distribution	Inverse link: $g(x) = 1/x$

The smooth function, $f(x_i)$, is represented using a basis which is a set of functions that collectively span a space of smoothers which contain $f(x_i)$ (or a close approximation to it) (Wood, 2017; Simpson, 2018). The functions in the basis which arise from a basis expansion of the covariate are called basis functions (Wood, 2017). If $b_j(x_i)$ is the jth basis function of x_i, then the smooth $f(x_i)$ can be represented as a weighted sum of basis functions:

$$f(x_i) = \sum_{j=1}^{k} b_j(x_t)\beta_j$$

where β_j is the weight applied to the jth basis function.

4.4.5.1 GAMs to determine the periods of changes of time series

In palaeolimnology, datasets of proxies are normally presented in time ordered sequences. So palaeolimnologists are generally interested in the following questions:

a) Does the sedimentary proxy change with time?
b) Is the degree of change constant over time?
c) If the degree of change is not constant, when does the change happen?

Except for a few cases with laminae or varves, most palaeolimnological datasets are arranged unevenly in time due to the variance in accumulation rates and compaction caused by overlying sediments (Battarbee et al., 2012; Simpson, 2018). Consequently, most palaeolimnological datasets are characterized by higher variance in younger sediments where each section represents fewer lake years than that of older sediments, acting as a time-varying high-cut filter of the annual depositional signal (Simpson 2018). Statistical analysis including the smoothers such as running means, locally weighted scatterplot smoother (LOESS) and simple linear trends have been used to estimate the trends in palaeolimnological time series (Simpson, 2018). However, the boundary problems caused by the width of filters in smoothers often results in the shortening of original datasets and the simple linear regression oversimplifies the trend. Modelling palaeolimnological time series datasets using GAMs has the advantages of revealing the trends in the data itself and resolving the uneven spacing of samples in time without shortening the dataset (Simpson, 2018).

Among the different kinds of basis in GAMs, such as the cubic regression splines and the thin plate regression splines, the cubic regression spline is widely used (Simpson, 2018). Figure 4.11 shows how the cubic regression spline (A, B) and the thin plate regression spline (C) work in the GAMs (Simpson, 2018). A cubic spline is a smooth curve which is composed of sections of cubic polynomials. These sections are joined at particular points which are called the knots. At each knot, the two sections of cubic polynomial that join have the same value and the same first and second derivate to guarantee that the different sections are joined smoothly and differentially (Wood, 2017). Typically, the knots are evenly distributed over the time series.

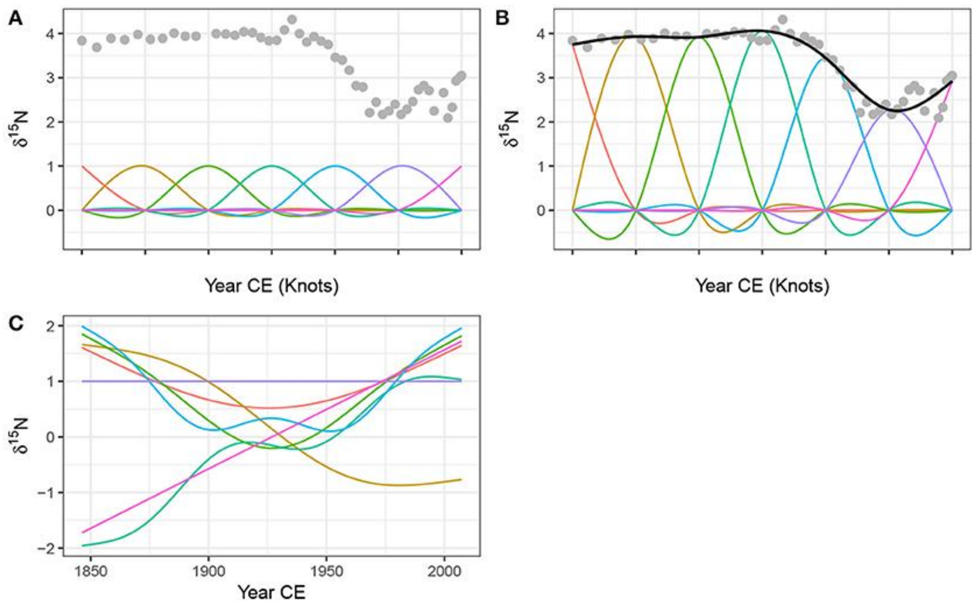

Figure 4.11 Basis functions for the time covariate and a palaeo-dataset. (A) A cubic regression spline composed of 7 basis functions with knots indicated by tick marks on the x axis; (B) Weighted cubic regression spline with estimated coefficients and the resulting GAM trend line; (C) A thin plate regression spline composed of 7 basis functions (from Simpson, 2018).

When modelling a palaeo-time series dataset using a simple linear regression model, the trend of the dataset can be obtained by calculating the first derivate which is the slope of the fitted model (Simpson, 2018). However, a simple linear regression which forces the proxy to change at a constant rate throughout the whole time series normally cannot reveal the real trend as most palaeo-time series datasets are complex and variable through time. In GAMs where the trends are developed from the data themselves, the slope of the trend is potentially different at every point in the time series (Simpson, 2018). The trend of the data at a time point over the time series can be revealed by the slope which is the first derivative at that point. Hence, the first derivative of the fitted model throughout the time series can be used to identify the period of changes in the palaeo-time series dataset (Simpson, 2018). In GAMs, the derivatives of the fitted model are calculated using the method of finite differences. For each derivative at any time point, an approximate pointwise confidence interval is given. If the first derivative is not statistically distinguishable from 0 (i.e. 0 is within the confidence interval of the first derivative), it means there is no trend in the data at that time point. If the first derivative is significantly larger than 0, it means the data increases at that time point, whereas if the first derivative is significantly smaller than 0 (0 on the right of the confidence interval on the first derivative), it means there is a decreasing trend of the data at that time point (Simpson, 2018).

In this study, GAMs were fitted to time series of pigment PCA axis 1 (since ~ 1800 CE) and the first derivative was calculated to detect the timing of changes in algal production in the lakes. Time series of z-scores of urban/industrial and agricultural archives, total annual rainfall, and mean annual temperature (since 1949 CE) were modelled using GAMs to investigate the timing of changes in urbanization/industrialization and agricultural activities, total annual rainfall and mean annual temperature in Chapter 6.

4.4.5.2 GAMs to detect the drivers of ecosystem change

Normally, environmental and ecological changes are driven by multiple factors. In palaeolimnology, the effects of each individual driver may vary in time and space (Smol et al., 2012). For example, the disproportionate increase in cyanobacteria relative to other phytoplankton in the northern temperate-subarctic regions was attributed to increasing nutrient loading and global warming (Taranu et al., 2015). Hence, it is of great importance to quantify the effects of each individual drivers for management and restoration purposes. Over the last several decades, the development in statistics, such as the emergence of variance partitioning analysis and regression tree analysis, has made it possible to quantify the relative magnitude of the effects of different drivers on ecosystem change (Hall et al., 1999; Cao et al., 2014; Taranu et al., 2015; Moorhouse et al., 2018). By using variance partitioning from sediment core data, Hall et al. (1999) revealed that the effects of agriculture and urbanization was larger than that of climate on the variance of algal and chironomid communities. Regression tree analysis showed that the establishment and upgrades of wastewater treatment plant and human population density were greater predictors of algal community changes in the low land (< 100 m.a.s.l.) lakes in the English Lake District, whereas those in the upland (> 100 m.a.s.l.) lakes in the area were predicted by climate (Moorhouse et al., 2018).

Though widely used in palaeolimnology, there is a major disadvantage of variance partitioning and regression tree analysis. Both are only able to identify the relative effects of each driver over the entire time series. In reality, the effects of different drivers may vary over time. Modelling the relationships between palaeolimnological datasets and potential drivers using GAMs has the advantage of answering questions of when and where different drivers may be driving the changes in the response variables (Simpson and Anderson, 2009; Dong et al., 2012; Capo et al., 2017). By using GAMs, Dong et al. (2012) revealed that diatom community changes were mostly driven by changes in soluble reactive phosphorus with lower influences of air temperature before 1975 CE in the Esthwaite Water in the English Lake District. After 1975 CE, air temperature started to have a stronger influence, while the influence of nutrients remained dominant.

In this study, GAMs were used to link the changes in algal production and N_2-fixing cyanobacteria (potential HABs taxa) with potential drivers since ~ 1950 CE. The response variable is the pigment PCA axis 1 (indicating algal production) or aphanizophyll (pigments from N_2-fixing cyanobacteria). The explanatory variable includes proxies of urbanization/industrialization (Z_U, z-scores of urban/industrial proxies), indicators of agricultural activities (Z_A, z-scores of agricultural proxies), mean annual temperature (T), total annual rainfall (R), (presence or absence) and local dam (LD, presence or absence). GAMs were conducted using the *gam()* function in RStudio (version 1.2.1335) (R Core Team, 2020) with the "*mgcv*" (version 1.8.31) package.

4.4.6 Constrained hierarchical cluster analysis

When palaeolimnological datasets are presented as stratigraphies of multiple measures, it is difficult to describe and interpret the dataset directly (Bennett, 1996). Hence, the dataset is normally reduced to manageable units, known as zones, for description and interpretation purposes (Bennett, 1996). Cluster analysis is widely used to separate the stratigraphical dataset into zones. There are different techniques to cluster palaeolimnological dataset, such as the binary techniques (Birks, 1974), optimal techniques (Birks and Gordon, 1985) and constrained cluster analysis (Grimm, 1987). Both the binary and optimal techniques depend on the whole sequence as they work in a way to minimize the sum of squares of the whole dataset. Truncation of the sequences may change the results of zonation. In contrast, constrained cluster analysis is built up locally (Bennett, 1996). In constrained cluster analysis, the zones are formed by hierarchical agglomeration of stratigraphically-adjacent samples, and hence it is more appropriate for the zonation of palaeolimnological datasets. The idea of cluster analysis is to partition the total variance of the dataset into separate components (Bennett, 1996). In the broken-stick model, the total variance is considered as a stick of unit length and the stick is separated into segments. The length of each segment is the proportion of total variance apportioned to each level of zonation if the sequence consisted of samples with no stratigraphic structure. Thus, if the reduction in variance for a particular zone exceeds the proportion expected from this model, the zone concerned accounts for more variance than would have been expected and consequently the zone may be considered significant (Bennett, 1996).

In this study, constrained cluster analysis was used for the zonation of chironomid and pigment datasets and the number of the zones was determined using the broken stick model. Constrained cluster analysis and the broken stick model were applied using the function *chclust()* and *bstick(),* respectively, in RStudio (version 1.2.1335) (R Core Team, 2020) with the package "*rioja*" (version 0.9-21) package (Juggins, 2017).

4.4.7 ANOVA

Analysis of variance (ANOVA), introduced by Ronald Fisher, tests for differences in the means of different groups (Miller, 1997). The null hypothesis for ANOVA is that there is no difference in the means of different groups. ANOVA statistically test the null hypothesis by partitioning the total variance of the dataset into different sources: difference between groups, also known as differences caused by systematic factors and the difference within groups or differences caused by random factors (Miller, 1997). Mathematically, the difference between groups is calculated by summing of the squared deviations between the means of different groups and the overall mean ($SS_{between}$) (Miller, 1997). The differences within the groups is the sums of squares within the groups (SS_{within}) (Miller, 1997). For a dataset (N samples) made up of k groups

$$SS_{between} = \sum_{j=1}^{k}\left(\bar{x_j} - \frac{\sum_{j=1}^{k} \bar{x_j}}{k}\right)^2;$$

$SS_{within} = \sum\left(x_{ij} - \bar{x}_j\right)^2$

where is $\bar{x}_j$ is the mean value of the *j*th group, x_{ij} is the value of the *i*th sample in the *j*th group.

In order to eliminate the difference in sample size in different groups and to get a normal variance, the mean squares between groups ($MS_{between}$) and the mean squares within groups (MS_{within}) are calculated by dividing the SSbetween and SSwithin by their degrees of freedom (df), which is $k - 1$ and $N - k$, respectively (Miller, 1997). Therefore,

$$MS_{between} = SS_{between}/(k - 1) = \frac{\sum_{j=1}^{k}\left(\bar{x}_j - \frac{\sum_{j=1}^{k}\bar{x}_j}{k}\right)^2}{k-1};$$

$$MS_{within} = SS_{within}/(N - k) = \frac{\sum\left(x_{ij} - \bar{x}_j\right)^2}{(N - k)}$$

The null hypothesis is tested using *F*-test (*F*-value = $MS_{between}/MS_{within}$), which depends on the $MS_{between}$, the MS_{within} and the sample size. The null hypothesis is rejected when the *F*-value is significantly larger than 1 (large $MS_{between}$ but small MS_{within}), which indicates the means are different between groups. The null hypothesis is accepted if the F-value ≈ 1 ($MS_{between} \approx MS_{within}$), which means there is no difference in the means between groups (Miller, 1997).

In this study, ANOVA was applied to test the difference in sedimentation conditions, pigments and sedimentary UVR index between lakes using the *anova()* function in RStudio (version 1.2.1335) (R Core Team, 2020).

CHAPTER 5 RESULTS

This chapter presents the results of sedimentary proxies (chlorophyll and carotenoid pigments, chironomids (excluding Dongting and Honghu Lakes), TOC, TN, total phosphorus (TP), C/N ratios, $\delta^{13}C$ and $\delta^{15}N$) in each individual lake and historical archives in the catchments. The ^{210}Pb activities for dating the sediment cores from Honghu, Luhu, Wanghu and Poyang are already published in Chen et al., (2019). TP analyses of sediment cores from Dongting, Honghu, Luhu, Wanghu and Poyang Lakes were provided by J. Ji and X. Chen from China University of Geosciences (Wuhan). The results of Futou Lake (pigments, chironomids, TOC, TN, TP and C/N ratios) are previously published in Zeng (2016) as part of an MSc study, but are summarised here again and used in new analyses for later chapters.

5.1 Dongting Lake

5.1.1 Chronology

In general, $^{210}Pb_{excess}$ decreased exponentially from the top to the bottom of the sediment core and reached equilibrium at ca. 60 cm (Figure 5.1). Therefore, the CRS model was used to establish the chronology of the sediment core. ^{137}Cs was first detected at 47 cm and reached a peak of 22.13 Bq kg^{-1} at 39 cm before markedly decreasing (Figure 5.1). Thus, the ^{137}Cs peak at 39 cm was assigned to the maximum radionuclide fallout in 1963 CE (Ritchie and McHenry, 1990). Before the 1940s CE, dry mass accumulation rate (DMAR) was low (< 0.4 g cm^{-2} yr^{-1}) in Dongting Lake (Figure 5.1). Since the 1940s CE, DMAR markedly increased, reaching ~ 1.1 g cm^{-2} yr^{-1} in the 1990s CE, before decreasing to ~ 0.3 g cm^{-2} yr^{-1} in the 2010s CE.

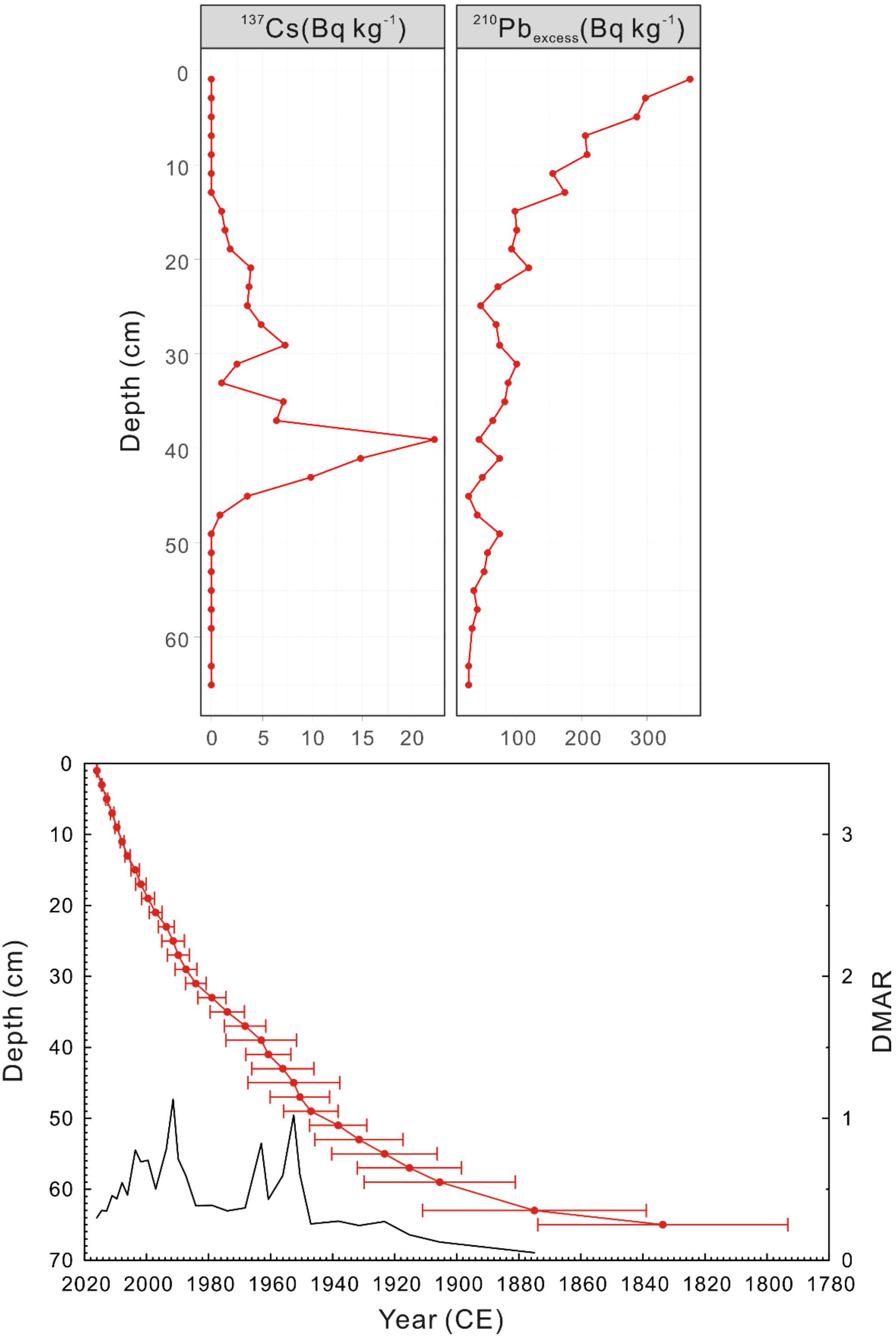

Figure 5.1 ^{137}Cs and ^{210}Pb activity profiles (upper) and age-depth model with error bar (red line) (lower) of the Dongting sediment core. DMAR (black solid line) is dry mass accumulation rate (g cm^{-2} yr^{-1}).

5.1.2 Sedimentary pigments

Generally, all sedimentary pigments showed an increasing trend throughout the whole sediment core with the exception of the UVR-absorbing compound which was not present in the top 9 cm of the sediment core (Figure 5.2). According to cluster analysis and the broken stick model, four major zones were identified in the sedimentary pigment profile. In Zone A (66-35 cm, ca. CE 1833-1974), concentrations of sedimentary pigments were low. All sedimentary pigments increased slightly in Zone B (35-21 cm, ca. CE 1974-1997), especially the UVR-absorbing compound (a mean concentration of 1.93 nmol g^{-1} TOC to > 11 nmol g^{-1} TOC in Zone B). In Zone C (21-9 cm, ca. CE 1997-2010), all sedimentary pigments further increased. For example, average concentration of alloxanthin increased more than 10-fold and β-carotene increased more than 13-fold in Zone C relative to Zone B. In Zone D (9-0 cm, ca. CE 2010-2016), all sedimentary pigments except the UVR-absorbing compound continuously increased. The most notable change in this zone is the sharp increase in aphanizophyll, a pigment from filamentous N_2-fixing cyanobacteria, which was not detected in previous zones; it sharply increased to 600 nmol g^{-1} TOC. In contrast, the UVR absorbing compound, which had a high concentration in Zone B and Zone C, was not detected in this zone.

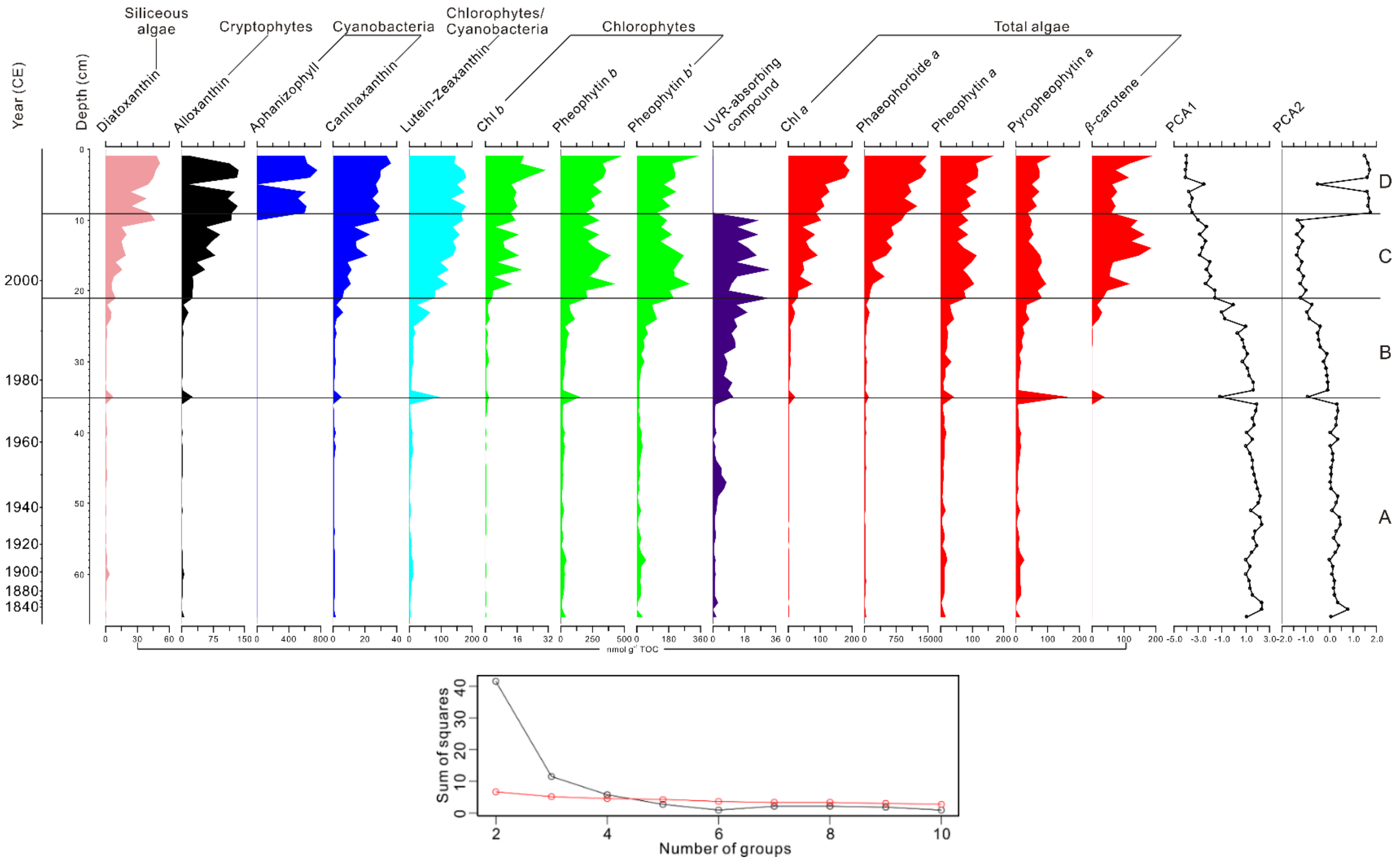

Figure 5.2 Changes in chlorophyll and carotenoid pigment concentrations and pigment PCA 1 and PCA 2 scores in the core from Dongting Lake (top). The capital letters on the right indicate the different pigment zones based on constrained cluster analysis and broken stick model. Group-by-sum of squares (SS) graph (bottom) comparing the dispersion of the classification at different fusion levels to a null model (black line) and the broken stick model (red line).

DCA showed that the gradient length of the pigment dataset was 1.07 SD, which is less than 2 SD, so PCA was used to summarize and simplify the pigment assemblages in Dongting Lake. The first PCA axis explained more than 80% of the variance in pigments and was significantly negatively correlated with all pigments ($R \leq -0.36$; $p < 0.005$) (Figure 5.3). The second PCA axis explained a further 12.7% of the variance in the pigments. PCA axis 2 was significantly positively correlated with aphanizophyll ($p < 0.0001$) and significantly negatively correlated with the UVR-absorbing compound ($p < 0.0001$). The four zones identified in constrained cluster analysis were distinctly identified in the PCA biplot (Figure 5.3). Samples in Zone A were distributed at the right of the biplot with little variance on the second PCA axis, characterized by low concentrations of all sedimentary pigments. Samples in Zone B gradually moved to the left and bottom of the biplot, indicating increases in all sedimentary pigments (except aphanizophyll), especially the UVR-absorbing compound. Samples in Zone C were distributed at the bottom left of the biplot, characterized by high concentrations of all sedimentary pigments except aphanizophyll. Samples in Zone D were distributed at the upper left of the biplot, characterized by high concentrations of all sedimentary pigments (except the UVR-absorbing compound), especially aphanizophyll.

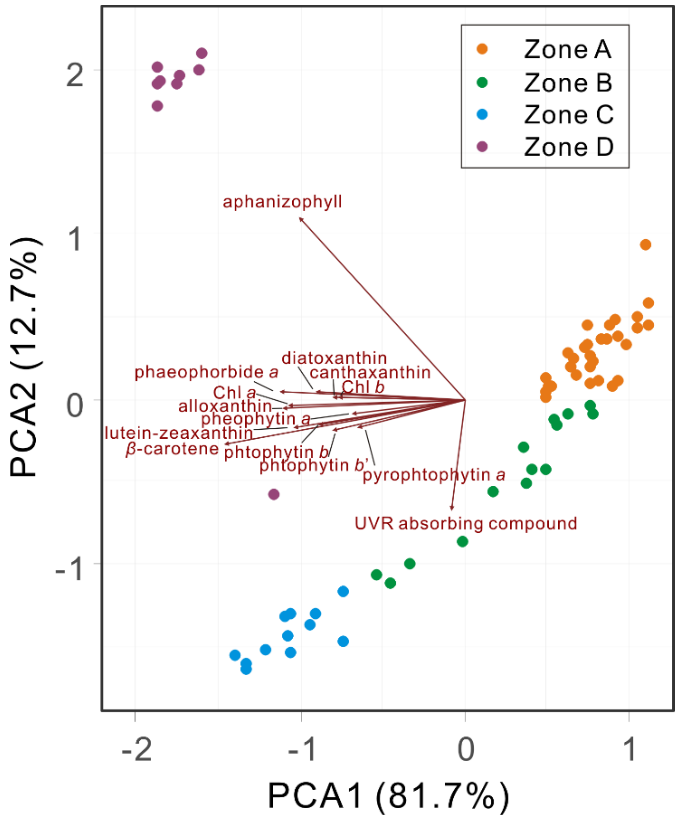

Figure 5.3 PCA ordination biplot of the pigments in the Dongting sediment core. Samples are classified based on the results of constrained cluster analysis and the broken stick model.

5.1.3 Sedimentary C and N mass and stable isotopes and TP

TOC (< 3 %) and TN (< 0.4 %) were low in the Dongting sediment core (Figure 5.4). Before ~2000 CE, TOC and TN slightly fluctuated at around 0.75% and 0.15%, respectively. After that, TOC and TN showed an upward trend before reaching a peak of 2.25% and 0.32% after 2008 CE. C/N ratios in the sediment core were low with a highest value of ~ 12. C/N ratios fluctuated at ~ 7 before ~ 1990 CE and increased between ~1990 CE and ~ 2005 CE. After 2005 CE, the C/N ratios remained at 8.3. Before ~ 1980s CE, $\delta^{13}C$ and $\delta^{15}N$ fluctuated at around –23.5‰ and 4.5‰, respectively. Since then, $\delta^{13}C$ gradually decreased to ~ –28‰ after 2010 CE, whereas $\delta^{15}N$ increased to 7.69‰ in 2010 CE and then slightly decreased to 7.28‰ in 2016 CE. TP showed a general increasing trend from the bottom to the top of the sediment core (Figure 5.4). TP fluctuated at around 0.055% before the 1950s CE, followed by a slight increase between the 1950s CE and the late 1980s CE. Since the late 1980s CE, TP sharply increased and remained at a peak at around 0.075% after 2010 CE.

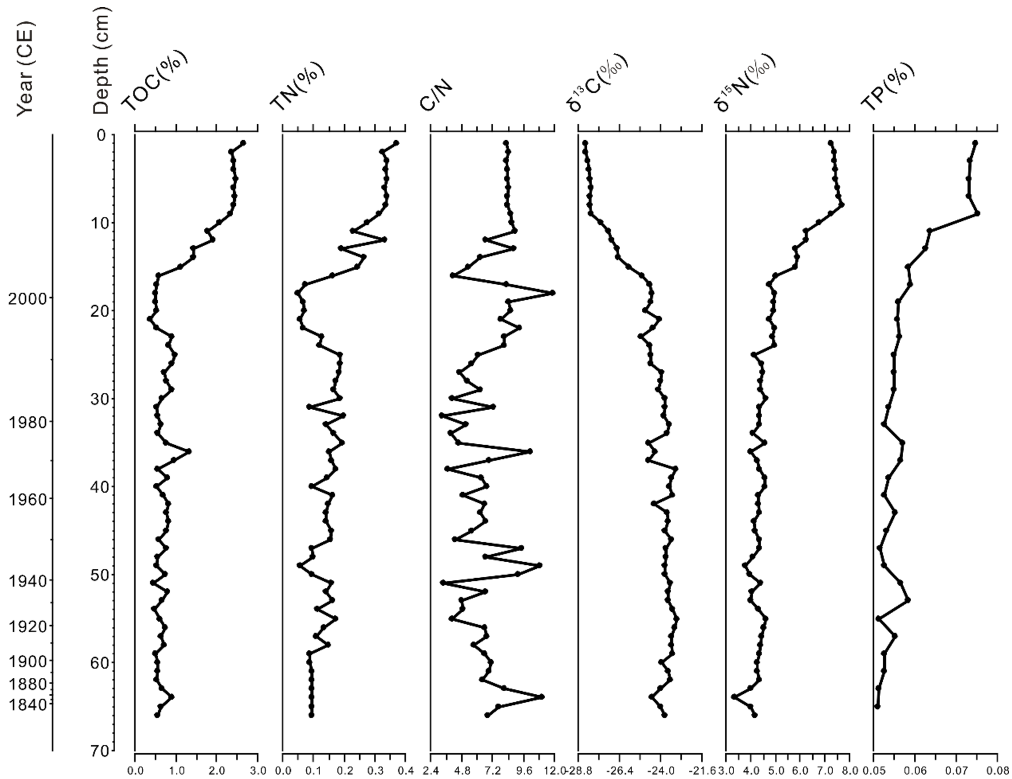

Figure 5.4 Changes in C and N mass, C/N ratios, $\delta^{13}C$, $\delta^{15}N$ and TP in the Dongting Lake sediment core. TP data was provided by J. Jin and X. Chen (China University of Geosciences (Wuhan)).

5.1.4 Historical archives

In 1949 CE, Hunan Province had a population of ca. 30 million, of which about 27.5 million (ca. 92.1%) lived in rural areas and the rest (7.9%) were in urban areas. After that, the population (mainly rural) experienced a 1.67-fold increase to ca. 46 million in 1980 CE (Figure 5.5a), except during the "Three Years of Great Famine" in the late 1950s CE and the early 1960s CE when the population decreased. Grain production in Hunan Province increased from 6.4 million metric tons in 1949 CE to more than 21 million metric tons in the early 1980s CE (Figure 5.5a). The usage of nitrogen fertilizers in Hunan Province increased from less than 10 thousand metric tons before the 1960s CE to about 480 thousand metric tons in 1980 CE and that of phosphorus fertilizers showed a ca. 25-fold increase from 5275 metric tons in 1958 CE to ca. 140 thousand metric tons in 1980 CE (Figure 5.5a). Aquaculture production was low before the 1980s CE (Figure 5.5a). Electricity and concrete production gradually increased from 4.27 billion kw·h and 150 thousand metric tons in 1958 CE to 11.9 billion kw·h and 5020 thousand metric tons in 1980 CE, respectively (Figure 5.5b). Urban population slightly increased from 2.36 million to 6.71 million, which accounted for 7.9% and 12.7% of the population in 1949 CE and 1980 CE, respectively (Figure 5.5b). The length of roads in the province was 3420 km and there were 1100 vehicles in Hunan Province in 1950 CE. In 1980 CE, the number had increased to 54897 km and 65200, respectively (Figure 5.5b).

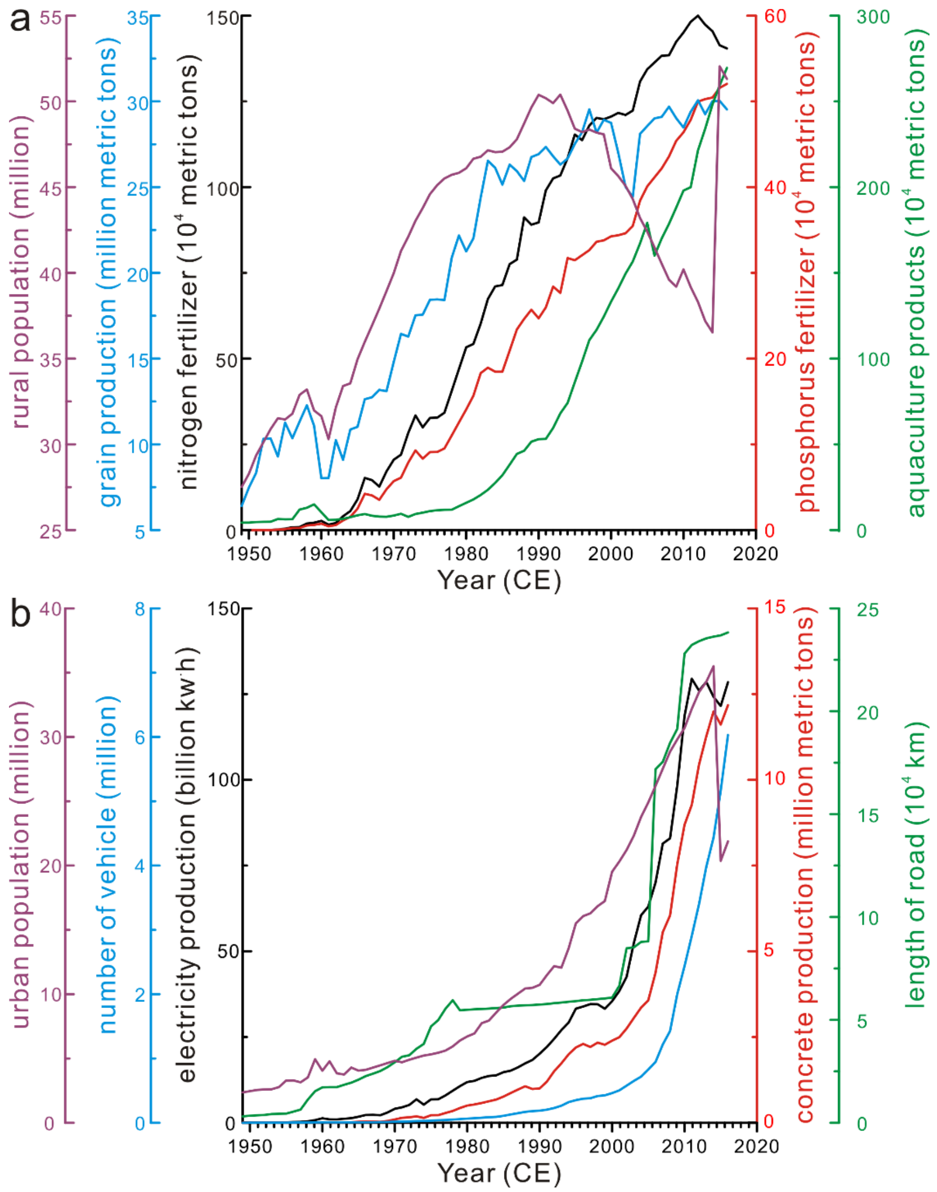

Figure 5.5 Historical archives of (a) agriculture and (b) industry and urbanization in Dongting Lake catchment.

Between 1980 CE and 2016 CE, there was a 39 percent increase in grain production from 21.2 million metric tons to 29.5 million metric tons, which was low compared with the 232 percent increase between 1949 CE and 1980 CE (Figure 5.5a). Rural population in Hunan Province gradually increased from ca. 46 million in 1980 CE to ca. 54 million in the middle 1990s CE and then decreased to 36.53 million in 2014 CE with urbanization (Figure 5.5a). At the same time, urban population showed an exponential increase from 6.7 million in 1980 CE to 35.5 million in 2014 CE (Figure 5.5b). By 2014 CE, about half of the population in Hunan Province were living in urban areas. The usage of nitrogen and phosphorus fertilizers increased from 478 thousand and 140 thousand metric tons in 1980 CE to 1259 thousand and 521 thousand metric tons in 2016 CE, respectively (Figure 5.5a). Compared with the gradual and slight increase before the 1980s CE, electricity production, concrete production, the number of vehicles and the length of road increased sharply since 1980 CE, especially after the late 1990s CE, a respective 272%, 420%, 1350% and 297% increase to 128.5 billion kw·h, 121.78 million metric tons, 6.03 million and 238.3 thousand km in 2016 CE (Figure 5.5b).

5.2 Honghu Lake

5.2.1 Chronology

^{210}Pb and ^{137}Cs profiles of the Honghu sediment core were published in Chen et al., (2019). In general, $^{210}Pb_{excess}$ exponentially decreased from the top to the bottom of the sediment core and reached equilibrium at ca. 54 cm (Figure 5.6). Therefore, the CRS model was used to establish the chronology of the sediment core. The CRS model gave a mean sedimentation rate of 0.33 cm yr^{-1} with the upper 54 cm representing 164 years of sediment accumulation. Chronology below 54 cm was established using a linear extrapolation from the lower four samples with measurable excess ^{210}Pb. DMAR was low in Honghu Lake (< 0.2 g cm^{-2} yr^{-1}) before the 1940s CE, followed by a rapid increase, reaching 0.8 g cm^{-2} yr^{-1} in the 1980s CE. Since the 1980s CE, DMAR decreased, reaching 0.2 g cm^{-2} yr^{-1} after 2010 CE (Figure 5.6).

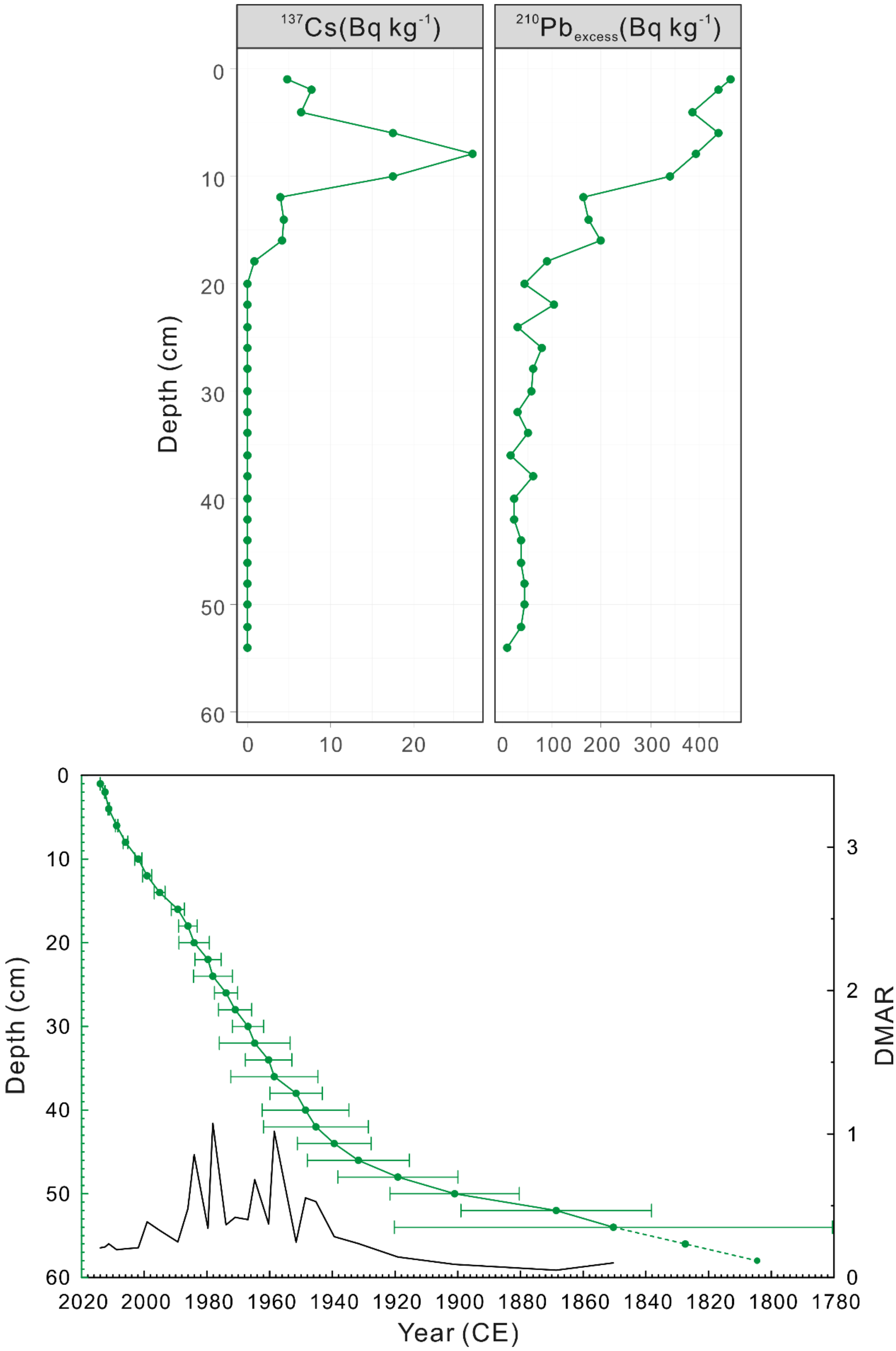

Figure 5.6 ^{137}Cs and ^{210}Pb activity profiles (upper) and age-depth model with error bar (green line) (lower) of the Honghu sediment core. The dashed line indicates results of linear extrapolation. Only dates after 1800 CE were shown. DMAR (black line) is dry mass accumulation rate (g cm^{-2} yr^{-1}). (Original data are from Chen et al., 2019).

5.2.2 Sedimentary Pigments

All sedimentary pigments showed an increasing trend throughout the whole sediment core with the exception of the UVR-absorbing compound which was not present in the top 4 cm of the sediment core (Figure 5.7). According to cluster analysis and the broken stick model, four major zones were identified in the sedimentary pigment profile. In Zone A (70-59 cm, ca. CE before 1800), concentrations of sedimentary pigments were low. In Zone B (59-40 cm, ca. CE before 1800-1949), pigment concentrations further decreased, with some below detection limit. In Zone C (40-13 cm, ca. CE 1949-1997), all sedimentary pigments increased compared with Zone A and B. In Zone D (13-0 cm, ca. CE 1997-2014), all sedimentary pigments continuously increased, with the exception of the UVR-absorbing compound. Although aphanizophyll (from N_2-fixing cyanobacteria) was not detected in previous zones, it appeared in Zone D for one sample. In contrast, the UVR absorbing compound, which had a high concentration in Zone C, sharply decreased and disappeared at the top of the core.

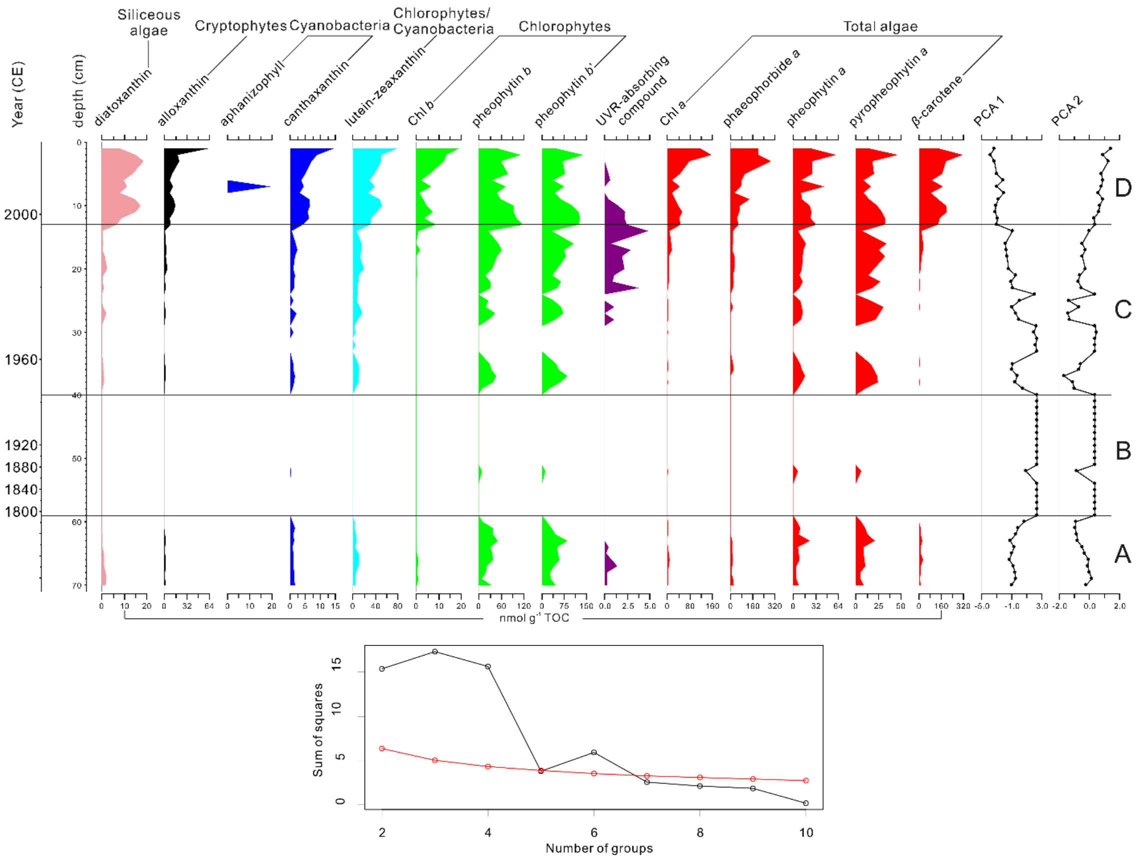

Figure 5.7 Changes in chlorophyll and carotenoid pigment concentrations and pigment PCA 1 and PCA 2 scores in the core from Honghu Lake (top). The capital letters on the right indicate the different pigment zones based on constrained cluster analysis and broken stick model. Group-by-sum of squares (SS) graph (bottom) comparing the dispersion of the classification at different fusion levels to a null model (black line) and the broken stick model (red line).

As the gradient length was less than 2 SD, PCA was used to extract the major trend in pigment dataset from Honghu sediment core. The first PCA axis explained more than 80% of the variance in pigments and was significantly negatively correlated with all pigments ($R \leq -0.43$; $p < 0.001$) except for aphanizophyll ($R = -0.19$; $p = 0.14$) (Figure 5.8). The second PCA axis explained a further 9.5% of the variance in pigments. The four zones identified in constrained cluster analysis were distinctly identified in the PCA biplot. Samples in Zone A were distributed at the centre of the biplot with little variance on the first PCA axis, characterized by relatively high concentrations of sedimentary pigments. Samples in Zone B gradually moved to the right of the biplot, indicating decreases in pigment concentrations. Samples in Zone C gradually moved to the left of the biplot, implying increases in pigment concentrations. Samples in Zone D were distributed at the upper left of the biplot, indicating sharp increases in pigment concentrations.

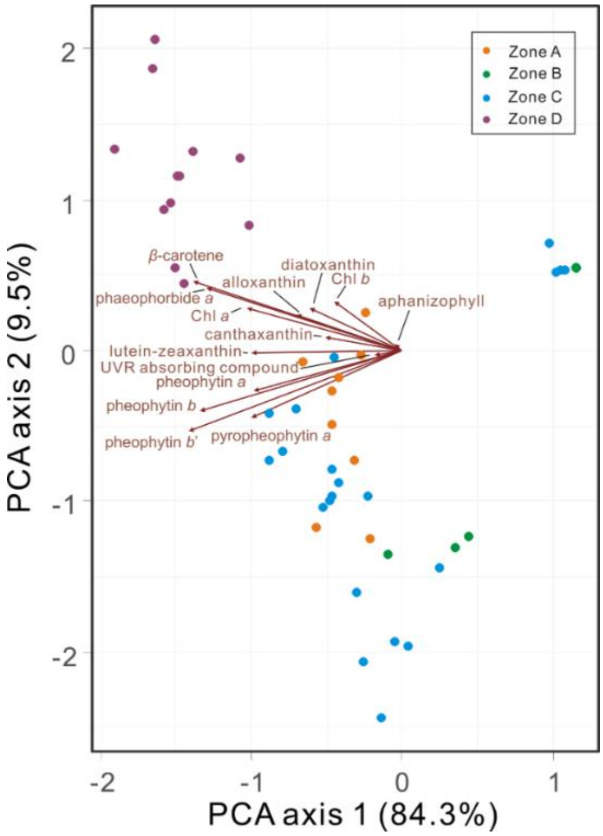

Figure 5.8 PCA ordination biplot of the pigments in Honghu sediment core. Samples are classified based on the results of constrained cluster analysis and the broken stick model.

5.2.3 Sedimentary C and N mass and stable isotopes and TP

Organic matter content in Honghu Lake was higher than that in Dongting Lake. TOC, TN and stable isotopes showed a four-section change in the sediment core (Figure 5.9). From the bottom of the sediment core to ~ the 1800s CE, TOC decreased from ~ 10% to ~ 1%; TN decreased from ~ 0.73% to ~ 0.1%, and C/N ratios decreased from ~ 17.5 to ~ 7.5. In contrast, $\delta^{13}C$ increased from ~ –27.5‰ to ~ –22.5‰ and $\delta^{15}N$ increased from ~ 2.0‰ to ~ 5.0‰. Between the 1800s CE and the 1970s CE, TOC, TN and the C/N ratios remained at low values, and $\delta^{13}C$ and $\delta^{15}N$ were high. From the 1970s CE to the 2010s CE, TOC and TN sharply increased to more than 20% and ~ 2%, respectively. $\delta^{13}C$ increased but $\delta^{15}N$ decreased during this period. Since the 2010s CE, TOC and $\delta^{13}C$ remained stable in Honghu Lake, and TN and $\delta^{15}N$ showed an upward trend. TP fluctuated at around 0.065% before the 1970s CE. Between the 1970s CE and the 2010s CE, TP slightly decreased from around 0.075% to 0.055%.

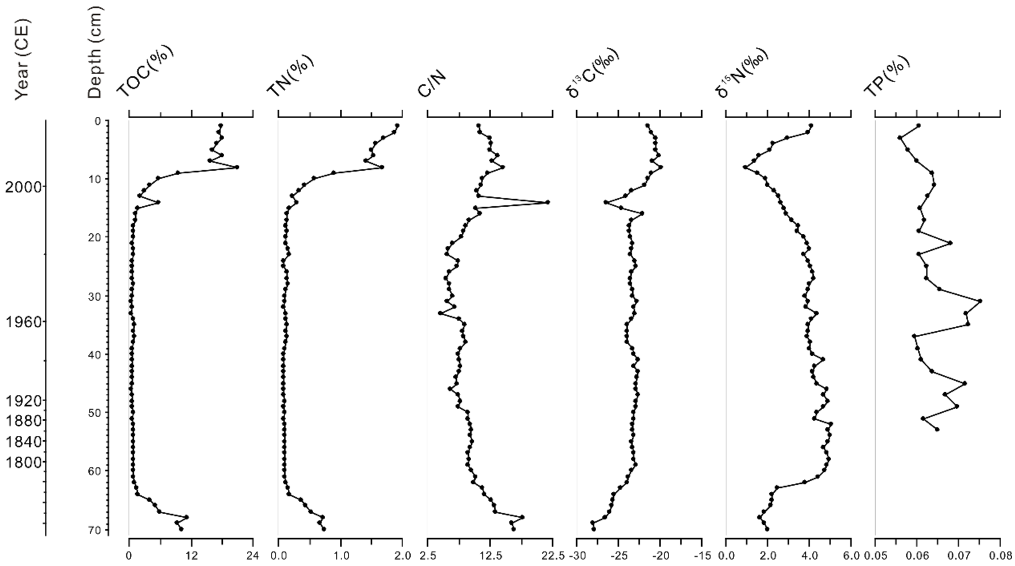

Figure 5.9 Changes in C and N mass, C/N ratios, $\delta^{13}C$, $\delta^{15}N$ and TP in the Honghu Lake sediment core. TP data was provided by J. Jin and X. Chen (China University of Geosciences (Wuhan)).

5.2.4 Historical archives

Agriculture developed extensively in Jingzhou between 1949 CE and the early 1980s CE (Figure 5.10a). Most of the population (ca. 90%) inhabited rural areas in Jingzhou before 1980 CE. The rural population experienced a 1.7-fold increase from 1.72 million in 1949 CE to 2.95 million in 1980 CE (Figure 5.10a). Accompanying the increase in population, grain production increased from ca. 0.7 million metric tons to about 2.5 million metric tons between 1949 CE and the early 1980s CE (Figure 5.10a). As an efficient way to increase the production of agricultural products, nitrogen and phosphorus fertilizer usage increased from ca. 12 and 4 metric tons in 1952 CE to ca. 43 and 13 thousand metric tons in 1980 CE, respectively (Figure 5.10a). In contrast to the agriculture trends, industry and urbanization developed more slowly between ~1950s CE and ~1980s CE, with a slight increase of urban population (from ca. 0.15 to ca. 3.5

million), electricity production (from about 0.01 to 0.6 billion kw·h), concrete production (from 0 to 175 thousand metric tons), the number of vehicles (from 6 to 2868) and the length of roads (from ca. 190 to 3541 km) (Figure 5.10b).

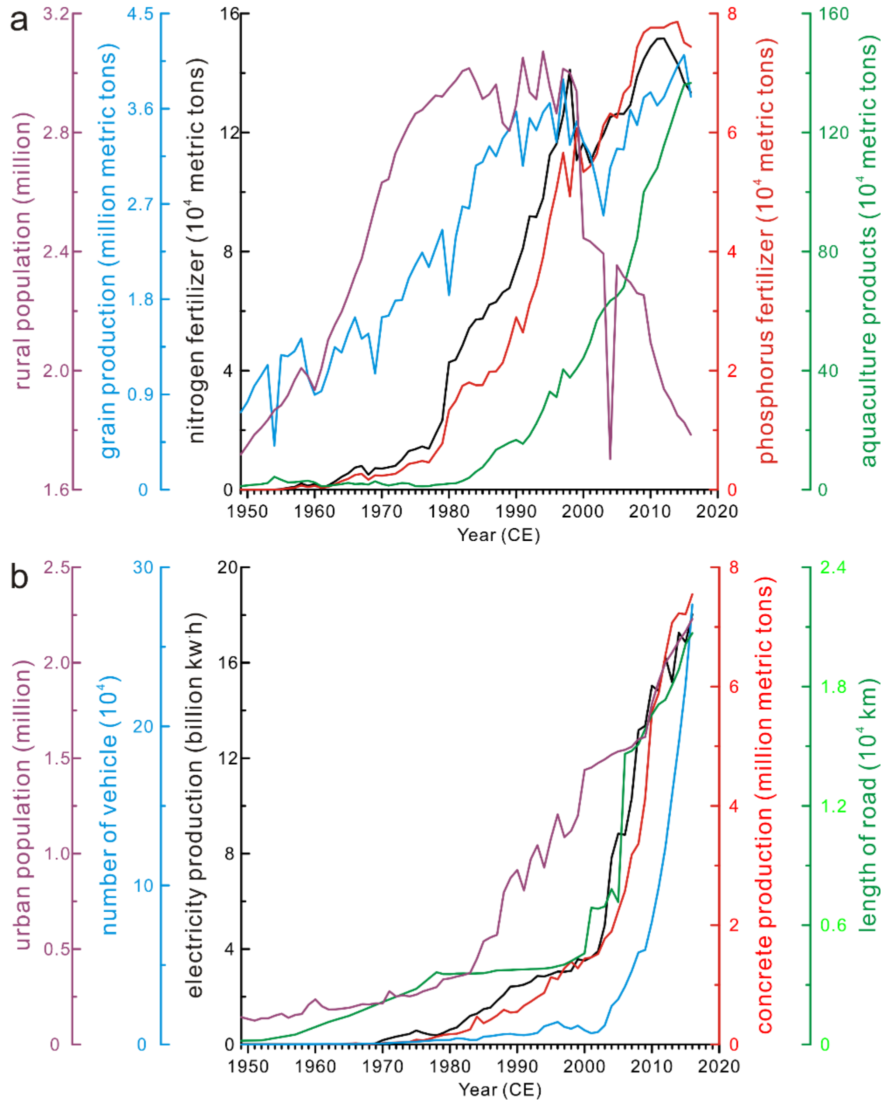

Figure 5.10 Historical archives of (a) agriculture and (b) industry and urbanization in the Honghu Lake catchment.

Since the early 1980s CE, industrial development and urban expansion intensified while the development of agriculture slowed down. Urban population gradually exceeded the agricultural population since 2012 CE (Figure 5.10b). In 2016 CE, there were 2.23 million people living in the urban area, accounting for 55.5% of the total population. After the 1980s CE, and especially since the late 1990s CE, the production of electricity and concrete, the number of vehicles and the length of road showed an exponential expansion from 0.6 billion kw·h, 175 thousand metric tons, 2868 and 3541 km in 1980 CE to 18 billion kw·h, 7.55 million metric tons, 276,659 and 20,699 km in 2016 CE, respectively (Figure 5.10b).

5.3 Futou Lake

Sedimentary results of the chronology, chlorophyll and carotenoid pigments, chironomids, TOC and TN content and C/N ratios are from Zeng (2016) and ^{210}Pb activities and chironomids are published in Zeng et al., (2018).

5.3.1 Chronology

$^{210}Pb_{excess}$ exponentially decreased from the top to the bottom of the sediment core and reached an equilibrium at ca. 65 cm (Figure 5.11). The ^{137}Cs peak was not obvious in the Futou Lake sediments so the chronology was established based upon the ^{210}Pb with the CRS model. The chronology below 65 cm was extrapolated from the lower three samples with measurable excess ^{210}Pb. DMAR was low (< 0.2 g cm^{-2} yr^{-1}) in Futou Lake before the 1900s CE. Between the 1900s CE and the 1930s CE, DMAR increased to ~ 0.4 g cm^{-2} yr^{-1} (Figure 5.11). Since the 1930s CE, DMAR further increased to ~ 0.8 g cm^{-2} yr^{-1} in the 1970s CE, followed by a gradual decrease, reaching 0.2 g cm^{-2} yr^{-1} in the 2010s CE.

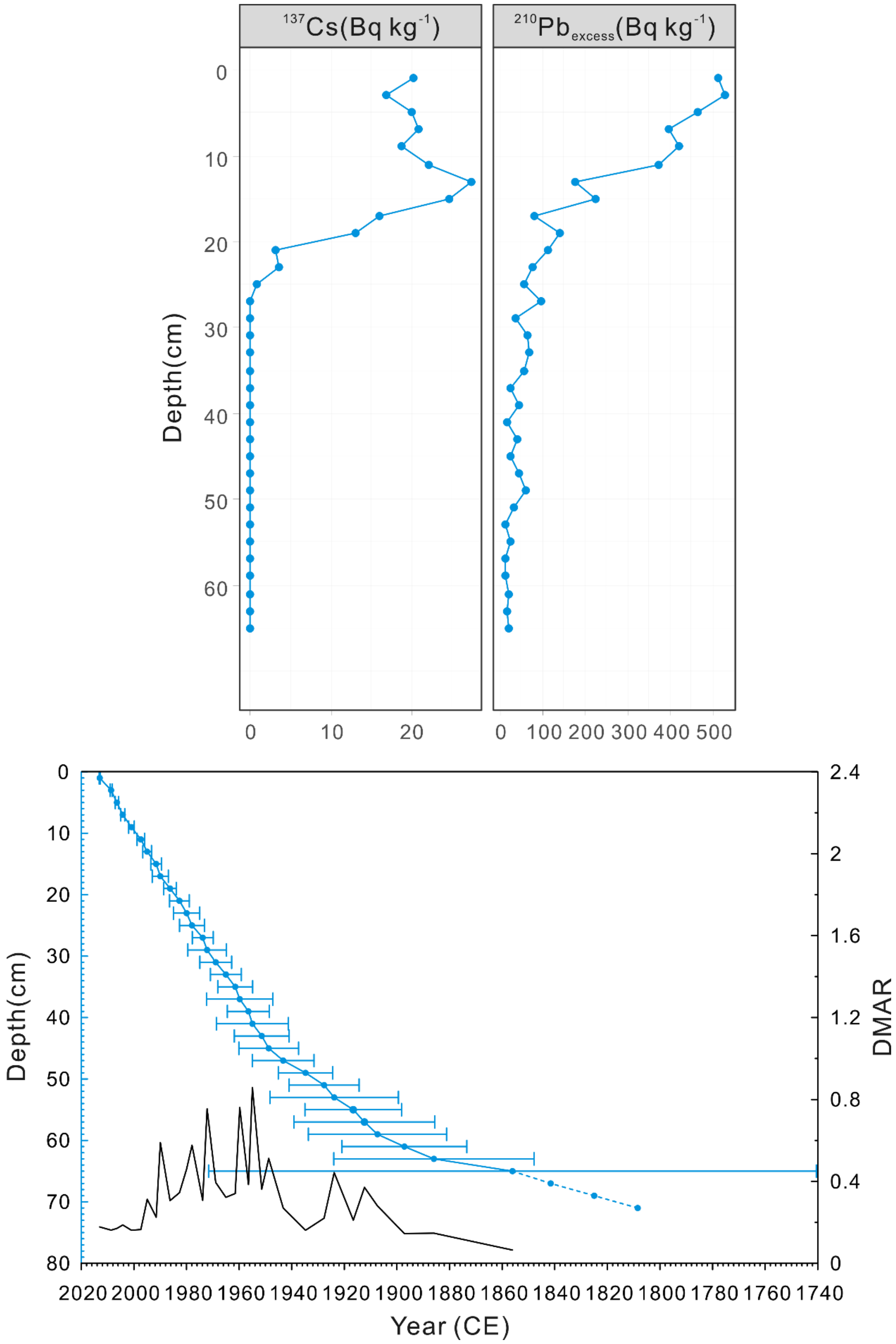

Figure 5.11 ^{137}Cs and ^{210}Pb activity profiles (upper) and age-depth model with error bar (blue line) (lower) of the Futou sediment core. The dashed line indicates results of linear extrapolation. Only dates after 1800 CE were shown. DMAR (black line) is dry mass accumulation rate (g cm^{-2} yr^{-1}). (Original data from Zeng, 2016).

5.3.2 Sedimentary pigments

Sedimentary pigments in Futou Lake showed an overall upward trend with the exception of the UVR-absorbing compound which decreased at the top of the sediment core (Figure 5.12). According to cluster analysis and the broken stick model, three major zones were identified in the sedimentary pigment profile. In Zone A (82-35 cm, ca. AD before 1800-1961), concentrations of sedimentary pigments were relatively low. In Zone B (35-8 cm, ca. AD 1961-2004), pigment concentrations gradually increased. Concentrations of all pigments further increased in Zone C (8-0 cm, ca. AD 2004-2013) with the exception of the UVR-absorbing compound which sharply decreased and vanished at the top of the core. In Futou Lake, aphanizophyll was not detected throughout the sediment core.

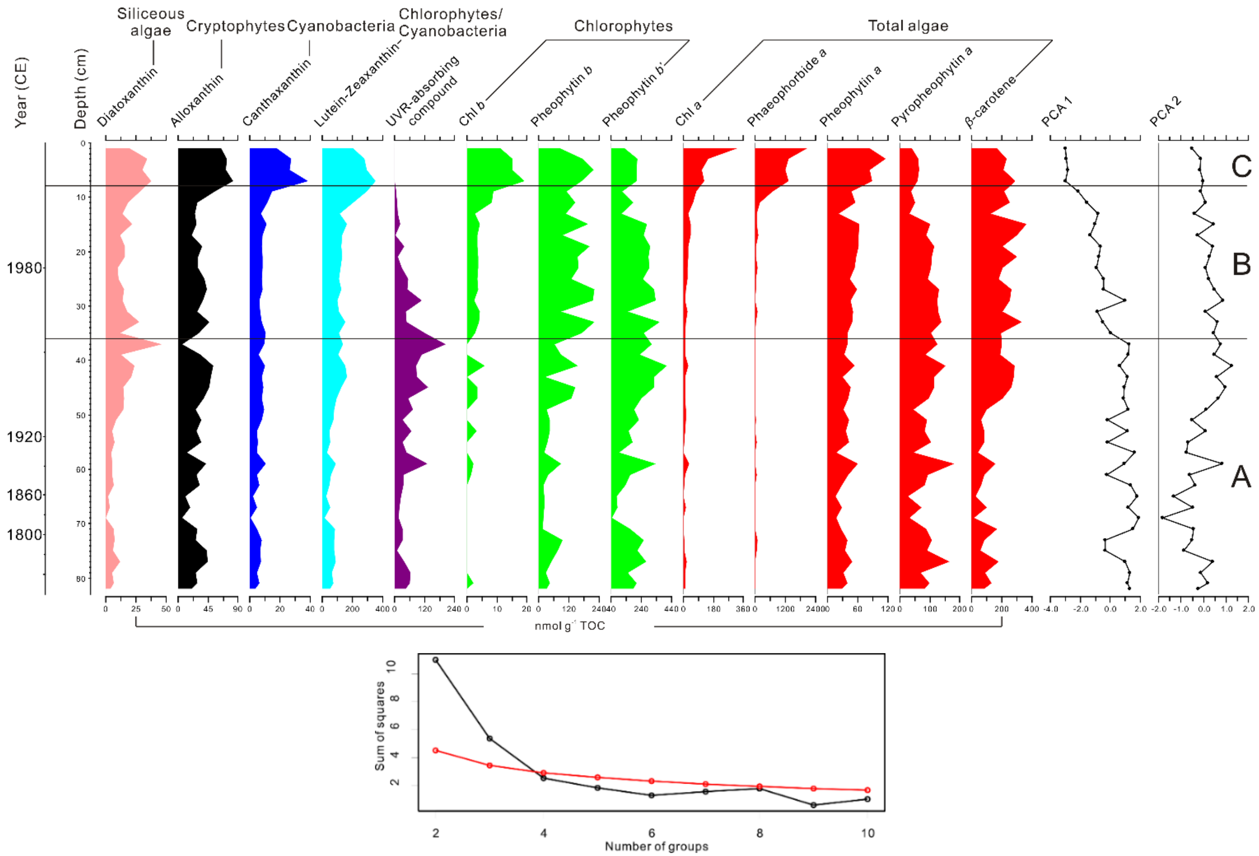

Figure 5.12 Changes in chlorophyll and carotenoid pigment concentrations and pigment PCA 1 and PCA 2 scores in the core from Futou Lake (top). The capital letters on the right indicate the different pigment zones based on constrained cluster analysis and broken stick model. Group-by-sum of squares (SS) graph (bottom) comparing the dispersion of the classification at different fusion levels to a null model (black line) and the broken stick model (red line). (Original data from Zeng, 2016).

DCA showed that the gradient length of the pigment dataset was 0.87 SD, which was less than 2 SD, so PCA was used to summarize and simplify the pigments in Futou Lake. The first PCA axis explained ~ 75% of the variance in pigments and was significantly negatively correlated with all pigments ($p < 0.005$) except pheophytin *b*' and pyropheophytin *a* (Figure 5.13), and significantly positively correlated with the UVR-absorbing compound. The second PCA axis explains a further 14.5% of the variance in pigments. PCA axis 2 was significantly negatively correlated with alloxanthin, diatoxanthin, pheophytin *b*, pheophytin *b*', *β*-carotene, pyropheophytin *a* and the UVR-absorbing compound ($p < 0.05$). The three zones identified in constrained cluster analysis are distinctly identified in the PCA biplot. Samples in Zone A are distributed at the right of the biplot, characterized by high concentration of the UVR-absorbing compound. Samples in Zone B gradually move to the left of the biplot, implying increases in all pigment concentrations with the exception of the UVR absorbing compound. Samples in Zone C are distributed at the leftmost of the biplot, indicating high concentrations of sedimentary pigments while low concentrations of the UVR-absorbing compound.

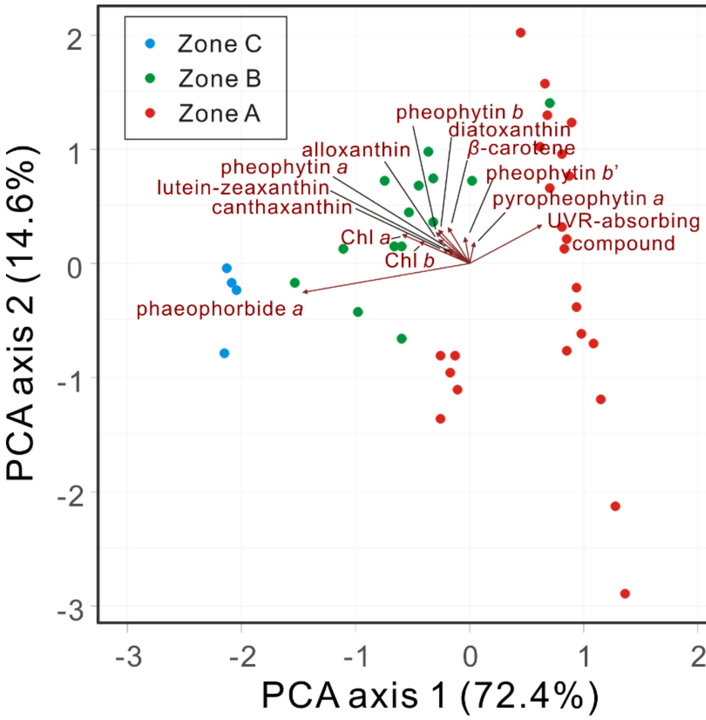

Figure 5.13 PCA ordination biplot of the pigments in Futou sediment core. Samples are classified based on the results of constraint cluster analysis and the broken stick model.

5.3.3 Sedimentary C and N mass and stable isotopes and TP

TOC and N mass and C/N ratios showed an upward trend in the Futou Lake sediment core (Figure 5.14). Before the 1980s CE, TOC and TN content were relatively low and stabilized at 1% and 0.12%, respectively. C/N ratios were low as well, slightly fluctuating at around 7. Since the 1980s CE, TOC and TN content in the sediments sharply increased, reaching ca. 6% and 0.48% after 2000 CE, respectively. $\delta^{13}C$ was generally low before the 1960s CE, fluctuating at around –25‰, followed by a slight increase, reaching ca. –22‰ at around 2000 CE. Since 2000 CE, $\delta^{13}C$ slightly decreased. $\delta^{15}N$ showed a similar trend to $\delta^{13}C$, which was relatively low before the 1960s CE (~ 3‰) and gradually increased to ~ 7‰ at around 2000 CE, followed by a slight decrease thereafter. TP content in the sediment core gradually decreased from 0.075% in the early

20th century to 0.06% in the late 1990s CE, followed by a sharp increase, reaching 0.085% in the 2010s CE.

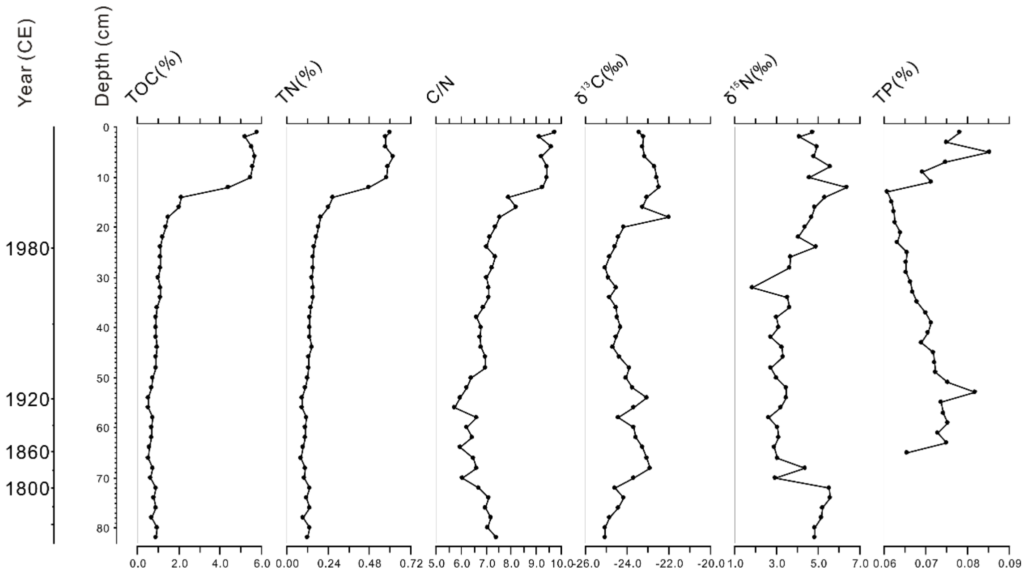

Figure 5.14 Changes in C and N mass, C/N ratios, $\delta^{13}C$, $\delta^{15}N$ and TP in the Futou Lake sediment core. (C and N mass, C/N ratios and TP data are from Zeng (2016), Zeng et al., (2018)).

5.3.4 Chironomids

In total, 42 chironomid species were identified in the Futou sediment core. Only those (25 taxa) occurring in at least two samples and with an abundance ≥ 2% in at least 1 sample were presented and used for analysis (Figure 5.15). Chironomids in Futou Lake were dominated by *M. tener*-type, *Paratanytarsus* sp., *P. penicillatus*-type, and *C. sylvestris*-type. According to cluster analysis and the broken stick model, two major zones were identified in the chironomid stratigraphic profiles (Figure 5.15). Zone A (81-19 cm, ca. CE before 1800-1986) can be divided into two subzones, A1 and A2. Subzone A1 (81-49 cm, ca. CE before 1800-1935) was dominated by *M. tener*-type (average ~ 38.9%), while *Paratanytarsus* sp., *P. penicillatus*-type, and *C. sylvestris*-type were rarely identified. In subzone A2 (49-19 cm, ca. CE 1935-1986), *M. tener*-type (average ~ 36.4%) was still abundant. Concurrently, the average abundance of

Paratanytarsus sp., *P*. *penicillatus*-type, and *C*. *sylvestris*-type increased to 9.1%, 13.1%, and 4.6%, respectively. Zone B (19-0 cm, ca. CE 1986-2013) was co-dominated by *Paratanytarsus* sp., *P*. *penicillatus*-type, and *C*. *sylvestris*-type, with the average abundance increased to 17.3%, 28.4 % and 17.8%, respectively. In contrast, abundance of *M. tener*-type rapidly decreased (average ~ 10.6%). Meanwhile, eutrophic species, such as *C. plumosus*-type, *G. severini*-type and *P. akamusi*-type which were rarely identified in Zone A, were more frequently identified in this zone.

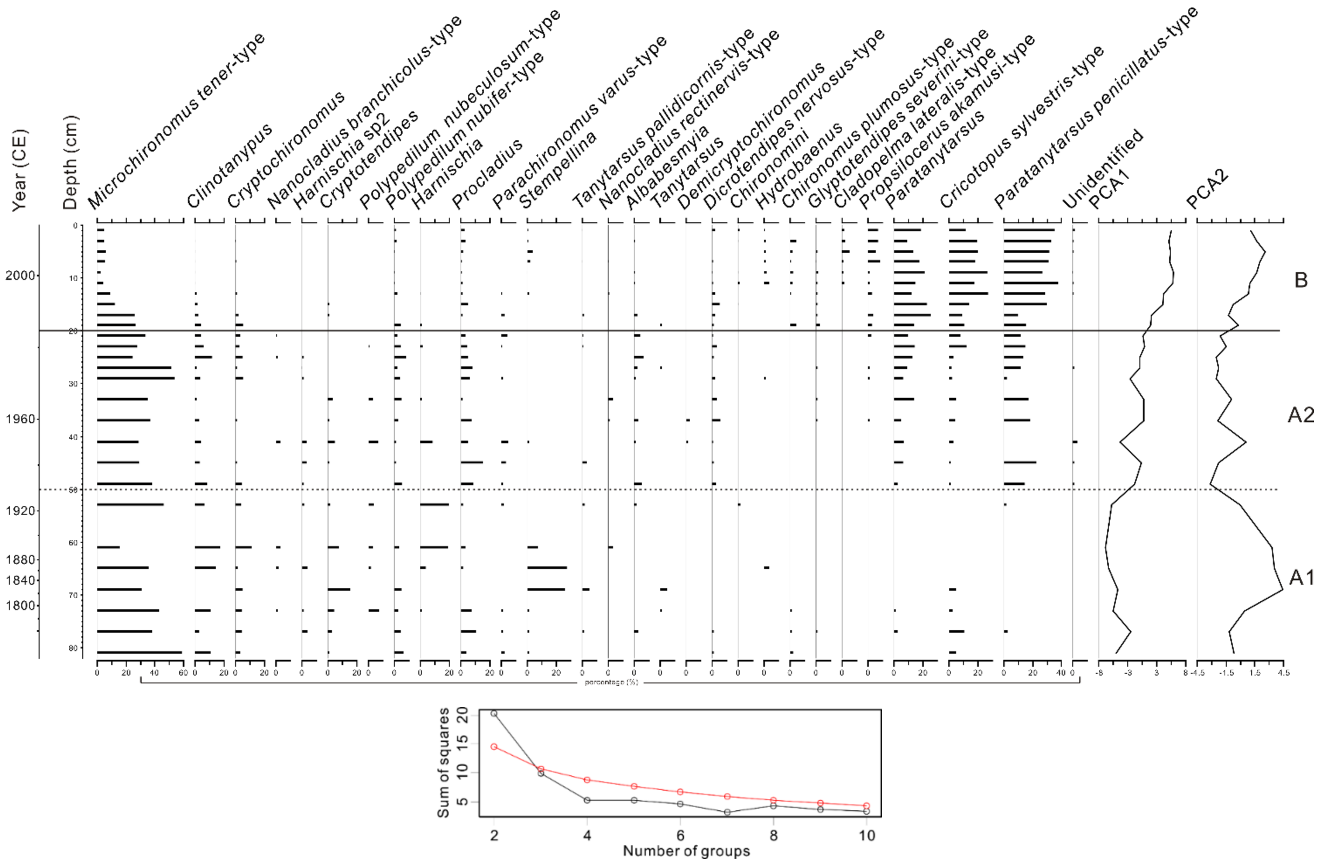

Figure 5.15 Changes in chironomid communities and PCA 1 and PCA 2 scores in the core from Futou Lake (top). The capital letters on the right indicate the different chironomid zones based on constrained cluster analysis and broken stick model. Group-by-sum of squares (SS) graph (bottom) comparing the dispersion of the classification at different fusion levels to a null model (black line) and the broken stick model (red line). (Original data from Zeng (2016)).

DCA showed that the gradient length of the chironomid dataset was 2.2 SD, so PCA was used to summarize chironomid assemblages in Futou Lake. The results showed that the first and second PCA axes explained 46.3% and 14.1% of the changes in chironomids, respectively (Figure 5.16). The first PCA axis was significantly and negatively correlated with species such as *M. tener*-type, and positively correlated with species such as *Paratanytarsus* sp., *P. penicillatus*-type, and *C. sylvestris*-type ($p < 0.001$). The three zones/subzones of chironomids were distinctly identified in the PCA biplot (Figure 5.16). Samples in Zone A1 were distributed at the left of the biplot with high variability on PCA axis 2, characterized by high concentrations of *M. tener*-type. Samples in Zone A2 gradually moved from the left to the right of the biplot, along the first PCA axis, while there were low sample scores on PCA axis 2. Samples in Zone B were distributed at the right of the biplot, with a strong relationship with species such as *Paratanytarsus* sp., *P. penicillatus*-type, and *C. sylvestris*-type.

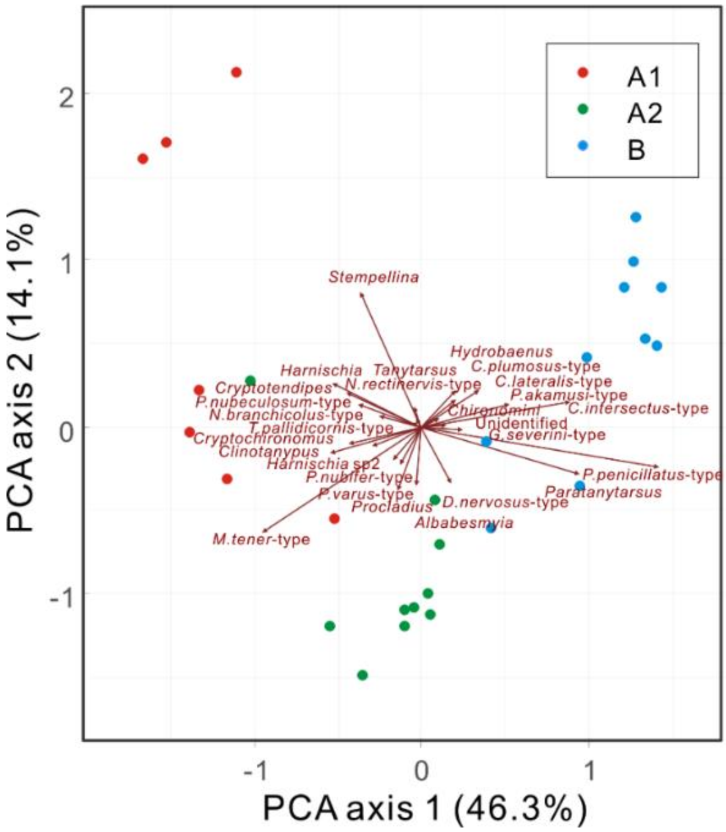

Figure 5.16 PCA ordination biplot of the chironomids in Futou sediment core. Samples are classified based on the results of constrained cluster analysis and the broken stick model.

5.3.5 Historical archives

The rural population in the Futou catchment experienced a ca. 5-fold increase from ca. 1.5 million in 1949 CE to more than 7.5 million in the 1980s CE (Figure 5.17a). Accompanying the increase in population, grain production increased from less than 0.4 million to more than 1.4 million between 1949 CE and the early 1980s CE (Figure 5.17a). Concurrently, nitrogen and phosphorus fertilizer usage increased from close to 0 in 1952 CE to ca. 90 and 45 thousand metric tons respectively in the 1980s CE (Figure 5.17a). In contrast to the agriculture trends, industry and urbanization developed more slowly during this period (Figure 5.17b).

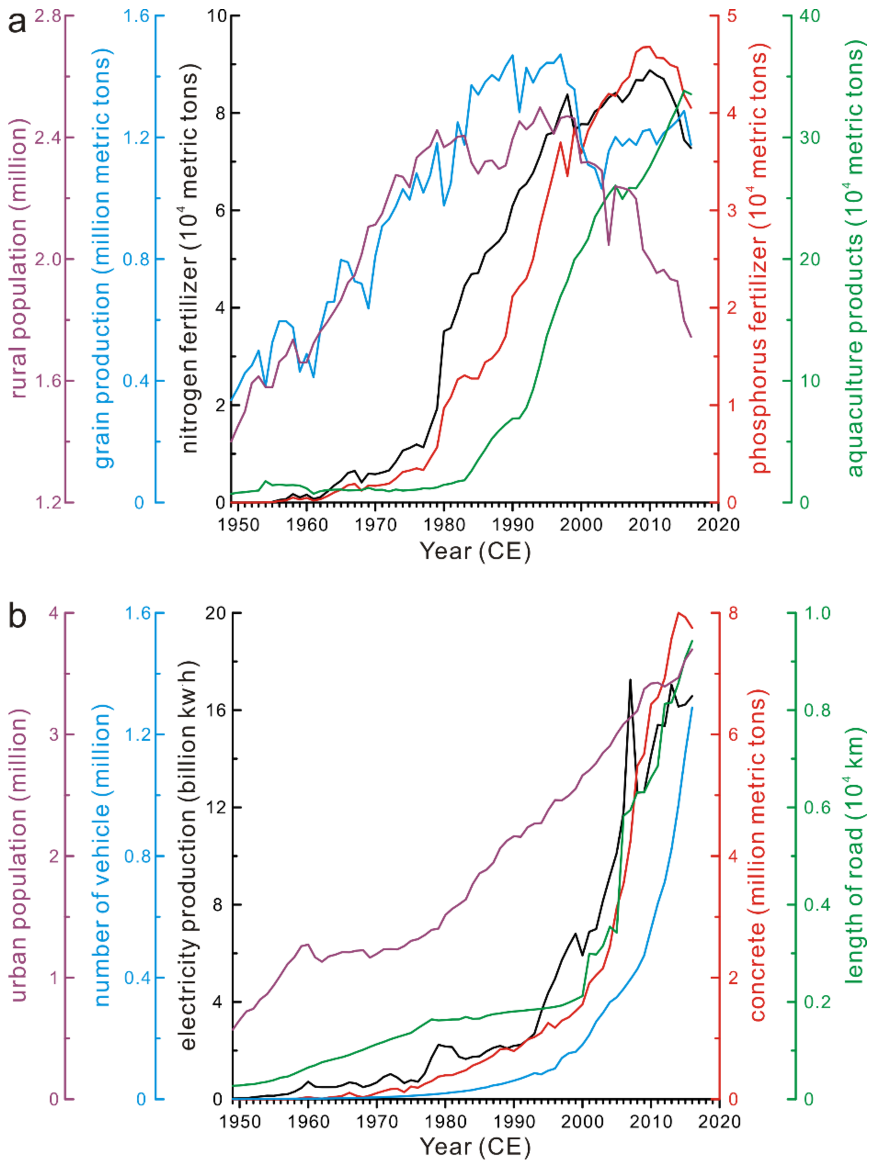

Figure 5.17 Historical archives of (a) agriculture and (b) industry and urbanization in the Futou Lake catchment.

Since the early 1980s CE, industrial development and urban expansion intensified (Figure 5.17b), whilst the development of agriculture slowed down (Figure 5.17a). Urban population exceeded the agricultural population after 2012 CE. In 2016 CE, there were more than 3.5 million people living in the urban area, accounting for ca. 70 % of the total population (Figure 5.17b). After the 1980s CE, and especially since the late 1990s CE, the production of electricity and concrete, the number of vehicles and the length of road showed an exponential expansion (Figure 5.17b). For example, electricity and concrete production increased from ca. 2 billion kw·h and 0.5 million metric tons in the early 1980s CE to more than 16 billion kw·h and ca. 8 million metric tons in 2016 CE, respectively (Figure 5.17b).

5.4 Luhu Lake

5.4.1 Chronology

^{210}Pb and ^{137}Cs of Luhu sediment core are presented in Chen et al. (2019). Excess ^{210}Pb activity in the sediment core showed an exponential declining trend from the top to the bottom of the sediment core and reached an equilibrium at 52 cm (Figure 5.18). The activity of ^{137}Cs was relatively low compared with other Northern Hemisphere lakes (Moorhouse, 2016) and did not have an obvious peak in the sediment core. Therefore, chronology of the sediment core was established using the ^{210}Pb with the CRS model, which gave a mean sediment rate of 0.31 cm yr^{-1} with the upper 52 cm covering 168 years. Chronology below 52 cm was calculated using a linear extrapolation from the last three samples with measurable excess ^{210}Pb. DMAR was low (< 0.2 g cm^{-2} yr^{-1}) in Luhu Lake before the 1930s CE, followed by a gradual increase to ~ 0.3 g cm^{-2} yr^{-1} in the 2010s CE (Figure 5.18).

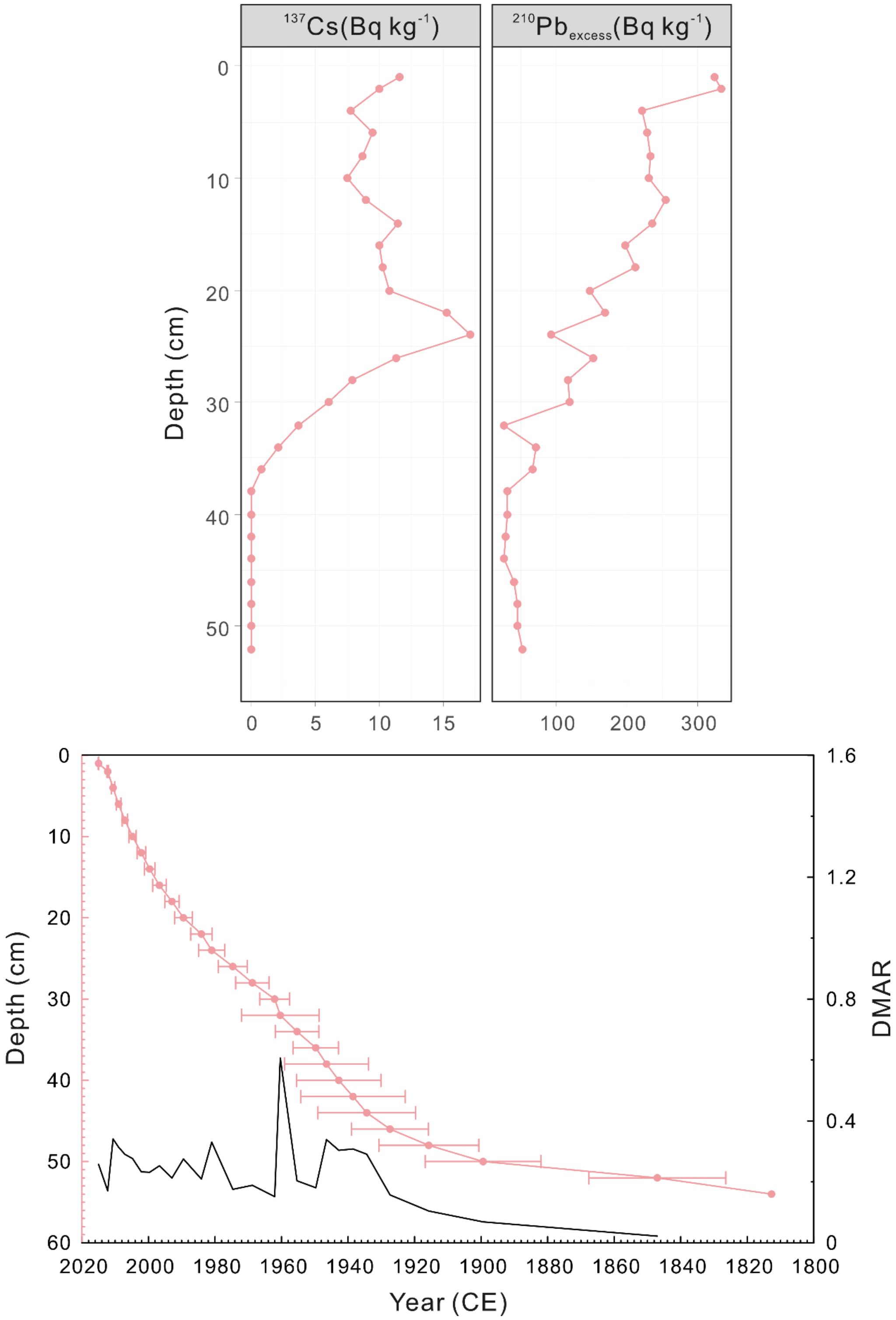

Figure 5.18 ^{137}Cs and ^{210}Pb activity profiles (upper) and age-depth model with error bar (pink line) (lower) of the Luhu sediment core. The dashed line indicates results of linear extrapolation. Only dates after 1800 CE were shown. DMAR (black line) is dry mass accumulation rate (g cm^{-2} yr^{-1}). (Original data were from Chen et al., 2019).

5.4.2 Sedimentary pigments

Similar to Dongting Lake, all sedimentary pigments in Luhu Lake showed a general increasing trend throughout the sediment core, with the exception of the UVR-absorbing compound (Figure 5.19). According to cluster analysis and the broken stick model, three zones were identified in the pigment profile (Figure 5.19). In Zone A (87-64 cm), concentrations of all sedimentary pigments were low. Pigments from N_2-fixing cyanobacteria (aphanizophyll) were not detected. In Zone B (64-13 cm, ca. CE before 1800-2001), all sedimentary pigments increased with the exception of aphanizophyll. For instance, the average concentration of *β*-carotene and Chl *a* doubled in Zone B relative to Zone A. In Zone C (13-0 cm, ca. CE 2001-2015), all pigments except the UVR-absorbing compound sharply increased. Canthaxanthin increased 4-fold, alloxanthin more than doubled. In this Zone, aphanizophyll appeared for the first time with a mean concentration of 467 nmol g^{-1} TOC, and the UVR-absorbing compound gradually declined to undetectable levels.

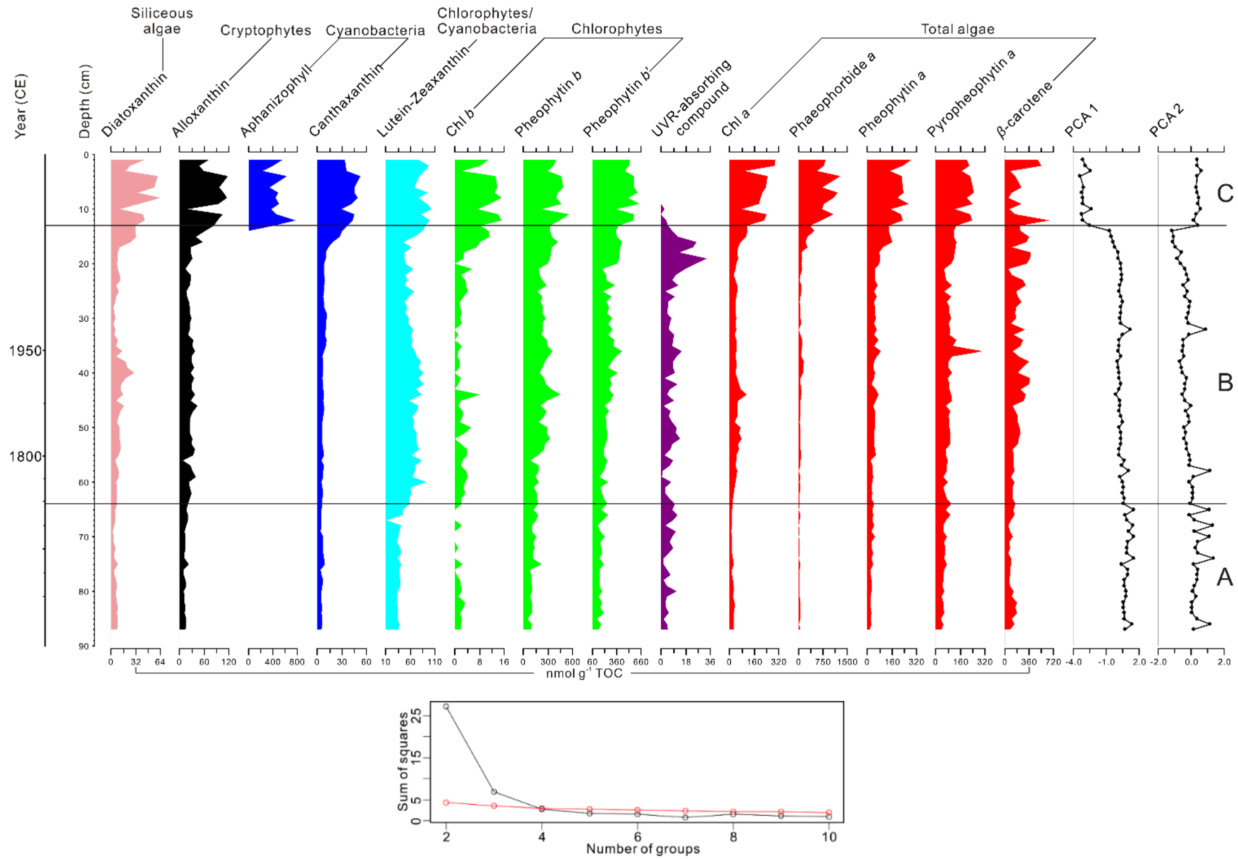

Figure 5.19 Changes in chlorophyll and carotenoid pigment concentrations and pigment PCA 1 and PCA 2 scores in the core from Luhu Lake (top). The capital letters on the right indicate the different pigment zones based on constrained cluster analysis and broken stick model. Group-by-sum of squares (SS) graph (bottom) comparing the dispersion of the classification at different fusion levels to a null model (black line) and the broken stick model (red line).

As DCA analysis showed that the gradient length of pigments is 0.72 SD which was less than 2 SD, PCA was used to summarize the major trends in pigments. The first and the second PCA axis explained 72.8% and 12.4% of the changes in pigments, respectively (Figure 5.20). The first PCA axis was significantly positively correlated with the UVR-absorbing compound ($R = 0.30$; $p < 0.005$) and significantly negatively correlated with the other pigments ($R \leq -0.36$; $p < 0.0001$). The second PCA axis was significantly positively correlated with aphanizophyll ($R = 0.28$; $p < 0.05$) while negatively correlated with UVR-absorbing compound ($R = -0.61$; $p < 0.0001$). The three pigment zones were clearly distinguished in the PCA biplot. Samples in Zone A were distributed at the upper and righthand quadrant of the biplot, characterized by low concentrations of all sedimentary pigments. Zone B samples were located at the right bottom of the biplot, indicating an increase of all pigments with the exception of aphanizophyll. Zone C samples were distributed at the upper left of the biplot, implying the increase in all pigments, especially aphanizophyll, alongside a decrease in the UVR-absorbing compound.

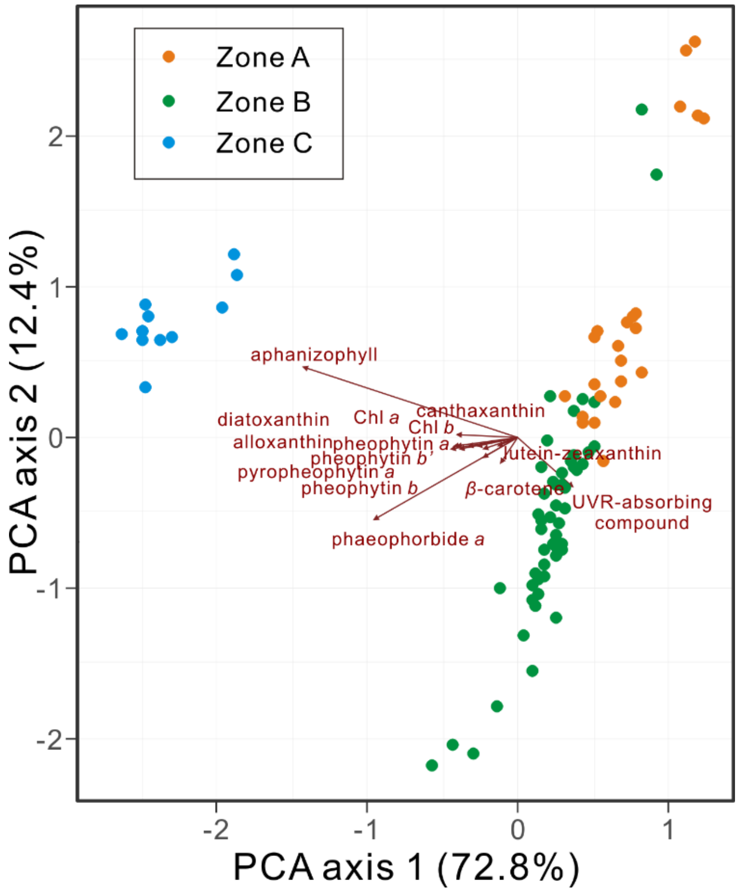

Figure 5.20 PCA ordination biplot of the pigments in Luhu sediment core. Samples are classified based on the results of constrained cluster analysis and the broken stick model.

5.4.3 Sedimentary C and N mass and stable isotopes and TP

TOC and TN showed an overall upward trend in the Luhu sediment core (Figure 5.21). From the bottom to around 70 cm, TOC and TN slightly decreased from about 1.5% and 0.2% to about 1% and 0.15%, respectively. TOC and TN remained at around 1% and 0.15% between 70 cm and 35 cm (ca. 1953 CE), respectively, followed by an increase thereafter. Between 35 cm and 18 cm (ca. 1950 to the late 1980s CE), TOC increased from 1% to ~ 1.5% and TN increased from 0.15% to ~ 0.2%. Between 18 cm and 11 cm (ca. the early 1990s to 2005 CE), TOC doubled from 1.5% to ~3% and TN increased from 0.2% to 0.4% and remained at their maxima thereafter. From the bottom to around 70 cm, C/N gradually decreased from 9 to 8. C/N ratios remained at a low values of 8 between 70 cm and 35 cm, followed by an increase to the peak at ca. 9 at 14 cm (ca. 2000 CE). Since 2000 CE, C/N ratios have fluctuated at around 8.75. $\delta^{13}C$ fluctuated at around −24.5‰ from the bottom of the sediment core to 49 cm, followed by a slight decrease to around −25‰ at 36 cm (ca. the early 1950s CE). After that, $\delta^{13}C$ gradually increased to a peak at ca. −23‰ at 26 cm (ca. 1975 CE), followed by a slight decrease. Between 14 cm and the top of the sediment core (ca. from 2000 to 2015 CE), $\delta^{13}C$ remained at low values (ca. −25.5‰). $\delta^{15}N$ gradually increased from 4.78 at the bottom of the sediment core to 6 at 65 cm. Between 65 cm and 14 cm, $\delta^{15}N$ fluctuated at a low value at around 4.5. Since then, $\delta^{15}N$ gradually increased to a peak at ca. 5.5‰, followed by a slight decrease in the top two centimetres. TP remained low at ca. 0.061% from the bottom of the sediment core to 20 cm (ca. 1990 CE), followed by a sharp increase to a peak of ca. 0.09% at 12 cm (ca. 2002 CE) and fluctuated at around 0.09% thereafter.

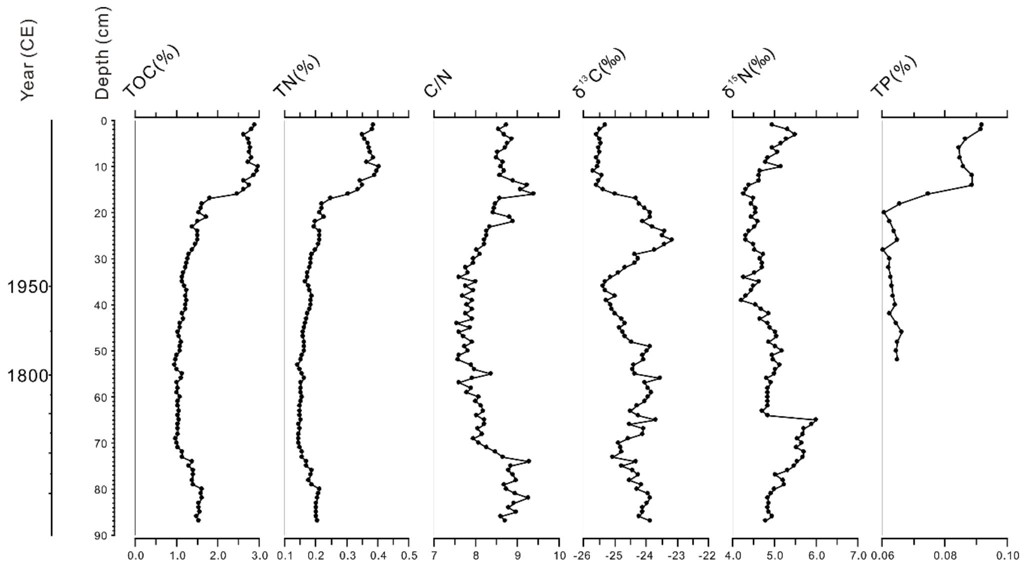

Figure 5.21 Changes in C and N mass, C/N ratios, $\delta^{13}C$, $\delta^{15}N$ and TP in the Luhu Lake sediment core. TP data was provided by J. Jin and X. Chen (China University of Geosciences (Wuhan)).

5.4.4 Chironomids

In total, 39 chironomid species were identified in the Luhu sediment core. Only those (25 taxa) occurring in at least two samples and with an abundance ≥ 2% were presented and used for analysis (Figure 5.22). Chironomids in Luhu sediment core were dominated by *M. tener*-type, *Paratanytarsus*, *P. penicillatus*-type, *C. intersectus*-type and *P. nubifer*-type. Two major zones were distinguished in the chironomid stratigraphic profiles by cluster analysis with a broken stick model (Figure 5.22). Zone A (80-21 cm, ca. CE before 1800-1987) was divided into two subzones. Subzone A1 (80-39 cm, ca. CE before 1800-1945) was dominated by *M. tener*-type (average ~ 30%), *P. nubifer*-type (average ~ 8%), *P. penicillatus*-type (average ~ 10%), *Paratanytarsus* (average ~ 10%) and *Procladius* (average ~ 7%). In subzone A2 (39-21 cm, ca. CE 1945-1987), *M. tener*-type (average ~ 29%), *P. penicillatus*-type (average ~ 8%), *Paratanytarsus* (average ~ 14%) and *Procladius* (average ~ 5%) remained dominant, but there was a slight decrease of *M. tener*-type and an increase in macrophyte-related species, *Stempellina*, to a peak of ca. 23% (average ~ 8%). In Zone B (21-3 cm, ca. CE 1987-2011), *M. tener*-type and *Stempellina* sharply decreased to a mean of ~ 10% and ~ 1%, respectively while eutrophic species, such as *M. tabarui*-type (average ~ 10%), *P. jacatius*-type (average ~ 6%) and *Tanypus* (average ~ 7%), which were rare in Zone A sharply increased to make up 24% of the chironomid community.

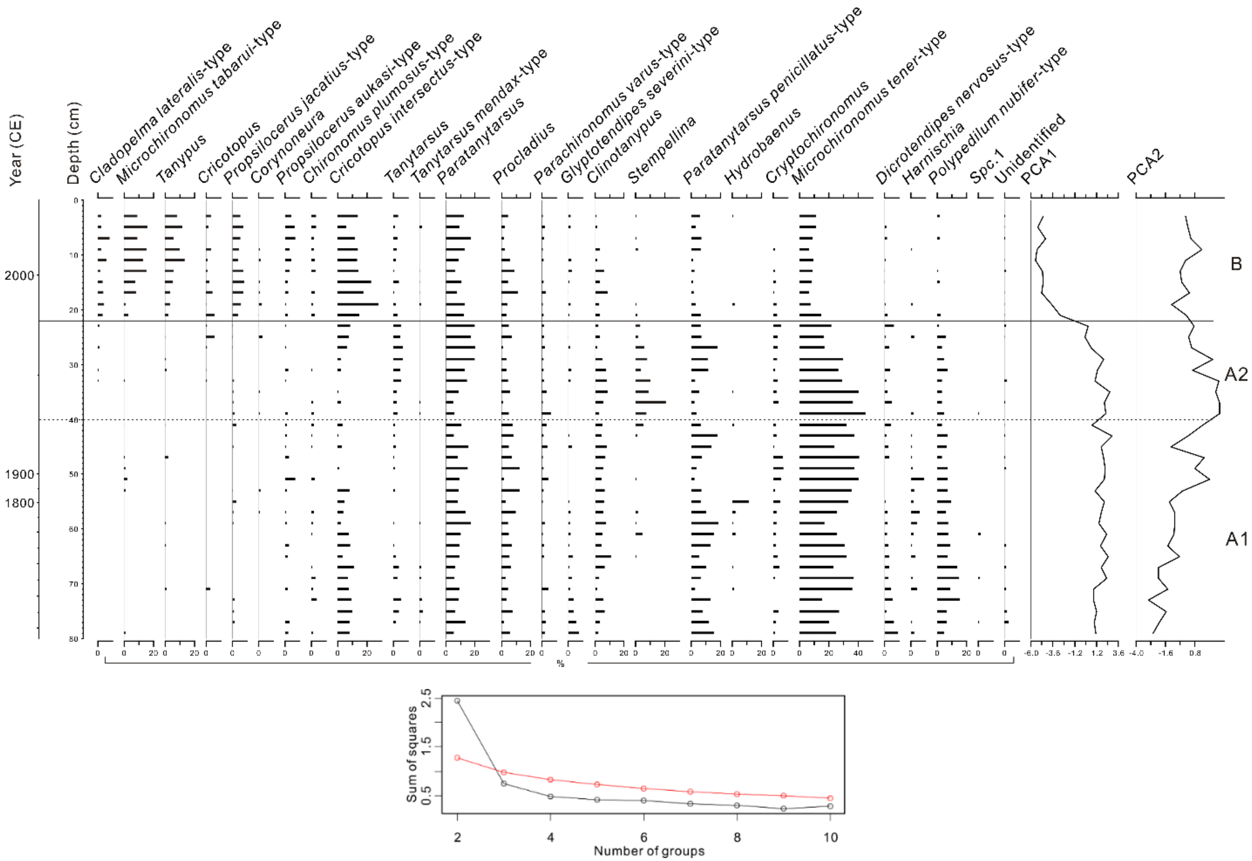

Figure 5.22 Changes in chironomid communities and PCA 1 and PCA 2 scores in the core from Luhu Lake (top). The capital letters on the right indicate the different chironomid zones based on constrained cluster analysis and broken stick model. Group-by-sum of squares (SS) graph (bottom) comparing the dispersion of the classification at different fusion levels to a null model (black line) and the broken stick model (red line).

As DCA analysis showed a gradient length of 1.29 SD (i.e., < 2 SD) for the chironomid assemblages, PCA was used to summarize the major trends. PCA analysis showed that the first and second PCA axes explained 41% and 12% of the changes in chironomids, respectively (Figure 5.23). The first PCA axis was significantly and positively correlated with species such as *M. tener*-type, *P. nubifer*-type, *Clinotanypus*, *P. penicillatus*-type, and negatively correlated with eutrophic species including *M. tabarui*-type, *Tanypus*, *C. plumosus*-type and *P. jacatius*-type. PCA axis 2 is positively correlated with *Stempellina*. The three zones/subzones of chironomids were distinctly identified in the PCA biplot (Figure 5.23). Samples in Zone A were distributed at the right of the biplot, characterized by high concentrations of *M. tener*-type, *P. nubifer*-type, *Clinotanypus* and *Procladius*. Zone A samples have similar scores on PCA axis 1 and variable PCA axis 2 scores. More specifically, samples in subzone A1 are characterized by negative PCA axis 2 scores whereas samples in subzone A2 are distributed at the upper section of the biplot, strongly related with *Stempellina*. Samples in Zone B were distributed at the left of the biplot with a strong relationship with eutrophic species (e.g., *M. tabarui*-type, *Tanypus*, *P. jacatius*-type).

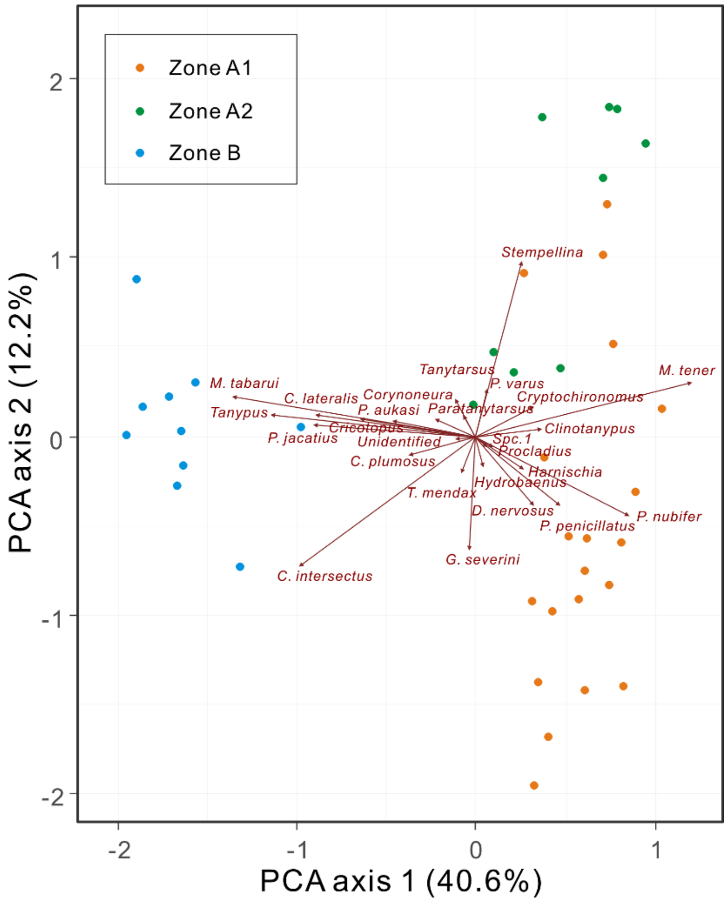

Figure 5.23 PCA ordination biplot of chironomid in the Luhu sediment core. Samples are classified based on the results of constraint cluster analysis and the broken stick model.

5.4.5 Historical archives

In 1949 CE, there were 1.71 million people living in rural areas and another 1.05 million people were based in urban areas in Wuhan, accounting for 62% and 38% of the total population, respectively (Figure 5.24a). This differs from Hunan Province and Honghu where about 90% of the population were in rural areas. From 1949 CE to 1960 CE, both rural and urban population increased sharply to 2.09 and 2.36 million, respectively (Figure 5.24). Between 1960 CE and 1980 CE, the increase of urban population slowed down while rural population continued to increase. In 1980 CE, the proportion of urban and rural population was 49.5% and 50.5%, respectively. Since the early 1980s CE, rural population in Wuhan remained stable, hovering around 2.9 million before it started to decrease at around 2000 CE (Figure 5.24a). However, urban population sharply increased from 2.81 million in 1980 CE to 5.98 million in 2016 CE (Figure 5.24b). In 2016 CE, urban population contributed 72% to the total population, which was about twice that of the rural population. Grain production increased from ca. 0.4 million metric tons in 1949 CE to around 1.6 million metric tons in the 1980s CE and then gradually decreased to about 1.2 million metric tons in the 2010s CE (Figure 5.24a). Negligible quantities of nitrogen and phosphorus fertilizers were used in Wuhan in the early 1950s CE. After that, the usage of nitrogen and phosphorus gradually increased to around 20 thousand and 5 thousand in the early 1980s CE and then boomed to the highest of ca. 85 thousand and 45 thousand metric tons in the 2000s CE before decreasing to ca. 60 thousand and ca. 33 thousand metric tons in 2016 CE, respectively (Figure 5.24a). Industry was poorly developed in Wuhan before the 1980s CE and then sharply increased since the 1980s CE (Figure 5.24b). In 1980 CE, the production of electricity and concrete, the number of vehicles and the length of road were 3.94 billion kw·h, 0.68 million metric tons, 37680 and 1012 km, respectively (Figure 5.24b). Since 1980 CE, especially after 2000 CE, they increased exponentially to reach 21.7 billion kw·h, 10.71 million metric tons, 2.4 million and 5704 km in 2016 CE, respectively (Figure 5.24b).

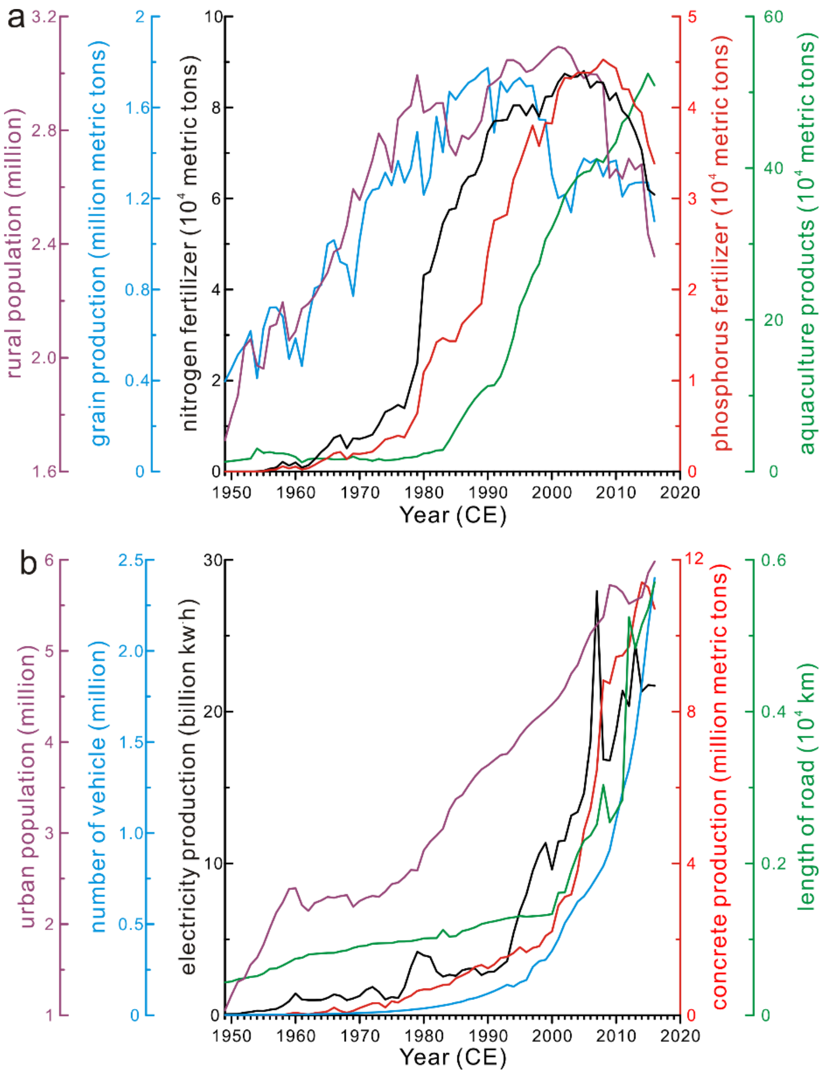

Figure 5.24 Historical archives of (a) agriculture and (b) industry and urbanization in the Luhu Lake catchment.

5.5 Wanghu

5.5.1 Chronology

^{210}Pb and ^{137}Cs in the Wanghu sediment core were presented in Chen et al. (2019). Generally, $^{210}Pb_{excess}$ decreased exponentially from the top to the bottom of the sediment core and reached an equilibrium at ca. 77 cm (Figure 5.25). Activity of ^{137}Cs was relatively low in the sediment core (less than 12 Bq kg^{-1}) and the peak was not obvious. Therefore, chronology of the Wanghu sediment core was established using the ^{210}Pb with the CRS model, which gave a mean sedimentation rate of 0.53 cm yr^{-1}, with the top 77 cm coving the past 145 years.

Chronology below 77 cm was linearly extrapolated from the lower two samples with measurable excess ^{210}Pb. DMAR was low (< 0.2 g cm^{-2} yr^{-1}) in Wanghu Lake before the 1930s CE, followed by a gradual increase, reaching the peak value of more than 1 g cm^{-2} yr^{-1} in the 1970s CE (Figure 5.25). Since then DMAR gradually decreased to ~ 0.4 g cm^{-2} yr^{-1} in the 2010s CE.

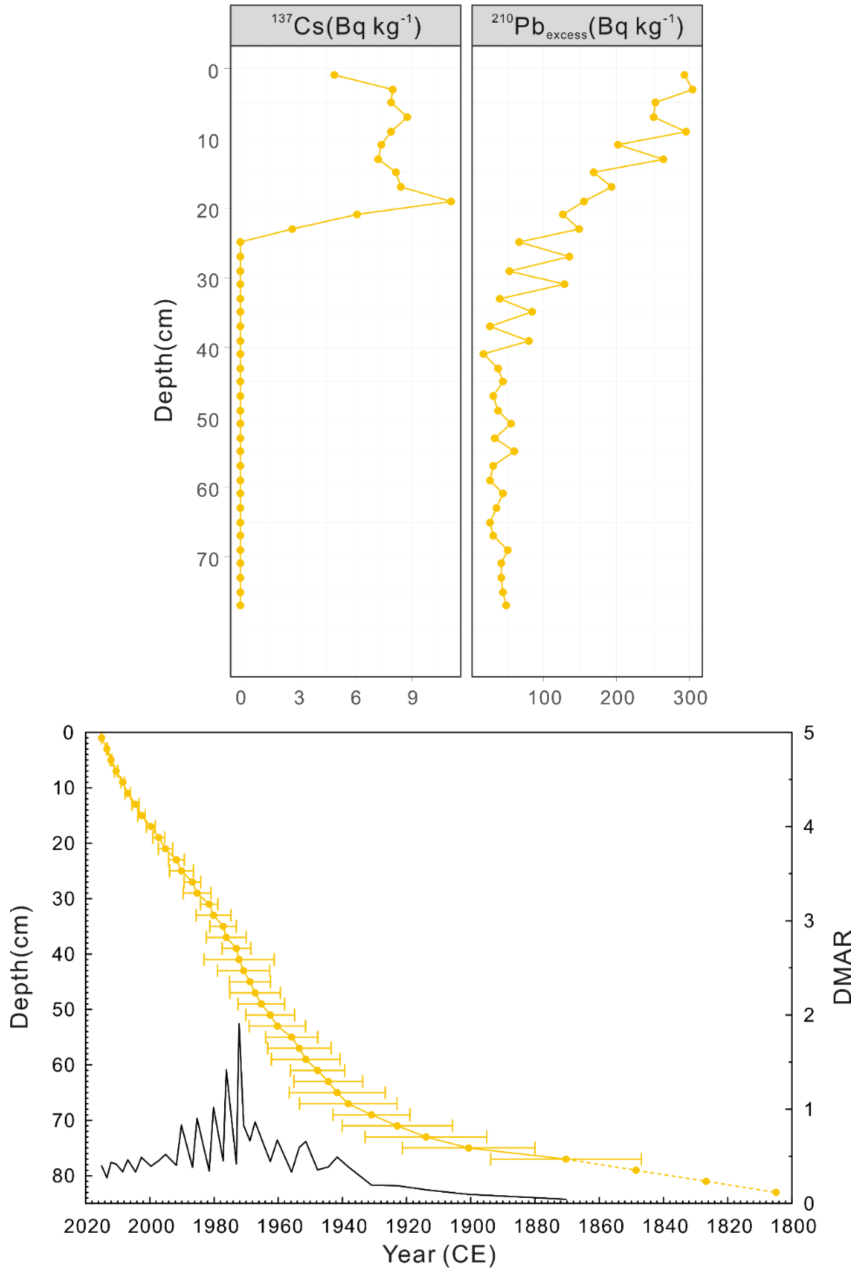

Figure 5.25 ^{137}Cs and ^{210}Pb activity profiles (upper) and age-depth model with error bar (yellow line) (lower) of the Wanghu sediment core. The dashed line indicates results of linear extrapolation. Only dates after 1800 CE were shown. DMAR (black line) is dry mass accumulation rate (g cm^{-2} yr^{-1}). (Original data from Chen et al., 2019).

5.5.2 Sedimentary pigments

All sedimentary pigments in Wanghu Lake showed an overall increasing trend with the exception of the UVR-absorbing compound (Figure 5.26). According to cluster analysis and the broken stick model (Figure 5.26), five zones were identified in the pigment profiles. In Zone A (90-49 cm, ca. CE before 1800-1965), concentrations of all sedimentary pigments were low. Mean concentration of β-carotene was 92 nmol g^{-1} TOC. Concentrations of most pigments were slightly lower in Zone B (49-27 cm, ca. 1965-1987 CE), with the exception of the UVR-absorbing compound, pheophytin *b*', pheophytin *a* and pyropheophytin *a*, mean concentrations of which increased. In Zone C (27-19 cm, ca. 1987-1997 CE) all sedimentary pigments increased. In Zone D (19-11 cm, ca. 1997-2007 CE), all sedimentary pigments sharply increased with the exception of the UVR-absorbing compound. In Zone E (11-0 cm, ca. 2007-2015 CE), most of the pigments except the UVR-absorbing compound remained at a high concentration. The most remarkable change in Zone E was the appearance of aphanizophyll, which was not present in the other zones, and the disappearance of the UVR-absorbing compound.

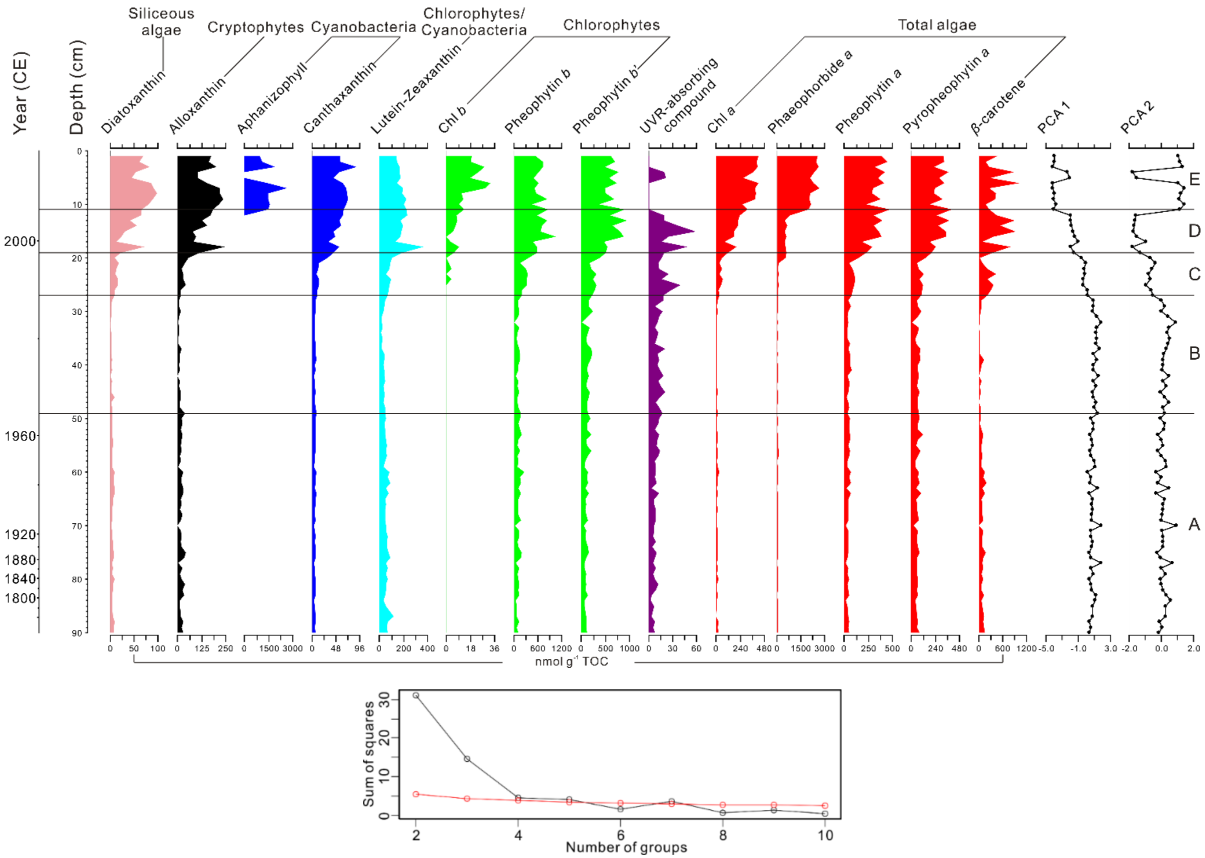

Figure 5.26 Changes in chlorophyll and carotenoid pigment concentrations and pigment PCA 1 and PCA 2 scores in the core from Wanghu Lake (top). The capital letters on the right indicate the different pigment zones based on constrained cluster analysis and broken stick model. Group-by-sum of squares (SS) graph (bottom) comparing the dispersion of the classification at different fusion levels to a null model (black line) and the broken stick model (red line).

DCA showed that the gradient length was 0.86 SD (<2 SD) and so PCA was used to extract the major trends in pigments (Figure 5.27). The first PCA axis explained 73.5% of the variance in pigments and the second PCA axis explained 14.6% of the variance. The first PCA axis was significantly negatively correlated with all sedimentary pigments with the exception of the UVR-absorbing compound ($R < -0.69$, $p < 0.0001$). The second PCA axis was significantly and positively correlated with aphanizophyll ($R = 0.54$, $p < 0.0001$) and negatively correlated with the UVR-absorbing compound ($R = -0.78$, $p < 0.0001$). The five zones identified in constrained cluster analysis were clearly identified in the PCA biplot. Samples in Zone A and B were distributed at the right of the biplot, characterized by low concentrations of all pigments. Samples in Zone C and D gradually moved to the left and bottom of the biplot, indicating an increase in pigment concentrations, especially of the UVR-absorbing compound. Zone E samples were located at the upper left of the biplot, suggesting further increases in all pigments, especially aphanizophyll, with a decrease in the UVR-absorbing compound.

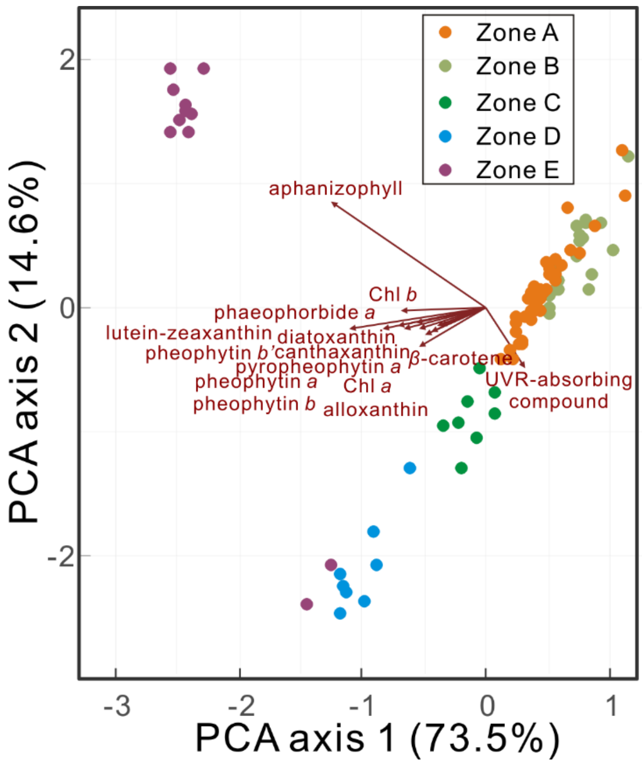

Figure 5.27 PCA ordination biplot of the pigments in Wanghu sediment core. Samples are classified based on the results of constrained cluster analysis and the broken stick model.

5.5.3 Sedimentary C and N mass and stable isotopes and TP

Similar to other study lakes, organic matter content (TOC) in Wanghu Lake was low (< 2.5%) (Figure 5.28). TOC and TN were generally low below 29 cm (before ~1985 CE), slightly fluctuating at around ~ 0.65% and ~ 0.12%, respectively. Since then, both TOC and TN sharply increased, reaching ~ 2.5% and ~ 0.35% in the top 8 cm (after ca. 2010 CE), respectively. C/N ratios in Wanghu Lake were low as well (< 10). C/N ratios fluctuated at around 6.4 below 49 cm (before ~ 1965 CE) and increased thereafter, reaching ~ 9 in the top 8 cm (after ca. 2010s CE). $\delta^{13}C$ gradually decreased from ~ –23.5‰ in the 1840s CE to ~ –26‰ in the late 1990s CE and then slightly increased to ~ –25.5‰ in the early 2000s CE. $\delta^{15}N$ changed within a small range in the Wanghu Lake (between ~ 4.8 and ~ 6.5‰) except three points with relatively high values. $\delta^{15}N$ in Wanghu Lake remained stable at ~ 6.5‰ before the 1930 CE and at ~ 6‰

between the 1930s CE and the mid-1960s CE. Between the mid-1960s CE and the mid-1990s CE, $\delta^{15}N$ gradually decreased from ~ 6‰ to ~ 5.2‰. After that, $\delta^{15}N$ increased to ~ 6.1‰ in 2010 CE and then decreased. TP stabilized at a low value at ca. 0.07% below 21 cm (before ca. 1995 CE), followed by a sharp increase from ca. 0.07% to ca. 0.2% between 21 cm and 11 cm (ca. 1995 to 2005 CE). In the top 11 cm (after 2005 CE), TP remained at a high value of ca. 0.2%.

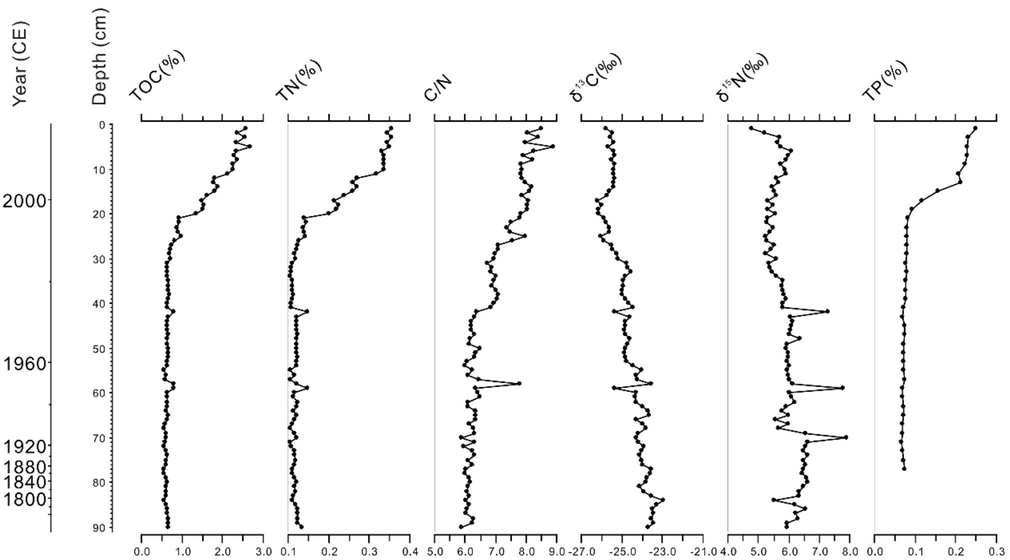

Figure 5.28 Changes in C and N mass, C/N ratios, $\delta^{13}C$, $\delta^{15}N$ and TP in the Wanghu Lake sediment core. TP data was provided by J. Jin and X. Chen (China University of Geosciences (Wuhan)).

5.5.4 Chironomids

A total of 33 chironomid species were identified in Wanghu sediment core. Only those (27 taxa) occurring in at least two samples and with an abundance ≥ 2% were presented and used for analysis. The most abundant chironomids in Wanghu sediment core were *M. tener*-type, *E. dissidens*-type, *E. albipennis*-type, *E. tendens*-type, *M. tabarui*-type, *P. jacatius*-type, *Procladius* and *Clinotanypus* (Figure 5.29). Three major zones were distinguished in the chironomid stratigraphic profiles by cluster analysis with a broken stick model (Figure 5.29). Zone A (81-51 cm, ca. 1827-1962 CE) was dominated by *M. tener*-type with an average abundance of 48.25%. Sub-dominant species were *H. conformis*-type (~5%), *Cricotopus* (~ 4%), *Harnishia* (~ 6%), especially at the bottom of the sediment core. Abundance of *Clinotanypus* and *Procladius* were relatively consistent throughout the whole sediment core, fluctuating at 8% and 10%, respectively. Zone B (51cm-25 cm, ca. 1962-1990 CE) was co-dominated by four species including *M. tener*-type, *E. tendens*-type, *E. albipennis*-type, *E. dissidens*-type. In Zone B, mean abundance of *M. tener*-type decreased to 27%, whereas macrophyte-related species including *E. tendens*-type, *E. albipennis*-type and *E. dissidens*-type sharply increased. Average relative abundance of the three species increased to 11%, 9% and 23%, respectively. The most notable change in Zone C (25-0 cm, ca. CE 1990-2015) was the shift from macrophyte-related chironomids to eutrophic species. More specifically, *E. tendens*-type (average ~ 1%), *E. albipennis*-type (average ~ 2%) and *E. dissidens*-type (average ~ 3%) sharply decreased and almost vanished while nutrient-tolerant species such as *C. plumosus*-type, *M. tabarui*-type, *P. jacatius*-type, *P. aukasi*-type and *Tanypus*, which were rarely reported below 25 cm, sharply increased. For example, average abundance of *M. tabarui*-type and *P. jacatius*-type increased from nearly 0% to more than 9% and 7% at ca. 2000 CE, respectively. Since then, eutrophic species further increased to eventually dominate the chironomid assemblages, with average relative abundances of *M. tabarui*-type and *P. jacatius*-type increasing to 30% and 15% after the 2010s AD, whereas *M. tener*-type further decreased to an average relative abundance of 9%.

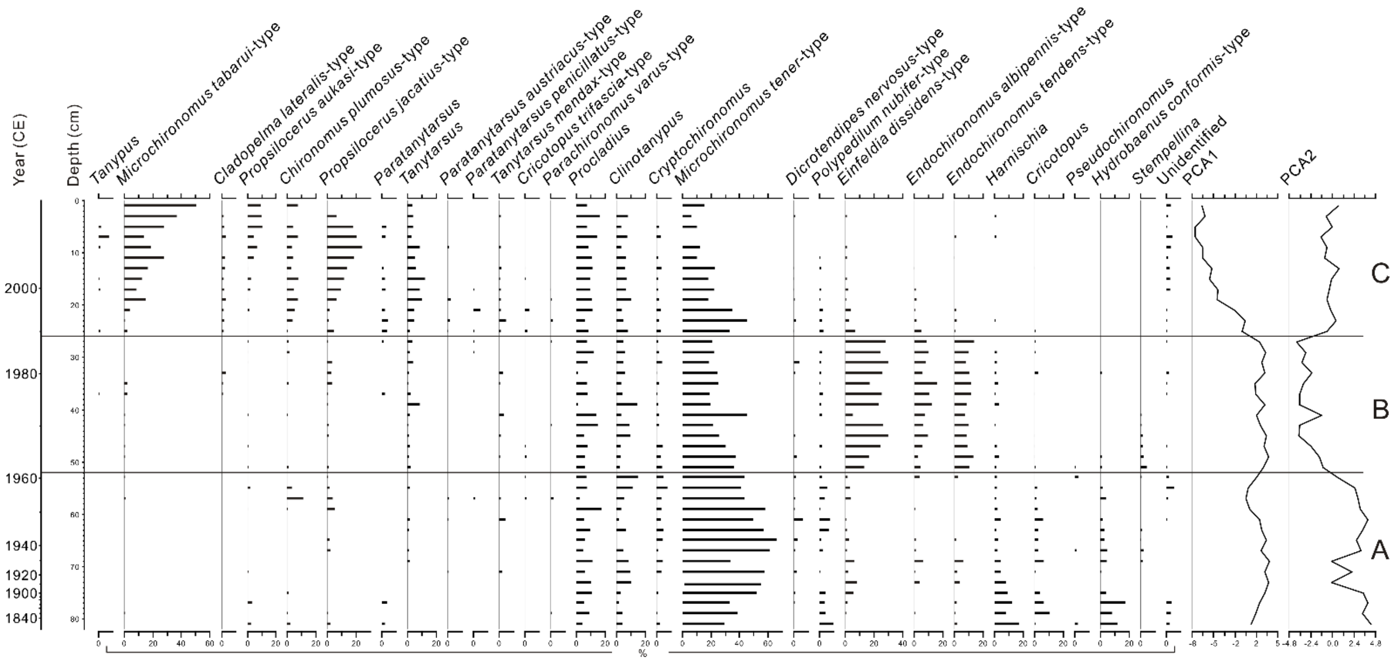

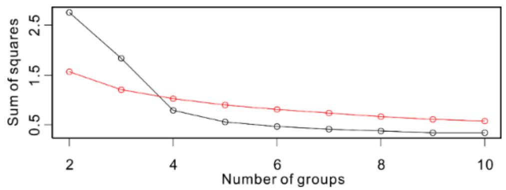

Figure 5.29 Changes in chironomid communities and PCA 1 and PCA 2 scores in the core from Wanghu Lake (top). The capital letters on the right indicate the different chironomid zones based on constrained cluster analysis and broken stick model. Group-by-sum of squares (SS) graph (bottom) comparing the dispersion of the classification at different fusion levels to a null model (black line) and the broken stick model (red line).

As DCA showed that the gradient length was 1.91 SD, which is less than 2 SD, PCA was used to extract the major trends in chironomids (Figure 5.30). The first PCA axis explained 40% of variance in the chironomid assemblages. PCA axis 1 was significantly positively correlated with species such as *M. tener*-type, *E. dissidens*-type, *E. albipennis*-type, *E. tendens*-type and *H. conformis*-type and negatively correlated with eutrophic species including *M. tabarui*-type, *C. plumosus*-type, *P. jacatius*-type and *Tanypus*. The second PCA axis explained a further 22% of the variance in chironomids, and was negatively correlated with macrophyte-related species such as *E. tendenis*-type, *E. albipennis*-type and *E. dissidens*-type. The three chironomid zones were clearly distinguished in the PCA biplot (Figure 5.30). Samples in Zone A were distributed in the upper right of the biplot, characterized by high abundance of species such as *Harnischia*, *M. tener*-type. Samples in Zone B were distributed at the right of the biplot but characterized by negative PCA axis 2 scores, strongly correlated with *E. tendens*-type, *E. albipennis*-type and *E. dissidens*-type. Samples in Zone C gradually moved to the left side of the biplot, characterized by high abundance of species such as *M. tabarui*-type and *C. plumosus*-type.

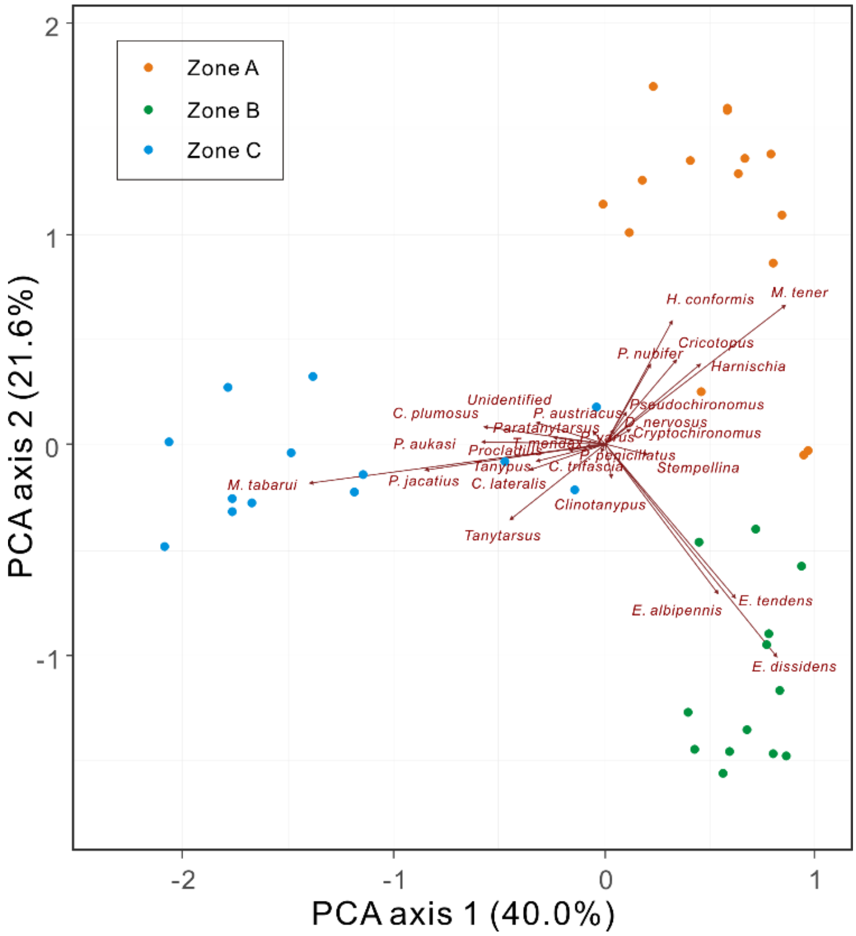

Figure 5.30 PCA ordination biplot of the chironomids in Wanghu sediment core. Samples are classified based on the results of constrained cluster analysis and the broken stick model.

5.5.5 Historical archives

In 1949 CE, there were about 0.76 million people in the catchment, of which 86.8% (0.66 million) lived in the rural areas and the rest 13.2% (0.1million inhabited urban areas (Figure 5.31)). Between 1949 CE and 1980 CE, there was a doubling of rural population from 0.66 million to ca. 1.2 million (Figure 5.31a). After that, rural population in the catchment stabilized at ca. 1.3 million before sharply decreasing since the late 2000s CE (Figure 5.31a). In contrast to the rural population, urban population showed a continuous increase since 1949 CE (Figure 5.31b). There were 0.53 million (30.5%) and 1.53 million (61.9%) people living in urban areas in 1980 CE and 2016 CE, respectively. Grain production increased from 0.19 million metric tons in 1949 CE to ca. 0.60

million metric tons in the 1980s CE and then fluctuated around at 0.6 million metric tons (Figure 5.31a). Between 1949 CE and 1980 CE, the usage of nitrogen and phosphorus fertilizers increased slowly from 0.04 and 0.013 metric tons to 9818 and 3327 metric tons, respectively (Figure 5.31a). Since the 1980s CE, the usage of both fertilizers increased sharply. In 2016 CE, 28.43 thousand metric tons of nitrogen fertilizers and 13.52 thousand metric tons of phosphorus fertilizers were applied in the catchment (Figure 5.31a). The production of electricity and concrete, the number of vehicles and the length of roads increased slowly from 0.014 billion kw·h, 22.9 thousand metric tons, 53 and 318 km to 2.17 billion kw·h, 5178.2 thousand metric tons, 15379 and 1629 km between 1949 CE and 2000 CE, respectively (Figure 5.31b). After that, they increased exponentially, reaching 10.42 million kw·h, 14.81 million metric tons, 174188 and 6842 km in 2016 CE, respectively (Figure 5.31b).

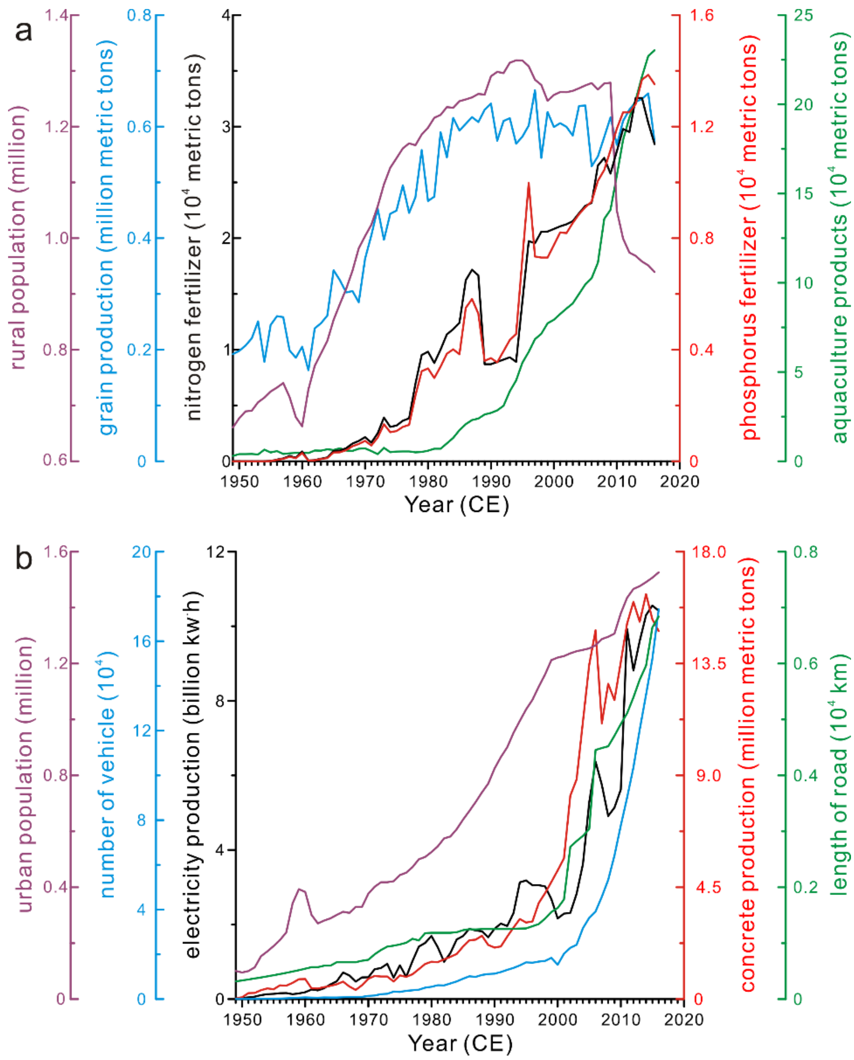

Figure 5.31 Historical archives of (a) agriculture, (b) industry and urbanization in the Wanghu Lake catchment.

5.6 Poyang Lake

5.6.1 Chronology

^{210}Pb and ^{137}Cs activities in the Poyang Lake sediment core are presented in Chen et al. (2019). In general, $^{210}Pb_{excess}$ showed an exponential decreasing trend from the top to the bottom of the sediment core (Figure 5.32). Activities of ^{137}Cs were below the detection limit (Figure 5.32). Chronology of the sediment core was established using the ^{210}Pb with the CRS model. DMAR was low (< 0.2 g cm^{-2} yr^{-1}) in Poyang Lake before the 1930s CE, followed by a gradual increase to more than 1 g cm^{-2} yr^{-1} in the early 2000s CE, and then a decline to ~ 0.8 g cm^{-2} yr^{-1} in the 2010s CE (Figure 5.32).

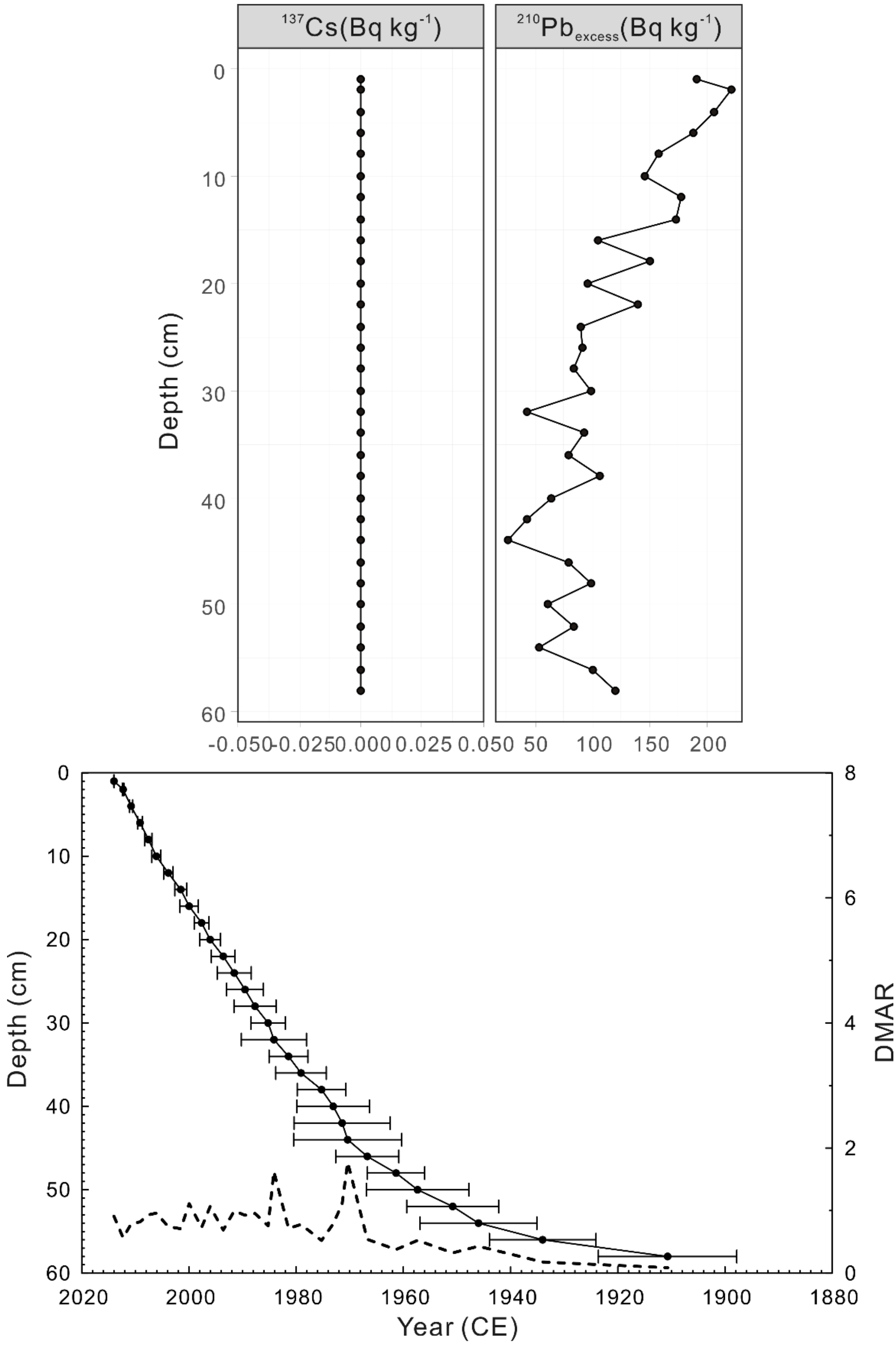

Figure 5.32 ^{137}Cs and ^{210}Pb activity profiles (upper) and age-depth model with error bar (black solid line) (lower) of the Poyang sediment core. DMAR (black dash line) is dry mass accumulation rate (g cm^{-2} yr^{-1}).

5.6.2 Sedimentary pigments

Similar to sediment cores from the other lakes, all the sedimentary pigments in Poyang Lake showed an upward trend with the exception of the UVR-absorbing compound (Figure 5.33). According to cluster analysis and the broken stick model (Figure 5.33), three zones were identified in the pigment profile. In Zone A (58-25 cm, ca. 1911-1991 CE), concentrations of all sedimentary pigments were low except the UVR-absorbing compound which had higher concentrations (mean of 8 nmol g^{-1} TOC) than the other Zones. In Zone B (25-11 cm, ca. 1991-2005 CE), with the exception of the UVR-absorbing compound and *β*-carotene which slightly decreased, concentrations of other pigments sharply increased relative to Zone A. For example, the concentration of alloxanthin increased ~ 10-fold from the start to the end of Zone B. In Zone C (11-0 cm, ca. 2005-2014 CE), concentrations of all sedimentary pigments further increased with the exception of the UVR-absorbing compound which sharply decreased to reach undetectable levels in this Zone. Aphanizophyll which was not preserved in Zones A and B sharply increased (mean concentration of 84 nmol g^{-1} TOC).

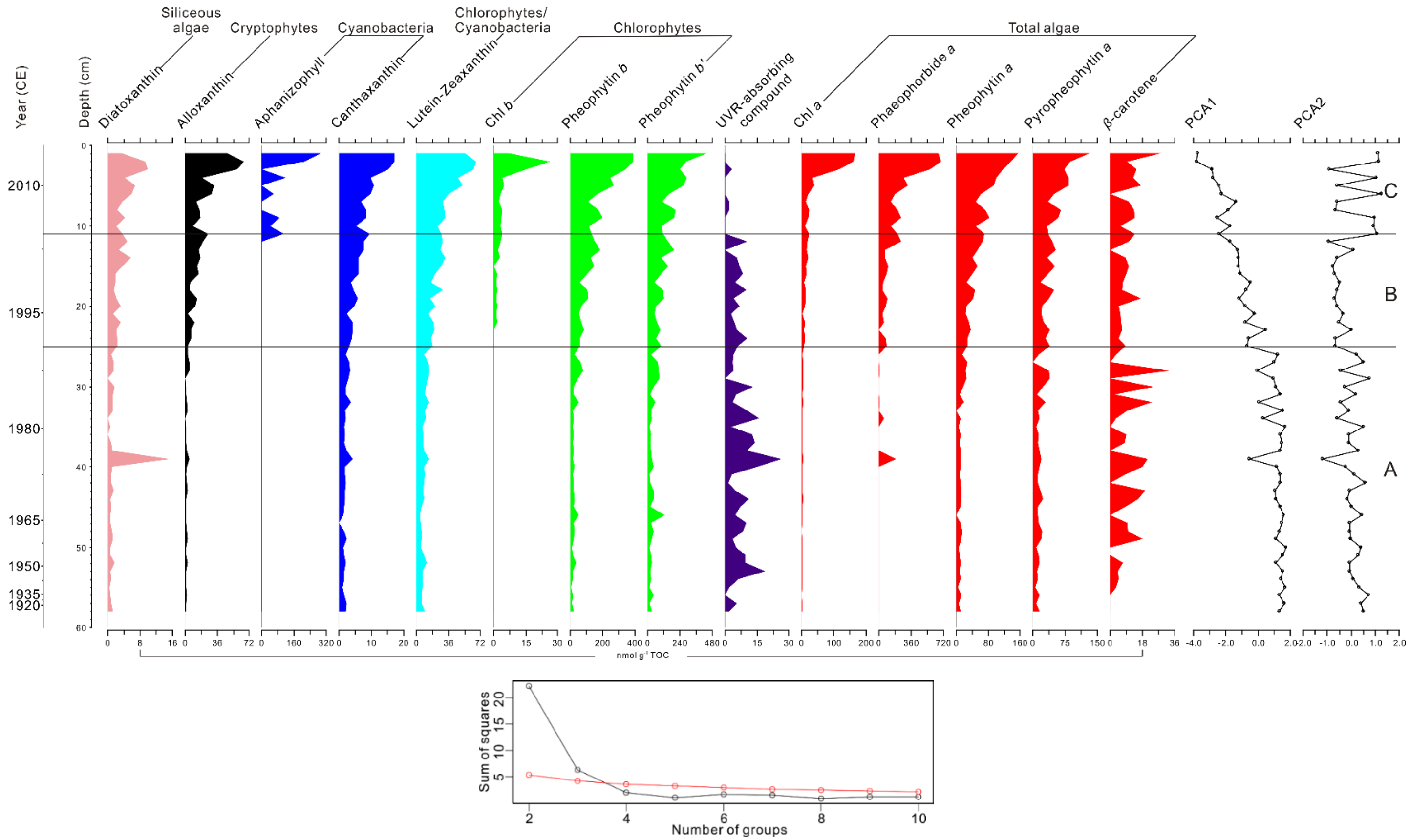

Figure 5.33 Changes in chlorophyll and carotenoid pigment concentrations and pigment PCA 1 and PCA 2 scores in the core from Poyang Lake (top). The capital letters on the right indicate the different pigment zones based on constrained cluster analysis and broken stick model. Group-by-sum of squares (SS) graph (bottom) comparing the dispersion of the classification at different fusion levels to a null model (black line) and the broken stick model (red line).

As the DCA gradient length was 1.14 SD (< 2 SD), PCA was used to summarize the major trends in pigments. The first PCA axis explains 73.0% of the variance in pigments and the second PCA axis explains a further 10.4% of the variance (Figure 5.34). The first PCA axis was significantly and positively correlated with the UVR absorbing compound ($R = 0.38$, $p < 0.005$), and negatively correlated with the other pigments ($R < -0.36$, $p < 0.01$). The second PCA axis was significantly positively correlated with aphanizophyll ($R = 0.56$, $p < 0.0001$) and negatively correlated with the UVR-absorbing compound ($R = -0.52$, $p < 0.0001$). The three zones were clearly distinguished in the PCA biplot. Samples in Zone A were distributed at the right of the biplot, characterized by low concentrations of all pigments. Sample in Zone B gradually moved to the left and the bottom of the biplot, implying the increases in pigments such as the UVR-absorbing compound and β-carotene. Samples in Zone C are located at the upper left of the biplot, characterized by high concentrations of all pigments, especially aphanizophyll, and low concentrations of the UVR-absorbing compound.

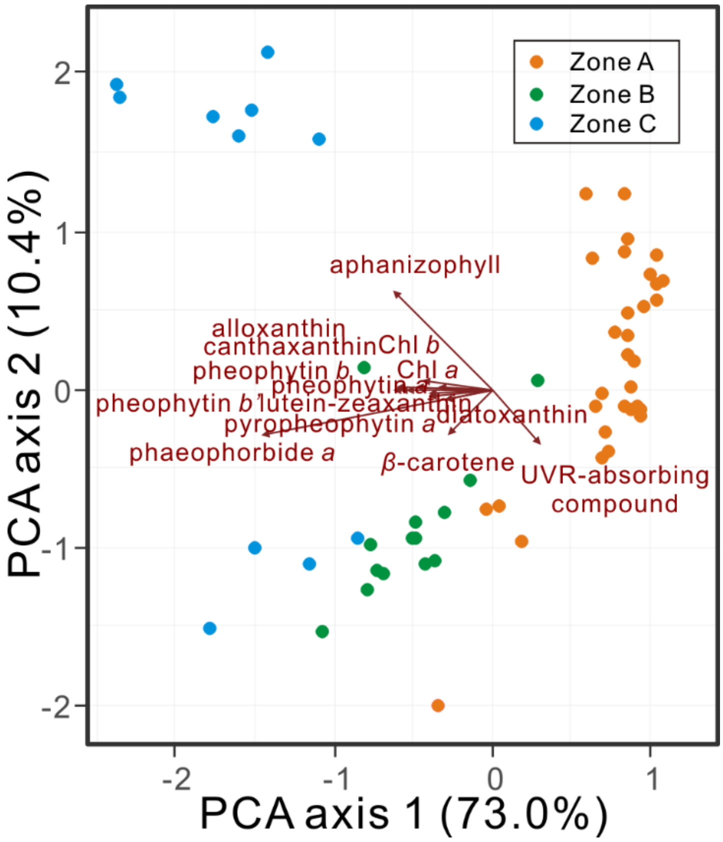

Figure 5.34 PCA ordination biplot of the pigments in Poyang sediment core. Samples are classified based on the results of constrained cluster analysis and the broken stick model.

5.6.3 Sedimentary C and N mass and stable isotopes and TP

TOC in Poyang Lake sediments was consistently lower than 1% (Figure 5.35). From the bottom of the sediment core to 35 cm (between the 1910s CE and early 1980s CE), TOC and TN fluctuated at around 0.75% and 0.12%, respectively. C/N ratio was generally low, fluctuating at around 7. From 35 cm to the top of the sediment core (ca. 1980 to 2015 CE), both TOC and TN showed a general upward trend, increasing from ca. 0.6% and ca. 0.0 % to ca. 0.95% and ca. 0.12%, respectively. C/N ratios rapidly increased to ca. 10 at ca. 32 cm and remained stable at 10 thereafter. $\delta^{13}C$ remained stable at ~ –22 ‰ below 35 cm (before the 1980s CE), followed by a gradual decrease to ~ –26‰ in the 2010s. $\delta^{15}N$ showed a upward trend in general, increasing from ~ 5.2‰ at the bottom of the sediment core (ca. the 1910s CE) to ~ 6.4‰ at the top of the sediment core (ca.

the 2010s CE). TP concentrations was ~ 0.05% before the 1980s CE and gradually increased to ~ 0.06% in the 2010s CE.

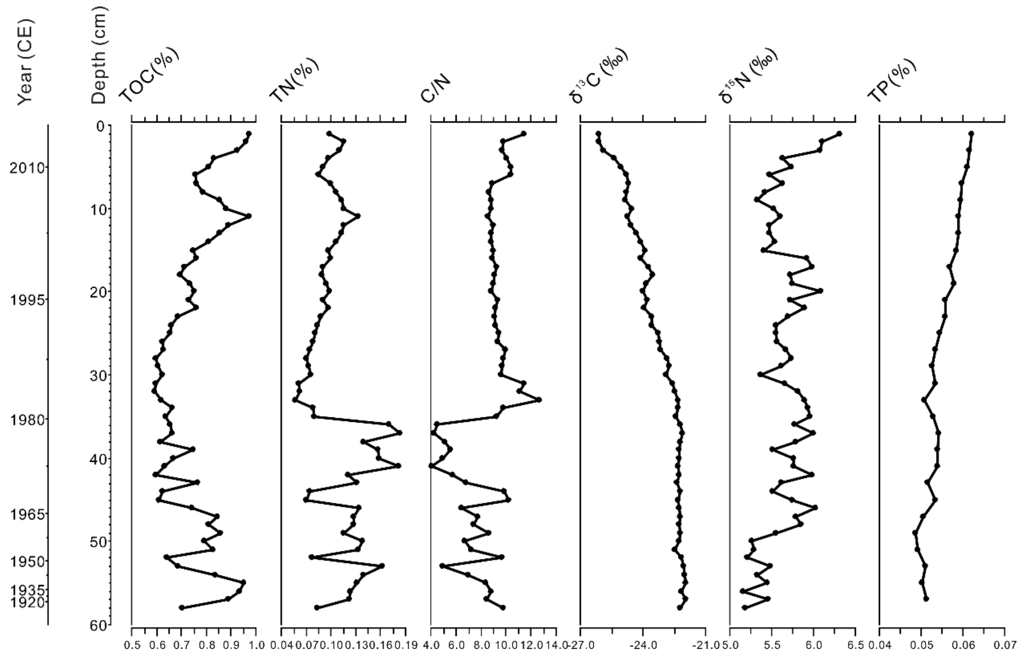

Figure 5.35 Changes in C and N mass, C/N ratios, δ^{13}C, δ^{15}N and TP in the Poyang Lake sediment core. TP data was provided by J. Jin and X. Chen (China University of Geosciences (Wuhan)).

5.6.4 Chironomids

In total, 29 chironomid taxa were identified in the Poyang sediment core. Only 22 taxa which occurred in at least two samples and with an abundance ≥ 2% were presented and used for analysis (Figure 5.36). The broken stick model shows that there were no obvious community shifts in chironomid assemblages (Figure 5.36). Chironomid assemblages in the Poyang sediment core were dominated by *M. tener*-type, *C. sylvestris*-type, *P. nubifer*-type and *Tanytarsus*. Abundance of *M. tener*-type, *C. sylvestris*-type, *P. nubifer*-type and *Tanytarsus* fluctuated at ca. 22%, 12%, 13% and 11%, respectively. Nutrient-tolerant species, such as *C. plumosus*-type (average percentage, ~ 0.47%), *M. tabarui*-type, *Tanypus* and *P. jacatius*-type, which were abundant in Luhu and Wanghu lakes, were less prevalent or not reported in the Poyang sediment core.

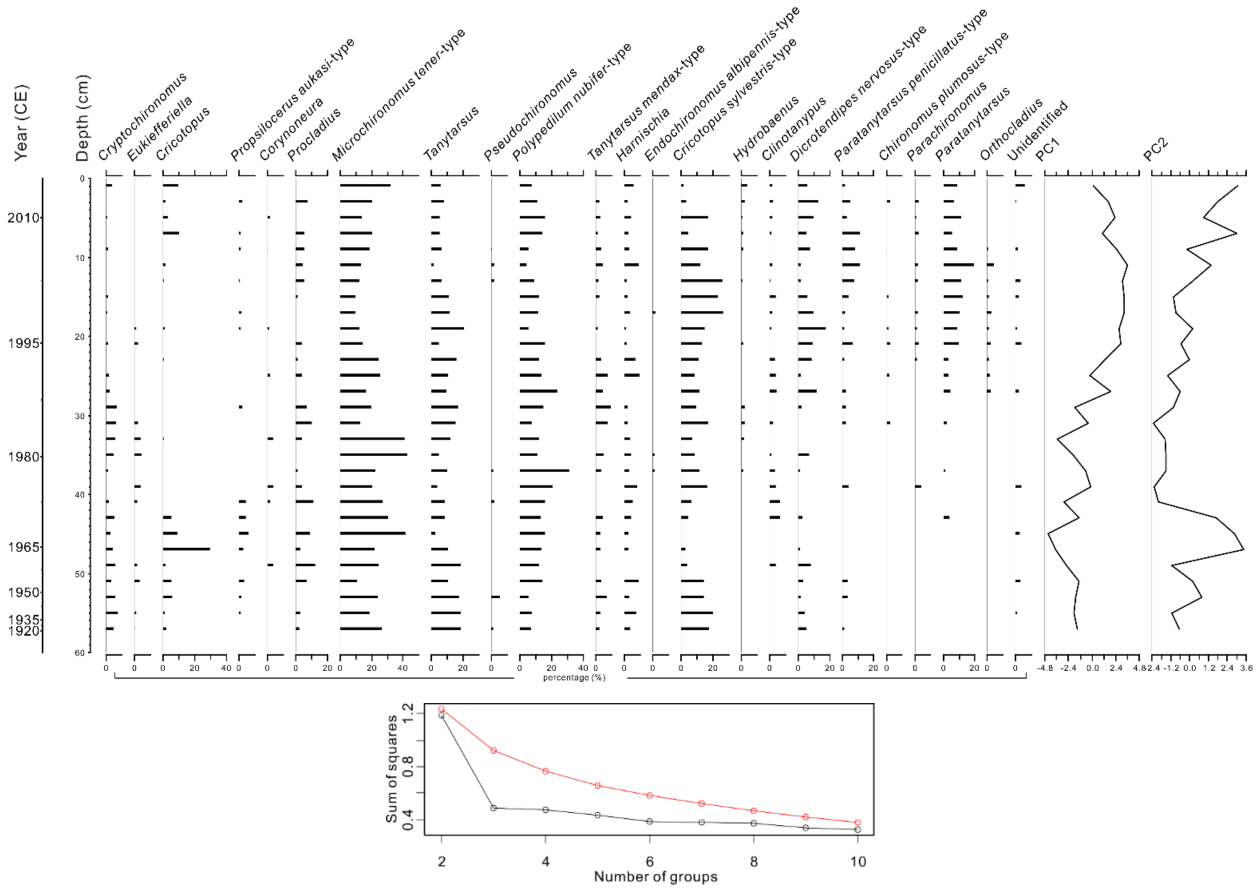

Figure 5.36 Changes in chironomids communities and PCA 1 and PCA 2 scores in the core from Poyang Lake (top). Group-by-sum of squares (SS) graph (bottom) comparing the dispersion of the classification at different fusion levels to a null model (black line) and the broken stick model (red line).

As DCA showed that the gradient length was 1.18 SD (< 2 SD), PCA was used to summarize the major trends in chironomids. The first PCA axis explained 28.0% of the variance in chironomids and was positively correlated with *Paratanytarsus*, *P. penicillatus*-type and *D. nervosus*-type and negatively correlated with *M. tener*-type, *Cryptochironomus* and *Procladius* (Figure 5.37). The second PCA axis further explained 13.5% of the variance in chironomids and was positively correlated with *Cricotopus* but negatively correlated with *C. sylvestris*-type, *Eukiefferiella* and *Corynoneura*. Samples moved from the left to the right of the biplot, implying a shift from species such as *M. tener*-type and *Cryptochironomus* to *Paratanytarsus*, *P. penicillatus*-type and *D. nervosus*, but the clusters were not distinctive.

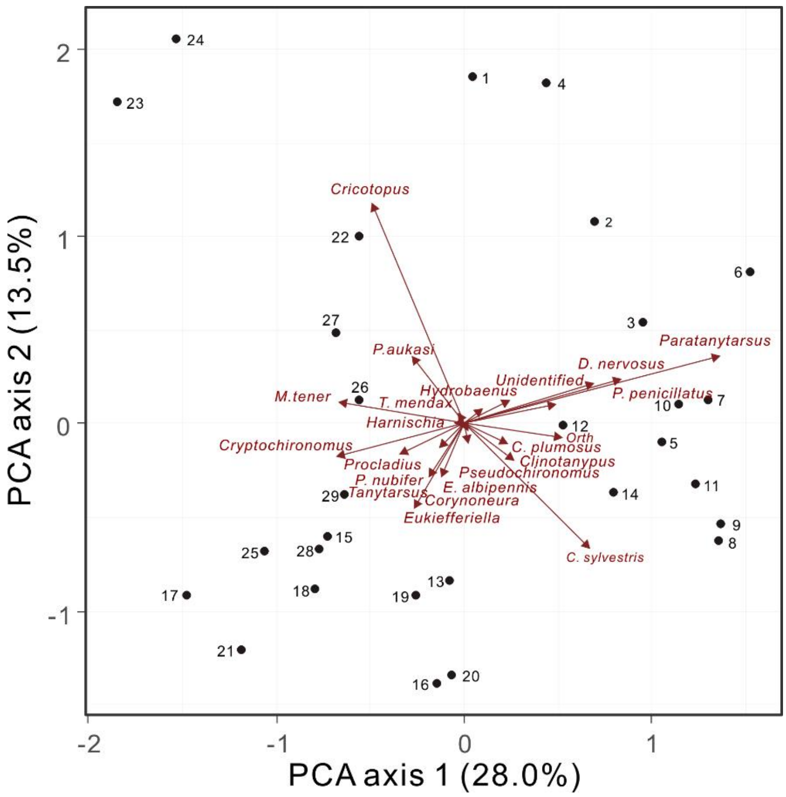

Figure 5.37 PCA ordination biplot of the chironomids in Poyang sediment core. The number near the point indicates the depth of the sample in the sediment core.

5.6.5 Historical archives

In 1949 CE, there were 11.47 million and 1.67 million people living in the rural and urban areas in the catchment, accounting for 87.3% and 12.7% of the total population, respectively (Figure 5.38a). Before the 1990s CE, both the rural and urban population increased, reaching ca. 30 million (75%) and ca. 10 million (25%) in the 1990s CE, respectively (Figure 5.38). Since the 1990s CE, the population living in rural areas decreased, while the number of people inhabiting urban areas increased rapidly, reaching 24.38 million, which makes up more than 50% of the total population (49.92 million). Grain production increased continuously from 3.88 million metric tons in 1949 CE to 21.38 million metric tons in 2016 CE (Figure 5.38a). Between the early 1950s CE and the early 1980s CE, the usage of nitrogen and phosphorus fertilizers increased from ca. 600 and 290 metric tons to 280 thousand and 112 thousand metric tons, respectively (Figure 5.38a). After the 1980s CE, both nitrogen and phosphorus fertilizers were increasingly used in the catchment, reaching more than 600 thousand and ca. 300 thousand metric tons in the late 1990s CE (Figure 5.38a). Since then, the usage of nitrogen fertilizers remained at around 600 thousand metric tons while that of phosphorus continued to increase, reaching more than 400 thousand metric tons in 2016 CE. Compared with agriculture, industry was weakly developed in Jiangxi Province before the 1980s CE. Between 1949 CE and 1980 CE, the production of electricity and concrete, the number of vehicles and the length of roads increased from 0.004 billion kw.h, 1.25 thousand metric tons, 17,535 and 4,739 km to 5.72 billion kw.h, 2010 thousand metric tons, 51,000 and 29,651 km, respectively (Figure 5.38b). After 1980 CE, electricity and concrete production and the number of vehicles increased at a higher speed, reaching 20.11 kw·h, 13.82 million metric tons and 247,000 in 2000 CE, respectively (Figure 5.38b). Since then, the four metrics (electricity production, concrete production, number of vehicles and the length of road) exponentially increased to 108.54 million kw·h, 95.13 million metric tons, 4,073,587 and 161,909 km in 2016 CE, respectively (Figure 5.38b).

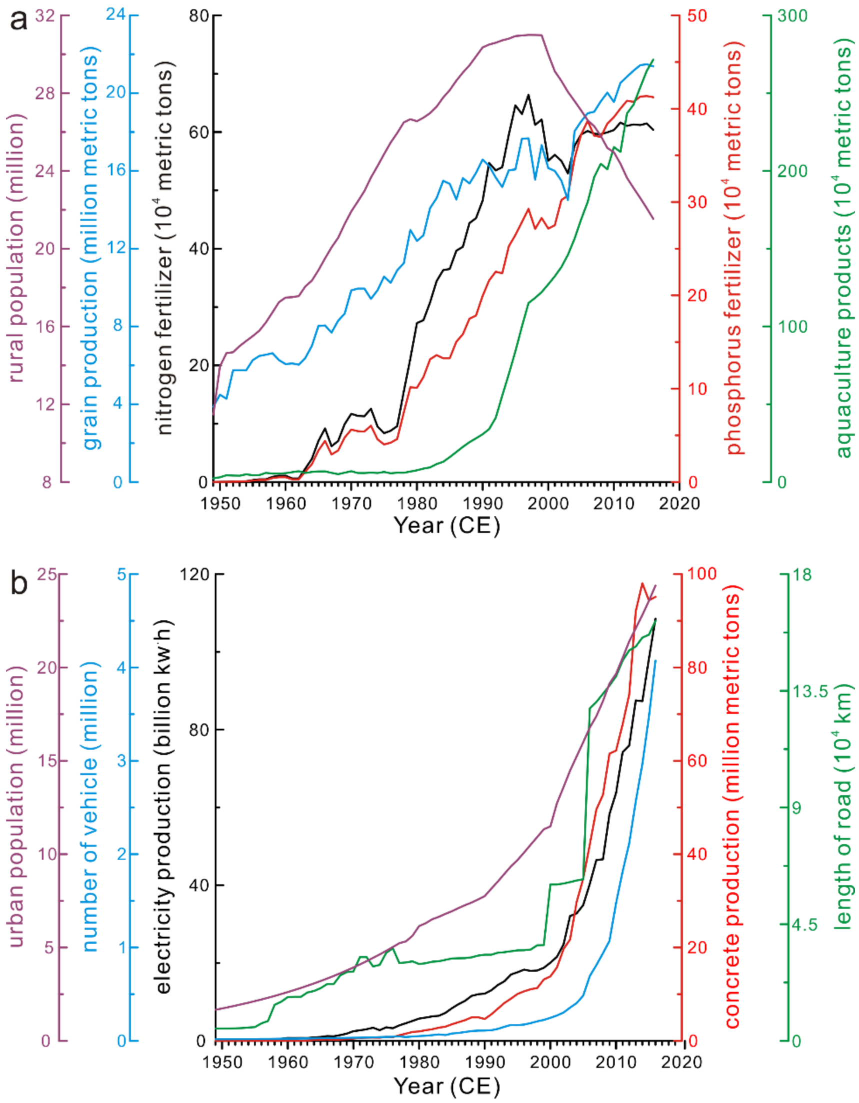

Figure 5.38 Historical archives of (a) agriculture and (b) industry and urbanization in the Poyang Lake catchment.

5.7 Summary

The results of sedimentary proxies revealed the changes in algal production (chlorophyll and carotenoid pigments), lake ecosystems (chironomids) and organic matter cycling (TOC, TN, C/N ratios, $\delta^{13}C$ and $\delta^{15}N$) in the middle Yangtze floodplain. Historical archival data showed the development of agricultural and industrial activities as well as urbanization in the catchments.

Sedimentary chlorophyll and carotenoid pigments showed an overall increasing trend in all six lakes, indicating the increase in algal production. HAB-associated biomarker pigments were uncommon in all lakes before increasing most markedly in Dongting, Poyang, Luhu and Wanghu Lakes after 2000 CE. In contrast, UVR-absorbing compound decreased in all lakes after 2000 CE, suggesting low light condition since then.

TOC, TN and C/N ratios increased in all the lakes. $\delta^{13}C$ showed a general upward trend in the two lakes with abundant submerged macrophytes (Futou and Honghu), but decreased in the other four lakes (Dongting, Poyang, Luhu and Wanghu) with pigments from N_2-fixing cyanobacteria. $\delta^{15}N$ varied among the lakes, suggesting different N cycling.

In hydrologically restricted drainage lakes (Futou, Luhu and Wanghu), chironomids revealed a shift from general species (i.e., *M. tener*-type) to macrophyte-related species after local dam construction, followed by the dominance of eutrophic species (i.e., *M. tabarui*-type, *C. plumosus*-type) in recent years with the exception of Futou Lake. In the hydrologically open Poyang Lake, there was no significant shift in chironomid community.

Historical archival data documented rapid development in agricultural activities from the late 1940s CE to the late 1970s CE, followed by the explosion of industrialization and urbanization since the 1980s CE.

More detailed interpretation of these sedimentary proxies will be discussed in the following chapters. As chronologies before 1800 CE were extracted from the ^{210}Pb chronologies and so are not as reliable, so the analyses that follow in subsequent chapters will mostly be restricted to the last two centuries (since ~ 1800 CE).

CHAPTER 6 ALGAL PRODUCTION AND COMMUNITY CHANGE IN THE MIDDLE YANGTZE BASIN SINCE THE 19TH CENTURY

6.1 Introduction

Cultural eutrophication and harmful algal blooms (HABs) caused by excessive nutrient loading (nitrogen and phosphorus) from anthropogenic activities (urbanization/industrialization and agriculture) have been widely reported worldwide (Conley et al., 2009; Smith and Schindler, 2009; Taranu et al., 2015). Debates on the causes of cultural eutrophication are sometimes controversial (Schindler et al., 2008; Leavitt et al., 2006; Burson et al., 2018). Evidence from bioassay, whole-lake experiments and other sources suggests that phosphorus (P) is the limiting element controlling eutrophication (Schindler, 1977; Schindler et al., 2008). Wastewater from urban and domestic point sources, which is rich in P, is more likely to cause HABs in freshwater ecosystems (Edmondson, 1970; Jenny et al., 2016). Recent studies on Lough Neagh (Northern Ireland) and Lake Winnipeg (Canada) revealed that nitrogen (N) from agricultural sources also enhances algal production, raising the argument that controlling pollution from agricultural diffuse sources, which has high N concentrations, is essential in regulating eutrophication (Bunting et al., 2007; Bunting et al., 2016).

The majority of eutrophication studies to date have been based on northern lakes in the temperate zone with longer histories of cultural enrichment. Evidence from floodplain lakes is relatively rare, although it is well established that lakes in the Yangtze floodplain have degraded recently (Yang et al., 2008). According to the Vollenweider model, P retained in lakes is inversely correlated with lake flushing rate (Vollenweider, 1976). In floodplain areas, hydrological connectivity with the main channel regulates water retention times and water exchange ratios, which might influence the P retention and hence algal production, and algae sedimentation and retention in floodplain lakes (Junk et al., 1989; McGowan et al., 2011; Chen et al., 2016). Therefore, gaining knowledge of the influence of nutrients and hydrology (influenced by climate and damming) on eutrophication and primary production is valuable for water management in floodplain lakes.

Over the last 70 years, extensive and intensive agricultural and industrial development and urbanization have profoundly modified the biogeochemical cycles of N and P in the Yangtze floodplain, resulting in the deterioration of water quality (Liu et al., 2016; Yu et al., 2019) and eutrophication of floodplain lakes (Yang et al., 2008; Dong et al., 2012). Concurrently, more than 50 thousand dams and reservoirs have been established in this area (e.g., TGD) for the benefits of hydropower, irrigation, flood control and water supply (Yang et al., 2011), which have modified the natural hydrological connection between the Yangtze River and the floodplain lakes (Chen et al., 2016; Chen et al., 2017). In recent years, increasing algal production and HABs are a common phenomenon in the Yangtze floodplain (Dong et al., 2016; Zong et al., 2019). This chapter aims to investigate how and whether algae and primary producers have responded to the intensification of agricultural and industrial/urban activities in the catchments and changes in hydrological connectivity in the middle Yangtze floodplain lakes. These questions will be addressed through analyses conducted both spatially (comparing among lakes) and temporally (looking at change in individual lakes) to assess the dominant drivers of water quality, with the following hypotheses tested:

1. Agricultural activities will increase N loading, and urbanization and industrialization will increase P loading into the middle Yangtze lakes.
2. The increase in nutrient loadings from human activities will increase algal production and HABs in these middle Yangtze floodplain lakes. High P loading from urbanization/industrialization will result in N limitation, promoting N_2-fixing cyanobacteria.
3. Connectivity with the Yangtze River will alleviate algal blooms and HABs caused by increasing nutrients by high lake flushing rates.

6.2 Methods

Methodological approaches: Chlorophyll and carotenoid pigments (i.e., diatoxanthin, alloxanthin, aphanizophyll, canthaxanthin, lutein-zeaxanthin, Chl *b*, pheophytin *b*, pheophytin *b*', Chl *a*, phaeophorbide *a*, pheophytin *a*, pyropheophytin *a*, *β*-carotene) from sediment cores of the six lakes were used as proxies to investigate the timing and extent of changes in algal production and community composition. Principal component analysis (PCA) was used to summarize the main trends in the pigment datasets (Chapter 4).

Spatial analyses (post 2000 CE): Recent densities of agricultural and industrial/urban activities (human drivers) across the middle Yangtze floodplain were studied and compared to recent lake sediments deposited after 2000 CE to assess whether there were relationships between the human development drivers (archival data), sedimentary TP and TN influx (nutrient response), and algal communities/HABs abundances (biological response).

Temporal analyses (trends since > 1800 CE): Archival data was used to establish how and when social-economic indices, hydrology/dams and climate have changed, and pigment data was used to determine when and how biota have changed. The influence of human drivers on nutrient fluxes and algal production/HABs was assessed in individual Yangtze floodplain lakes by comparing historical records with pigment biomarkers from the six study lakes using GAMs. Due to the limits of ^{210}Pb (< 150 years) and extrapolation of the dating models, this study focused on sediments deposited after 1800 CE to assess "baseline" conditions prior to the intensive period of modernisation (Bennion et al., 2011).

6.3 Results

6.3.1 Historical archives

6.3.1.1 Spatial comparisons of recent (after 2000 CE) intensity of human activities across the mid-Yangtze

The 10 historical datasets (Chapter 5) were divided by the administrative area to allow the comparison of densities across the region as a proxy for the intensity of agricultural and industrial/urban activities (Figure 6.1). Densities of all the variables were lower in the Dongting and Poyang catchments, indicating low intensity of both agricultural and urban/industrial activities. The biggest metropolis in central China, Wuhan (Luhu catchment), has the highest density of all archives except concrete production, indicating high intensity of both agricultural and industrial/urban activities. Apart from the Luhu catchment, the densities of grain production, aquaculture products, nitrogen and phosphorus fertilizers usage were higher in the Honghu and Futou catchments than the others, indicating more intensive agricultural activities. In contrast, electricity and concrete production were higher in the Wanghu catchments relative to other catchments, indicating intensive urban/industrial activities. Vehicle density was similar in all the catchments, with the exception of Wuhan which had the highest vehicle densities. However, road density was similar in all the six catchments. To summarize, agricultural activity is generally more intensive in the Honghu and Futou catchments, while industry and urbanization indices are more intensive in the Wanghu catchments. The Luhu catchment is intensive in both agricultural and urban/industrial activities. In contrast, both agricultural and urban/industrial activities are less intensive in the Dongting and Poyang catchments.

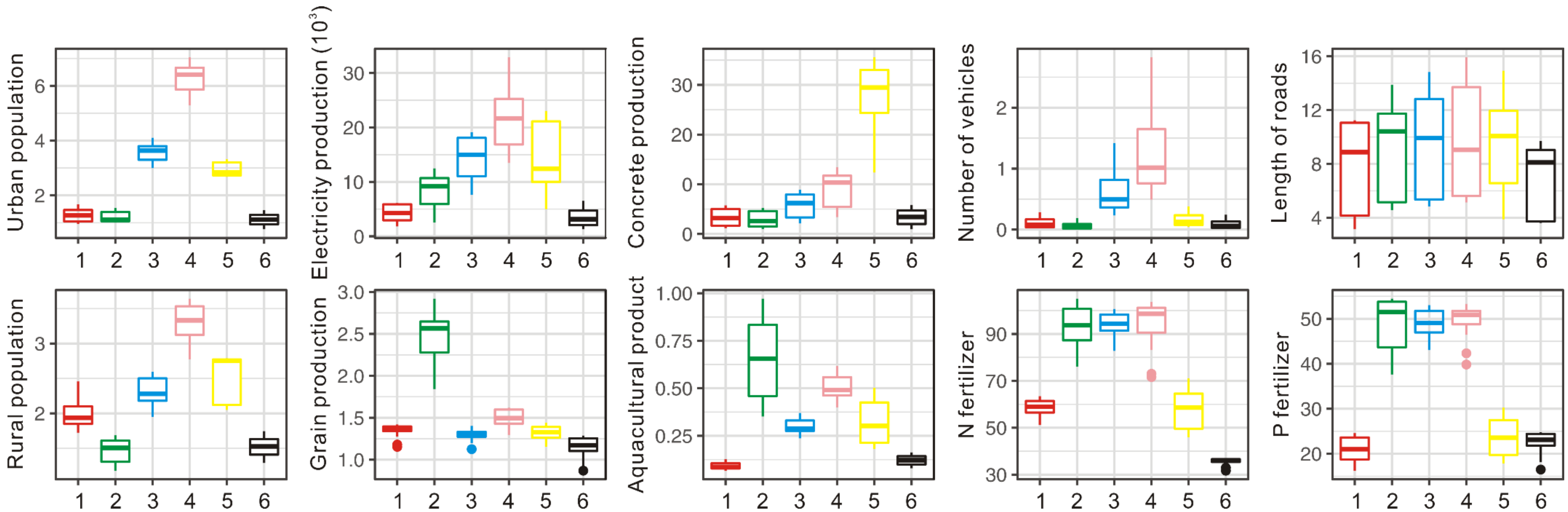

Figure 6.1 Densities of industrial/urban (upper) and agricultural (lower) variables after 2000 CE reflecting the intensity of human activities in the catchments. Industrial and urban archives include urban population (unit: per ha), electricity production (unit: kw h per ha), concrete production (unit: ton per ha), number of vehicles (unit: per ha) and length of roads (unit: m per ha). Agricultural archives include rural population (unit: per ha), grain production (unit: ton per ha), aquacultural product (unit: ton per ha), N fertilizer (unit: kg per ha) and P fertilizer (unit: kg per ha). Number 1 to 6 on the x-axis indicate the catchments, 1 = Dongting; 2 = Honghu; 3 = Futou; 4 = Luhu; 5 = Wanghu; 6 = Poyang.

6.3.1.2 Temporal variation of human activity intensity in the catchments

In general, the six lake catchments showed a similar history of agricultural development and urbanization/industrialization over the last 7 decades (Chapter 5). Agricultural activities and industrialization/urbanization were less intense in all catchments before the early 1950s CE (Chapter 5). In terms of the social-economic structure, agriculture was dominant, compared to industry and urbanization, between the 1950s CE and the late 1970s CE. Rural population comprised more than 85% of the total population in each administrative region except for the metropolis Wuhan, where about 62% of the population were based in rural areas. Rural population and grain production increased from the early 1950s CE to the late 1970s CE and remained at a peak before decreasing since 2000 CE. Fertilizer usage was low in the 1950s CE and gradually increased in the 1960s CE, followed by marked increase since the 1970s CE. In contrast to rural population, urban population showed a continuous increase over the last 70 years and gradually became dominant component of the total population since the late 1970s CE, especially in regions in the lower reaches (Wuhan, Huangshi and Jiangxi), where urban population accounted for more than 50% of the total population in 2016 CE. With the release of the "Reform and Opening" policy in the early 1980s CE, the socio-economic structure transformed from agriculturally-dominated towards the development of industry and urbanization. Electricity and concrete production, the number of vehicles, and the length of roads showed an exponentially increasing trend with low values before the 1980s CE and major increases thereafter.

To eliminate the differences in units or scales of measurements, the 10 historical archives were standardized using z-scores and then the 5 indicators of agriculture (rural population, grain production, N fertilizers, P fertilizers and aquaculture production) and 5 urban and industrialization archives (urban population, electricity and concrete production, number of vehicles and length of roads) were each summed to be used as proxies for agricultural (Z-agriculture) and urban/industrial (Z-urban) development. GAMs were then fitted to detect the periods of change in agricultural development and urbanization/industrialization.

Proxies of agricultural and urban/industrial development indicate that significant changes in Z-agriculture preceded those in Z-urban in all lake catchments (Figure 6.2a, b). There was a period of sustained agricultural growth between 1949 CE and the mid-1990s CE (slope = ca. 0.25 in each catchment) in all six catchments with the exception of a hiatus in growth between 1955 CE and the early 1960s CE associated with the Great Famine, and followed by a reduction in growth rate afterwards (slope = ca. 0.15 in each catchment), associated with rural depopulation as people moved into cities (Figure 6.2a) (Yang, 2013). Z-urban increased exponentially with a slow and significant increase starting around the 1980s CE associated with the release of the “Reform and Opening” policy, which accelerated in all catchments in the early 2000s CE (Figure 6.2b). The scale of change in Z-urban (z-scores between ~ −5 and ~ 15), was almost double that of Z-agriculture (z-score between ~ −7.5 and ~ 7.5), reflecting a more pronounced growth in urban and industrial sectors than in agriculture.

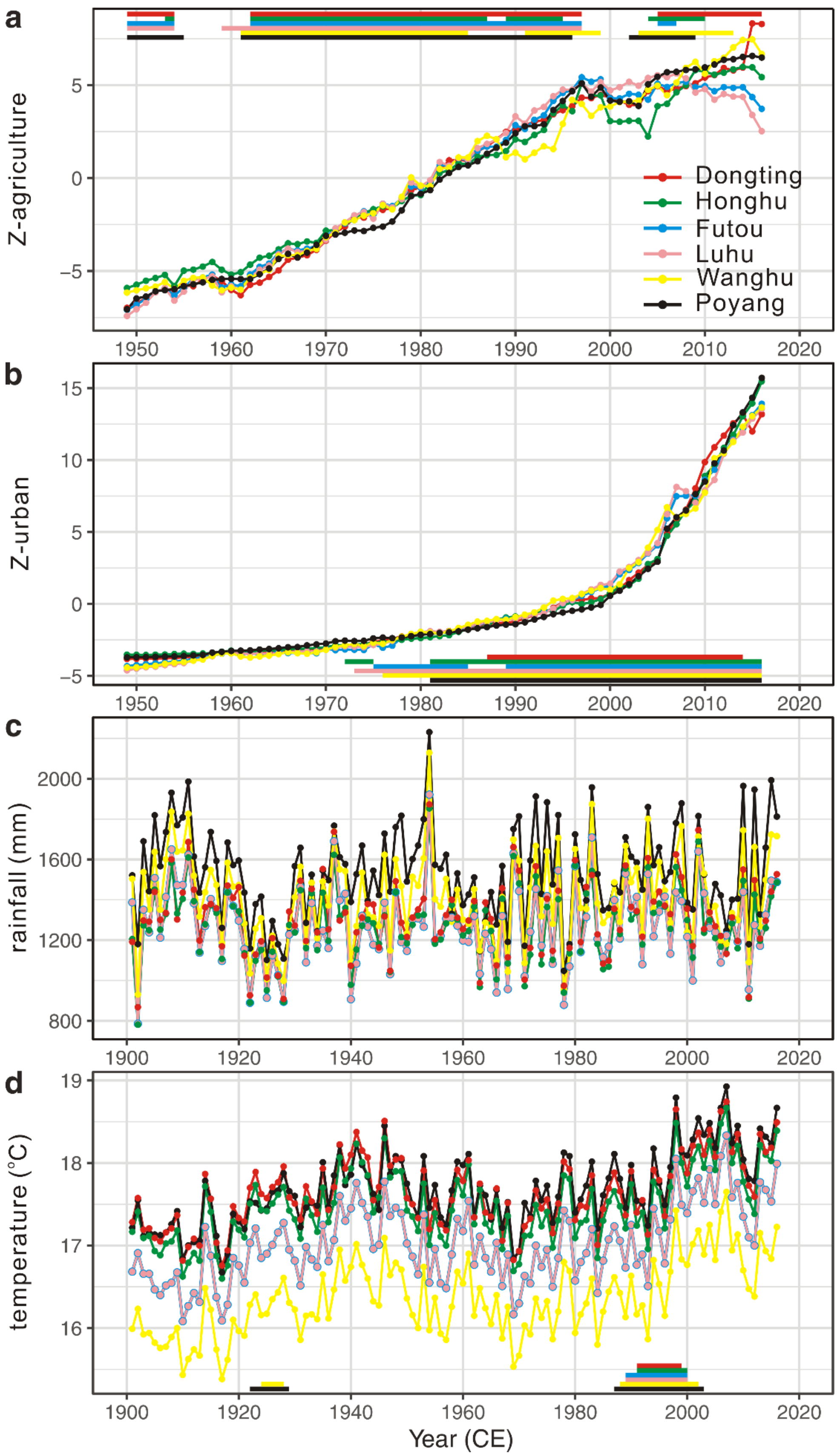

Figure 6.2 Z-scores of agricultural (a) and industrial/urban (b) drivers and total annual rainfall (c) and mean annual temperature (d). The horizontal bars in a, b and d indicate the period when the first derivative of the GAM fitted values of the z-score is significantly larger than 0 in each catchment.

Both total annual rainfall and mean annual temperature showed the same trend of variation in all catchments over the last ~120 years (Figure 6.2c, d). Total annual precipitation fluctuated at around 1350 mm with no overall directional trend through time (Figure 6.2c). Mean annual surface temperatures fluctuated around ~ 16.2 °C in the Wanghu catchment and ~17.0 °C in other catchments before the 1990s CE, followed by a significant increase between the 1990s CE and ~ 2000 CE before fluctuating since ~ 2000 CE (Figure 6.2d).

6.3.2 Spatio-temporal pattern of sedimentary TN and TP flux

6.3.2.1 Spatial comparisons of recent (post 2000 CE) sediment composition among lakes

The two large, open lakes (Poyang and Dongting) had the highest recent (post 2000 CE) dry mass accumulation rate (DMAR), followed by Luhu and Wanghu Lakes (Figure 6.3 A). DMARs were lowest in Honghu and Futou Lakes (Figure 6.3 A). In contrast, sedimentary N: P ratios were higher in Honghu and Futou Lakes (> 15) than the other four lakes (< 10) (Figure 6.3 B). Similarly, TOC was higher in Honghu and Futou Lakes (> 5%) compared with the other four lakes (Dongting, Luhu, Wanghu and Poyang) (~ 3%) after 2000 CE (Figure 6.3 C). The distribution of C/N ratios was similar to that of TOC, with higher values (> ~ 10) in Honghu and Futou Lakes and lower values (< ~ 10) in the others (Figure 6.3 D).

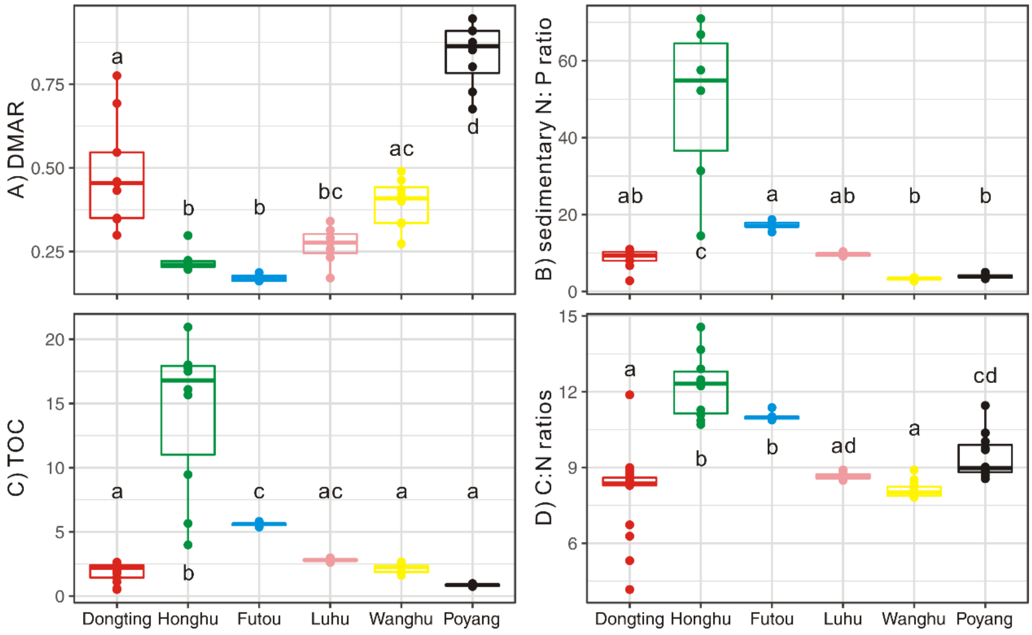

Figure 6.3 Boxplot showing the spatial difference in (A) DMAR (dry mass accumulation rate, unit: g · cm^{-2} · year^{-1}), (B) sedimentary N: P ratios (molecular), (C) TOC and (D) C/N ratios among sediments of the six lakes deposited since 2000 CE. Differences among groups (p < 0.05) were assessed using one-way ANOVA. Different letters on the boxes indicate significant differences between groups.

6.3.2.2 Temporal variance of sedimentary TN and TP fluxes in the lakes

Dated sediment cores provide a record of chronological changes in fluxes of nutrient pollutants to the lakes, allowing the consequences of human development in the catchments to be assessed. Here, major increases in the fluxes of N and P to all lakes, relative to fluxes before ~ 1950 CE, were documented (Figure 6.4). Between the 1950s CE and the 2010s CE, TN fluxes in the lakes increased from less than 0.05 g·cm^{-2}·year^{-1} to more than 0.10 g·cm^{-2}·year^{-1} with highly variable fluxes (Figure 6.4). TP fluxes also increased in all lakes since the 1950s CE, but temporal trends differed among lakes (Figure 6.4). Before the 1950s CE, sedimentary TP fluxes in the lakes were generally low (~ 0.01 g·cm^{-2}·year^{-1}). Since then, TP fluxes increased to ca. 0.04 g·cm^{-2}·year^{-1} by the 1980s CE, followed by a decrease in Dongting, Honghu and Futou Lakes. However, TP fluxes continued to increase in Luhu, Wanghu and Poyang Lakes from 1950 CE onwards. In the 2010s CE, sedimentary TP fluxes were more than 0.025 g·cm^{-2}·year^{-1} in Dongting, Luhu, Wanghu and Poyang Lakes, which was ca. 2-fold of that in Honghu and Futou Lakes (~ 0.01 g·cm^{-2}·year^{-1}) (Figure 6.4). N and P are strongly associated with lake eutrophication and sourced from agricultural fertilizers, urban wastewaters and fossil fuel burning, and increases fluxes in recent lake sediments mostly likely indicated long-term nutrient pollution.

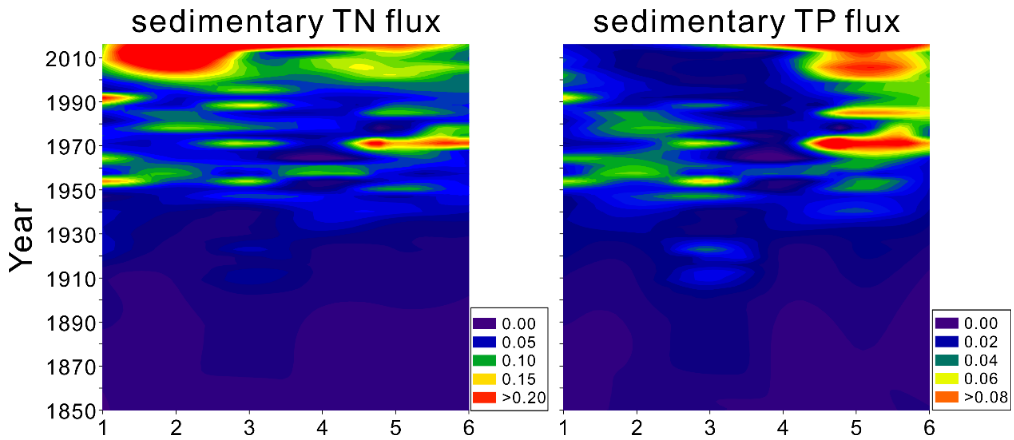

Figure 6.4 TN and TP fluxes of the lakes (unit: g · cm^{-2} · year^{-1}) (number 1 to 6 on the x-axis indicate the lakes, 1 = Dongting; 2 = Honghu; 3 = Futou; 4 = Luhu; 5 = Wanghu; 6 = Poyang).

6.3.3 Pigments

All sedimentary pigments from the six lakes showed an overall upward trend since ~ 1800 CE, indicating increasing primary production from algae including diatoms (diatoxanthin), cryptophytes (alloxanthin), chlorophytes (Chl *b*, pheophytin *b*, pheophytin *b*', lutein), cyanobacteria (aphanizophyll, canthaxanthin, zeaxanthin) and total algae (Chl *a*, phaeophorbide *a*, pheophytin *a*, pyropheophytin *a*, β-carotene). To investigate pigment changes on a common scale among different lakes, a single PCA was performed using log(x+1)-transformed pigment data from all six lakes to summarize and simplify the pigment dataset. The first PCA axis of pigments (PCA axis 1) explained 74.8 %

of the variance (Figure 6.5) and was significantly negatively correlated with all pigments ($R < -0.38$, $p < 0.001$), capturing the pigment abundance and composition in the lakes well. The second PCA axis of pigments explained a further 11.8 % of the variance and was significantly correlated with aphanizophyll ($R = -0.61$, $p < 0.001$) (Figure 6.5). Pigment PCA axis 2 clearly distinguished lakes with aphanizophyll. In recent years, samples from Dongting, Luhu, Wanghu and Poyang Lakes moved towards the negative direction of the second pigment PCA axis, characterized by high concentrations of aphanizophyll (Figure 6.5).

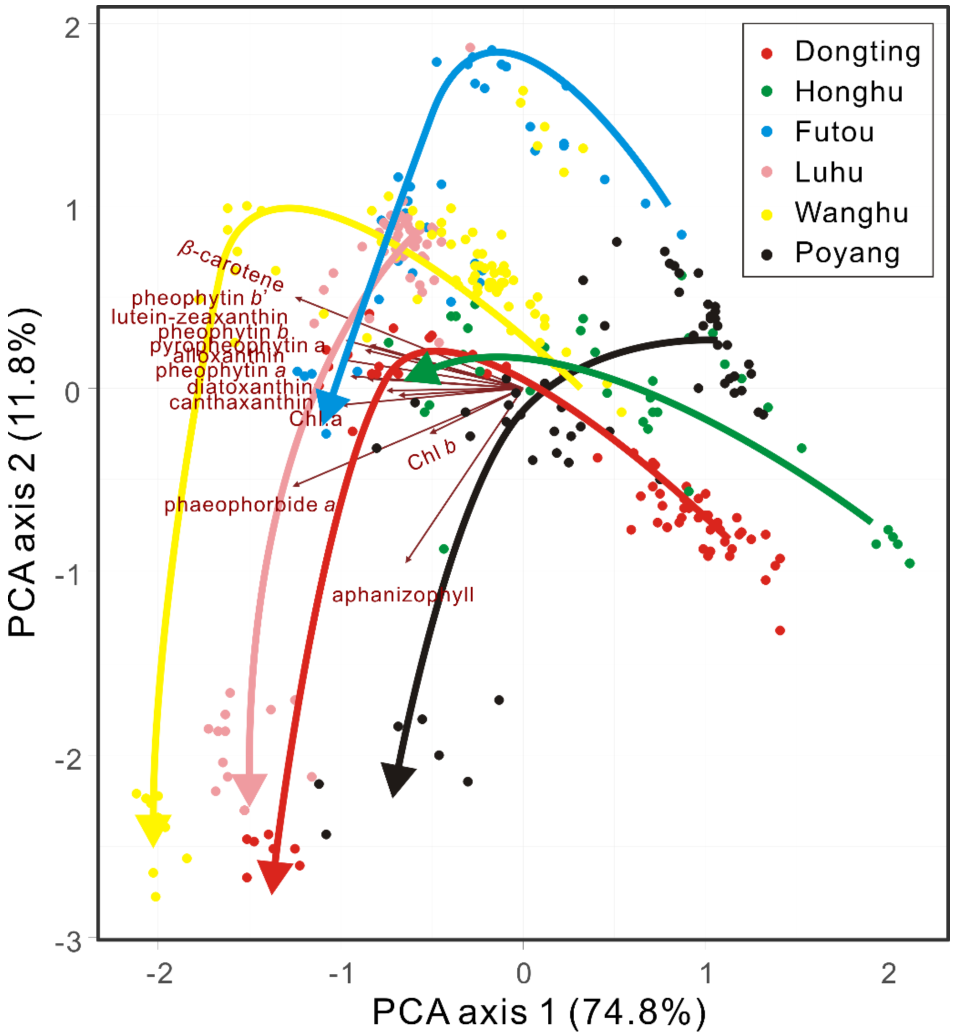

Figure 6.5 Biplot of joint PCA using pigments from all six lakes. PCA performed using pigment data from all six lakes. The coloured arrows indicate the trajectory from older to younger aged samples.

6.3.3.1 Spatial comparisons of recent (post 2000 CE) algal communities and HABs among lakes

Luhu and Wanghu Lakes had lower recent (post 2000 CE) pigment PCA axis 1 sample scores (and so higher pigment abundance) than Dongting, Poyang, Futou and Honghu Lakes (Figure 6.6 A). Similarly, concentrations of pigments from colonial cyanobacteria (canthaxanthin) were also higher in recent sediments of Luhu and Wanghu Lakes than the others (Figure 6.6 B). The distribution of pigments from filamentous N_2-fixing cyanobacteria (aphanizophyll) was different (Figure 6.6 C). Aphanizophyll was only preserved in Dongting, Luhu, Wanghu and Poyang Lakes but was barely detected in Honghu and Futou Lakes (Figure 6.6 C). In the four lakes with aphanizophyll, the concentrations of aphanizophyll were higher in Luhu and Wanghu Lakes. In terms of algal community composition, the ratio of pigments from colonial cyanobacteria to siliceous algae was similar in all six lakes with the exception of Poyang Lake which had a relatively higher ratio of canthaxanthin to diatoxanthin (Figure 6.6 D). In the four lakes with pigments from filamentous N_2-fixing cyanobacteria, there was no difference in the relative concentration of aphanizophyll to diatoxanthin (Figure 6.6 E). Similar to pigment concentrations, the accumulation rates of canthaxanthin (Figure 6.6 F) and aphanizophyll (Figure 6.6 G) were higher in Luhu and Wanghu Lakes compared with the other four lakes.

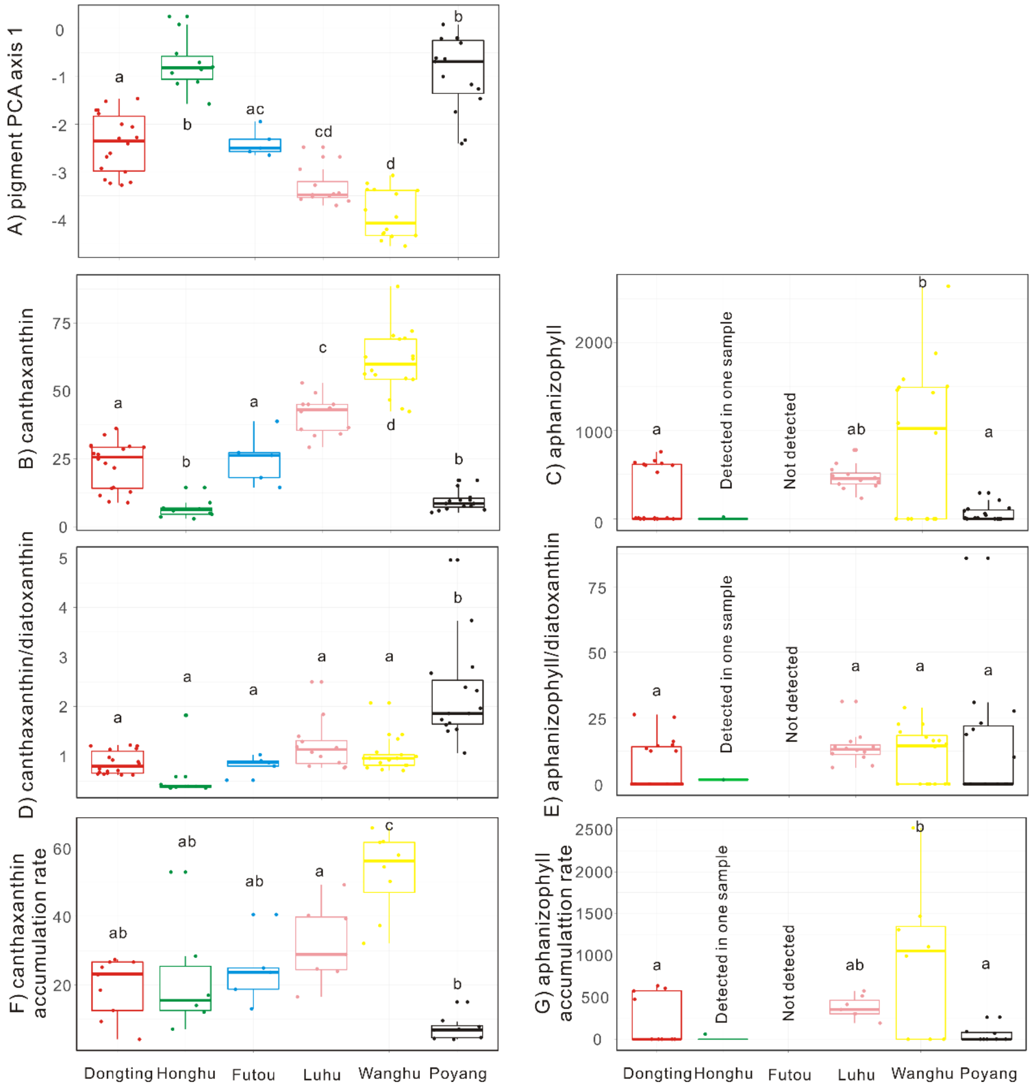

Figure 6.6 Boxplot showing the spatial difference in (A) algal production (indicated by pigment PCA axis 1), (B) canthaxanthin concentration (unit: nmol g^{-1} TOC), (C) aphanizophyll concentration (unit: nmol g^{-1} TOC), (D) aphanizophyll/diatoxanthin, (E) canthaxanthin/diatoxathin, (F) canthaxanthin accumulation rate (unit: nmol cm^{-2} yr^{-1}) and (G) aphanizophyll accumulation rate (unit: nmol cm^{-2} yr^{-1}) among the six lakes since 2000 CE. Differences among groups ($p < 0.05$) were assessed using one-way ANOVA. Different letters on the boxes indicate significant differences between groups.

6.3.3.2 Temporal variation of sedimentary pigments in each lake

The Mann-Kendall coefficient values (tau) of pigment PCA axis 1 was significantly smaller than 0 (tau ≤ –0.37; $p < 0.001$), implying an overall decreasing trend in pigment PCA axis 1 (Figure 6.7), which indicates an increase in algal production in all of the lakes since ~ 1800 CE. Although all lakes experienced an overall increase in algal production over the last 200 years, the timing and trends of algal assemblage shifts were different among the lakes (Figure 6.7). In Honghu Lake, the first derivatives of the GAM-fitted pigment PCA axis 1 were indistinguishable from 0 before 1952 CE and were significantly smaller than 0 ($p < 0.05$) thereafter, indicating a significant decrease in pigment PCA axis 1 scores since 1952 CE (Simpson, 2018). For Futou Lake, the first derivatives of the GAMs fitted pigment PCA axis 1 were negative ($p < 0.05$) after 1932 CE (Figure 6.7). In Dongting, Luhu, Wanghu and Poyang Lakes, the pigment PCA axis 1 scores were relatively stable before ca. 1980 (Figure 6.7). It was not until ca. 1980 (±2) CE ($p < 0.05$) that the first derivatives of the GAM fitted to pigment PCA axis 1 scores were significantly smaller than 0 (1980 CE, 1982 CE, 1979 CE and 1982 CE in Dongting, Luhu, Wanghu and Poyang, respectively) (Figure 6.7). Therefore, according to the GAM, algal production started to increase since 1952 CE in Honghu and 1932 CE in Futou Lakes, whereas the increases in algal production were later in Dongting, Luhu, Wanghu and Poyang Lakes, starting from ca. 1980 (±2) CE.

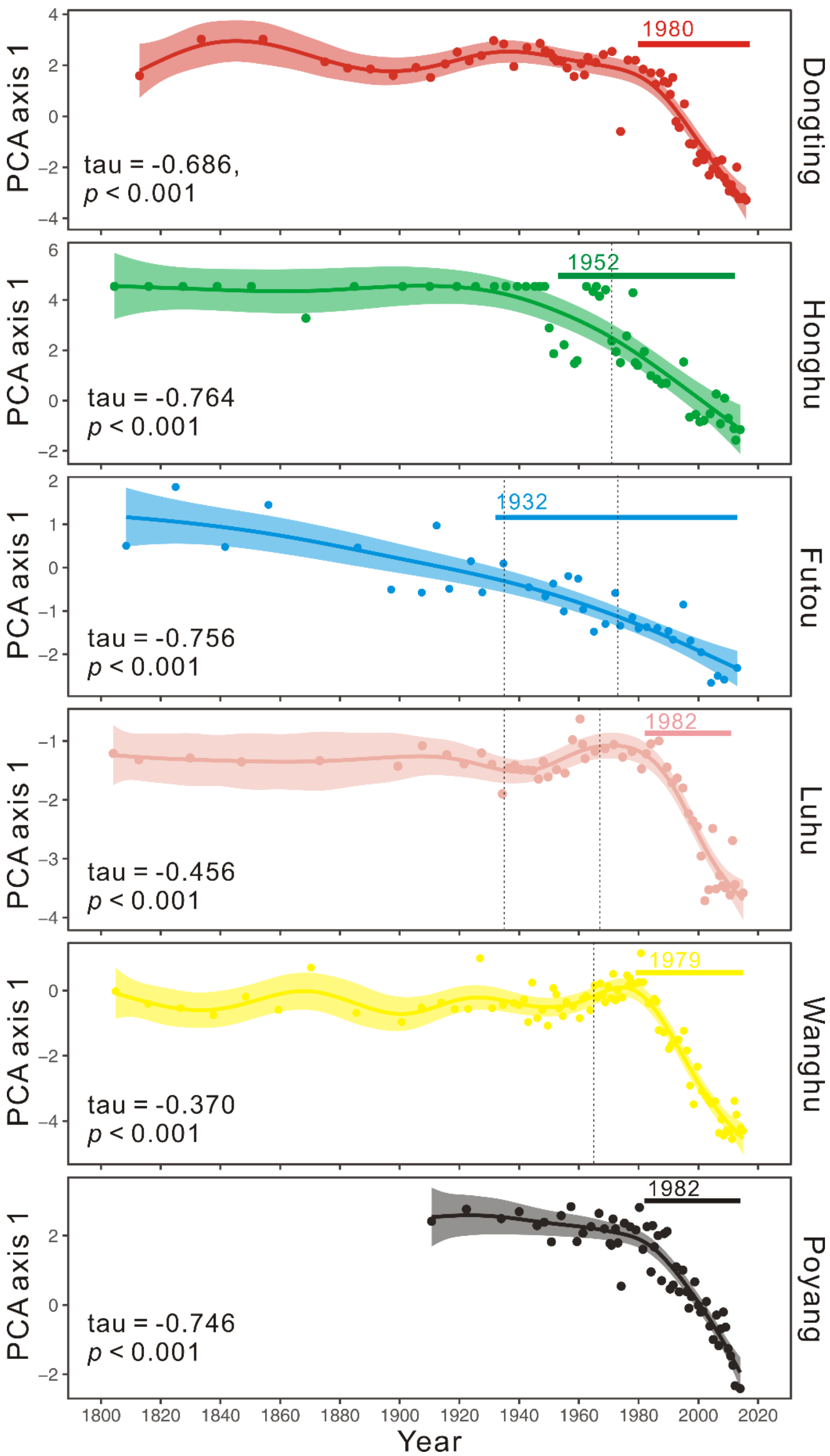

Figure 6.7 Observed and GAM fitted values for joint pigment PCA axis 1 scores for the lakes. The band is the 95% pointwise confidence interval on the fitted values. The horizontal line shows the period when the first derivative of pigment PCA axis 1 is significantly different from 0. The number on the line indicates the start of the period. The vertical dashed line indicates local dam construction. tau is the MK coefficient values, *p* is the significance level.

6.3.4 Summary of results

Since 2000 CE Luhu and Wanghu Lakes which have more intensive urban/industrial activities in the catchments, have had higher algal production (as pigment PCA axis 1) (Figure 6.6 A) and concentrations of colonial cyanobacteria (as canthaxanthin) (Figure 6.6 B) compared to other lakes. In contrast, pigments of filamentous N_2-fixing cyanobacteria (as aphanizophyll) were only preserved in Dongting, Luhu, Wanghu and Poyang Lakes which had lower sedimentary N: P ratios (< 10), and were barely detected in Honghu and Futou Lakes which had higher sedimentary N: P ratios (> 15) (Figure 6.6 C). In the four lakes with pigments from filamentous N_2-fixing cyanobacteria, concentration and sedimentation rate of aphanizophyll were lower in hydrologically open Dongting and Poyang Lakes compared with Luhu and Wanghu Lakes, which are influenced by local dams.

Sedimentary pigments showed an overall upward trend over the last 200 years, implying the increases in algal production in these middle Yangtze floodplain lakes (Figure 6.7). In Honghu and Futou Lakes, which have more intensive agricultural activities in the catchments (Figure 6.1), major increases in algal production started from the ~ 1940s (±10) CE (Figure 6.7), in correspondence with the timing of agricultural development in the catchments (Figure 6.2). Rapid increases in algal production occurred since ~ 1980 CE in Dongting, Luhu, Wanghu and Poyang Lakes, coinciding with the timing of urbanization/industrialization in the catchments (Figure 6.7).

6.4 Statistical analysis

6.4.1 Spatial comparison among the lakes

6.4.1.1 Relationship between recent (post 2000 CE) catchment human activities and sedimentary TN and TP flux

To explore how agricultural and industrial/urban activity intensity in the catchment affect nutrient conditions in the lakes, the relationship between recent (post 2000 CE) sedimentary TN and TP flux in the lakes and historical archives in the catchments was compared among the six lakes. The result showed that sedimentary TN flux was significantly positively correlated with all agricultural archives, with the exception of rural population which was negatively correlated with TN flux. Sedimentary TP flux was positively correlated with concrete production and negatively correlated with agricultural archives (grain production, aquaculture products, and N and P fertilizer).

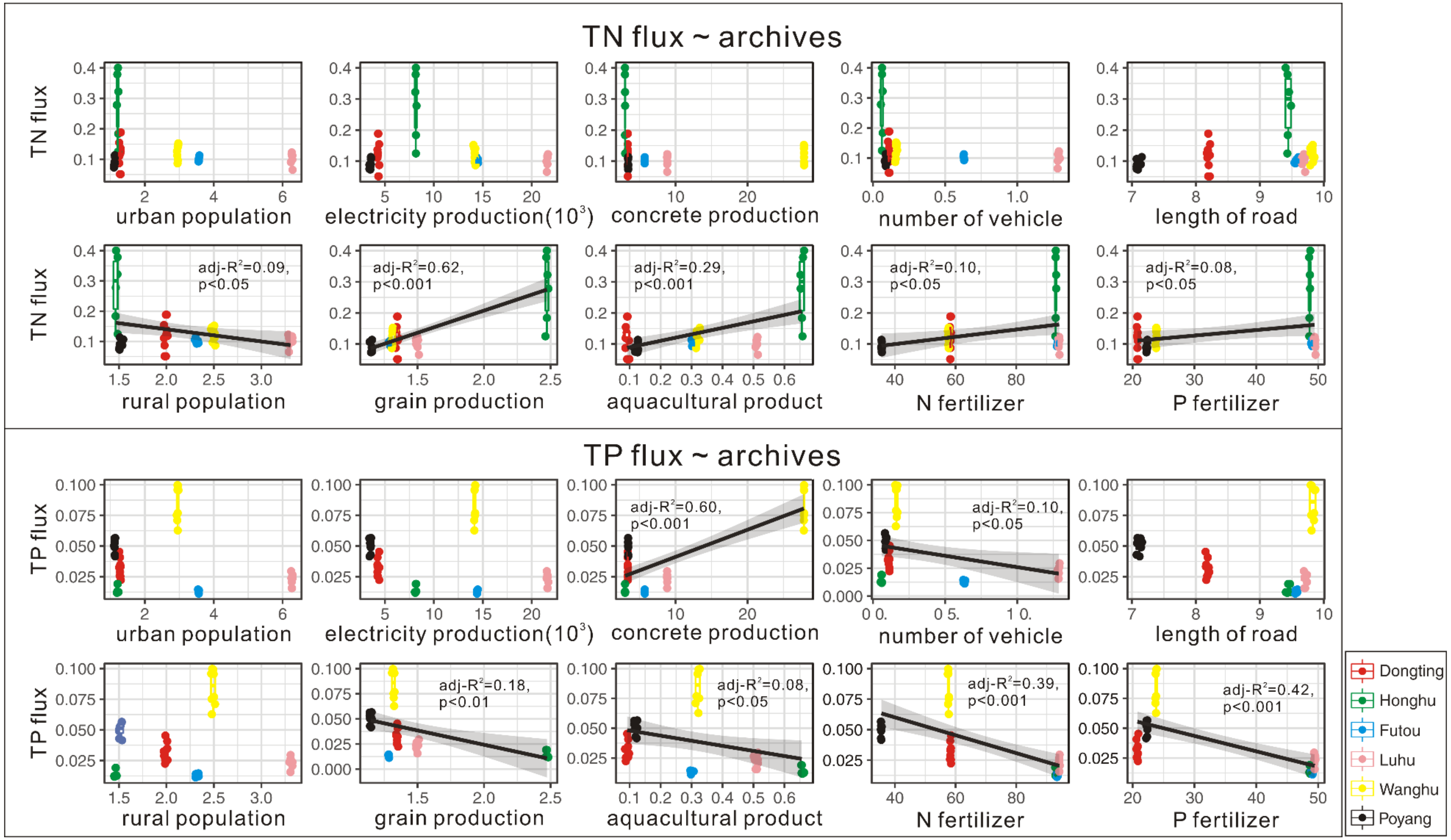

Figure 6.8 Linear regression between recent (after 2000 CE) sedimentary TN (upper) and TP (lower) flux in the lakes and the density of historical archives in the catchments. The shaded band surrounding the fitted line indicates the approximate 95 % confidence intervals.

6.4.1.2 Relationship between recent (post 2000 CE) water quality (TN and TP concentrations) and pigments

To explore how HABs and algal production response varied with water quality among the lakes, recent (post 2000 CE) pigments from filamentous N_2-fixing cyanobacteria (aphanizophyll) and joint pigment PCA axis 1 scores were plotted against the TN and TP in the water column acquired from water survey in the summer of 2017 CE. The results showed that recent aphanizophyll concentration was significantly correlated with both TN (adj-R^2 = 0.23; p < 0.001) (Figure 6.9 A) and TP (adj-R^2 = 0.32; p < 0.001) (Figure 6.9 B) concentrations in the water column. Similarly, there was also a significant correlation between recent pigment abundance (as pigment PCA axis 1) and both TN (Figure 6.9 C) and TP (Figure 6.9 D) in the water column.

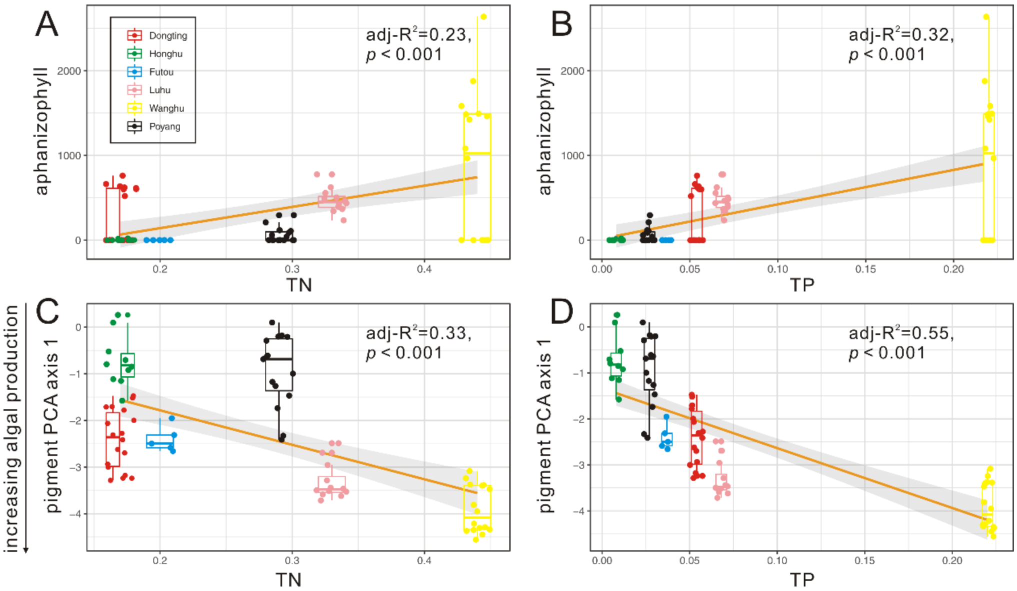

Figure 6.9 Linear regression between recent (after 2000 CE) filamentous N_2-fixing cyanobacteria (as aphanizophyll, unit: nmol g^{-1} TOC) and algal production (joint PCA axis 1 scores) and water column TN and TP (unit: mg L^{-1}) in the lakes. (A) aphanizophyll against TN; (B) aphanizophyll against TP; (C) pigment PCA axis 1 against TN; (D) pigment PCA axis 1 against TP. The shaded band surrounding the fitted line indicates the approximate 95 % confidence intervals.

6.4.1.3 Relationship between recent (post 2000 CE) DMAR and HABs among lakes with aphanizophyll

According to the Vollenweider (1976) model, hydrology (water flushing rates) is important in regulating nutrient (mainly P) sedimentation and retention in lake, which may influence algal production and HABs. To explore the relationship between hydrology and algal production and HABs, recent (after 2000 CE) joint pigment PCA axis 1 scores (indicating algal production) and pigments from filamentous N_2-fixing cyanobacteria (aphanizophyll) were plotted against the DMAR among lakes with HABs. The result showed that both recent algal production and aphanizophyll were significantly correlated with DMAR (Figure 6.10).

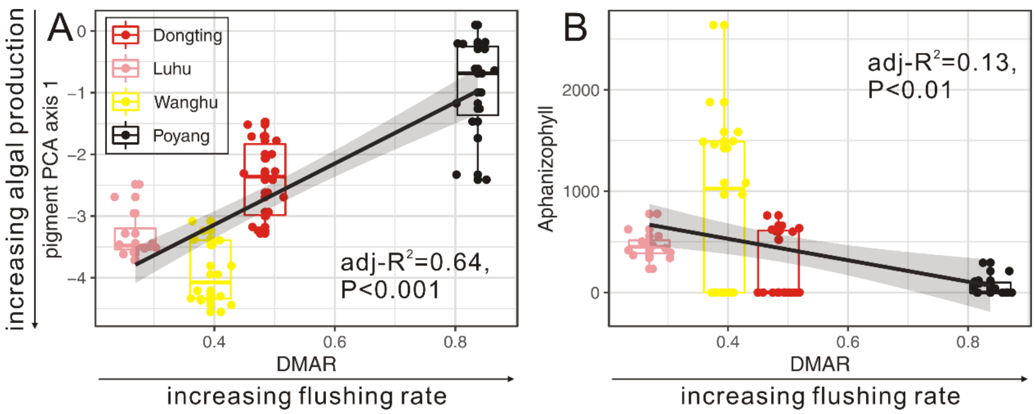

Figure 6.10 Linear regression between recent (after 2000 CE) (A) pigment (as pigment PCA axis 1) and (B) filamentous N_2-fixing cyanobacteria (as aphanizophyll, unit: nmol g^{-1} TOC) abundance and DMAR (dry mass accumulate rate, unit: g cm^{-2} yr^{-1}) among lakes with HABs.

6.4.2 Temporal variation in the sediment cores

6.4.2.1 Relationship between TN and TP fluxes and pigment PCA axis 1 since ~ 1850 CE

In an attempt to investigate the linkages between nutrient fluxes and algal production changes since ~1850 CE, linear regression analysis was used to quantify the relationship between sedimentary TN and TP fluxes and algal pigments in each lake. For algal production, PCA was performed using log(x+1)-transformed pigment data on an individual lake basis. The first PCA axis of pigments in each lake explained more than 75% of the variance in pigments and was significantly negatively correlated with all pigments ($R < -0.37$; $p < 0.01$), with the exception of pheophytin *b*' ($R = -0.12$; $p = 0.50$) and pyropheophytin *a* ($R = 0.10$; $p = 0.55$) in Futou Lake and β-carotene ($R = -0.13$; $p = 0.34$) in Luhu Lake, which captured the pigment abundance and composition in the lakes well (Figure 6.11). Lower sample scores on the first pigment PCA axis indicated higher algal production. Therefore, the first PCA axis of pigments which represents algal production was used as the response variable, and the explanatory variable was sedimentary TN or TP fluxes.

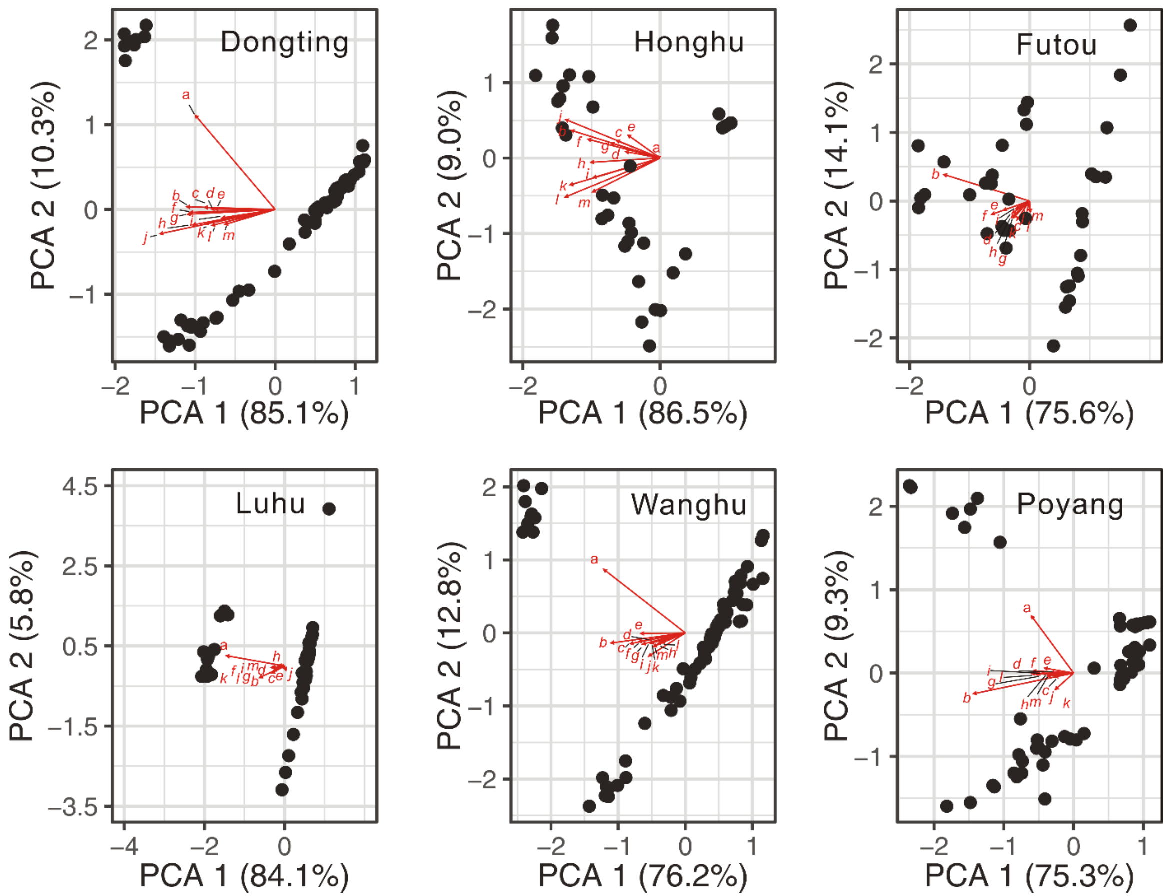

Figure 6.11 PCA biplot of pigments from each individual lake (a = aphanizophyll, b = phaeophorbide *a*, c = diatoxanthin, d = canthaxanthin, e = Chl *b*, f = Chl *a*, g = alloxanthin, h = lutein-zeaxanthin, i = pheophytin *a*, j = *β*-carotene, k = pheophytein b, l = pheophytin *b*', m = pyropheophytein *a*). PCA performed using pigment dataset from each individual lake.

Pigment composition in lakes in the middle Yangtze floodplain showed different relationships with TN and TP fluxes since ~ 1850 CE (Table 6.1, Figure 6.12). In Dongting, Honghu and Futou Lakes, the first PCA axis of pigments was significantly correlated with TN flux but not with TP flux. In Luhu and Wanghu Lake, both TN and TP flux were significantly correlated with pigment PCA axis 1. In Poyang Lake, there were no significant correlations between TN and TP flux and PCA axis 1 of pigments.

Table 6.1 Significance level of simple linear regression between pigment PCA axis 1 and TN and TP flux of the lakes.

	pigment PCA axis 1					
	Dongting	Honghu	Futou	Luhu	Wanghu	Poyang
TN flux	*	***	***	***	**	n.s.
TP flux	n.s.	n.s.	n.s.	*	**	n.s.

***<0.001; **<0.01; *<0.05; n.s. no significance

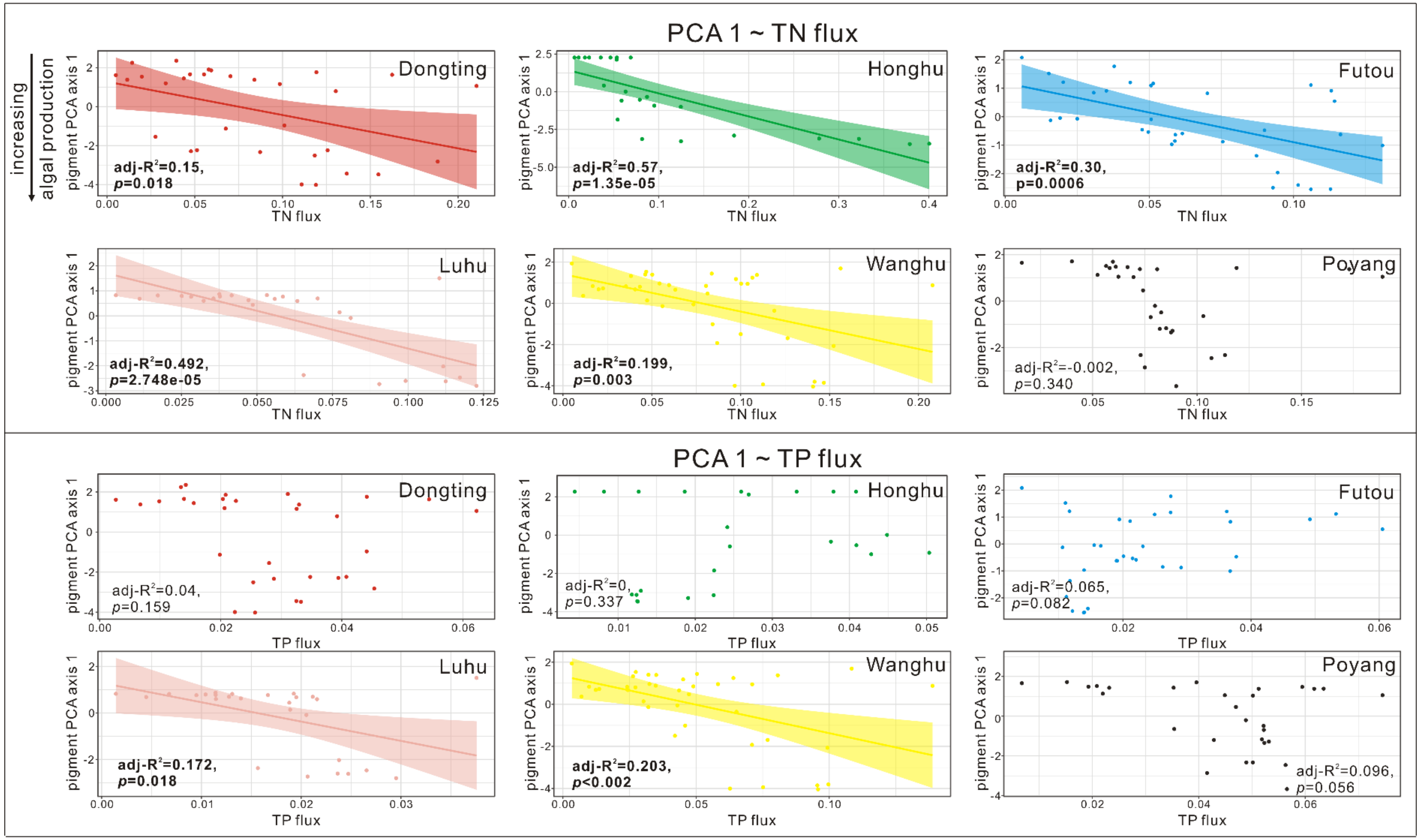

Figure 6.12 Linear regression between the first PCA axis of pigments and TN (upper) and TP (lower) flux of the lakes. Regression line was presented in plots with significant relationship (p < 0.05) were shown. The shaded band surrounding the fitted line indicates the approximate 95 % confidence intervals.

6.4.2.2 Relationship between sedimentary pigments and historical archives since ~ 1950 CE

As historical archives were available from 1949 CE, GAMs were applied to investigate the relationships between algal production (as pigment PCA axes 1) and HABs (as cyanobacterial biomarker pigments, aphanizophyll) and potential environmental drivers in each individual lake since ~ 1950 CE. Explanatory variables in the analyses included indicators of agricultural development (Z-agriculture) and industrial activities and urbanization (Z-urban), mean annual temperature, total annual rainfall and dam construction (present or absent), which may potentially influence algal production and community change.

Relationship between algal production (pigment PCA axis 1) and historical archives

In general, GAMs showed that algal production was significantly and positively correlated with agricultural development, but not urbanization/industrialization indicators in Dongting, Honghu and Futou Lakes (Table 6.2). In contrast, algal production was only significantly related with urban/industrial activities in Luhu Lake. In Wanghu and Poyang Lakes, algal production was significantly related with both agricultural and urban/industrial development.

Table 6.2 Results of the significance level of drivers to PCA axis 1 and aphanizophyll from GAMs (Z_A and Z_U are short for Z-agriculture and Z-urban, respectively; T is temperature; R is rainfall; TGD is Three Gorges Dam; LD stands for local dam).

		Z-A	Z-U	T	R	TGD	LD
Dongting	PCA1	***	n.s.	n.s.	n.s.	n.s.	-
	aphanizophyll	n.s.	***	*	n.s.	n.s.	-
Honghu	PCA1	*	n.s.	n.s.	**	n.s.	**
	aphanizophyll	-	-	-	-	-	-
Futou	PCA1	*	n.s.	n.s.	n.s.	**	n.s.
	aphanizophyll	-	-	-	-	-	-
Luhu	PCA1	n.s.	***	n.s.	n.s.	n.s.	n.s.
	aphanizophyll	n.z.	***	n.s.	*	*	n.s.
Wanghu	PCA1	**	***	n.s.	n.s.	n.s.	n.s.
	aphanizophyll	n.s.	***	n.s.	n.s.	n.s.	n.s.
Poyang	PCA1	***	***	n.s.	*	n.s.	-
	aphanizophyll	n.s.	***	n.s.	n.s.	n.s.	-

***<0.001; **<0.01; *<0.05; n.s. no significance; - no data

In Dongting Lake, the GAM results indicated a negative relationship between PCA axis 1 of pigments and z-score of agriculture (Z_A) (p < 0.001) (Figure 6.13; Table 6.2). The pigment PCA axis 1 was relatively stable when the z-score of agriculture (Z_A) was less than 0 (before ca. 1980 CE). When the Z_A was larger than 0, sample scores on the pigment PCA axis 1 sharply decreased with increasing Z_A, indicating the increase in algal production as Z_A increases.

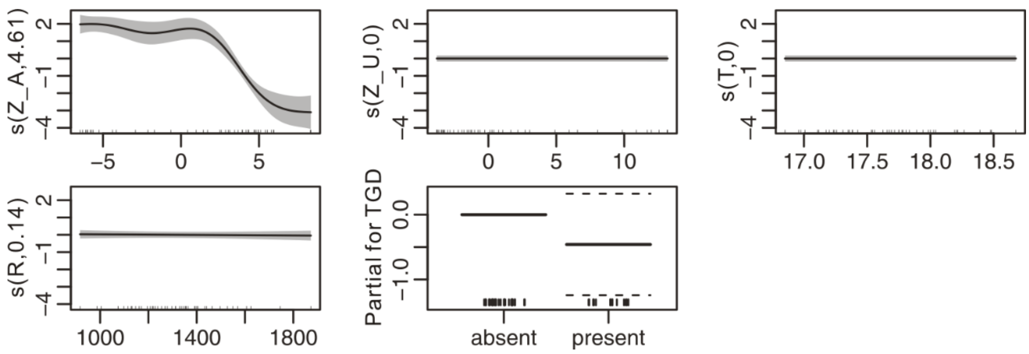

Figure 6.13 The fitted smooth function for covariates from the GAM for the pigment PCA axis 1 in Dongting Lake. The grey bands are approximate 95% pointwise confidence intervals on the fitted functions. The numbers in brackets on the y-axis are the effective degrees of freedom for each smooth function. (Z_A and Z_U are short for z-score of agriculture and z-score of urbanization/industrialization, respectively; T is temperature; R is rainfall; TGD is Three Gorges Dam).

In Honghu Lake, pigments PCA axis 1 was significantly related with z-score of agriculture (Z_A) ($p < 0.01$), rainfall ($p < 0.01$) and local dam construction ($p < 0.01$) (Figure 6.14; Table 6.2). To be more specific, pigment PCA axis 1 responded to Z_A in a unimodal way. Sample scores on pigment PCA axis 1 increased (representing decreases in algal production) with the increase in Z_A before ~ 1975 CE when Z_A was less than −1.5, and decreased (implying increases in algal production) with the increase in Z_A after ~ 1975 CE when Z_A was larger than −1.5. Different from Z_A, pigment PCA axis 1 was negatively correlated with precipitation. When total annual precipitation was below ~ 1,200 mm, there was a negative relationship with pigments (PCA axis 1 sample scores), whereas when rainfall was higher than ~ 1200 mm, sample scores were unresponsive. After local dam (LD) construction there were significant increases in algal production (significantly lower sample scores on pigment PCA axis 1).

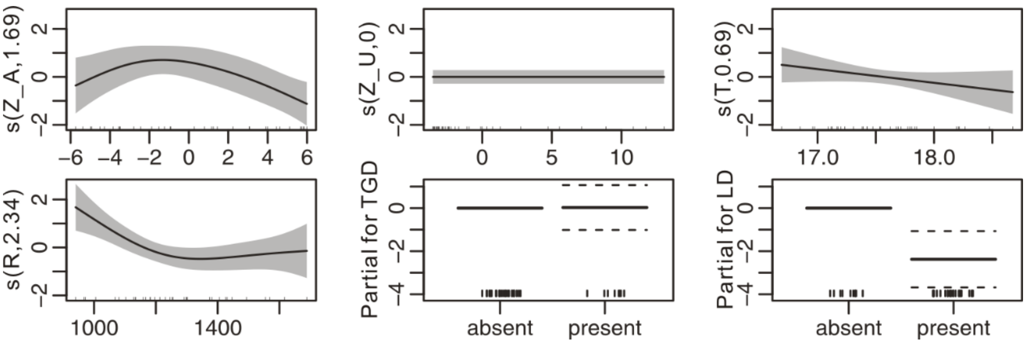

Figure 6.14 The fitted smooth function for covariates from the GAM for the pigment PCA axis 1 in Honghu Lake. The grey bands are approximate 95% pointwise confidence intervals on the fitted functions. The numbers in brackets on the y-axis are the effective degrees of freedom for each smooth function. (Z_A and Z_U are short for z-score of agriculture and z-score of urbanization/industrialization, respectively; T is temperature; R is rainfall; TGD is Three Gorges Dam; LD stands for local dam).

Both Z-agriculture ($p < 0.05$) and TGD ($p < 0.01$) were significantly related with pigments PCA axis 1 in Futou Lake (Figure 6.15; Table 6.2). Sample scores on the first pigment PCA axis linearly decreased with the increase in Z_A, indicating increases in algal production as Z_A increased. There was a significant decrease in the sample scores on pigment PCA axis 1 after the construction of TGD, which indicated increases in algal production, but no significant response to local damming.

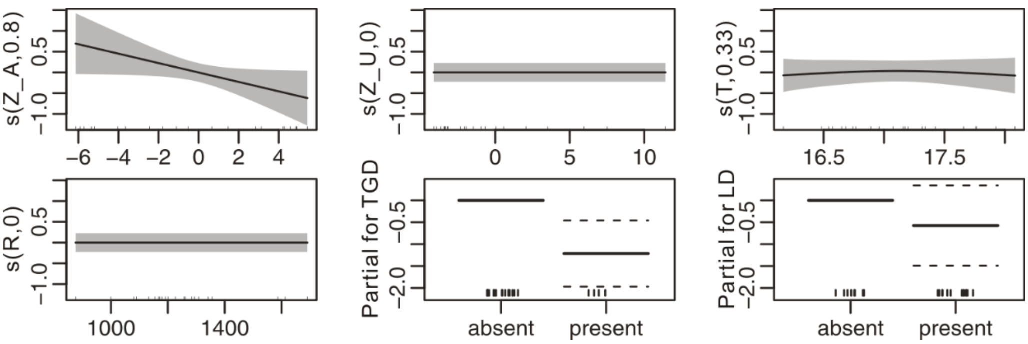

Figure 6.15 The fitted smooth function for covariates from the GAM for the pigment PCA axis 1 in Futou Lake. The grey bands are approximate 95% pointwise confidence intervals on the fitted functions. The numbers in brackets on the y-axis are the effective degrees of freedom for each smooth function. (Z_A and Z_U are short for z-score of agriculture and z-score of urbanization/industrialization, respectively; T is mean annual temperature; R is total annual rainfall; TGD is Three Gorges Dam; LD stands for local dam).

In Luhu Lake, the z-score of urbanization and industrialization (Z_U) was the only explanatory variable significantly related with pigment PCA axis 1 ($p < 0.001$) (Figure 6.16; Table 6.2). Sample scores on pigment PCA axis 1 were relatively stable when Z_U was less than −2 (before ~ 1980 CE). Between ~ 1980 CE and ~ 2005 CE when Z_U increased from ~ −2 to ~ 5, sample scores on the first pigment axis sharply decreased, implying the increase in algal production. After ~ 2005 CE, samples scores hovered at a low value as Z_U increased to more than 5.

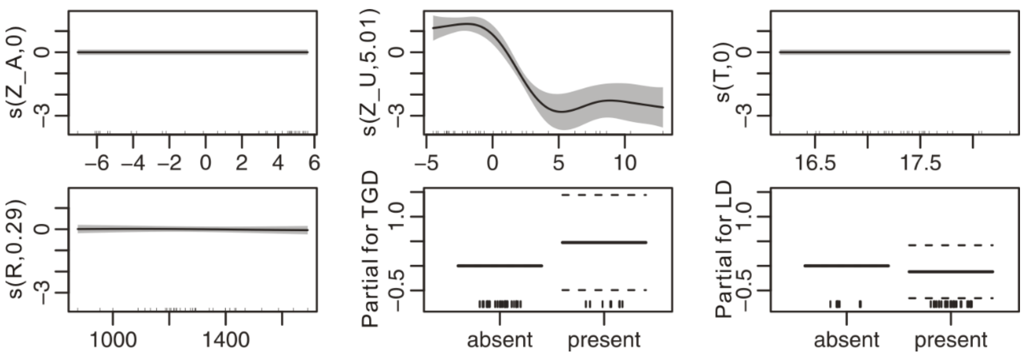

Figure 6.16 The fitted smooth function for covariates from the GAM for the pigment PCA axis 1 in Luhu Lake. The grey bands are approximate 95% pointwise confidence intervals on the fitted functions. The numbers in brackets on the y-axis are the effective degrees of freedom for each smooth function. (Z_A and Z_U are short for z-score of agriculture and z-score of urbanization/industrialization, respectively; T is mean annual temperature; R is total annual rainfall; TGD is Three Gorges Dam; LD stands for local dam).

Although both were significant, Z_U (effective degrees of freedom (edf) = 3.63; $p < 0.001$) had a larger influence on the variance in sample scores on pigment PCA axis 1 compared to Z_A (edf = 1.84; $p < 0.05$) in Wanghu Lake, indicating more significant influence of urbanization and industrialization on algal production (Figure 6.17; Table 6.2). Before ~ 1980 CE when Z_U < −2, sample scores on the first pigment PCA axis maintained at a high value. When −2 < Z_U < 7.5 (between ~ 1980 CE and ~ 2010 CE), sample scores on pigment PCA axis 1 sharply decreased (representing increasing algal production) with increases in

Z_U. When Z_U > 7.5, sample scores on the first PCA axis of pigments were hovering at a low value. As for Z_A, sample scores slightly decreased with the increases in Z_A after ~ 1980 CE when Z_A > 0.

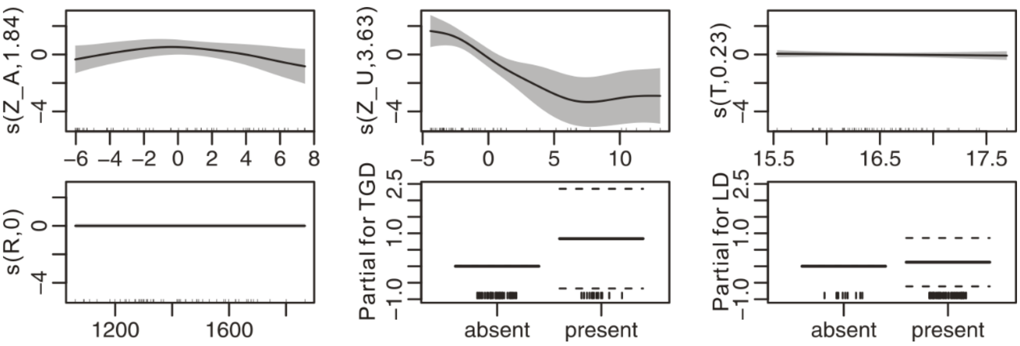

Figure 6.17 The fitted smooth function for covariates from the GAM for the pigment PCA axis 1 in Wanghu Lake. The grey bands are approximate 95% pointwise confidence intervals on the fitted functions. The numbers in brackets on the y-axis are the effective degrees of freedom for each smooth function. (Z_A and Z_U are short for z-score of agriculture and z-score of urbanization/industrialization, respectively; T is mean annual temperature; R is total annual rainfall; TGD is Three Gorges Dam; LD stands for local dam).

In Poyang Lake, the pigments PCA axis 1 was significantly correlated with z-score of agriculture (Z_A) ($p < 0.001$), z-score of urbanization/industrialization (Z_U) ($p < 0.001$) and rainfall ($p < 0.05$), in which Z_A had the largest edf (2.92), implying the largest influence (Figure 6.18, Table 6.2). Sample scores showed a negative relationship with both Z_A and Z_U. Different from Z_U, which had a linearly negative relationship with pigment PCA axis 1, the relationship between Z_A and pigment PCA axis 1 varied. Sample scores on pigment PCA axis 1 stabilised at a high value when Z_A < 0 and rapidly decreased (representing increase in algal production) with the increase in Z_A when Z_A > 0.

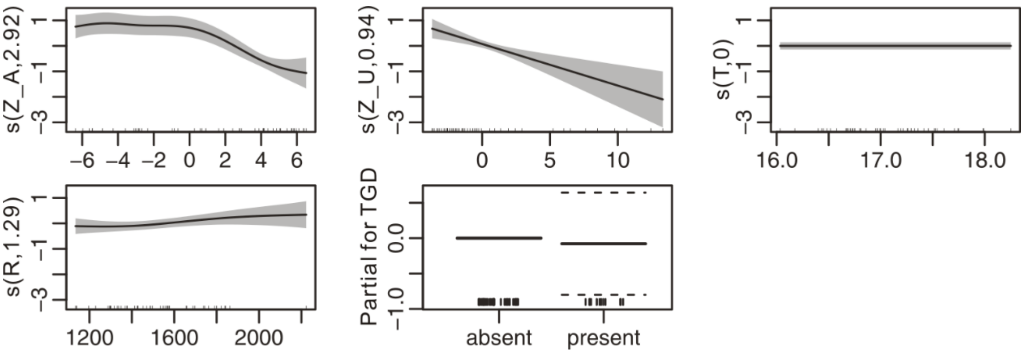

Figure 6.18 The fitted smooth function for covariates from the GAM for the pigment PCA axis 1 in Poyang Lake. The grey bands are approximate 95% pointwise confidence intervals on the fitted functions. The numbers in brackets on the y-axis are the effective degrees of freedom for each smooth function. (Z_A and Z_U are short for z-score of agriculture and z-score of urbanization/industrialization, respectively; T is mean annual temperature; R is total annual rainfall; TGD is Three Gorges Dam).

Relationship between N_2-fixing cyanobacteria (aphanizophyll) and historical archives

To look at patterns in HABs, pigments from filamentous N_2-fixing cyanobacteria (aphanizophyll) were used as the response variable in GAMs. As aphanizophyll was barely detected in Honghu and Futou Lakes, GAMs were only fitted in Dongting, Luhu, Wanghu and Poyang Lakes.

The results of GAMs showed that aphanizophyll was significantly related with z-score of urbanization/industrialization (Z_U) in all the four lakes (Figure 6.19, Table 6.2), indicating the role of urbanization/industrialization in causing HABs. Nevertheless, the pattern of the relationship between aphanizophyll and Z_U in Luhu (Figure 6.19 B) and Wanghu (Figure 6.19 C) Lakes was different from that in Dongting (Figure 6.19 A) and Poyang (Figure 6.19 D) Lakes. In both Luhu and Wanghu Lakes, concentrations of aphanizophyll was low and stable when Z_U < 1 (before ~ 2000 CE). When 1 < Z_U < 7, aphanizophyll rapidly increased with the increases in Z_U in the two lakes. After ~ 2000 CE when Z_U >7, aphanizophyll was maintained at a high value. Different from Luhu and Wanghu

Lakes, aphanizophyll concentrations were low and stable when Z_U < 7, and consistently increased with the increases in Z_U when Z_U > 7.

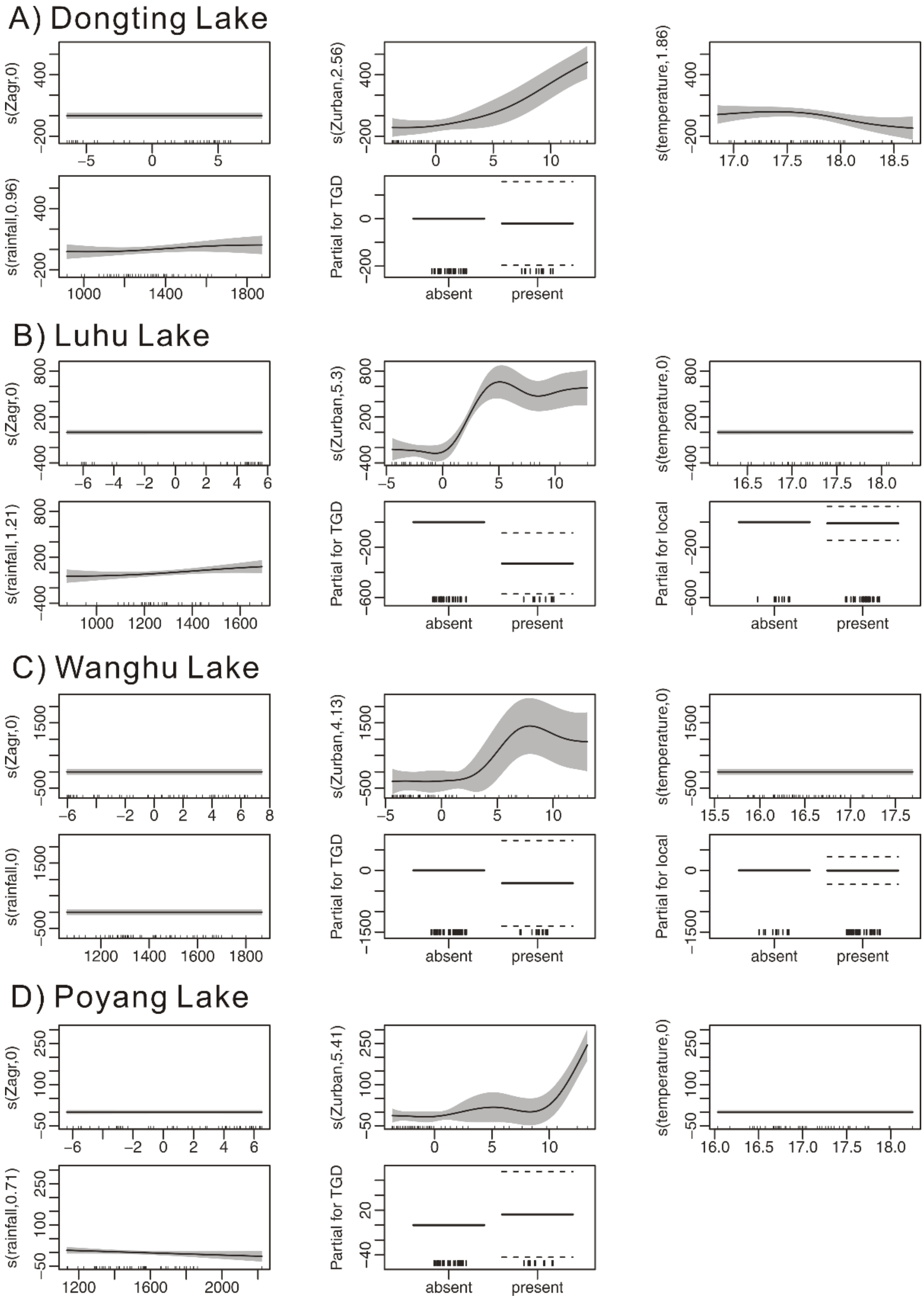

Figure 6.19 Summary of the fitted smooth function for covariates from the GAM for aphanizophyll in the lakes. The grey bands are approximate 95% pointwise confidence intervals on the fitted functions. The numbers in brackets on the y-axis are the effective degrees of freedom for each smooth function. Z_A and Z_U are short for Z-agriculture and Z-urban, respectively; T is temperature; R is rainfall; TGD is Three Gorges Dam; LD stands for local dam.

6.5 Discussion

Lakes in this study encompass a wide variety of intensity in agricultural and urban/industrial activities in their catchments (Figure 6.1) and hydrological connectivity with the Yangtze River (Table 3.1). This makes the study suitable to examine the effects of human activities and hydrology on nutrient condition and algal production in floodplain lakes. Historical archives show that agriculture has rapidly developed since ~ the late 1940s CE and urbanization/industrialization rapidly developed since ~ the late 1970s CE (Figure 6.2). Regression analysis shows that sedimentary TN and TP flux were correlated with agricultural and industrial/urban activities, repectively. Sedimentary TN and TP flux indicate that nutrient loading increased in the lakes with the intensification of agricultural and urban/industrial activities in the catchment (Figure 6.4). Sedimentary pigments indicate an overall increase in algal production in the middle Yangtze floodplain lakes over the last two centuries (Figure 6.7), including HABs in some of the lakes (Dongting, Honghu, Luhu and Wanghu) after 2000 CE. The significant correlations between TN and TP and pigment PCA axis 1 scores (indicating algal production) indicates that nutrients were the fundamental factor influencing algal production and HABs (Figure 6.9). In the four lakes with aphanizophyll, both recent (> 2000 CE) algal production and aphanizophyll concentration were higher in Luhu and Wanghu Lakes (with local dam) than Dongting and Poyang Lakes (open), while the algal community composition were similar (Figure 6.6). The significant correlation between pigment PCA axis 1 scores and aphanizophyll concentration and DMAR indicates that hydrology might influence the pigment concentrations in these Yangtze floodplain lakes (Figure 6.10).

6.5.1 Influence of dam construction and catchment agricultural and industrial/urban activities on sedimentary TN and TP flux

Recent (post 2000 CE) DMAR was significantly higher in open Dongting and Poyang Lakes than the other four lakes with local dam (Figure 6.3), suggesting that hydrological connectivity with the Yangtze River was an important factor regulating sediment flux in these Yangtze floodplain lakes (Xiang et al., 2002; Chen et al., 2016). It is well established that bulk sediment accumulation rate is influenced by various factors, such as the allochthonous sediment influx (e.g., catchment soil erosion) and autochthonous organic matter production (e.g., algal production) (Rose et al., 2011; Xu et al., 2017). In a river-floodplain system, the main channel is an important source of external sediments for floodplain lakes (Junk et al., 1989). Evidence from floodplain lakes in the Mackenzie Delta and the Slave River Delta shows that hydrologically open lakes receive large quantities of sediment from the main channel, resulting in high sediment rates (Squires et al., 2002; Sokal et al., 2008). The Yangtze River is rich in sediment load (ca. 470 Mt per year before the 1980s CE) (Milliman and Farnsworth, 2011). Therefore, Dongting and Poyang Lakes, which are freely connected with the Yangtze River, are characterized by high DMAR. In contrast, local dam construction blocked the transport of suspended particles from the Yangtze River, resulting in the lower DMAR in Honghu, Futou, Luhu and Wanghu Lakes.

It is assumed that the sedimentation of nutrients is proportional to nutrient loadings into a lake (Vollenweider, 1976; Ostrofsky, 2012). Therefore, sedimentary N and P flux have been used to reflect the loading of N and P into lakes, respectively, in palaeolimnology (Rippey and Anderson, 1996; Rose et al., 2004). In Taihu Lake (lower Yangtze), the sedimentary N and P profiles well recorded the history of water quality degradation and eutrophication over the last several decades (Rose et al., 2004). Previous evidence shows that untreated wastewaters from industrial and urban point sources are rich in nutrients (especially P) (Edmondson, 1970; Dixit et al., 2000; Jenny et al., 2016; Hobbie et al., 2017), and agricultural activities may lead to enhanced nutrients (especially N) loading through the runoff and leaching of nutrients and soils fertilized by synthetic fertilizers (Bunting et al., 2007; Yu et al., 2019). In this study, the significant positive correlation between recent (post 2000 CE) sedimentary TN flux and agricultural proxies (grain production, aquaculture product, N and P fertilizers) among the lakes indicates that agricultural activities were the main source of N pollution (Figure 6.8). In contrast, recent (post 2000 CE) sedimentary TP flux is positively correlated with concrete production (Figure 6.8). In China the most remarkable signal of urbanization is the spread of “concrete jungles” across the country (Huang et al., 2018). Therefore, concrete production can be used an index of urbanization/industrialization, which suggests that urban/industrial activities were the main source of P loading in the middle Yangtze floodplain. Therefore, Honghu and Futou Lakes with more intensive agricultural activities in the catchments received more N loading and were characterized by higher (> 15) sedimentary N: P ratios than other lakes (< 10) (Figure 6.3 B).

Temporal analysis shows that sedimentary TN and TP flux increased since ~ the 1950s CE in these middle Yangtze floodplain lakes (Figure 6.4), which was in accordance with the intensification of agricultural and urban/industrial activities in the catchments (Figure 6.2). Before the 1940s CE both agricultural and urban/industrial activities were less intense in the middle Yangtze floodplain (Figure 6.2), resulting in the low sedimentary TN and TP flux (Figure 6.4). After the foundation of the People's Republic of China in 1949 CE, agriculture rapidly developed in this area (Figure 6.2). Chemical fertilizers were widely and intensively used to promote grain production in order to meet the increasing food demands of the increasing population (Yu et al., 2019). In both the Honghu and Futou catchments, N fertilizer usage increased more than 15-fold between the 1950s CE and the 2010s CE (Figure 5.10 a; Figure 5.17 a). Concurrent with the decreases in fertilizer use efficiency, farmlands in the catchments became over saturated with nutrients, which promoted the agricultural nutrient (mainly N) loading into the lakes (Ma et al., 2013; Yu et al., 2019). In the Taihu Lake (lower Yangtze), annual N runoff and leaching from paddy soil was 55.3-93.1 kg N ha^{-1} between 2007 CE and 2010 CE (Zhao et al., 2012). With the release of the Opening and Reform policy in the late 1970s CE, China has been experiencing rapid urbanization and industrialization from a previously agriculture-based economy. Urbanization rate experienced a ~ 2.5-fold increase between 1980 CE and 2012 CE from 19.4 % to 52.6 % (Yang, 2013). In combination with the wide use of P-based detergents, large quantities of nutrients are transported into freshwaters from industrial and urban point sources (Van Drecht et al., 2009; Yan et al., 2016), resulting in the further increases in sedimentary TP flux.

Although sedimentary TN and TP flux are useful in reflecting the historical loading of nutrients into lakes (Rippey and Anderson, 1996), it is worth noting that hydrology (e.g., water flush rates) may influence the nutrient retention and sedimentation in lakes as well (Vollenweider, 1976). It is well established that P sedimentation increases with higher water retention times (Vollenweider, 1976). In floodplain areas, dam construction results in reduced water flushing rates (Chen et al., 2016; Chen et al., 2020). Therefore, it is possible that the concurrent hydrological modification could have accelerated the increase in sedimentary P flux in lakes with local dam construction, apart from the direct increases in P loadings with the intensification of human activities in the catchments since ~ the 1950s CE (Vollenweider, 1976).

After being retained and deposited in lakes, N and P in the sediments may be released and recycled in the water column via processes such as sediment resuspension, microbial processes and redox, which might cause bias in using sedimentary nutrient influx to interpret the changes in nutrients in water column (Søndergaard et al., 2003; Ding et al., 2019). In eutrophic lakes, internal nutrient loading from sediments sometimes accounts for a large proportion of nutrients in the water column and causes HABs (Søndergaard et al., 2003; Ostrofsky, 2012). Evidence shows that the shift from eutrophic to mesotrophic and oligotrophic state of lakes often takes years after the reduction in external nutrient loading, and the hysteresis has been attributed to the internal nutrient loading from sediments (Søndergaard et al., 2007; Ding et al., 2019).

6.5.2 Influence of nutrients on algal production and HABs

It has been widely reported that lakes in the Yangtze floodplain have been suffering from severe environmental degradation and declines in ecosystem services with the extensive and intensive social-economic development in the catchment since the 1950s CE (Dearing et al., 2012; Yang et al., 2008; Xu et al., 2017). Sedimentary pigments from this study agrees with this, suggesting that algal production (including HABs) have increased in lakes in the middle Yangtze floodplain lakes over the last 200 years (Figure 6.7), which is in correspondence to the period of increasing nutrient influx into the lakes (Figure 6.4). Consistent with previous knowledge (Dearing et al., 2012; Xu et al., 2017; Zhang et al., 2018), both spatial and temporal analysis of sedimentary pigments support the idea that increasing nutrient loading from agricultural and industrial/urban activities in the catchments is the fundamental factor regulating algal communities in these Yangtze floodplain lakes. However, the timing of changes in algal production increases varied along the middle Yangtze region (Figure 6.7), and shows a different relationship with sedimentary TN and TP flux (Figure 6.12).

It is well established that N and P are two key elements regulating algal production and community composition in freshwater ecosystems, although there is constant debate on whether P and N solely or both are important in regulating eutrophication and HABs (Bunting et al., 2006; Schindler et al., 2008; Paerl et al., 2012). According to the resource competition theory, algal production and community composition is fundamentally determined by the availability of limiting nutrients (Paerl et al., 2016; Burson et al., 2018). Algal production is low when the availability of both N and P are low; increasing P will promote algal production until N runs out and becomes limiting, and *vice versa* (Xu et al., 2010; Paerl et al., 2016). HABs form when both N and P are abundant, and the relative abundance of N: P may shift algal community composition and HAB-forming species (Schindler et al., 2008; Paerl et al., 2014). High N: P ratios are more favourable for HABs with non-N_2-fixing species (e.g., *Microcystis* spp.), whereas N_2-fixing species (e.g., *Anabaena* spp., *Aphanizomenon* spp.) increase when N: P ratios are low (Paerl et al., 2014). Due to the variance in intensity of agricultural and industrial/urban activities over time and space in the catchments, N: P ratios may vary through time and across different lakes (Elser et al., 2007; Yan et al., 2016), resulting in changes in algal production and bloom-forming species over time and space. A study on Taihu Lake (lower Yangtze) showed that phytoplankton production changed from P-limitation to N-limitation with the decreases in N: P ratios from winter/spring to summer (Xu et al., 2010).

The dominant activities in the catchments of Honghu and Futou Lakeas are agriculture (Figure 6.1). In the middle Yangtze floodplain, agricultural activities were the main source of N flux (Figure 6.8). In Honghu and Futou Lakes algal production increased since the ~ 1940s (± 10) CE (Figure 6.7), in accordance with the intensification of agricultural activities in the catchments (Figure 6.4). This indicates that N from agricultural diffuse sources was the main factor regulating algal production in Honghu and Futou Lakes. Consistent with this interpretation, pigment PCA axis 1 was significantly correlated with sedimentary TN flux in these two Lakes (since ~ 1850 CE) (Figure 6.12; Table 6.1). Diffuse nutrient pollution from agriculture is strongly associated with increased algal production across lakes in the northern temperate zone (Bunting et al., 2007; Stevenson et al., 2016). In Lough Neagh, diffuse N loading from agriculture resulted in the increases in algal production during the 20th century (Bunting et al., 2007). Before the 1940s CE agricultural and industrial/urban activities were less intensive in the catchments (Figure 6.2), and low algal production was accompanied with the lower nutrient influx into Honghu and Futou Lakes (Figure 6.4). The sustained growth in agriculture since the late 1940s CE promoted N loading into the lakes, as indicated by increasing sedimentary TN fluxes (Figure 6.4), resulting in the increases in algal production. Therefore, the increase in algal production since ~ the 1940 (± 10) CE in Honghu and Futou

Lakes might be attributed to the increasing nutrient loading, especially N, with the intensification of agricultural activities in the catchments.

The Luhu and Wanghu catchments are dominated by urban and industrial activities which were the main source of P flux in the middle Yangtze floodplain (Figure 6.8). In contrast to Honghu and Futou Lakes, major increases in algal production started from ~ the 1980s CE in Luhu and Wanghu Lakes (Figure 6.7), which was coincident with the intensification of urbanization/industrialization (Figure 6.2). This indicated that P from urban and industrial point sources appeared to play an important role in controlling algal production change in Luhu and Wanghu Lakes, which was consistent with the significant correlation between pigment PCA axis 1 and both sedimentary TP flux (Figure 6.12; Table 6.1). Since the late 1970s CE, both the Luhu and Wanghu catchments have experienced intensive urbanization and industrialization (Figure 6.2), resulting in the increases in P loading into the lakes, as shown by the rapid increase in sedimentary TP flux (Figure 6.4), which promoted algal production. In temperate lakes there are many examples of where P from urban industrial point sources have resulted in the increase in algal production (Edmondson, 1970; Dixit et al., 2000; Moorhouse et al., 2018). In Lake Washington P effluent from wastewater plants was the limiting element of algal production (Edmondson, 1970). In Wuhan, TP has been regarded as the principal factor influencing algal production in lakes fed by untreated industrial and domestic sewage (Lv et al., 2011). Therefore, the increase of algal production in Luhu and Wanghu Lakes after ~1980s CE from a previously stable baseline (Figure 6.7) might be attributed to the rapid increase in nutrient loading, especially P, due to extensive and intensive industrial development and urbanization in the catchments.

In agreement with previous studies (Xu et al., 2010; Paerl et al., 2014), the relative availability of P to N appeared to be an important factor regulating HAB-forming species in these floodplain lakes after 2000 CE. The marked increase in aphanizophyll (pigments from filamentous N_2-fixing cyanobacteria) in recent sediments indicated the blooms of N_2-fixing cyanobacteria in Dongting, Poyang, Luhu and Wanghu Lakes which were characterized by lower sedimentary N: P ratios (< 10). On the contrary, aphanizophyll were barely detected in lakes (Honghu and Futou) with relatively higher sedimentary N: P ratios (> 15) (Figure 6.6). This was in accordance with previously published phytoplankton counts showing that Honghu and Futou Lakes were dominated by bacillariophytes, whereas cyanobacteria were more abundant in Luhu and Wanghu Lakes (Table 3.1). Sedimentary TN and TP flux showed that both N and P influx increased in these middle Yangtze floodplain lakes with the consistent intensification of agricultural and industrial/urban activities after 2000 CE (Figure 6.4), while the relative availability of N to P was different among the lakes (Figure 6.3). Honghu and Futou Lakes, where agricultural activities dominate in the catchments, had higher availability of N relative to P (high sedimentary N: P ratios, > 15), whereas the other lakes were characterized by low sedimentary N: P ratios (< 10) (Figure 6.3). In waterbodies with low N: P ratios, algal production is limited by the availability of N, whereas P becomes the limiting element when N: P ratio is high (Xu et al., 2010; Paerl et al., 2016). Therefore, Honghu and Futou Lakes which were characterized by high sedimentary N: P ratios (> 15) due to the intensive agricultural activities in the catchments were rich in N and were limited by P after 2000 CE. As a result, aphanizophyll (pigments from N_2-fixing cyanobacteria) were barely detected in these two lakes. In comparsion, Dongting, Luhu, Wanghu and Poyang Lakes, which had low recent sedimentary N: P ratios (< 10) (Figure 6.6), were rich in P and were limited by the availability of N after 2000 CE, promoting the growth of N_2-fixing cyanobacteria (Edmondson, 1970; Schindler et al., 2008; Paerl et al., 2016). Different from Taihu Lake (lower Yangtze) where non-N_2-fixing cyanobacteria (*Microcystis* spp.) were dominant in the bloom-forming species (Paerl et al., 2014), HABs were formed by N_2-fixing species in lakes in this study, which might be attributed to the high availability of N in Taihu Lake (Paerl et al., 2014).

Apart from the high N: P ratios, Honghu and Futou Lakes are rich in macrophytes (Deng et al., 2008; Zeng et al., 2018), as shown by the high C/N ratios (> 10) (Figure 6.3, more details in Chapter 8) and high abundance of macrophyte-related chironomids (more details in Chapter 7), which may partially explain the low algal production and HABs in these two lakes. It is well established that macrophytes may supress the phytoplankton production and HABs through several mechanism under the aquatic stable state transition (Scheffer et al., 1993). First, macrophytes may compete with phytoplankton for nutrients (Jeppesen et al., 1998). Second, macrophytes can provide refuges to zooplanktons which feed on phytoplankton through food-web interactions (Jeppesen et al., 1998). Third, the development of macrophytes may limit the resuspension of sediments and hence the release of nutrients from the sediments (Scheffer et al., 1993). Therefore, it is possible that the presence of macrophytes could partly explain the low algal production and the rare existence of HABs in Honghu and Futou Lakes.

6.5.3 Influence of hydrology on algal production and HABs

In agreement with the third hypothesis, algal production and HABs appeared to be related with hydrology in these Yangtze floodplain lakes. In Dongting Lake which is characterized by agricultural activities in the catchment, it was not until ~ 1980 CE that algal production started to increase (Figure 6.6), although TN fluxes (since ~ 1850 CE) (Figure 6.12; Table 6.1) and agricultural activities (since ~ 1950 AD) (Figure 6.13; Table 6.2) appeared to be the main driver of algal production change. In Poyang Lake, the significant correlation between algal production and agricultural and urban/industrial proxies since ~ 1950 CE indicated that agricultural and industrial activities and urbanization in the catchment were the fundamental driver of algal production (Figure 6.18; Table 6.2). However, there was nonsignificant correlation between algal production and sedimentary TN/TP fluxes in Poyang Lake (Figure 6.12; Table 6.1). Poyang Lake (~ 2933 km^2) and Dongting Lake (~ 2500 km^2) are the largest and second largest freshwater lakes in China by area and are freely connected and experience intensive water exchange with the Yangtze River. Water retention times in Poyang Lake and Dongting Lake are approximately 30 and 29 days, respectively, which is about 1/6 of that in hydrologically isolated lakes (i.e., ~ 190 days in Honghu) (Wang and Dou, 1998). The difference in water surface area during the flooding (> 4000 km^2) and non-flooding (< 3000 km^2) season is more than 1000 km^2 in Poyang Lake (Shankman and Liang, 2008). Free hydrological connectivity with the main channel may conceal the relationship between sedimentary pigments and sedimentary nutrients in floodplain lakes (Pan et al., 2009; Liu et al., 2017). Firstly, the highly variable hydrological condition in open lakes may suppress the original production of algae (Elliott, 2010; McGowan et al., 2011). Secondly, after production, algae are easily flushed out rather than being retained and deposited in lakes freely connected with the main channel (Vollenweider, 1976; Tockner et al., 1998). Thirdly, the circulation and sedimentation of TN and TP in open lakes are complex and are influenced by various factors. On one hand, the main channel is a potential source of nutrients in open lakes (Van den Brink, 1994). On the other hand, the free hydrological connection with the Yangtze River may flush nutrients out of the lakes, impeding them being utilized by phytoplankton and being retained (Vollenweider, 1976; Chen et al., 2016). Moreover, the periodical flooding and drawdown in open lakes may accelerate the release and decrease the affinity of P in sediments (Attygalla et al., 2016). Therefore, free hydrological connectivity may delay the response of algal production in Dongting Lake to anthropogenic nutrient loading until ~ 1980 CE, when the concentration of nutrients from further intensification of agricultural activities and urbanization/industrialization in the catchment exceed the influence of hydrology. For Poyang Lake, the free hydrology connection with the Yangtze River might hide the relationship between algal production and sedimentary TN and TP flux.

In the four lakes with pigments from N_2-fixing cyanobacteria, recent (after 2000 CE) pigment abundance (as pigment PCA axis 1) (Figure 6.6 A) and concentrations of canthaxanthin (Figure 6.6 B) and aphanizophyll (Figure 6.6 C) were higher in restricted drainage lakes (Wanghu and Luhu) than Dongting and Poyang Lakes which are freely connected with the Yangtze River, which also suggests that hydrology was an important factor influencing pigment abundance and HABs in the middle Yangtze floodplain lakes. Different from previous knowledge which suggests that highly variable and turbulent hydrological conditions most likely lead to an increase in diatoms over cyanobacteria in large and well-flushed lakes (Elliott, 2010; Paerl and Paul, 2012), algal community composition was similar between the four lakes, as revealed by the comparable canthaxanthin/ diatoxathin (Figure 6.6 D) and aphanizophyll/ diatoxanthin (Figure 6.6 E) ratios. In Poyang Lake, the canthaxanthin/ diatoxanthin ratio was even higher. This indicates that hydrology only influence the concentration and abundance of algae and N_2-fixing cyanobacteria, without modifying the algal community composition in these Yangtze floodplain lakes. For lakes (Luhu and Wanghu) with local dams, more nutrients were deposited and retained in lakes due to the low water flushing rates (Vollenweider, 1976). The release and recycling of nutrients from sediments may fuel algal production and HABs in Luhu and Wanghu Lakes. Besides, the low water flushing rates were favourable for the deposition and sedimentation of algae and HABs. On the contrary, fewer nutrients were retained in open lakes (Dongting and Poyang) due to the high flushing rates, resulting in lower algal production, and the frequent water exchange with the Yangtze River might directly flush algae and HABs out before forming blooms in hydrologically open Dongting and Poyang Lakes (Vollenweider, 1976). Therefore, the concentrations and sedimentation rate of pigments were lower in open lakes (Figure 6.6 F, G).

6.6 Summary

This study provides clear evidence that nutrient loading has increased in these Yangtze floodplain lakes with the intensification of agricultural and industrial/urban activities in the catchments over the last 200 years. Compared with agricultural activities, urbanization and industrialization were more likely to increase P loading into these lakes. Sedimentary pigments indicate that increasing nutrient loading from agriculture and industrialization/urbanization led to significant increases in algal production in the middle Yangtze floodplain lakes since the 1940s CE and ~ 1980 CE, respectively, which is in accordance with the great acceleration in the Anthropocene (Waters et al., 2016). Pigments from filamentous N_2-fixing cyanobacteria were uncommon in all lakes, before increasing markedly in lakes (Dongting, Poyang, Luhu and Wanghu) with low sedimentary N: P ratios (< 10), whilst barely detected in lakes with high sedimentary N: P ratios (> 15) after ~ 2000 CE. In comparison with dammed lakes, pigment abundance (including HABs) was lower in hydrologically open lakes (Poyang and Dongting) which are freely connected with the Yangtze River, while the algal community composition was similar across the four lakes. This indicated that nutrients were the fundamental factor influencing algal community composition (mainly HABs) in these highly eutrophic Yangtze floodplain lakes. Free hydrological connectivity with the Yangtze River can alleviate HABs by flushing algae including cyanobacteria out of the lakes before forming blooms.

This study emphasizes the role of social-economic structure and hydrology in shaping algal production and HABs in floodplain lakes. Though agricultural management of cropland nitrogen is efficient at reducing nitrogen discharge to freshwaters (Yu et al., 2019), the management of urban and industrial wastewater treatment, which have monetary and energy costs, is essential and efficient as they are useful to alleviate HABs (Moorhouse et al., 2018; Schindler et al., 2008). Furthermore, maintaining free hydrological connection with the main channel is efficient at relieving the symptoms of eutrophication resulting from anthropogenic disturbance in floodplain lakes (Paerl et al., 2012).

CHAPTER 7 CHANGES IN LAKE ECOSYSTEM STATE INFERRED FROM PIGMENTS AND CHIRONOMIDS

7.1 Introduction

Phytoplankton and benthic communities (macrophytes, benthic algale) are two important components of shallow freshwater ecosystems. Theoretical evidence suggests that ecosystem structure and function of shallow freshwater lakes are determined by a complex combination of physical, chemical and biological processes controlled by nutrients and light availability under the theory of aquatic stable state transition (Scheffer et al., 1993; Vadeboncoeur et al., 2003; Schindler et al., 2008). Under low nutrient conditions, lakes are in a macrophyte-dominated state characterized by high underwater light availability (Scheffer et al., 1993). Enhanced nutrient loading increases phytoplankton production, including some bloom-forming cyanobacteria which may shade out the benthic competitors, turning the lakes into an algal-dominated turbid state with low underwater light conditions (Scheffer et al., 1993).

In floodplain areas, hydrological connectivity with the main channel is important in determining the hydrological conditions (i.e., water level fluctuations, water retention times, and water exchange ratios) and suspended particle concentrations in floodplain lakes (Junk et al., 1989). Water level fluctuations and suspended particle concentrations can influence light attenuation and therefore the underwater light availability (Scheffer, 2001; Cantonati et al., 2014; Ersoy et al., 2020). Water retention times and water exchange ratios are important factors controlling nutrient availability in lakes (Cross et al., 2014;

Chen et al., 2016). By proxy, hydrological connectivity may therefore influence the light and nutrient conditions, and hence ecosystem structure in shallow floodplain lakes (Squires and Lesack, 2003). Primary production appears to be a trade-off between the supply of nutrients and light in relatively pristine floodplain lakes, which rely on rivers to supply nutrients, but turbid river waters can also impede light. Therefore, the highest primary production can occur in lakes with intermediate connection with the main channel in northern systems with limited human modification (Knowlton and Jones, 1997; Squires and Lesack, 2002; Wiklund, 2012). In river-floodplain systems where nutrient concentrations in rivers are lower than those in floodplain lakes, primary production shows a monotonic downward trend along the closed to open hydrological gradient (Sokal et al., 2008; Sokal et al., 2010).

In the densely-populated and highly-developed Yangtze floodplain, extensive and intensive human activities have exerted heavy burdens on shallow freshwater lakes (Yang et al., 2008; Dong et al., 2012) (Chapter 6). Lake area shrinkage and eutrophication has become a widespread phenomenon in almost all the floodplain lakes (Yang et al., 2008; Du et al., 2011). Besides, the construction of dams and reservoirs for various social-economic benefits have modified the natural hydrological conditions of these lakes, such as prolonging water retention times, reducing water exchange ratios and stabilizing water level fluctuation (Chen et al., 2016). To explore how hydrological modification caused by local dam construction and anthropogenic disturbance have influenced light penetration and ecosystem structure in the Yangtze floodplain lakes, sedimentary pigments and chironomids in lakes experiencing different hydrological connectivity with the Yangtze River were analysed. The following hypothesises were tested:

1. Water level fluctuations will influence underwater light conditions in these Yangtze floodplain lakes, especially in the two large, hydrologically open lakes (Poyang and Dongting) which experience high water level fluctuations during the flooding and non-flooding seasons.
2. Local dam construction will improve water clarity in lakes, by impeding the transport of suspended particles from the Yangtze main channel and stabilizing water level fluctuations.
3. Anthropogenic nutrient loading from agricultural, industrial and urban development in the catchment will stimulate algal production, resulting in algae-induced turbidity.
4. Improved light conditions and stable water levels due to local dam construction will stimulate the growth and development of benthic communities.
5. Local dams will amplify the symptoms of eutrophication by increasing water retention times and stimulate the growth of eutrophic species, whereas free hydrological connection with the Yangtze River will alleviate the negative effects caused by nutrients.

7.2 Methodological approaches

Over exposure to certain wavelengths of radiation causes damaging effects on algae (Leavitt et al., 1997; McGowan et al., 2018). Empirical evidence revealed that variable exposure to light induced by water level fluctuations may result in distinctive benthic cyanobacteria and algae communities with different sheath colours (Cantonati et al., 2014). Cyanobacteria in shallow littoral areas are characterized by protective yellow-brown sheaths, whereas cyanobacteria in deeper waters have colourless sheaths (Cantonati et al., 2014). Acting as photo-protectants, ultraviolet radiation (UVR)-absorbing compounds (e.g., scytonemin) are a group of pigments generated by benthic algae to protect them from the damage caused by over exposure to UV which can be damaging (Leavitt et al., 1997; McGowan et al., 2007). Leavitt et al (1997) proposed one way of inferring UVR (and hence light) exposure in lakes by calculating the abundance of UVR-absorbing compounds relative to the sum of indicator carotenoids produced by cyanobacteria (alloxanthin, diatoxanthin, lutein and zeaxanthin). The UVR index has been used as an indicator in lake sediment records to study historical underwater clarity across various environments (Leavitt et al., 1997; Stevenson et al., 2016; McGowan et al., 2018). A higher UVR index indicates conditions where more clear water exposes phototroph to UVR, whereas lower values result from lower UVR exposure. In this chapter, the UVR index derived from sedimentary pigments was calculated to infer how underwater light conditions have changed in all six of the study lakes.

Chironomids are sensitive to various environmental factors (Brooks et al., 2007). Previous studies have shown that macrophytes, which provide refuge and food resources to chironomids (Cao et al., 2014; Zeng et al., 2018), and nutrients (Zhang et al., 2006) are major factors influencing chironomid communities in the Yangtze floodplain lakes. In this study, changes in chironomid assemblages were analysed to help understand how ecosystem structure in Yangtze lakes has changed through time using groupings according to “macrophyte-related” and “eutrophic” species. Macrophyte-related species include *C. lateralis*-type, *C.*

intersectus-type, *D. nervosus*-type, *Paratanytarsus*, *P. penicillatus*- type, *P. nubifer*-type, *Stempella*, *E. dissidens*-type, *E. albipennis*-type, and *E. tendens*-type (Langdon et al., 2010; Vermaire et al., 2013; Cao et al., 2014; Zeng et al., 2018). *C. plumosus*-type, *M. tabarui*-type, *P. aukasi*-type, *Tanypus* have an optimal phosphorus tolerance of > 2 mg L^{-1} and are abundant in eutrophic waterbodies in the Yangtze floodplain (Zhang et al., 2006; Zhang et al., 2012; Cao et al., 2014) and therefore these four species were grouped as proxies of eutrophic chironomid species in this study. Following chironomid analysis, changes in light conditions (inferred from the UVR index) and changes in nutrient loading (inferred from sedimentary TP fluxes) were compared with chironomid assemblages to try to understand the drivers of ecosystem state change in Yangtze floodplain lakes. As chironomids were poorly preserved in Dongting and Honghu Lakes, this analysis was only conducted on Futou, Luhu, Wanghu and Poyang Lakes. The results of Futou Lake were from Zeng (2016). The scope of this study encompasses the last two centuries (since ~ 1800 CE) when ^{210}Pb dating could provide a reasonable chronology.

7.3 Results

7.3.1 UVR index

The UVR index exhibited different patterns of variation in lakes with different degrees of hydrological connection with the Yangtze River over the last 200 years (Figure 7.1). In Dongting and Poyang Lakes, which are freely connected with the Yangtze River, the UVR index was low before the ~ 1940s CE, followed by an increase between the ~ 1940s CE and the early 1990s CE before sharply decreasing thereafter. In Honghu, Luhu and Wanghu Lakes, the UVR index was low when they were freely connected with the Yangtze River, followed by an increase to the maximum after dam constructions before sharply decreasing to undetectable values in the 2010s CE. The UVR index in Futou Lake was relatively high and fluctuated between 0 and ~ 100 between the early 1800s CE and the 1990s CE, but declined to 0 during the 2010s CE.

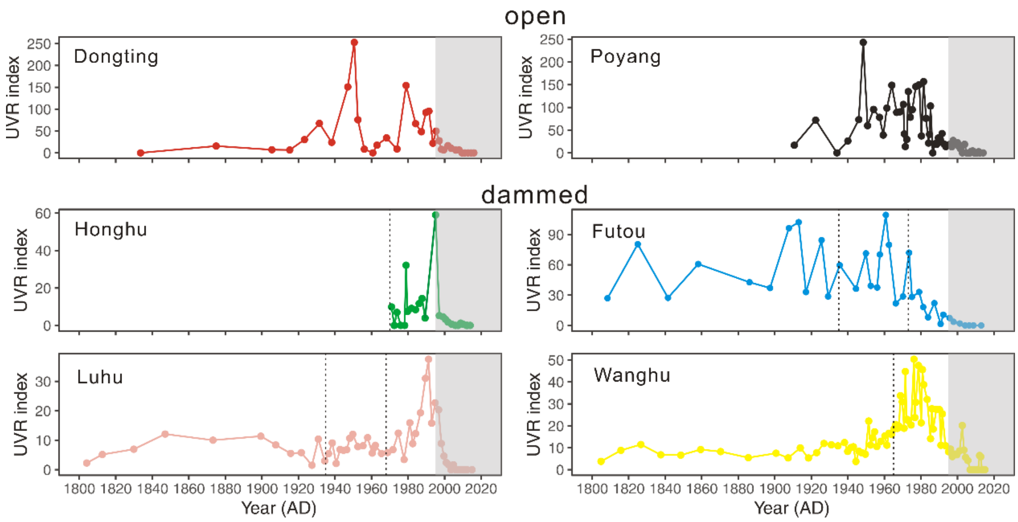

Figure 7.1 UVR index in the six lakes. The dashed line indicates the timing of local dam construction and the grey bar indicates the period of highest algal production (Chapter 6). In Honghu Lake, concentrations of UVR-absorbing compounds, alloxanthin, diatoxanthin, and lutein-zeaxanthin before the 1970s CE were below the detection limits of HPLC. Therefore, UVR index which is the quotient of these pigments could not be assessed and was left blank in this section.

Levene's test was used to test the homogeneity of variance of the UVR index between the lakes. The results showed that the UVR index in the two larger open drainage lakes (Dongting and Poyang) was significantly higher than the smaller lakes with local dam construction, with the exception of Futou Lake (Figure 7.2). In the two open lakes, Dongting and Poyang, the UVR index showed a wide range of change, varying between 0 and 250, whereas the UVR index changed between 0 and 60 in the lakes with local dam construction (Honghu, Luhu and Poyang), except Futou Lake in which the UVR index varied between 0 and 120.

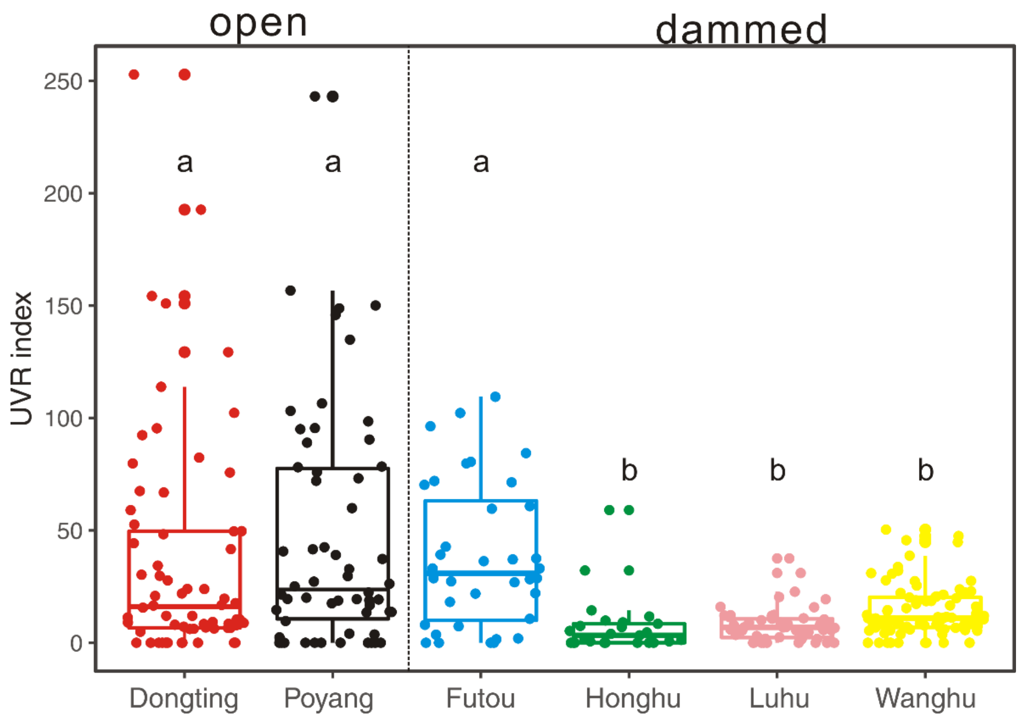

Figure 7.2 Boxplot of the UVR index of the lakes (Differences among groups (*p* < 0.05) was assessed using Levene's test. Different letters indicate significant differences between groups. The dotted line separates the open and dammed lakes).

7.3.2 Ecological changes in Futou Lake (with local dam, agricultural catchment)

When Futou Lake was freely connected with the Yangtze main channel via the Jinshui River before 1935 CE (Figure 7.3a), sedimentary TP flux was relatively low (Figure 7.3b) and the relatively high UVR index value indicated good water clarity (Figure 7.3b). At this time, pigment PCA axis 1 scores were high (Figure 7.3c), implying low algal production in the lake (Chapter 6). Proportions of macrophyte-related chironomid species were low (< 40%) and eutrophic species were barely identified (Figure 7.3c). After the construction of the local dams in 1935 CE and 1973 CE, the lake changed into a hydrologically restricted drainage basin. Concurrently, the catchment of lake experienced intensive agricultural activities between the late 1940s CE and the late 1980s CE, as revealed by the increase in z-score of agriculture (Figure 7.3a). During this period, sedimentary TP flux increased (Figure 7.3b), indicating that more nutrients were retained in the lake. Algal production gradually increased as revealed by the decreases in pigment PCA axis 1 scores (Figure 7.3c), whereas proportions of macropyte-related chironomids species increased from < 40 % to ~ 80% (Figure 7.3c), implying the growth of macrophytes during this period. Since the 1990s CE, the z-score of agriculture further increased and z-score of industrialization/urban exponentially increased (Figure 7.3b). The UVR index gradually decreased towards 0 in the 2010s CE (Figure 7.3b), indicating a decline in water clarity in the lake. Sample scores on pigment PCA axis 1 sharply decreased after the 1990s CE (Figure 7.3c), reflecting a rapid growth in algal production. The chironomid community was dominated by macrophyte-related species although their proportions slightly decreased during this period (Figure 7.3c). In contrast, eutrophic species, which were sparse before the 1990s CE, slightly increased.

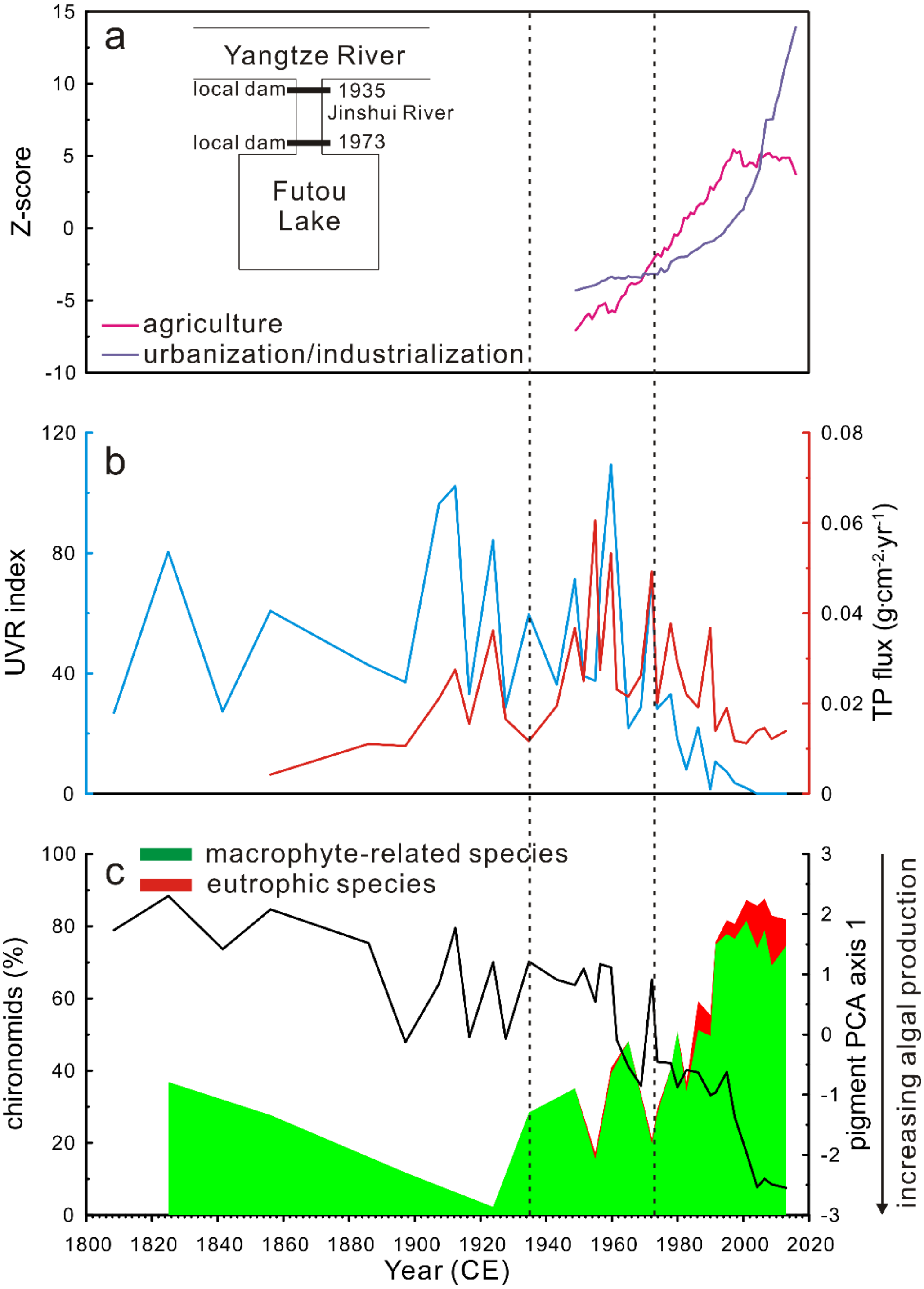

Figure 7.3 (a) The history of dam construction (black bar) and anthropogenic perturbation in the Futou Lake catchment, (b) sedimentary TP flux (g ·cm^{-2} ·yr^{-1}) and UVR index and (c) the first PCA axis of sedimentary pigments and percentages of macrophyte-related and eutrophic chironomids in Futou Lake (the black vertical dash line indicates the timing of local dam construction). (original data of pigments, chironomids and sedimentary TP flux from Zeng (2016)).

7.3.3 Ecological change in Luhu Lake (with local dam, urban catchment)

Before 1935 CE, Luhu Lake was freely connected with the Yangtze River via the Jinshui River (Figure 7.4a). At this time, sedimentary TP flux in the lake was generally low (less than 0.01 g $\cdot cm^{-2} \cdot yr^{-1}$) and UVR index fluctuated slightly around ~ 10, indicating low-moderate water clarity (Figure 7.4b). Concentrations of sedimentary pigments were low, implying low algal production (high pigment PCA axis 1 scores) (Figure 7.4c). At this time, proportions of both macrophyte-related species (~ 25%) and eutrophic species (~ 10%) were low in the chironomid community. In 1935 CE, a local dam was established at the junction of the small river and the Yangtze River, which changed the lake into a restricted drainage water body (Figure 7.4a). The TP flux and UVR index increased between 1935 CE and the late 1960s CE, indicating more nutrients were retained and the improvement of light condition (Figure 7.4b). The first PCA axis score remained at a high value, indicating low algal production (Figure 7.4c). At this time, the abundance of macrophyte-related chironomid species gradually increased to ca. 50%, which implies the growth and development of macrophytes in the lake (Figure 7.4c). Another local dam was established at the conjunction of the small river and Luhu Lake in 1967 CE. Agricultural indicators (Z-agriculture) gradually increased in the Luhu Lake catchment since 1949 CE (Figure 7.4a) and TP flux further increased (Figure 7.4b). The UVR index sharply increased to ca. 40 in the late 1980s CE (Figure 7.4b). The first pigment PCA axis slightly decreased, indicating increasing algal production between 1935 CE and the 1990s CE (Figure 7.4c). The chironomid community was dominated by macrophyte-related species, with an average abundance of 50%, whereas abundance of eutrophic species was low during this period (Figure 7.4c). Since the 1980s CE, urbanization/industrialization exponentially increased in the Luhu Lake catchment, as revealed by the rapid increase in Z-urban around the 1980s CE (Figure 7.4a). Meanwhile, Z-agriculture remained at a high value, indicating sustained agricultural intensity. Sedimentary TP flux further increased, reaching 0.03 g $\cdot cm^{-2} \cdot yr^{-1}$ around the early 2010s CE (Figure 7.4b). In contrast, the UVR index sharply decreased and remained at 0 after the 2010 CE, indicating a decline in water clarity (Figure 7.4b). Scores on the first PCA axis 1 sharply decreased since the 1990s CE, implying a rapid growth in algal production (Figure 7.4c). There was shift in the dominant chironomids from macrophyte-related species to eutrophic species during this period (Figure 7.4c). Abundance of macrophyte-related species decreased from more than 50% to less than 30%, whereas eutrophic species increased from less than 10% to more than 40%.

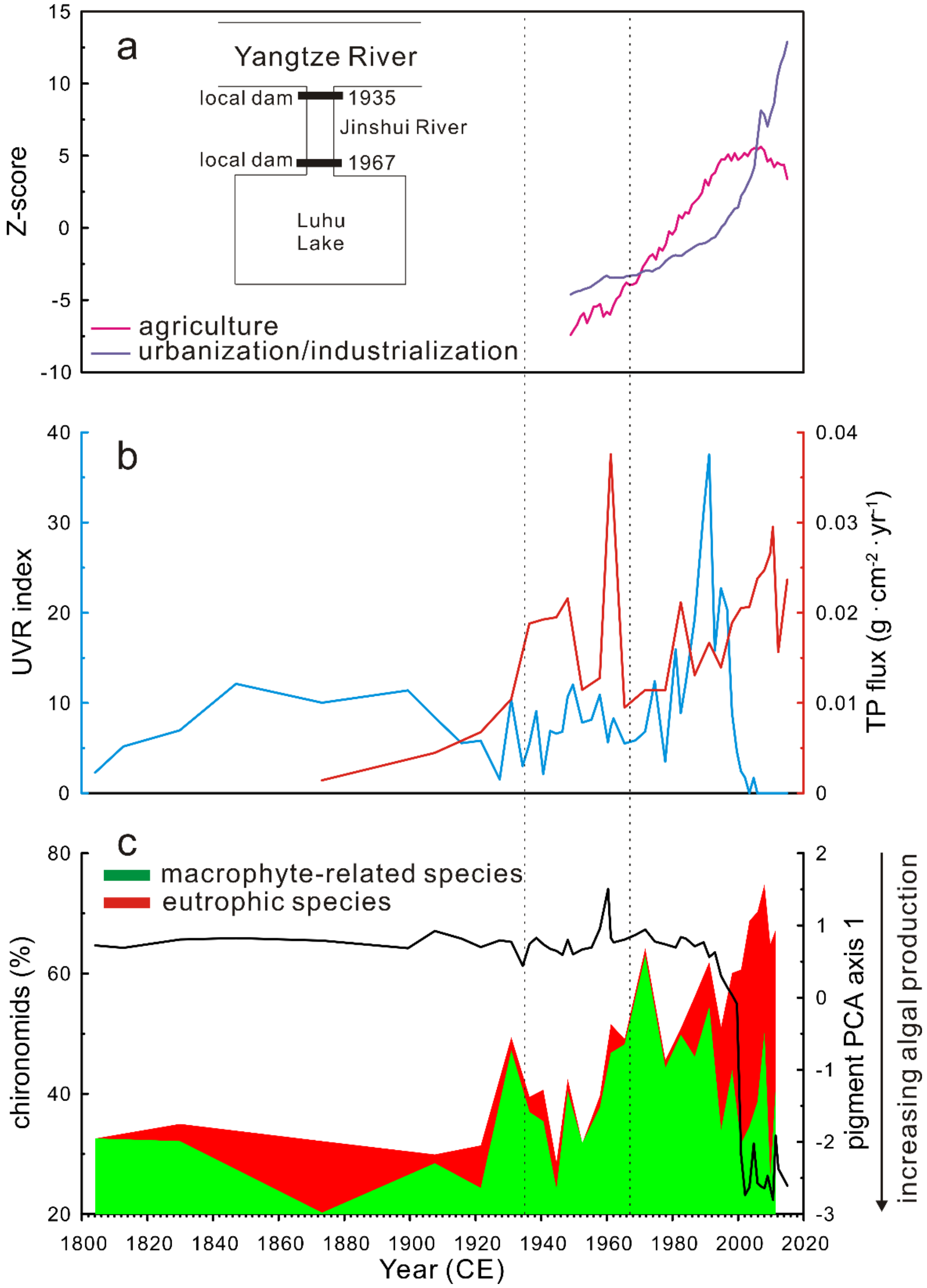

Figure 7.4 (a) The history of dam construction (black bar) and anthropogenic perturbation in the Luhu Lake catchment, (b) sedimentary TP flux (g ·cm^{-2} ·yr^{-1}) and UVR index and (c) the first PCA axis of sedimentary pigments and percentages of macrophyte-related and eutrophic chironomids in Luhu Lake (the black vertical dashed line indicates the timing of local dam construction).

7.3.4 Ecological change in Wanghu Lake (with local dam, urban catchment)

Before 1965 CE, Wanghu Lake was freely connected with the Yangtze River via the Fushui River (Figure 7.5a). Urbanization/industrialization were barely developed in the Wanghu Lake catchment, whereas agriculture gradually developed since 1949 CE (Figure 7.5a). Sedimentary TP flux (less than 0.04 g $\cdot cm^{-2}$ $\cdot yr^{-1}$) and UVR index (fluctuating at around 10) were generally low (Figure 7.5b), which probably indicated the low nutrient and restricted light conditions in the lake. Sample scores on the first PCA axis of pigments were high, indicating low algal production (Figure 7.5c). Abundance of both macrophyte-related and eutrophic chironomid species were stable and low, with an average value of ca. 10% and 2% (Figure 7.5c). In 1965 CE, a local dam was established at the junction of the Fushui River and Wanghu Lake. Agriculture continued to develop after 1965 CE until the late 1980s CE. Z-scores of urbanization/industrialization increased slightly during this period (Figure 7.5a). During this period, sedimentary TP flux and the UVR index increased to a mean value of ca. 0.08 g $\cdot cm^{-2}$ $\cdot yr^{-1}$ (indicating high nutrient conditions) and 30 (indicating high water clarity), respectively (Figure 7.5b). Pigments PCA axis 1 scores remained at a relatively high values, indicating low algal production during this period (Figure 7.5c). Macrophyte-related chironomid species substantially increased and became dominant with a mean abundance of ca. 70% between 1965 CE and the late 1980s CE (Figure 7.5c). Since the 1980s CE, Z-urban exponentially increased and Z-agriculture further developed (Figure 7.5a). Sedimentary TP flux sharply increased from ca. 0.04 g $\cdot cm^{-2}$ $\cdot yr^{-1}$ in the early 1990s CE to ca. 0.10 g $\cdot cm^{-2}$ $\cdot yr^{-1}$ in the 2010s CE (Figure 7.5b). At the same time, the UVR index sharply decreased from ca. 30 to 0 during this period, indicating a decline in water clarity (Figure 7.5b). Sample scores on the first PCA axis of pigments substantially declined since the early 1990s CE, indicating much higher algal production (Figure 7.5c). The dominant chironomids shifted markedly from macrophyte-related species (decreased from ~ 30% to ~ 2%) to eutrophic species (increased from ~ 5% to ~ 70%) (Figure 7.5c).

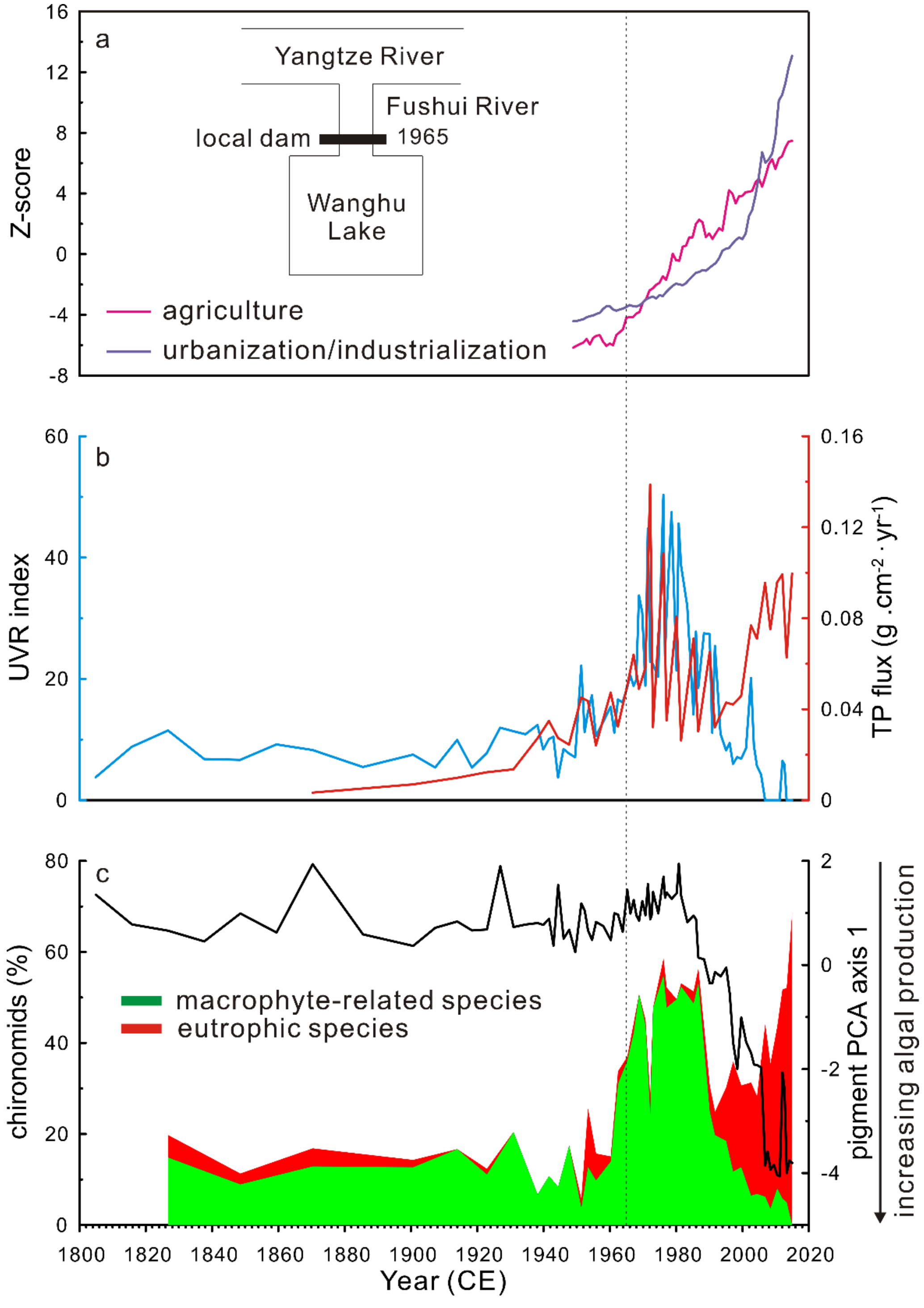

Figure 7.5 (a) The history of dam construction (black bar) and anthropogenic perturbation in the Wanghu Lake catchment, (b) sedimentary TP flux (g .cm^{-2} .yr^{-1}) and UVR index and (c) the first PCA axis of sedimentary pigments and percentages of macrophyte-related and eutrophic chironomids in Wanghu Lake (the black vertical dash line indicates the timing of local dam construction).

7.3.5 Ecological change in Poyang Lake (large, hydrologically free)

Poyang Lake is freely connected with the Yangtze River (Figure 7.6a). Agriculture gradually developed in the Poyang Lake catchment between the late 1940s CE and the 1980s CE, as revealed by the sustained increase in Z-agriculture (Figure 7.6a), whereas the relatively low values of Z-urban indicated that industrial activities and urbanization were low. Concurrently, the area of Poyang Lake sharply decreased during this period (Figure 7.6a). Sedimentary TP flux was generally low (mean value = 0.02 g $\cdot cm^{-2} \cdot yr^{-1}$) before the 1950s CE, followed by a rapid increase to ~ 0.05 g $\cdot cm^{-2} \cdot yr^{-1}$ (Figure 7.6b). UVR index was low (~ 50) before the 1940s CE and fluctuated around ~ 100 between the 1940s CE and the 1980s CE, indicating the improvement of underwater light condition (Figure 7.6b). The chironomid community was dominated by macrophyte-related species before the 1980s CE, the abundance of which fluctuated substantially between ~ 10% to ~ 50% (Figure 7.6c). The abundance of eutrophic chironomid species was less than 5 % during this period (Figure 7.6c). Since the 1980s CE, agriculture further developed in the Poyang Lake catchment as indicated by the sustained increase in Z-agriculture and urbanization/industrialization (Z-urhan) substantially intensified. Sedimentary TP flux was high after the 1980s CE, fluctuating around 0.05 g $\cdot cm^{-2} \cdot yr^{-1}$ (Figure 7.6b). The UVR index sharply decreased from ca. 150 in the early 1980s CE to 0 after 2010 CE (Figure 7.6b). Sample scores on the first PCA axis of pigments decreased sharply, implying a significant increase in algal production (Figure 7.6c). The chironomid community was dominated by macrophyte-related species, fluctuating at around 40% while the abundance of eutrophic chironomids remained low (~ 3%) (Figure 7.6c).

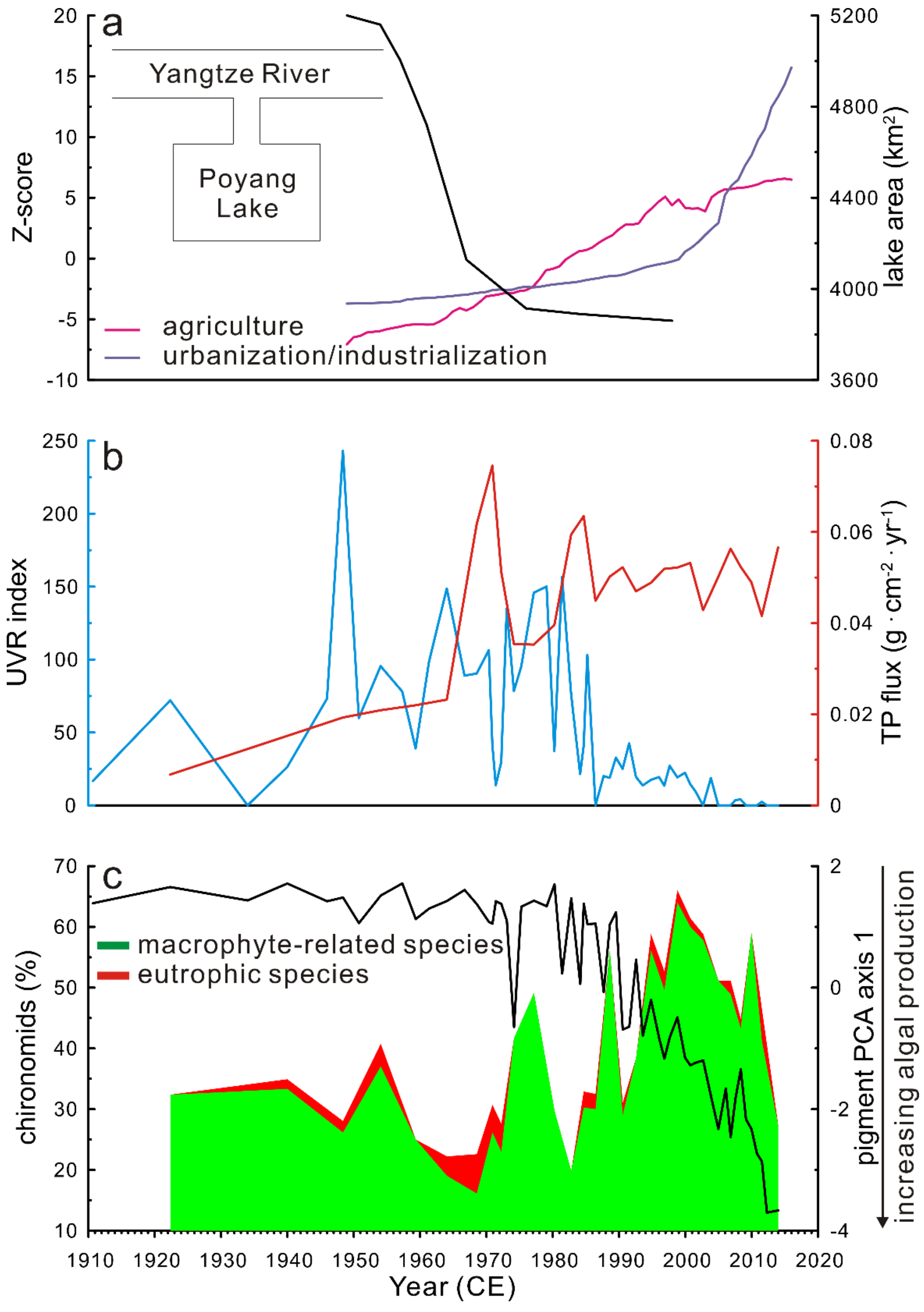

Figure 7.6 (a) The history of dam construction (black bar) and anthropogenic perturbation in the Poyang Lake catchment, (b) sedimentary TP flux (g .cm^{-2} .yr^{-1}) and UVR index and (c) the first PCA axis of sedimentary pigments and percentages of macrophyte-related and eutrophic chironomids in Poyang Lake.

7.4 Discussion

The distinct characteristics of the UVR index and chironomid community compositions between the hydrologically open drainage and dammed lakes, as well as agricultural and urban/industrial activity in the catchments, indicates that hydrological connection with the Yangtze main channel and catchment characteristics are two important factors regulating the light condition and ecosystem structure of the Yangtze floodplain lakes. The wide range of variation in the UVR index in the hydrologically open drainage lakes indicates the role of water level fluctuations and suspended particle concentration in regulating UV attenuation. The increase in the UVR index and macrophyte-related species after local dam construction implies that, in some cases, local damming appeared to improve light conditions, and hence stimulate the development of benthic communities in these floodplain lakes. Since the 1990s CE, the UVR index decreased abruptly, while algal production rapidly increased, the dominant chironomids shifted from macrophyte-related to eutrophic species and HABs emerged in dammed Luhu and Wanghu Lakes which have the most extensively urbanized/industrialized catchments. In the dammed lake with an agricultural catchment (Futou), water clarity declined as algal production increased but macrophyte-related chironomid species remained dominant and HAB associated pigments were barely detected (Chapter 6). In contrast, eutrophic species were sparse and algal production were relatively low in Poyang Lake, indicating that free hydrological connectivity with the main channel may conceal eutrophication in these Yangtze floodplain lakes.

7.4.1 Hypothesis 1:

Water level fluctuations will influence light conditions in these Yangtze floodplain lakes, especially the two large, hydrologically open lakes (Poyang and Dongting) which experience high water level fluctuation during the flooding and non-flooding seasons.

In agreement with the first hypothesis, light conditions varied more, and UVR index was higher in the two large, hydrologically open lakes (Doting and Poyang) (Figure 7.1; Figure 7.2), suggesting that the more extensive water level fluctuations in these lakes might be responsible for the variation of underwater light availability (Bucak et al., 2012; Cantonati et al., 2014). It is well-established that water level fluctuations are a key factor shaping ecosystem structure and may induce the aquatic stable state transitions in shallow lakes, although observations to date have been mostly confined to north temperate and Mediterranean lakes (Bucak et al., 2012; Cantonati et al., 2014; Ersoy et al., 2020). Dongting and Poyang Lakes are freely and directly connected with the Yangtze River and they are the largest (~2933 km^2) and second largest freshwater (~2500 km^2) lakes in China, respectively. Yangtze water flows into the lakes during the flooding season between May and October, and back into the Yangtze main channel in the dry season (November to April), which results in large fluctuations of water level (Harris and Zhuang, 2010). For instance, water depth varied from > 8 m in the flooding season to less than 15 cm in the winter dry season in Poyang Lake (Harris and Zhuang, 2010). Therefore, the high water level fluctuations resulted in the wide range of UVR exposure for biota of the two large open lakes (Cantonati et al., 2014).

Since the 1940s CE, UVR index increased in both Dongting and Poyang Lakes, indicating the improvement of water clarity (Figure 7.1). The Yangtze River which ranks fourth in the world in terms of sediment loads has high suspended particles in its water column (Milliman and Farnsworth, 2011; Wang et al., 2012). Large quantities of suspended particles are transported into the two large, open Poyang and Dongting Lakes from the Yangtze River, resulting in the siltation of sediments. For Dongting Lake, 80% of the sediment load ($\sim 1.21 \times 10^8$ m^3 each year) is from the Yangtze River (Du et al., 2001). Combined with land reclamation caused by the human activities, the areas of the two lakes have markedly shrunk since the 1940s CE (Du et al., 2001; Shankman and Liang, 2003). Between the 1930s CE and the late 1990s CE, the area of Dongting Lake declined by ~ a half from 4955 km^2 to 2500 km^2 (Zhao et al., 2005). The continuous siltation and shrinkage of lake areas were likely to shallow the lakes and reduce light attenuation in the water column, thus promoting benthic irradiance and increasing the UVR index in the sediments.

Apart from water level fluctuations, the concentrations of suspended particles influence light attenuation in shallow freshwater lakes (Scheffer 1997; Swift et al., 2006; Hannouche et al., 2011). Suspended particles in the water column may absorb and scatter light (Scheffer 1997). Therefore, waterbodies with high suspended particle concentrations are characterized by high turbidity and low underwater light conditions (Scheffer 1997; Swift et al., 2006). Before the 1940s CE, annual sediment load varied markedly in the middle Yangtze River, fluctuating between ~ 250 million metric tons and > 620 million metric tons (Wang et al., 2008). The two large lakes (Dongting and Poyang) are directly connected with the Yangtze River and receive highly variable quantities of suspended particles from the Yangtze River, resulting in high fluctuations of the UVR index. In comparison, the four dammed lakes are indirectly connected with the Yangtze River through small tributaries and the water surface areas are smaller (40-350 km^2). Therefore, the UVR index varied across a smaller range in these four small lakes.

7.4.2 Hypothesis 2:

Local dam construction will improve the water clarity of lakes by impeding the transport of suspended particles from the Yangtze main channel and stabilizing water level fluctuations.

There is tentative evidence to support the second hypothesis that local dam construction improved water clarity in the dammed Yangtze floodplain lakes (Honghu, Futou, Luhu and Wanghu). In three of the dammed lakes (Honghu, Luhu and Wanghu), the UVR index was generally low before dam construction and increased after damming, suggesting improved light conditions in these sites following hydrological restriction (Figure 7.1). Open lakes which are susceptible to flooding generally receive high suspended particle influxes from the main channel, and tend to have lower water clarity than closed drainage lakes (Wiklund, 2012). Water retention times in the dammed lakes (~ 190 days in Honghu Lake) is about six times that of hydrologically open lakes (~ 30 days in Poyang and ~ 29 days in Dongting) (Wang and Dou, 1998). The amount of suspended particles transported into the lakes from the Yangtze River are much smaller in these four dammed lakes compared with the two open large lakes, as revealed by the low recent (> 2000 CE) dry mass accumulation rates (Figure 6.3A). Therefore, the observations in this study seem to suggest that light conditions may have been improved by damming of the inflow to three of the four dammed lakes, but there was a complacent response to damming in Futou Lake. In this lake, water clarity apparently remained high before and after damming, and may be consistent with the observation that this lake has retained macrophyte cover through this period up until the present day. Macrophytes are well known to buffer against the effects of turbidity in shallow lakes through several mechanisms (Scheffer et al., 1993; Jeppesen et al., 1998). First, macrophytes may compete with phytoplankton for nutrients (Jeppesen et al., 1998). Second, macrophytes can provide refuges to zooplankton which feed on phytoplankton through food-web interactions (Jeppesen et al., 1997). Third, the development of macrophytes may limit the resuspension of sediments (Scheffer et al., 1993). Compared with Dongting and Poyang Lakes which are directly connected with the Yangtze River, the other four lakes are obliquely connected with the Yangtze River via tributaries. The length of the river connecting Futou Lake and the Yangtze River (> 42 km) is more than twice as that of the other three lakes (Honghu, Luhu and Wanghu) (< 20 km). This long distance may buffer the effects of hydrology, leading to an insensitive response of Futou Lake to the sediment influx from the Yangtze River, resulting in a lake that also had high water clarity and macrophyte cover before damming.

7.4.3 Hypothesis 3:

Anthropogenic nutrient loading from agricultural, industrial and urban development in the catchment will stimulate algal production and result in phytoplankton-induced turbidity.

In correspondence to the third hypothesis, light conditions gradually deteriorated in all lakes after the 1990s CE, concurrent with the period of high algal production and, in some lakes, potential HABs (Chapter 6). With the closure of the Yangtze River for the construction of the TGD since the late 1990s CE, ca. 150 million tons of suspended particles have been trapped in the TGD reservoir each year (Wang et al., 2008; Yang et al., 2011; Yang et al., 2014). As a result, water released from the TGD is sediment starved. Instrumental data shows that annual sediment load in the middle Yangtze River decreased by more than a half from > 320 million metric tons between 1991 CE and 1998 CE to < 160 million metric tons between 1999 CE and 2013 CE (Wang et al., 2008). As mentioned in section 7.4.2, the decrease in suspended particles in water column might potentially improve light conditions in the floodplain lakes. However, the UVR index sharply decreased since the late 1990s CE in all six lakes and reached 0 after the 2010s CE, which indicates a decline in water clarity (Figure 7.1). Despite the reduction in sediment supply, all mid-Yangtze lakes (and especially the free-flowing lakes) showed a reduction in water clarity (more turbid waters) (Yang et al., 2008). Together with the concurrent increase in algal production (Chapter 6), this provides compelling evidence that water clarity has been regionally affected by increases in algal production, and not primarily by the reduction in sediment supply. Increasing nutrient influxes from agricultural and industrial development as well as urbanization in the catchments have largely promoted algal production in these floodplain lakes (Chapter 6). The high phytoplankton concentrations in the water column led to shading and scattering of light, resulting in high light assimilation in the water column, and therefore the decline in irradiance at the bottom of the lakes (Scheffer et al., 1993; Scheffer et al., 1997; Swift et al., 2006). Therefore, the decrease in the UVR index since the late 1990s CE in these Yangtze floodplain lakes seems likely to be attributed to the increase of algal production due to anthropogenic nutrient loading.

7.4.4 Hypothesis 4:

Improved light conditions and the stable water levels due to local dam construction will stimulate the growth and development of benthic communities.

In agreement with the fourth hypothesis, local dam construction appeared to promote the growth of benthic communities in these Yangtze floodplain lakes (Futou, Luhu and Wanghu). As observed in the floodplain lakes, light penetration (as estimated by the UVR index) was generally low when lakes were freely connected with the main channel as more suspended particles were transported into the Yangtze floodplain lakes (Squires and Lesack, 2002; Wiklund, 2012). The exception to this was Futou Lake, where water clarity appeared to be high in the pre-dam period as well. In all lakes, the proportion of macrophyte-related chironomids was at moderate or low levels before damming, suggesting that freely connected lakes sometimes provide a suitable habitat for macrophyte growth. The variable chironomid community composition in the large, hydrologically open Poyang Lake supports the idea that macrophyte development in regularly-flooded lakes varies through time (McGowan et al., 2011). Therefore, as well as altering the light conditions, it appears that water level fluctuations and disturbances from flooding result in intermediate levels of plant coverage over decadal timescales, and this is likely due to substantial seasonal or inter-annual variability. After local dam installation, there was a substantial increase in the abundance of macrophyte-related species in Wanghu Lake (e.g., *E. tendens*-type, *E. albipennis*-type, *E. dissidens*-type) and Luhu Lake (e.g., *Stempellina*), with a more muted increase in Futou Lake (e.g., *Cricotopus*, *Paratanytarsus*). It is possible that improvements in light conditions initiated the spread of macrophytes, as recorded by the concurrent increase in the

UVR index in Wanghu and Luhu Lakes. In Futou Lake the UVR index suggests that water clarity was high before and after dam construction, possibly explaining the more moderate increase in plant-associated chironomids, and suggesting stable coverage through this period.

7.4.5 Hypothesis 5:

Local dams will amplify the symptoms of eutrophication by increasing water retention times and stimulate the growth of eutrophic species, whereas free hydrological connection with the Yangtze River will alleviate the negative effects caused by nutrients.

The ecosystem response to the intensive eutrophication period during the 1990s CE was different among the lakes. There was a sharp increase in eutrophic chironomids in Wanghu and Luhu Lakes accompanied by a marked decline in macrophyte-associated taxa. In contrast, macrophytes appeared to increase during the most eutrophic period in Futou and Poyang Lakes. This provides evidence that Futou and Poyang Lakes are responding to eutrophication by the spread of macrophytes, which is common in early stages of eutrophication (Sayer et al., 2010); whilst there has probably been a shift from the macrophyte-dominated to the turbid state in Luhu and Wanghu Lakes (Scheffer et al., 1993).

Since the 1980s CE, extensive and intensive agricultural and industrial activities and urbanization in the middle Yangtze floodplain have substantially enhanced the nutrient loadings into Luhu and Wanghu Lakes (Chapter 6). Concurrently, the construction of local dams have prolonged the water retention times and hence the nutrient retention in the lakes, as indicated by the high sedimentary TP flux after 2000 CE (> 0.025 g cm^{-2} yr^{-1}) (Figure 6.3A). In the Yangtze floodplain lakes, it has been widely reported that the installation of dams may accelerate the regime shifts from a clear water state to a turbid state caused by nutrients (Chen et al., 2016; Dong et al., 2016). Hence, dominant chironomids shifted from macrophyte-related to eutrophic species and algal production, including HABs, rapidly increased in Luhu and Wanghu Lakes. Although the hydrologically restricted Futou Lake has experienced intensive human disturbance in the catchment, macrophyte-related species were dominant after the 1990s CE, which might be attributed to the difference in the catchments. In the middle Yangtze floodplain, urbanization and industrialized induced large amount of P loading into the lakes (Chapter 6). Therefore Futou Lake (TP 0.037 mg L^{-1}; TN 0.20 mg L^{-1}), which is dominated by agriculture in the catchment was less polluted compared with Luhu (TP 0.068 mg L^{-1}; TN 0.33 mg L^{-1}) and Wanghu (TP 0.22 mg L^{-1}; TN 0.44 mg L^{-1}) Lakes, which are located in more urban/industrially-influenced catchments. In accordance with this, sedimentary pigments showed that algal production was lower and aphanizophyll (pigments from N_2-fixing cyanobacteria) was barely detected in Futou Lake, whereas algal production was higher and HAB-associated pigments rapidly increased in Luhu and Wanghu Lakes after 2000 CE (Chapter 6). However, the emergence and the gradual increase in nutrient tolerant chironomid species (e.g., *C. plumosus*-type, *P. akamusi*-type) as well as the decreases in the UVR index after the middle and the late 1990s CE showed early signals of water quality deterioration in Futou Lake. It is sensible to expect that if nutrients continuously increase, Futou Lake may become more and more vulnerable and turn into an algal dominant turbid state in the future.

Compared with other lakes (Luhu and Wanghu) where urban and industrial activities are prevalent in the catchment, eutrophic chironomid species were sparse in the large, hydrologically open Poyang Lake, probably reflecting the role of hydrology in regulating eutrophication. It has been widely reported that free hydrological connection with the main channel may conceal the symptoms of eutrophication in floodplain lakes (Paerl et al., 2011). First, free hydrological condition can alleviate eutrophication in open lakes by diluting the nutrient-enriched lake water with the nutrient-poor main channel water (Sokal et al., 2010). For instance, importing the relatively "clean water" from the Yangtze main channel has been regarded as a method to restore the severely eutrophic Taihu Lake in the lower Yangtze floodplain (Hu et al., 2010). Second, the high flushing rate in hydrologically open lakes may reduce the water retention times and hence flush the nutrients out of the lake (Chen et al., 2016). Local dam construction which blocks the free hydrological connection between the lakes and the main channel prolongs the water retention time and reduces the water exchange ratio. The prolonged water retention time and reduced water exchange may promote the utilization of nutrients, amplifying the symptoms of eutrophication (Sokal et al., 2010; Chen et al., 2016). Consistent with this, TP concentration was lower in Poyang Lake (0.027 mg/L) compared with Luhu (0.068 mg/L) and Wanghu (0.22 mg/L) Lakes. In agreement with chironomids, algal production and concentrations of sedimentary pigments (aphanizophyll and canthaxanthin) from HABs were higher in the dammed lakes (Luhu and Wanghu) than the open Poyang Lake, although algal production sharply increased in all these lakes (Chapter 6). Therefore, the data supports the idea that free hydrological connection can alleviate eutrophication while local dam construction exacerbates eutrophication in floodplain lakes.

7.5 Summary

This study suggests that hydrological connection with the main channel has a clear influence on light and nutrient conditions, and hence the ecosystem structure of lakes in floodplain areas. When lakes were freely connected with the Yangtze River before local dam construction, large quantities of suspended particles were transported into them, which promotes the attenuation of light in the water column, resulting in poor underwater light condition. When agricultural and industrial/urban activities were low in the catchments lake nutrients were scarce, causing algae and macrophytes to be sparsely developed. After the construction of local dams, which impeded the hydrological interaction between the floodplain lakes and the main channel, light conditions in lakes was improved due to the reduced suspended particle concentrations in the water column, stimulating the growth of macrophytes. With the intensification of agricultural and industrial activities as well as urbanization in the catchment, large quantities of nutrients from anthropogenic sources were transported into the lakes. In combination with local dam construction which blocked water exchange with the relatively less polluted main channel and prolonged water retention times, more nutrients were retained in the lake, which resulted in a substantial increase in algal production. Shading of phytoplankton resulted in poor light conditions at the bottom of the lakes, which was not favourable for the growth and development of benthic communities. This sedimentary evidence suggests that the lakes (Luhu and Wanghu) shifted from a macrophyte-dominated state with high UV penetration to an algal dominated state which was turbid (Scheffer et al., 1993). Overall, this study revealed that the weakened hydrological connection caused by local dam construction would amplify the symptoms of eutrophication in lakes with nutrient enrichment, promoting higher algal production and eutrophic species. In contrast, the free hydrological interaction with the Yangtze River can mitigate the effects of eutrophication.

CHAPTER 8 CHANGES IN CARBON AND NITROGEN CYCLING IN THE MIDDLE YANGTZE FLOODPLAIN SINCE ~ 1800 CE

8.1 Introduction of C/N ratios and $\delta^{13}C$

Potential sources of organic matter preserved in lake sediments include allochthonous (derived externally to the lake) land plants and autochthonous (derived from within the lake) algae and macrophytes. The different sources of carbon (i.e., CO_2 vs. HCO_3^-) and the different pathways (i.e., C_3 vs. C_4) used in photosynthesis may leave distinct isotopic signature and C/N ratios in organic matter from different sources (Meyers and Teranes, 2001; Leng et al., 2006). C_3 plants which use the Calvin photosynthetic pathway in photosynthesis to transform atmospheric CO_2 into organic matter are characterized by a $\delta^{13}C$-value (PDB) of about −27‰ (Meyers and Teranes, 2001). C_4 plants which use the Hatch-Slack pathway in photosynthesis have an average $\delta^{13}C$-value (PDB) of about −14‰ (Smith and Samuel, 1971; O'Leary, 1981; 1988; Hassan et al., 1997; Meyers and Lallier-Vergés, 1998).

For autochthonous organic matter, empirical evidence from deep lakes, where phytoplankton are the dominant source of organic matter, suggests that lakes experiencing increasing productivity are often accompanied by an enrichment of $\delta^{13}C$ (Meyers and Teranes, 2001). When primary productivity increases to a level at which aqueous CO_2 is insufficient, algae use bicarbonate (HCO_3^-) as the carbon source, resulting in a further increase of $\delta^{13}C$ as bicarbonate ($\delta^{13}C$ = 1‰) is more rich in ^{13}C than CO_2 ($\delta^{13}C$ = −7‰). In shallow lakes, benthic communities (i.e., submerged macrophytes, benthic algae) are an important source of autochthonous organic matter (Sayer et al., 2010). Submerged macrophytes and benthic algae which grow at the bottom of lakes have been reported to have distinct isotopic signal from phytoplankton species (Goericke, 1994; Wu et al., 2006). Therefore, it is sensible to expect that aquatic stable state transitions between macrophyte-dominated and algal dominated states may leave an isotopic footprint in sediments.

As demonstrated in Chapter 6 and Chapter 7, human activities including hydrological modification caused by local dam construction and agricultural and industrial activities as well as urbanization have heavily influenced the catchment processes and lake ecosystems (i.e., phytoplankton, macrophytes and benthic invertebrates) in the Yangtze floodplain. Carbon and nitrogen content and carbon stable isotopes preserved in lake sediments can provide fruitful information quantifying the amount and identifying the sources of organic matter related with ecosystem evolution and organic matter cycling (Meyers and Teranes, 2001; Leng et al., 2006). In this section, C/N ratios and carbon isotopic signatures of catchment plants, aquatic plants, catchment soils, and surface sediments were investigated to define the geochemical characteristics of potential organic matter sources. Then, C/N ratios and stable carbon isotopes in sediment cores from the lakes were studied, aiming to provide a regional overview of carbon cycling and sequestration in the middle reaches of the Yangtze floodplain over the last 200 years. By synthesising sedimentary pigments, chironomids and isotopes, this chapter further aims to understand long term (~ 200 years) dynamics of organic matter cycle in large river-floodplain systems undergoing hydrological modification and receiving human emitted pollutants. The following hypothesis were tested:

1. Increases in productivity of algae and HABs caused by enhanced nutrient loadings from agricultural and industrial activities and urbanization in the catchment will increase $\delta^{13}C$ in the sediments.
2. The growth and development of macrophytes after local dam construction will leave an isotopic signature in the sediments similar to that of submerged macrophytes.

8.2 Methodological approaches of C/N ratios and $\delta^{13}C$

C/N ratios and $\delta^{13}C$ in the sediment cores were analysed at the Natural Environmental Research Council (NERC) Isotope Geoscience Laboratory at the British Geological Survey using the methodology outlined in Chapter 4 to investigate carbon cycling over the last 200 years. In addition, $\delta^{13}C$ and C/N ratios in land plants, submerged, emergent and floating plants, catchment soils and surface sediments were analysed to facilitate the interpretation of downcore changes.

8.3 Results of C/N ratios and $\delta^{13}C$

8.3.1 C/N ratios and $\delta^{13}C$ of aquatic plants, catchment land plants and soils

Analysis of modern samples showed that aquatic plants (emergent, floating and submerged) and catchment land plants had distinct isotopic characteristics across the lakes in the middle Yangtze floodplain (Figure 8.1; Table8.1). Submerged plants were generally less depleted in $\delta^{13}C$ (–21.4 ± 4.6‰) compared with floating (–27.4 ± 1.4‰) ($p < 0.05$) and emergent (–25.2 ± 6.4‰) ($p = 0.43$) plants. In terms of land plants, maize (*Zea mays*), a common C_4 plant, was characterized by a relatively positive $\delta^{13}C$ value (–12.0 ± 0.6‰). Other catchment plants, such as woody plants (–29.6 ± 0.7‰) and *Oryza sativa* (–29 ± 0.3‰), had a negative carbon isotopic composition. C/N ratios of aquatic plants (19.4 ± 7.8) and land plants (19.2 ± 8.0) were undistinguishable from one another (p = 0.96). As for catchment land plants, the C/N ratios of *Zea mays* was different from that of other catchment plants in the Yangtze floodplain. C/N ratios of *Zea mays* were 13.3 ± 1.5, whereas the C/N ratios of other catchment plants were 24.7 ± 7.4. Rice (*Oryza sativa*) had intermediate C/N ratios (14 ± 4.7), ranging from ca. 10 - 20. Both carbon isotope and C/N ratios of paddy soils in the middle Yangtze Basin have a wide range of variation from ca. –27‰ to –14‰ and ca. 12 to 42, respectively.

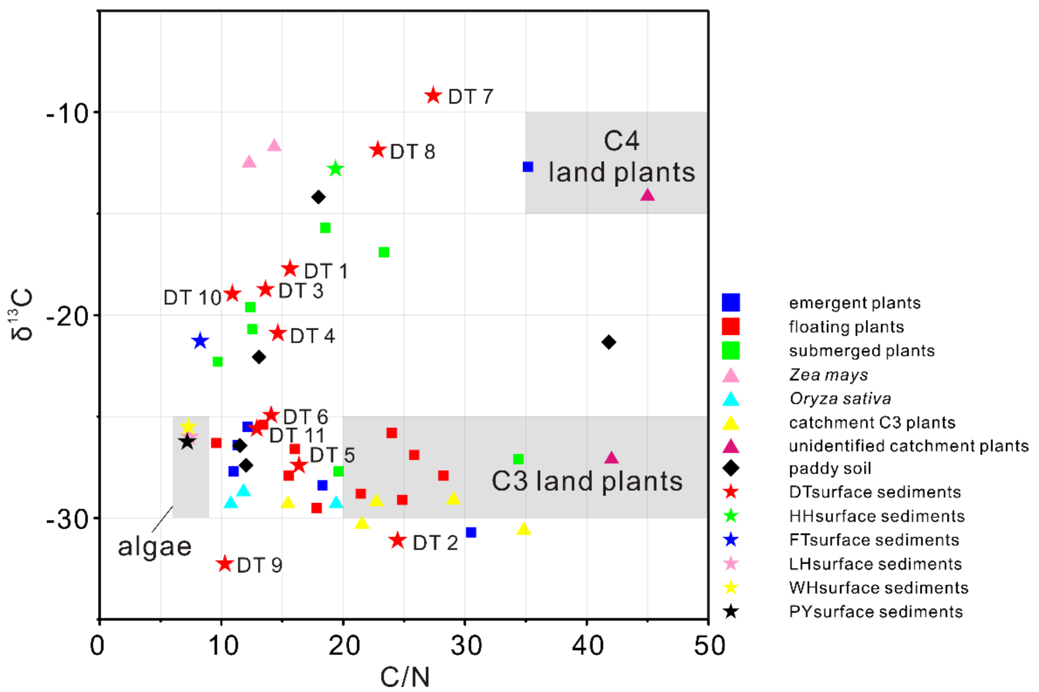

Figure 8.1 Biplot showing the C/N ratios and δ^{13}C of aquatic plants (submerged, emergent and floating), land plants, catchment soils and surface sediments in the six lakes. DT(Dongting Lake), HH (Honghu Lake), FT (Futou Lake), LH (Luhu Lake), WH (Wanghu Lake), PY (Poyang Lake). The grey bars indicate typical values of algae, C_3 and C_4 plants from Meyers and Teranes, 2001.

Table 8.1 C/N ratios and $\delta^{13}C$ of aquatic plants (submerged, emergent and floating), land plants, catchment soils in the middle Yangtze floodplain.

	name	C/N ratios	$\delta^{13}C$
submerged	*Potamogeton* 1	34.4	-15.7‰
	Potamogeton 2	12.5	-20.7‰
	Ceratophyllum demersum	18.5	-27.7‰
	Vallisneria natans 1	19.6	-19.6‰
	Vallisneria natans 2	12.4	-22.3‰
	Vallisneria natans 3	23.4	-27.1‰
	Myriophyllum verticillatum	9.7	-16.9‰
floating	*Eichhornia crassipes* 1	21.4	-28.8‰
	Eichhornia crassipes 2	25.8	-26.9‰
	Eichhornia crassipes 3	17.8	-29.5‰
	Eichhornia crassipes 4	28.2	-27.9‰
	Trapa spp. 1	24.0	-25.8‰
	Trapa spp. 2	16.0	-26.6‰
	Trapa spp. 3	9.6	-26.3‰
	Salvinia spp.	15.5	-27.9‰
	Nuphar spp.	13.4	-25.4‰
	floating seed	24.8	-29.1‰
emergent	*Nelumbo nucifera* 1	11.0	-27.7‰
	Nelumbo nucifera 2	12.1	-25.5‰
	Nelumbo nucifera 3	11.3	-26.4‰
	Phragmites adans 1	30.5	-30.7‰
	Phragmites adans 2	18.3	-28.4‰
	Phragmites commuis	35.2	-12.7‰
catchment plants	*Graminae*	29.1	-29.0‰
	Artemisia selengensis 1	22.7	-29.1‰
	Artemisia selengensis 2	15.5	-29.2‰
	Carex sp	34.8	-30.5 ‰
	Oryza sativa 1	10.8	-29.2 ‰
	Oryza sativa 2	11.8	-28.6 ‰
	Oryza sativa 3	19.4	-29.2 ‰
	Zea mays 1	14.3	-11.6‰
	Zea mays 2	12.3	-12.4‰
	Pinaceae	21.5	-30.2 ‰
	Unidentified	44.8	-13.9 ‰
	Unidentified	42.2	-27.0‰
catchment soil	paddy soil 1	18.0	-14.2‰
	paddy soil 2	11.5	-26.4‰
	paddy soil 3	41.8	-21.3‰
	paddy soil 4	12.0	-27.4‰
	paddy soil 5	13.1	-22.1‰

8.3.2 C/N ratios and $\delta^{13}C$ in surface sediments

$\delta^{13}C$ and C/N ratios of surface sediments in Poyang, Luhu and Wanghu Lakes which experienced HABs (filamentous N_2-fixing cyanobacteria, aphanizophyll)

(Chapter 6, Figure 6.6) were similar to that of algae, characterized by negative $\delta^{13}C$ (ca. −26 ‰) and low C/N ratio (ca. 7) (Figure 8.1). In the two lakes (Futou and Honghu) with no pigments from N_2-fixing cyanobacteria (aphanizophyll) but abundant macrophytes (Chapter 6), $\delta^{13}C$ was less depleted (Figure 8.1). The $\delta^{13}C$ and C/N ratios of surface sediments from Futou Lake were −21‰ and ca. 8, respectively. In Honghu Lake, $\delta^{13}C$ was −12.5‰ and C/N ratios was ca. 19 (Figure 8.1). The 11 surface sediments from Dongting Lake varied from ca. −32‰ and 10 to ca. −9‰ and 27 for $\delta^{13}C$ and C/N, respectively (Figure 8.1).

8.3.3 C/N ratios and $\delta^{13}C$ in the sediment cores

In the two large, hydrologically open drainage Donging and Poyang Lakes, $\delta^{13}C$ was relatively stable before the 1980s CE, hovering between −24‰ and −22‰, respectively (Figure 8.2). In contrast, C/N ratios fluctuated widely between 3 and 13 during this time. Since the 1980s CE, $\delta^{13}C$ gradually decreased to −28‰ in Dongting Lake and to −26‰ in Poyang Lake, whilst C/N ratios increased in both lakes. In the four smaller lakes (Honghu, Futou, Luhu and Wanghu) C/N ratios had similar values before local dam construction, which slightly varied between 6 and 8 (Figure 8.2). After local dam construction, especially since the 1980s CE, C/N ratios increased in all the four lakes, with higher values in Honghu (~ 13) and Futou (~ 11) and slightly lower values in Luhu (~ 8.5) and Wanghu (~ 8.5) by the 2010s CE. $\delta^{13}C$ was relatively stable in all the four lakes before dam construction, hovering at −24‰, −23.5‰, −24.5‰ and −24‰ in Honghu, Futou, Luhu and Wanghu, respectively. After local dam construction, $\delta^{13}C$ exhibited a different pattern of variation. In Honghu and Futou, $\delta^{13}C$ increased after local dam construction, especially after the 1980s CE, reaching ca. −20‰ and −22‰, respectively, in the early 2000s CE, followed by a slight decrease thereafter. In Luhu Lake, $\delta^{13}C$ increased from ~ −25.5‰ to ~ −23‰ after local dam construction. Since the 1980s CE, $\delta^{13}C$ gradually decreased in both Luhu and Wanghu Lakes, reaching −26‰ in the early 2010s CE.

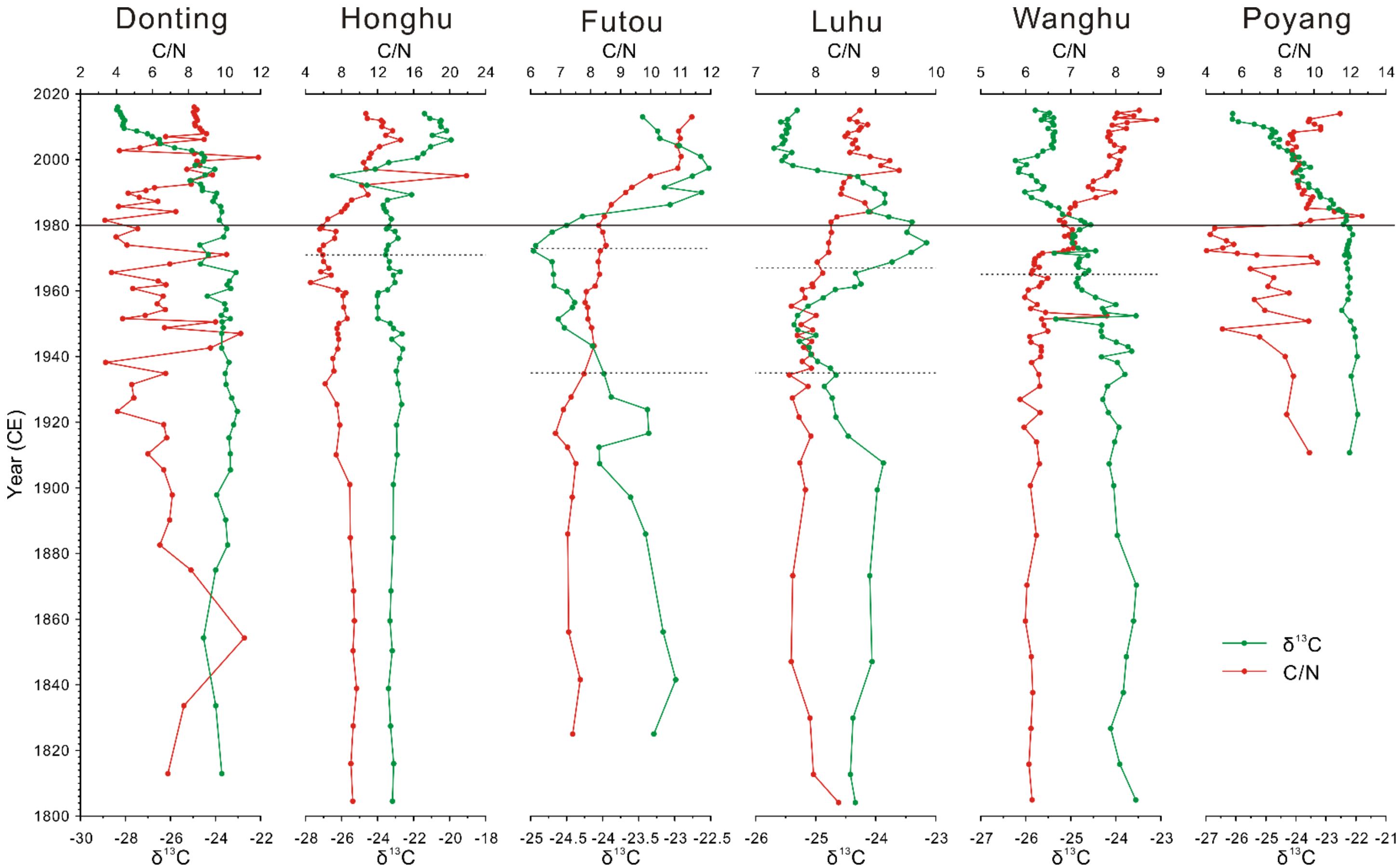

Figure 8.2 C/N ratios (red) and $\delta^{13}C$ (green) of the sediment cores from the six middle Yangtze floodplain lakes since the 19th century. The horizontal solid line indicates of start of the “Opening and reform” in the late 1970s CE. The horizontal dashed lines indicate the timing of local dam construction.

8.3.4 Statistical analysis

8.3.4.1 Spatial survey of Dongting Lake

In order to aid the interpretation of $\delta^{13}C$ in sediment core samples from all sites, linear regression was used to investigate the relationship between water depth and $\delta^{13}C$ and C/N ratios in surface sediments at Dongting Lake. The result showed that there is a significant positive relationship (p = 0.016) between $\delta^{13}C$ and water depth (Figure 8.3a), while the relationship between C/N and water depth was not significant (p = 0.56) (Figure 8.3b).

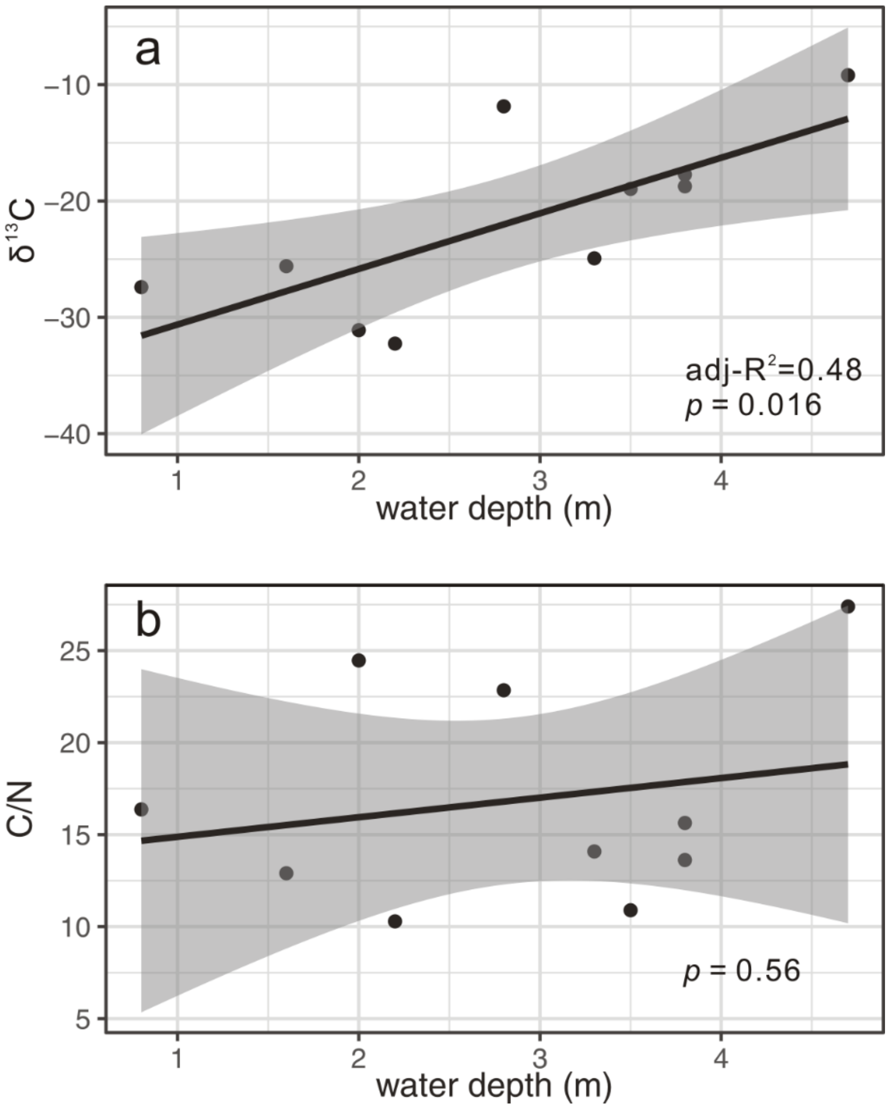

Figure 8.3 Linear regression between water depth and (a) C/N ratios and (b) $\delta^{13}C$ of organic matter in surface sediments in Dongting Lake. The shaded band around the fitted line indicates the 95 % confidence interval.

8.3.4.2 Sediment core samples

Mann-Kendall coefficients

Mann-Kendall trend analysis was used to test the overall trends of C/N ratios and $\delta^{13}C$ profiles in the sediment cores. The results revealed that C/N ratios showed an overall upward trend in all six lakes over the last 200 years ($p < 0.05$) (Table 8.2). In contrast, $\delta^{13}C$ decreased in Dongting, Luhu, Wanghu and Poyang Lakes ($p < 0.001$) over the last 200 years, and no significant trend was found in $\delta^{13}C$ for Futou and Honghu Lakes.

Table 8.2 Mann-Kendall trend coefficients (tau) of C/N ratios and $\delta^{13}C$ in sediment cores from the six middle Yangtze floodplain lakes (Dongting, Honghu, Futou, Luhu, Wanghu and Poyang) since the 19th century.

	C/N ratios		$\delta^{13}C$	
	tau	*p*	tau	*p*
Dongting	0.175	*	-0.659	***
Honghu	0.229	*	0.144	n.s.
Futou	0.786	***	-0.007	n.s.
Luhu	0.636	***	-0.320	***
Wanghu	0.745	***	-0.710	***
Poyang	0.182	*	-0.856	***

*** < 0.001; ** < 0.01; * < 0.05; n.s. no significance

Simple linear regression between $\delta^{13}C$ and algal production (pigment PCA axis 1)

As the first PCA axis of pigments captured the algal abundance and composition in the lakes (Chapter 6), $\delta^{13}C$ was used as response variable and pigment PCA axis 1 was used as explanatory variable in a regression to study the relationship between $\delta^{13}C$ and algal production. The result showed that $\delta^{13}C$ significantly decreased with the lower PCA axis 1 scores of pigments (indicating increases in algal production) in Dongting, Luhu, Wanghu and Poyang (Figure 8.4). In contrast, $\delta^{13}C$ increased with the decreases in pigment PCA axis 1 in Honghu and Futou, although the relationship was not significant in Futou Lake (Figure 8.4).

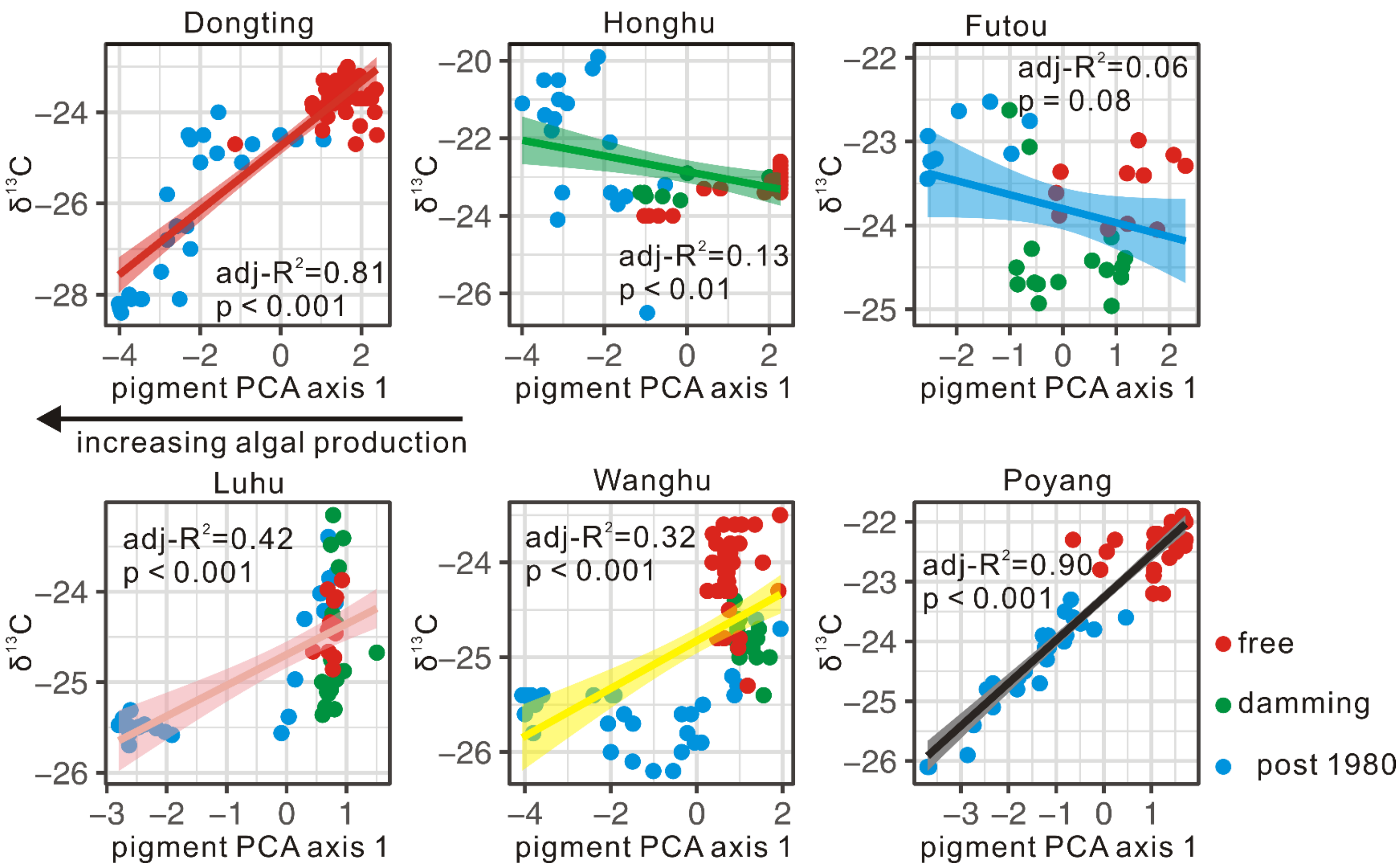

Figure 8.4 Linear regression between $\delta^{13}C$ and algal production (pigment PCA axis 1) in the sediment cores from the lakes. The shaded band around the fitted line indicates the 95 % confidence interval.

8.4 Discussion – C/N ratios and $\delta^{13}C$

The modern survey of catchment and aquatic plants indicates that organic matter from different sources have distinct C/N ratios and $\delta^{13}C$ in the middle Yangtze floodplain. Variation in C/N ratios and $\delta^{13}C$ in the sediment cores were heavily influenced by the changes in source of organic matter caused by human disturbance in the catchment. Local dam construction which promoted the development and growth of submerged macrophytes left a sedimentary C/N ratios and $\delta^{13}C$ similar to that of submerged macrophytes in Futou and Honghu which are less eutrophic (Figure 8.6). As the lakes changed into an algal dominated turbid state with intensive human activities in the catchment, algae became the main source of organic matter, and therefore, C/N ratios and $\delta^{13}C$ were closer to that of algae in Dongting, Luhu, Wanghu and Poyang.

8.4.1 Modern survey

Allochthonous land C_3 plants (*Oryza sativa*) (−29.4 ± 0.6‰) and C_4 plants (*Zea mays*) (−12.0 ± 0.6‰) are characterized by distinct $\delta^{13}C$ in the middle Yangtze floodplain (Figure 8.1), which is similar to values published by Meyers and Teranes (2001). Terrestrial plants use atmospheric CO_2 (~ −7‰) as the carbon source for photosynthesis. C_3 plants (i.e., *Oryza sativa*, *Gossypium*) which use the Calvin photosynthetic pathway in photosynthesis cause an average isotopic discrimination of ~ −20‰ from the ratio of atmospheric CO_2, while C_4 plants (*Zea mays*) use the Hatch-Slack pathway in photosynthesis resulting in higher $\delta^{13}C$ ranges of −6‰ to −4‰ (Hassan et al., 1997; Meyers and Lallier-Vergés, 1998). Therefore, organic matter produced by C_3 plants is characterized by a lower $\delta^{13}C$ value of about −27‰ compared to C_4 plants (−13‰ to −11‰) (Smith and Samuel, 1971; O'Leary, 1981; 1988; Hassan et al., 1997; Meyers and Lallier-Vergés, 1998).

$\delta^{13}C$ and C/N ratios of catchment soil are determined by the carbon signature of catchment plants and the subsequent processes in soils (Ehleringer et al., 2000). In the Yangtze floodplain, arable land dominated by C_4 plants (which are less depleted in $\delta^{13}C$) only account for 0.04 %, 10.08 % and 0.63 % of the total arable land in Hunan, Hubei and Jiangxi Provinces, respectively (NBSC, http://data.stats.gov.cn/index.htm). Instead C_3 plants (mainly *Oryza sativa*) with a more negative $\delta^{13}C$ signature (−29.4 ± 0.6‰), are the major agricultural plant in the catchment. In soils oxidizing reactions and microbial reactions preferentially utilize the lighter carbon (^{12}C) (Ehleringer et al., 2000), causing the slight increase of $\delta^{13}C$ in paddy soils, although the values (−22.3 ± 5.2‰) are highly variable in the middle Yangtze floodplain (Figure 8.5).

Autotrophs in lakes potentially use atmospheric CO_2, aqueous CO_2 and HCO_3^- as carbon sources (Meyers and Lallier-Vergés, 1998; Meyers and Teranes, 2001; Leng et al., 2006). Atmospheric and aqueous CO_2 has a similar isotopic signature as atmospheric CO_2 (−7‰), whereas HCO_3^- ($\delta^{13}C$ = ~ 1‰) is less depleted in $\delta^{13}C$ due to the fractionation during the hydration process (Deuser and Degens, 1967). Therefore, emergent and floating plants (−26.6±4‰), found at the surface and margins of lakes, are able to more easily access carbon as CO_2 and hence are depleted in $\delta^{13}C$ (−26.6 ± 4‰). In contrast, submerged macrophytes, which inhabit the bottom of lakes, are more likely to utilize HCO_3^- for photosynthesis when aqueous CO_2 is insufficient in these alkaline Yangtze floodplain lakes (Brenner et al., 2006). In addition, the difference in fractionation during carbon fixation between higher plants and cyanobacteria may influence δ^{13}C as well (Goericke, 1994; Wu et al., 2006). During photosynthesis, inorganic carbon is fixed under the influence of the enzyme ribulose 1,5-bisphosphate carboxylase-oxygenase (Rubisco) (Goericke, 1994). The isotopic fractionation of higher plants for Rubisco is 10‰ higher than that of photosynthetic bacteria (Goericke, 1994). Therefore, submerged macrophytes are less depleted in δ^{13}C (Hassan et al., 1997; Meyers and Lallier-Vergés, 1998; Brenner et al., 2006), and are in the range of −21.4 ± 4.6‰ in this study (Figure 8.5). In terms of C/N ratios, land plants, emergent and (to a lesser extent) floating plants and submerged plants are rich in cellulose, characterized by high C/N ratios (Figure 8.5).

8.4.2 Lake survey in Dongting Lake

Theoretically, organic matter in lake sediments of the Yangtze floodplain lakes has four potential sources, a) allochthonous land plants (mainly C_3 plants) and catchment soils; b) autochthonous emergent and floating plants; c) autochthonous submerged plants; and d) autochthonous algae (Figure 8.5). Organic matter from these sources have distinctive characteristics of C/N ratios and δ^{13}C in the middle Yangtze floodplain (Figure 8.1; Figure 8.5).

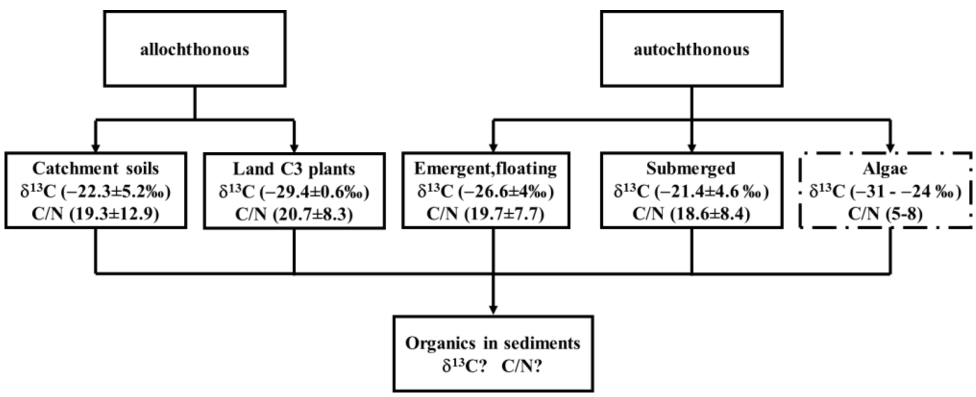

Figure 8.5 The characteristics of C/N ratios and δ^{13}C of organic matters from potential sources in the middle Yangtze floodplain. C/N ratios and δ^{13}C of algal (dashed line) were from cited Meyers and Teranes, 2001.

The lake survey of recently-deposited surface sediments in Dongting Lake showed that $\delta^{13}C$ is elevated with increases in water depth (Figure 8.3a), resulting in an increasing gradient from littoral areas to central parts of the lakes (Chen et al., 2017). Dongting Lake is the second largest freshwater lake in China with annual water surface area fluctuation between the flooding and drought season more than 1,200 km^2 (Ke et al., 2017). The advance and retreat of the lake margin during the flooding and non-flooding seasons integrate a large amount of allochthonous organic matter into the lake (Chen et al., 2017). In addition, the littoral areas are more favourable for emergent and floating plants which are depleted in $\delta^{13}C$. Therefore, littoral areas in Dongting which receive more allochthonous organic matter and are abundant in emergent and floating-leaved plants that are depleted in $\delta^{13}C$. In contrast, central parts of the lake, which are more favourable for the growth and development of submerged macrophytes and are less influenced by terrestrial organic matter, are characterized by less depleted $\delta^{13}C$ (Chen et al., 2017). As a result, $\delta^{13}C$ gradually increased from the littoral areas to the central parts of the lakes as the source of organic matter transformed from allochthonous land plants and emergent and floating plants to submerged macrophytes. However, the relationship between C/N ratios and water depth was not significant, which can be attributed to the similar C/N ratios of allochthonous land plants (20.7 ± 8.3), emergent and floating plants (19.7 ± 7.7) and submerged macrophytes (18.6 ± 8.4) and the high variation of C/N ratios in each group (Figure 8.1; Figure 8.5).

8.4.3 Sediment cores

8.4.3.1 Before intensive anthropogenic disturbance

When anthropogenic activities were less intensive in the catchments (defined as before local dam construction at hydrologically-restricted drainage lakes, and before 1980 CE for hydrologically open drainage lakes), lake sediments were characterized by intermediate $\delta^{13}C$ values (~ −24‰ in Dongting, ~ −23‰ in Honghu, ~ −23.5‰ in Futou, ~ −24.5‰ in Luhu, ~ −24‰ in Wanghu, and ~ −22.5‰ in Poyang) compared with allochthonous terrestrial plants (−29.4 ± 0.6‰), floating and emergent plants (−26.6 ± 4‰), algae (−31‰ to −24‰) which are low in $\delta^{13}C$ and submerged macrophytes (−21.4 ± 4.6 ‰) which is high in $\delta^{13}C$ (Figure 8.6; Figure 8.7). During this less anthropogenic disturbance period, influx of allochthonous organic matter and algal production in the lakes was low as nutrient loadings into the lakes were low due to the less intensive human activities in the catchments (Chapter 6). At the same time, water level fluctuations and disturbances from flooding resulted in low to intermediate levels of submerged macrophyte coverage (Chapter 7). Therefore, the intermediate $\delta^{13}C$ values in the sediments might indicate sedimentation of organic matter from different sources.

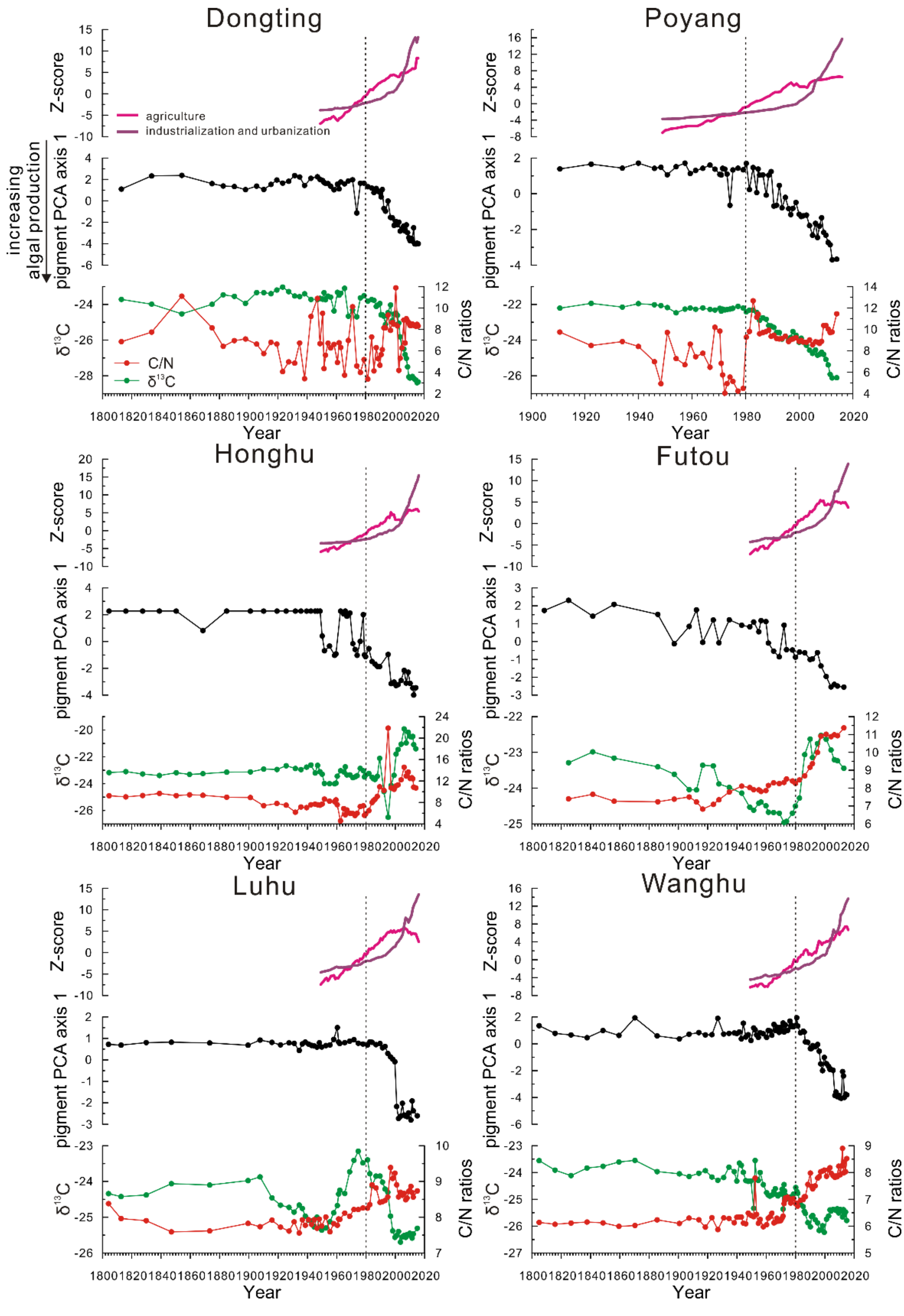

Figure 8.6 Changes in Z-score of agriculture and industrialization/industrialization, algal production (indicated by pigment PCA axis 1), C/N ratios and $\delta^{13}C$ for Dongting, Poyang, Honghu, Futou, Luhu, and Wanghu Lakes since 1800 CE.

During the period with less intensive anthropogenic disturbance, C/N ratios were highly variable in the two large, hydrologically open lakes (Dongting and Poyang) (C/N ratios, 3 to 13) (Figure 8.6). In contrast, C/N ratios of sediments were relatively stable in Honghu, Futou, Luhu and Wanghu Lakes which are connected with the Yangtze main channel through tributaries and are smaller in water surface area (Figure 8.6). This indicates that hydrological variation may be a factor influencing C/N ratios (Liang et al., 2016). Dongting and Poyang Lakes which are freely and directly connected with the Yangtze River experience high water level fluctuations and recurrent moving littoral zones (Harris and Zhuang, 2010; Chen et al., 2016; Ke et al., 2017). Therefore, the high variability in C/N ratios for Dongting and Poyang Lakes can be attributed to the combination of organic matter from different sources (Liang et al., 2016).

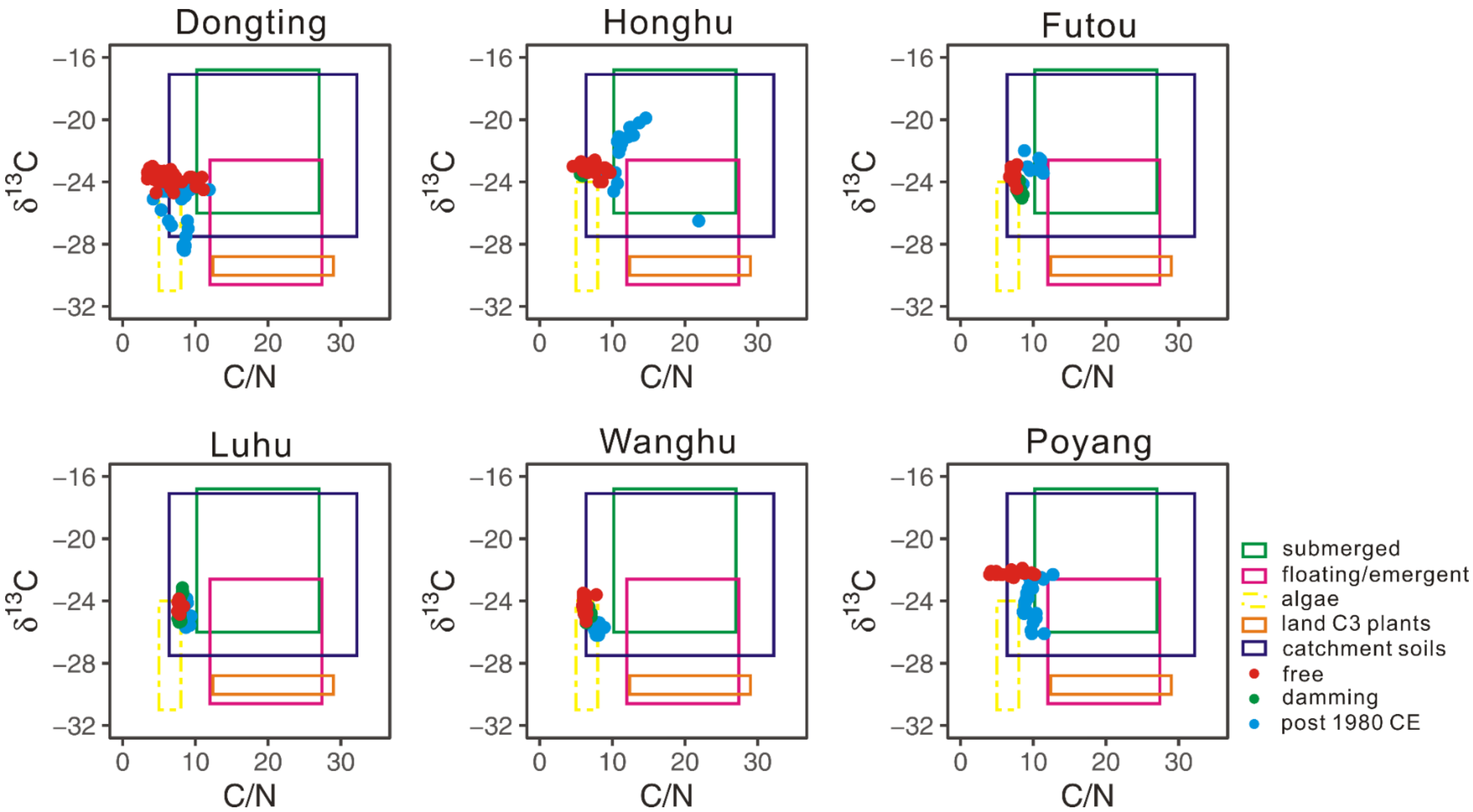

Figure 8.7 Atomic C/N ratios vs. $\delta^{13}C$ values of sediment organic matter in the middle Yangtze floodplain lakes since 1800 CE against values of land plants in the catchment, submerged, emergent and floating plants in the middle Yangtze floodplain (rectangles in solid line, showing the mean and 1 standard deviation of $\delta^{13}C$ and C/N ratios for each group) and algae from Meyers and Teranes (2001) (rectangle in yellow dashed line).

8.4.3.2 Intensive anthropogenic disturbance

Influence of nutrient loading from human activities - The increase of algal production appeared to lead to a decrease in $\delta^{13}C$ in Dongting, Luhu, Wanghu and Poyang Lakes. Since the 1980s CE, intensive human activities have increased nutrient loading in the lakes, resulting in the increase in algal production (Chapter 6). During this period, the $\delta^{13}C$ and C/N ratios of sediments gradually moved from the previously intermediate values to values closer to algae (Figure 8.7), suggesting that algae was the main source of organic matter in these four lakes. Consistent with this, regression analysis shows a significant positive relationship between $\delta^{13}C$ and sample scores on the first PCA axis of sedimentary pigments (Figure 8.4) which was negatively correlated with algal production (Chapter 6). With the decrease in pigment PCA axis 1 scores (increase in algal production), $\delta^{13}C$ has significantly decreased since the 1980s CE (Figure 8.4; Figure 8.6).

In deep lakes, phytoplankton preferentially assimilate lighter carbon (^{12}C) for photosynthesis, resulting in the enrichment of ^{13}C in the remaining inorganic carbon pool and newly generated organic matter (Meyers and Teranes, 2001). Thus, lakes experiencing increasing algal production are often accompanied by an increase in $\delta^{13}C$ (Meyers and Teranes, 2001). On the contrary, increases in algal production induced the depletion in $\delta^{13}C$ in Dongting, Luhu, Wanghu and Poyang Lakes. Lakes in the middle Yangtze floodplain are shallow and are more suited to the growth and development of submerged macrophytes compared with deep lakes (Chapter 7). Therefore, submerged macrophytes are an important source of autochthonous organic matter in addition to phytoplankton (Sayer et al., 2010). In shallow lakes, the increase in phytoplankton is often accompanied by a reduction in submerged macrophytes according to the aquatic stable state transition (Scheffer et al., 1993). Since the ~ 1980s CE, increasing nutrients due to agricultural development and urbanization, as well as industrialization in the catchments has stimulated algal production and HABs in these four lakes (Donting, Poyang, Luhu and Wang) (Figure 8.6; Chapter 6). During this time, the contribution of algae in the autochthonous organic matter pools increased (Chapter 6). Concurrently, the contribution of submerged macrophytes decreased (Chapter 7). In the middle Yangtze floodplain, submerged macrophytes are less depleted in $\delta^{13}C$ compared with algae (Figure 8.5). Therefore, the decrease in $\delta^{13}C$ in these four lakes after 1980 CE might be attributed to the increase in algal production and decrease in benthic communities caused by increasing nutrient loadings from human activities in the catchment.

Although the hydrologically restricted Futou and Honghu Lakes have also experienced intensive human disturbance in the catchments, C/N ratios (~ >10) and $\delta^{13}C$ were high and gradually moved from previously intermediate values to values closer to submerged macrophytes after local dam construction (Figure 8.6). This is because Honghu and Futou Lakes were less polluted than the other lakes and were in early stages of eutrophication as they were characterized by agricultural activities in the catchments (Chapter 7). Compared with the other four lakes (Dongting, Poyang, Luhu and Wanghu) which had high sedimentary TP flux (> 0.025 g cm^{-2} yr^{-1}) and high concentrations of pigments from filamentous N_2-fixing cyanobacteria (aphanizophyll), sedimentary TP flux was low (~ 0.01 g cm^{-2} yr^{-1}) and aphanizophyll was barely detected in Honghu and Futou after 2000 CE (Chapter 6). In accordance with their early stages of eutrophication, both Futou and Honghu have a high coverage of submerged macrophytes (Cao et al., 2014; Zeng et al., 2018). In Honghu Lake submerged macrophytes including *Myriophyllum spicatum*, *Potamogeton maackianus*, *Ceratophyllum demersum* and *Hydrilla verticillata* are widely developed (Song et al., 2016). The coverage of *M. spicatum* and *P. maackianus*, increased from 6 % and 10 % in the 1950s CE to 65 % and 65 % in the 1990s CE, respectively (Song et al., 2016). Submerged macrophytes are less depleted in $\delta^{13}C$ in the middle Yangtze floodplain lakes (Figure 8.5). Therefore, the concurrent increases in $\delta^{13}C$ and C/N ratios in Honghu and Futou after the 1980s CE might be attributed to the increasing contribution of submerged macrophytes to the organic matter pool in the early stage of eutrophication.

After ~ 2000 CE, although $\delta^{13}C$ of sediments in Honghu and Futou Lakes was closer to that of submerged macrophytes, it showed a slightly decreasing trend (Figure 8.6), which indicated increased contribution of organic matter depleted in $\delta^{13}C$. Agriculture and industry activities continued to develop in Honghu and Futou catchments after 2000 CE. For example, more than 70 % of the water area was used for aquaculture in Honghu Lake in 2010 CE (Song et al., 2016). With the continuously extensive human disturbance in the catchments, both Honghu and Futou Lakes showed early signs of water quality deterioration in recent years (Chapter 7). In Futou Lake abundance of eutrophic chironomids increased and the UVR index were low in both lakes after 2000 CE (Chapter 7). As a result, the coverage of submerged macrophytes slightly decreased in Honghu and Futou (Song et al., 2016; Zeng et al., 2018). The coverage of *M. spicatum* and *P. maackianus* decreased from ~ 65% to 15 % and 38 % by 2014 CE in Honghu, respectively (Song et al., 2016). On the contrary, algal production further increased in these two lakes as shown by sedimentary pigments (Chapter 6). With the combined influence of the decrease in submerged macrophytes and increases in algal production, $\delta^{13}C$ slightly decreased after ~ 2000 CE. These changes may be compounded by strong agricultural and industrial activities which increased the influx of allochthonous organic matter from the catchments.

Influence of allochthonous organic matter - Although the low C/N ratios (< ~10) (Figure 8.6) and the significant relationship between sedimentary pigment PCA axis 1 and $\delta^{13}C$ (Figure 8.4) revealed that algae was the main source of organic matter, C/N ratios showed an upward trend in Dongting, Luhu, Wanghu and Poyang Lakes ($p < 0.05$) (Table 8.2), which indicated the increase in the contribution of cellulose-rich organic matter (Meyers and Teranes, 2001). In these shallow Yangtze floodplain lakes, potential sources of cellulose-rich organic matter include allochthonous land C_3 plants and catchment soil and autochthonous emergent, floating, and submerged plants (Figure 8.5). As mentioned in Chapter 7, the contribution of submerged plants decreased with the increases in algal production since ~ 1980 CE in these lakes (Chapter 7). Hence, the increase in C/N ratios is unlikely to be caused by submerged macrophytes. The middle Yangtze floodplain has experienced extensive and intensive human activities including agricultural development since the late 1940s CE and urbanization/industrialization since the 1980s CE (Figure 8.7). Human activities such as land reclamation, deforestation, aquaculture and lake area shrinkage may enhance the influx of allochthonous organic matter (land C_3 plants and catchment soil) which are rich in cellulose from the catchment, resulting in the increase in C/N ratios and depletion of $\delta^{13}C$ (Chen et al., 2017). Therefore, the increase in C/N ratios may be attributed to the contribution of allochthonous land C_3 plants and catchment soils.

Influence of local dam construction –In agreement with the second hypothesis, local dam construction seemed to increase the C/N ratios and $\delta^{13}C$ in the Yangtze floodplain lakes. In Luhu Lake $\delta^{13}C$ increased after local dam construction. In the middle Yangtze floodplain lakes, the improvement of light condition and the stabilization of hydrological condition after local dam construction stimulated the growth and development of submerged macrophytes (Chapter 7), resulting in the increase in $\delta^{13}C$. However, the increase in $\delta^{13}C$ after local dam construction is not obvious in Honghu, Futou and Wanghu Lakes. One possible explanation of this is the synchronous increase in the contribution of allochthonous organic matter and algae (low in $\delta^{13}C$). In these Yangtze floodplain lakes, the timing of local dam construction (~ 1950s ± 10 CE) was concurrent with the period of intensive anthropogenic activities in the catchments (Chapter 6). Anthropogenic activities might enhance the influx of allochthonous land C_3 plants and catchment soil as well as algal production which have low $\delta^{13}C$ (Figure 8.5), compensating the increase in $\delta^{13}C$ with enhance contribution of submerged macrophytes after local dam construction.

8.5 Summary - $\delta^{13}C$ and C/N

$\delta^{13}C$ and C/N revealed similar baseline values in the middle Yangtze floodplain lakes when human activities were less intensive in individual lake catchments. Local dam construction and agricultural and industrial activities as well as urbanization since the 1980s CE have left distinctive $\delta^{13}C$ and C/N ratio signatures in the sediment records. The less polluted Honghu and Futou Lakes are in the early stage of eutrophication and are abundant in macrophytes. Therefore, sedimentary $\delta^{13}C$ and C/N ratios are similar to submerged macrophytes. In the four heavily polluted lakes (Dongting, Poyang, Luhu and Wanghu), $\delta^{13}C$ decreased and gradually moved to values closer to that of algae with the intensification of agricultural and industrial activities and urbanization in the catchments after 1980 CE.

8.6 N isotopes

$\delta^{15}N$ in lake sediments is also a useful proxy in palaeolimnology to provide information on the source of organic matter, in-lake processes, anthropogenic activities in the catchments and climate (Meyers and Teranes, 2001; Leng et al., 2006). However, $\delta^{15}N$ is not as widely used as $\delta^{13}C$ due to its complexity in interpretation (Meyers and Teranes, 2001). Nitrogen is influenced by various biogeochemical processes, such as nitrification fixation, nitrification, denitrification and volatilization (Meyers and Teranes, 2001). All of these processes may regulate the fractionation of nitrogen isotope, and influence the $\delta^{15}N$ in lake sediments. For example, wastewater from domestic and urban point sources which goes through ammonia volatilization and denitrification during the treatment processes can have a $\delta^{15}N$ signature of over +20‰. The growth of N_2-fixing cyanobacteria which utilize atmospheric N_2 can also cause the decrease of $\delta^{15}N$ (McGowan et al., 2012; Chen et al., 2017). For in-lake processes, organisms preferentially assimilate lighter N isotopes (^{14}N), resulting in the progressive enrichment of $\delta^{15}N$ in newly generated organic matter (Meyers and Teranes, 2001). In this study $\delta^{15}N$ in catchment and aquatic plants and sediment core samples were analysed, trying to provide more evidence of the influence of human activities and hydrology on floodplain ecosystem.

8.6.1 N isotopes in catchment plants

The catchment survey showed that $\delta^{15}N$ in aquatic and terrestrial plants is variable and indistinct in the middle Yangtze floodplain (Figure 8.8). The $\delta^{15}N$ of floating plants is highly variable (6.37 ± 4.75‰) when compared with the $\delta^{15}N$ of emergent plants which is smaller and less variable (4.70 ± 2.83‰). Submerged plants have a distinct $\delta^{15}N$ signature (6.42 ± 1.02‰). As for terrestrial plants, corn (*Zea mays*) is distinctive and depleted in $\delta^{15}N$ (0.32 ± 0.25‰) compared with *Oryza sativa* (7.00 ± 4.43‰) and other catchment plants (4.56 ± 2.22‰).

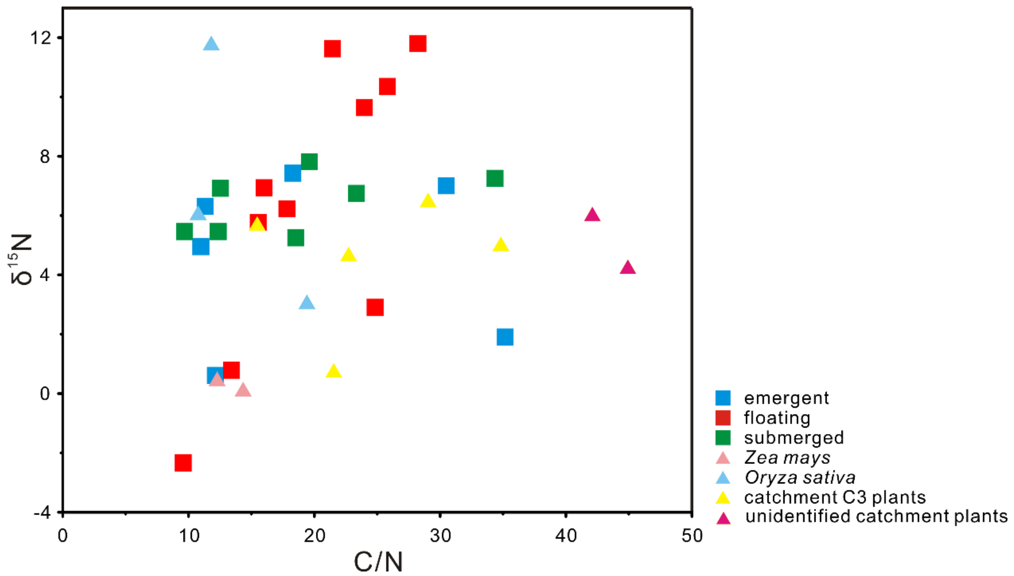

Figure 8.8 Biplot showing the C/N ratios and $\delta^{15}N$ of aquatic plants (submerged, emergent and floating) and catchment land plants in the middle Yangtze floodplain.

Table 8.3 $\delta^{15}N$ of aquatic plants (submerged, emergent and floating) and catchment land plants in the middle Yangtze floodplain.

	name	$\delta^{15}N$
submerged	*Potamogeton* 1	7.3‰
	Potamogeton 2	6.9‰
	Ceratophyllum demersum	5.3‰
	Vallisneria natans 1	7.8‰
	Vallisneria natans 2	5.5‰
	Vallisneria natans 3	6.8‰
	Myriophyllum verticillatum	5.5‰
floating	*Eichhornia crassipes* 1	11.6‰
	Eichhornia crassipes 2	10.4‰
	Eichhornia crassipes 3	6.2‰
	Eichhornia crassipes 4	11.8‰
	Trapa spp. 1	9.6‰
	Trapa spp. 2	6.9‰
	Trapa spp. 3	-2.3‰
	Salvinia spp.	5.8‰
	Nuphar spp.	0.8‰
	floating seed	2.9‰
emergent	*Nelumbo nucifera* 1	5.0‰
	Nelumbo nucifera 2	0.6‰
	Nelumbo nucifera 3	6.3‰
	Phragmites adans 1	7.0‰
	Phragmites adans 2	7.4‰
	Phragmites commuis	1.9‰
catchment plants	*Graminae*	6.5‰
	Artemisia selengensis 1	4.7‰
	Artemisia selengensis 2	5.7‰
	Carex spp.	5.0‰
	Oryza sativa 1	6.1‰
	Oryza sativa 2	11.8‰
	Oryza sativa 3	3.1‰
	Zea mays 1	0.2‰
	Zea mays 2	0.5‰
	Pinaceae	0.8‰
	Unidentified	4.2‰
	Unidentified	6.1‰

8.6.2 Sediment core

Generally, $\delta^{15}N$ in the middle Yangtze floodplain lake sediments was low and varied over a small range over the last 200 years: between ~ 3‰ and 8‰ in Dongting Lake, ~ 1‰ and 5‰ in Honghu Lake, ~ 2‰ and 6‰ in Futou Lake, ~ 4‰ and 6‰ in Luhu Lake, ~ 5‰ and 7‰ in Wanghu Lake, and ~ 5‰ and 6‰

in Poyang Lake (Figure 8.9). Different from the $\delta^{13}C$ patterns, temporal and spatial variability in $\delta^{15}N$ was less coherent among the middle Yangtze floodplain lakes (Figure 8.9). One possible reason for this is that $\delta^{13}C$ was from organic matter preserved in the sediments, while $\delta^{15}N$ was from bulk sediments, which indicates that there were more potential sources of N (i.e., inorganic materials) regulating $\delta^{15}N$ in the sediments. Besides, biogeochemical processes mediating $\delta^{15}N$ were more complex compared to $\delta^{13}C$, such as primary productivity, N_2-fixing, denitrification and ammonification (Leng et al., 2006). Moreover, post sedimentation decomposition may influence the $\delta^{15}N$ footprint in lake sediments as well (Meyers and Teranes, 2001).

In the middle Yangtze floodplain area, both the source of nitrogen (i.e., agriculture, fertilizer, urbanization) and the biogeochemical processes (i.e., increasing productivity, appearance of N_2-fixing cyanobacteria) changed concurrently and coherently over the last 200 years, especially since the 1950s CE (Figure 8.9). However, N from urban and industrial sewage, agriculture, fertilizers, and atmospheric deposition are characterized by distinct $\delta^{15}N$ signature and the biogeochemical processes have different influences on $\delta^{15}N$, which may compensate or consolidate the response of sedimentary $\delta^{15}N$ (Meyers and Teranes, 2001). Taken together, these factors might confound simple directional responses of $\delta^{15}N$ in individual lakes.

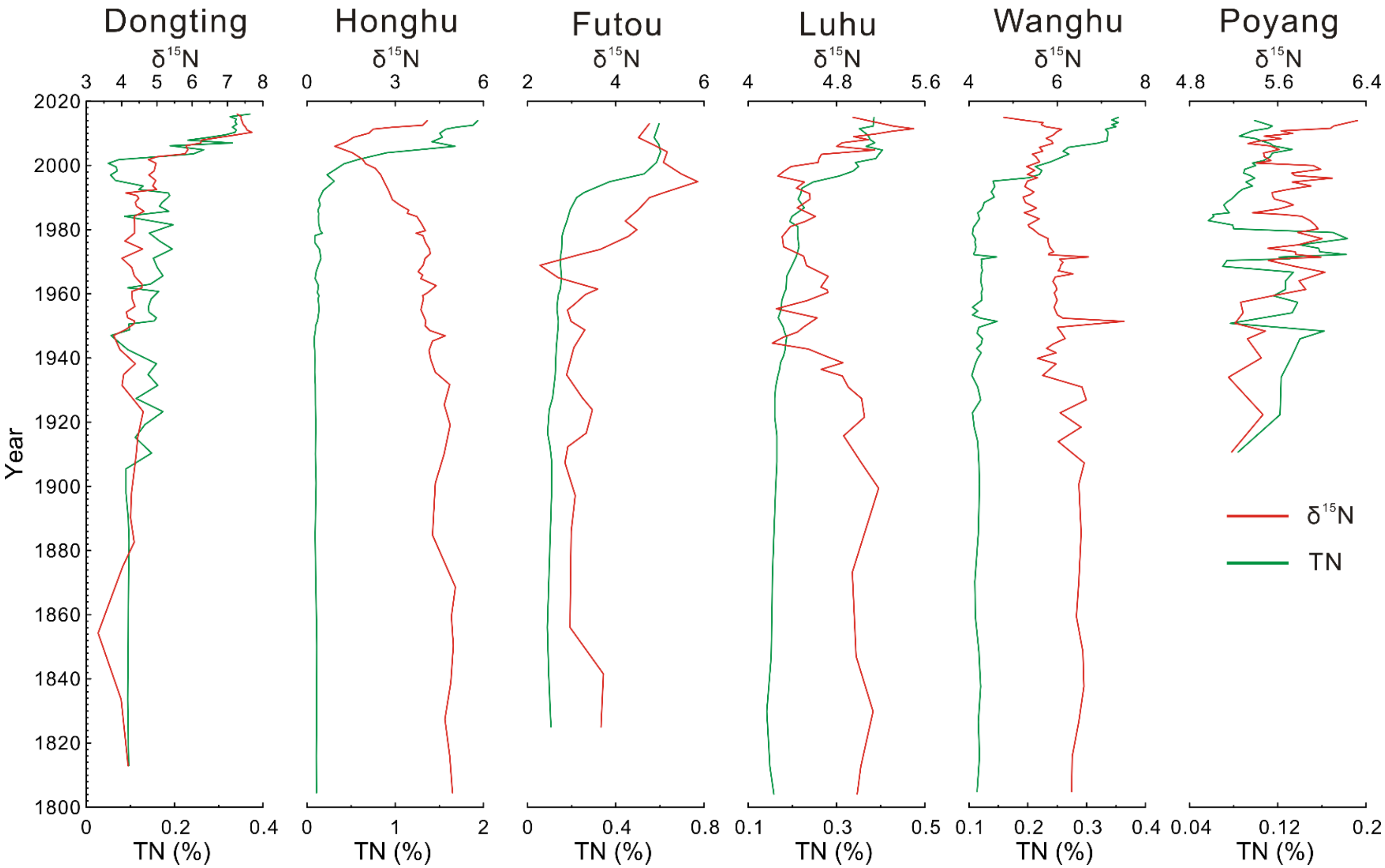

Figure 8.9 δ^{15}N of the sediment cores from the six middle Yangtze floodplain lakes since the 19th century.

Effects of urbanization/urbanization - After ~ 2000 CE $\delta^{15}N$ rapidly increased in all the lakes (Dongting, Honghu, Luhu, Wanghu and Poyang) except Futou Lake (Figure 8.10). Similarly, sedimentary TN flux in these lakes increased during this period (Figure 8.10). The increase in $\delta^{15}N$ and sedimentary TN flux was in correspondence with the exponential booming in industrialization and urbanization in the catchments (Figure 8.10). The middle Yangtze floodplain experienced exponential increases in urbanization and industrialization starting around the 1980s CE with the release of the "Reform and Opening" policy, which accelerated in the early 2000s CE (Figure 8.10a; Chapter 6). Urbanization experienced a ~ 2.5 fold increase from less than 20% to more than 50% during this period (Yang, 2013). As a result, large amounts of treated and untreated urban and industrial wastewater were exported into the lakes. Municipal wastewater produced in the Yangtze Basin increased by more than 40% from 1998 CE to 2014 CE (Wang et al., 2017). Taking Chaohu Lake in the lower Yangtze floodplain as example, ~ 45% of the nitrogen was from domestic wastewater (Wang et al., 2012). It is widely recognised that sewage from industrial and urban sources are characterized by enriched $\delta^{15}N$ (> 10‰) due to the volatilization of ammonia (Wayland and Hobson, 2001; Leavitt et al., 2006; Kendall et al., 2007). In the Qu'Appelle River catchment, Canada, lakes receiving urban sewage were characterized by enriched $\delta^{15}N$ in the sediments (Leavitt et al., 2006). Therefore, the rapid increases in $\delta^{15}N$ after ~ 2000 CE might be attributed to the contribution of municipal sewage with the intensification of urbanization and industrialization in the catchments during this period.

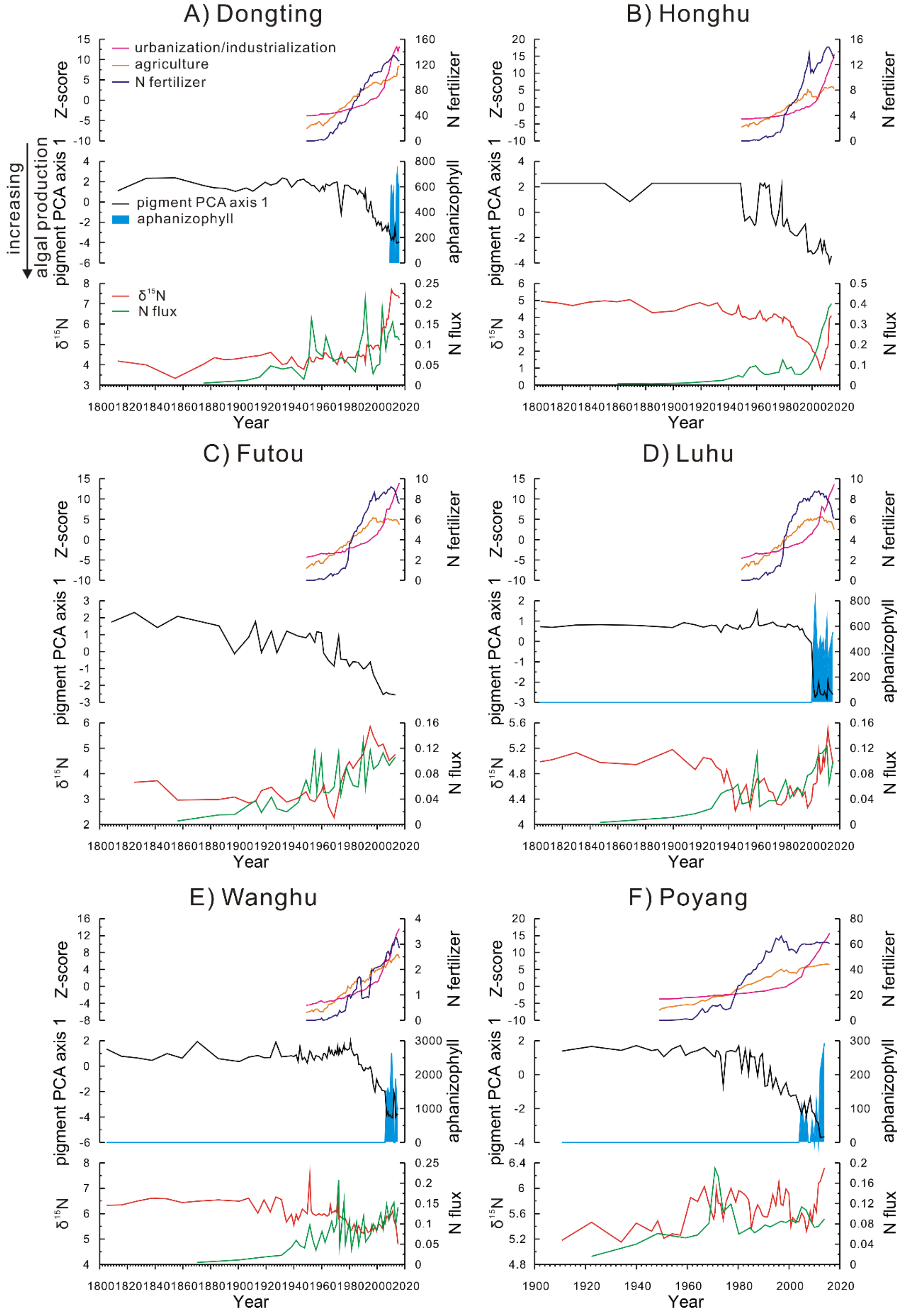

Figure 8.10 Changes in Z-score of agriculture and industrialization/industrialization and N fertilizer (unit: 10^4 tons), algal production (indicated by pigment PCA axis 1) and N_2-fixing cyanobacteria (indicated by aphanizophyll), and $\delta^{15}N$ and sedimentary TN flux of (A) Dongting, (B) Honghu, (C) Futou, (D) Luhu, (E) Wanghu and (F) Poyang Lakes over the last 200 years.

Effects of primary production - Apart from the concurrent change with urbanization and industrialization, the increase in $\delta^{15}N$ after ~ 2000 CE appeared to be synchronized with the rapid increases in algal production (indicated by the rapid decreases in sample scores on the first pigment PCA axis 1) in Dongting, Honghu, Luhu, Wanghu and Poyang Lakes (Figure 8.10A, B, D, E, F). Increasing productivity induced enrichment of $\delta^{15}N$ has been widely reported (Meyers and Teranes, 2001). Similar to carbon, algae preferentially assimilate lighter nitrogen (^{14}N), resulting in the enrichment of ^{15}N in the remaining nitrogen pool. Therefore, organic matter generated afterwards are progressively enriched in ^{15}N (Meyers and Teranes, 2001). Algal production rapidly increased in these middle Yangtze floodplain lakes with the intensification of agricultural and industrial activities as well as urbanization in the catchments, some were even suffering from HABs after ~ 2000 CE, which might be a reason of the rapid increases in $\delta^{15}N$.

Effects of N_2-fixing cyanobacteria - In Dongting, Luhu and Wanghu Lakes, $\delta^{15}N$ slightly decreased after ~ 2010 CE, which was in correspondence with the bloom of N_2-fixing cyanobacteria (indicated by the rapid increases in aphanizophyll) (Figure 8.10A, D, E). Intensive urbanization and industrialization in the catchments has resulted in the disproportionate increase of phosphorus relative to nitrogen in these lakes, which promoted the growth of N_2-fixing cyanobacteria in the lakes (Chapter 6). N_2-fixing cyanobacteria are capable of assimilating atmospheric N_2 which is depleted in $\delta^{15}N$ (~ 0‰) to supplement the deficiency in nitrogen (Schindler et al., 2008), resulting in the slight decreases in $\delta^{15}N$.

In Poyang Lake $\delta^{15}N$ continued to increase after ~ 2010s CE, although N_2-fixing cyanobacteria rapidly increased (Figure 8.10F). The average concentration of aphanizophyll after 2005 CE was ~ 80 nmol g^{-1} TOC in Poyang Lakes, which was relatively lower than that in Dongting (~ 380 nmol g^{-1} TOC), Luhu (~ 450 nmol g^{-1} TOC) and Wanghu (~ 1200 nmol g^{-1} TOC) Lakes (Chapter 5). One possible explanation of the consistent increase in $\delta^{15}N$ in Poyang Lake might be that the isotopically depleted atmospheric nitrogen fixed by cyanobacteria in Poyang might not compensate the enrichment of $\delta^{15}N$ caused by urban and industrial sewage.

Effects of agriculture – Concurrent with the increase in sedimentary TN flux, $\delta^{15}N$ gradually decreased in Honghu, Luhu and Wanghu Lakes since the ~ 1960s CE, in accordance with the increases in nitrogen fertilizer and the development of agriculture in the catchments as indicated by the increases in Z-agriculture (Figure 8.10C and F). Since the 1950s CE, N fertilizers were applied for agriculture to promote grain production and aquaculture, in order to meet the food demands of the growing population (Chapter 6). Between the 1950s CE and the 2010s CE, the usage of N fertilizer increased more than 1000-fold in the middle Yangtze floodplain (Chapter 5). Produced via industrial atmospheric N_2 fixation, synthetic fertilizers are depleted in $\delta^{15}N$ (~ 0‰) (Kendall et al., 2007). It has been widely reported that increased input of synthetic nitrogen fertilizer might cause the depletion of $\delta^{15}N$ in sediments (Wu et al., 2006; Botrel et al., 2014). Therefore, the decrease in $\delta^{15}N$ in Honghu, Luhu and Wanghu Lakes might be attributed to the direct contribution of nitrogen fertilizers.

In contrast, the increases in $\delta^{15}N$ started from the ~ 1940s CE in Futou and Poyang Lakes, which is concurrent with the intensification of agricultural in the catchments. Although nitrogen fertilizers are depleted in $\delta^{15}N$, the biogeochemical processes such as denitrification and ammonium volatilization which occur after fertilizer application cause the enrichment of $\delta^{15}N$ in soils (> 15‰) (Kendall et al., 2007). Intensive agricultural activities such as reclamation and ploughing increase the influx of catchment soil. Once leaching into the lakes, the soil from the catchment might result in the enrichment of the sediments.

8.7 Summary

With the concurrent variance in the sources of nitrogen and the biogeochemical processes, $\delta^{15}N$ varied in a small range and individually in the middle Yangtze floodplain lakes. Agriculture caused the decrease in the $\delta^{15}N$ since the 1960s CE with the direct input of synthetic fertilizers. With the intensification of urbanization and industrialization and the resultant rapid increase in algal production, $\delta^{15}N$ increased since ~ 2000 CE. Since the 2010s CE, severe eutrophication induced growth and blooming of N_2-fixing cyanobacteria caused a slight decrease in $\delta^{15}N$ in some lakes.

Chapter 9 SUMMARY

This chapter summarises the main findings of the thesis and tries to provide suggestions for the sustainable management of the water quality and ecosystem wellbeing of the Yangtze floodplain.

9.1 Responses to the aims and hypothesis

Aim 1: Investigate how and whether algae and primary producers have responded to the intensification of agricultural and industrial/urban activities in the catchments and changes in hydrological connectivity in the middle Yangtze floodplain lakes (Chapter 6).

Response: Algal production increased in the middle Yangtze floodplain lakes over the last 200 years with the intensification of human activities in the catchments, corresponding to the history of water quality degradation in this area (Liu et al., 2016; Zhang et al., 2018; Yu et al., 2019). The profound increase in algal production happened since the ~ 1940s CE in lakes with agriculturally dominant catchments (Honghu and Futou). In lakes where urbanization and industrialization dominated the catchment activities (Luhu and Wanghu), the rapid increases in algal production were later (since the ~ 1980s CE). Free hydrological connection with the Yangtze River might conceal the response of algal production in Dongting and Poyang Lakes to agricultural and industrial activities as well as urbanization in the catchments.

Nutrients overrode hydrology and acted as the fundamental factor influencing algal production and HABs in these Yangtze floodplain lakes (Liu et al., 2019). Since 2000 CE, the disproportional increase of P relative to N from urban and industrial point sources caused HABs (indicated by aphanizophyll, pigments from N_2-fixing cyanobacteria) in Dongting, Poyang, Luhu and Wanghu Lakes (sedimentary N: P ratios < 10). In lakes (Honghu and Futou) located in predominantly agricultural catchments, sedimentary N: P ratios (> 15) were high and pigments from N_2-fixing cyanobacteria were barely detected. The free hydrological conditions in the large and open Poyang and Dongting Lakes alleviated HABs directly by flushing phytoplankton out, without reshaping the algal community composition.

Aim 2: Explore how hydrological modifications caused by local dam construction and anthropogenic disturbance have influenced light penetration and ecosystem structure in the Yangtze floodplain lakes (Chapter 7).

Response: Combined with the intensification of agricultural and industrial activities and urbanization in the catchments, hydrological connection with the main channel played an important role in regulating the light and nutrient conditions and ecosystem structure in the middle Yangtze floodplain lakes (Junk et al., Chen et al., 2016). The highly variable water level fluctuations in hydrologically open lakes resulted in variable UVR penetration. Local dam construction which stabilized the water level and blocked the transport of suspended particles from the Yangtze main channel enhanced light penetration and stimulated the growth and development of macrophytes (Zeng et al., 2018). With the increase of algal production due to the intensification of human activities in the catchments, under water light condition gradually deteriorated in all the lakes since the 1990s CE. The severely polluted and hydrologically restricted drainage lakes (Luhu and Wanghu) gradually shifted from macrophyte-dominated clear water state into algal dominated turbid state, as reported in other lakes in this area (Dong et al., 2016). The less polluted Honghu and Futou Lakes were in earlier stages of eutrophication, characterized by high coverage of macrophytes. The free hydrological connection with the main channel alleviated the symptoms of eutrophication in Dongting and Poyang Lakes.

Aim 3: Understand long term (~ 200 years) dynamics of organic matter cycling in large river-floodplain systems undergoing hydrological modification and receiving human emitted pollutants.

Response: Before intensive human disturbance, sedimentary organic matter in these Yangtze floodplain lakes originated from various sources including allochthonous land plants and catchment soils, emergent and floating plants, submerged plants and algae. After ~ the 1980s CE, organic matter buried in different lakes were from different sources, depending on the state of the lakes. Autochthonous algae was the main source of organic matter in severely polluted lakes suffering from HABs, whereas submerged macrophytes made a large contribution to the organic matter in lakes (Honghu and Futou) which were less polluted and in a clear water state. Concurrently, the contribution of allochthonous terrestrial organic matter gradually increased.

9.2 Conceptual model of the response of lake ecosystem to human activities in the middle Yangtze floodplain

Different from floodplain lakes in relatively undisturbed areas where hydrology regulates both light (via suspended particles) and nutrient availability as the main channel is the main source of both suspended particles and nutrients (Figure 2.6a), light and nutrient availability in lakes in the middle Yangtze floodplain are influenced by hydrology (suspended particles from Yangtze River) and agricultural and industrial/urban activities (anthropogenic nutrients) in the catchments, respectively. Before intensive human disturbance when the lakes were freely connected with the Yangtze River and agricultural and indusial activities and urbanization were less intensive, nutrient loading into the lakes were low and light conditions were variable due to the highly variable water level fluctuations and high supply of suspended particles (Figure 9.1). During this period, lakes in the middle Yangtze floodplain were characterized by low algal production and low to intermediate coverage of macrophytes. With the gradual intensification of human activities in the catchments, hydrologically open lakes and lakes with local dam construction showed different responses to human disturbance.

Open lakes – With the intensification of human activities (e.g., land reclamation, agriculture, urbanizaiton, industrialization) in the catchments, nutrient loadings into the lakes increased. As a result, algal production, including some potentially bloom-forming cyanobacteria, rapidly increased in the lakes since the 1980s CE with the intensification of urbanization and industrialization. The increase in algal production enhanced the attenuation of light in the water column, causing low UV irradiance at the bottom of the lakes. As the lakes are freely connected with the Yangtze River, the periodic water exchange with the Yangtze River continuously flushed nutrients and algae out. During this period, the lakes were in the early stage of eutrophication, characterized by a moderate coverage of macrophytes.

Lakes with local dam – The installation of local dams blocked the interaction between the lakes and the Yangtze River, which stabilized the hydrological conditions and reduced the concentrations of suspended particle concentrations in the lakes. Consequently, light availability at the bottom of the lakes increased, promoted the development and growth of benthic communities. With the intensification of human activities in the catchments, nutrient loading into the lakes increased. Lakes with agricultural catchments were less polluted and were in the early state of eutrophication. In urban and industrial areas, lakes were severely polluted. In combination with the prolonged water retention times after local dam construction, increasing concentrations of nutrients were retained in the lakes, resulting in the abrupt increase of algal production. As a result, water clarity decreased, which suppressed the growth of benthic communities and changed the lakes into an algal-dominated turbid state.

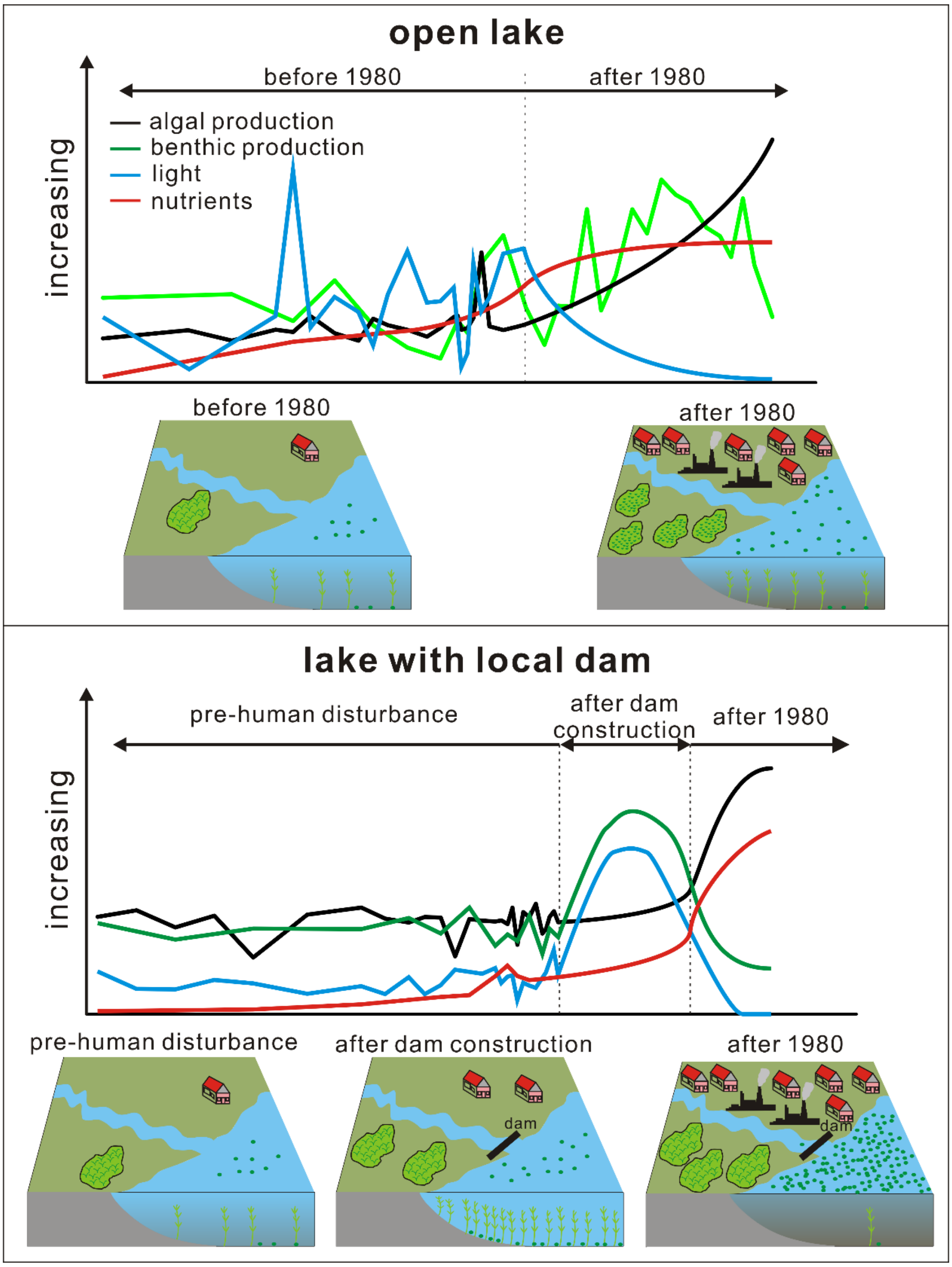

Figure 9.1 Conceptual model showing the variation of human activities in the catchment and the response of lake ecosystems in the middle Yangtze floodplain.

9.3 Contribution of this study

9.3.1 Timing and causes of water degradation and HABs in the middle Yangtze floodplain

By using palaeolimnological proxies including chlorophyll and carotenoid pigments, chironomids, C/N ratios, $\delta^{13}C$ and $\delta^{15}N$, this thesis deciphered the history of water quality degradation and ecosystem evolution in the middle Yangtze floodplain lakes since ~ 1800s CE. Consistent with previous evidence (Zhang et al., 2018; Yu et al., 2019), this study reinforced the two key dates in water degradation in the middle Yangtze floodplain depending on the catchment characteristics. In agricultural areas major increases in algal production started from ~ the late 1940s CE with the increase in nitrogen loading from agricultural activities in the catchments (Zhang et al., 2006; Chen et al., 2011). In lakes dominanted by urban/industrial activities in the catchments, it was not until ~ the 1980s CE that algal production started to increase, attributed to the increase in P loading from urban and industrial sources (Zhang et al., 2018). After 2000 CE, the disproportional increase of P relative to N caused HABs in some of the lakes (Dongting, Luhu, Wanghu and Poyang).

9.3.2 Local dam construction on Yangtze floodplain lake ecosystem

Palaeolimnological evidence from this thesis suggests that local dam construction which blocked the transportation of suspended particles and stabilized the hydrological conditions might improve water clarity and promote benthic communities provided that nutrient conditions are low (Liu et al., 2012). This may buffer against a lake shift into an algal-dominated state caused by eutrophication (Zeng et al., 2018). Under high nutrient conditions, local dam construction, which prolongs water retention times and reduces water exchange ratios in lakes, might amplify the symptoms of eutrophication and accelerat the aquatic stable state transition into an algal dominated turbid states (Chen et al., 2016; Dong et al., 2016). In contrast, free hydrological connectivity appears to conceal the side effects caused by eutrophication, such as HABs, by diluting the nutrient-rich lake water with the less polluted Yangtze River waters and flushing algae out of the lakes before forming blooms (Hu et al., 2010; Paerl et al., 2012).

9.3.3 History of water clarity in the Yangtze floodplain

This thesis is the first piece of work to investigate changes in underwater light conditions after local dam construction and during aquatic stable state transitions in the middle Yangtze floodplain by using the UVR index calculated with UVR-absorbing compounds produced by benthic algae. Light conditions varied widely in hydrologically open lakes which freely connected with the Yangtze main channel when human activities were less intensive in the catchments. In hydrologically closed drainage lakes, light conditions improved after local dam construction blocked the transportation of suspended particles from the main channel and stabilized the water level. As more and more nutrients were transported into the lakes with the intensification of agricultural and industrial activities as well as urbanization, the rapid growth and development of phytoplankton blocked the penetration of UV radiation, which shaded out the benthic algae.

9.3.4 Influence of algal production on $\delta^{13}C$ in shallow lakes

This thesis provides new insights into the variation of sedimentary $\delta^{13}C$ during aquatic stable state transitions in shallow floodplain lakes. Different from evidence from deep lakes which suggests that increasing algal production results in the increase in $\delta^{13}C$ (Meyers and Teranes, 2001; Leng et al., 2006), $\delta^{13}C$ decreases with nutrient induced increases in algal production. This is because submerged macrophytes which have higher $\delta^{13}C$ than phytoplankton species are an important source of organic matter in shallow lakes (Brenner et al., 2006).

According to the aquatic stable state, the increase in algal production is accompanied by the decrease in submerged macrophytes (Scheffer et al., 1993), resulting in the decreases in $\delta^{13}C$ with increases in algal production.

9.4 Future work

Based on palaeolimnological proxies preserved in the sediments, this thesis uncovered the history of water degradation on six large lake ecosystems in the middle Yangtze floodplain. Limnological studies comparing the suspended particle concentrations, turbidity, algal production and community composition between hydrological open and dammed lakes during the flooding and non-flooding seasons using sediment traps would aid and boost the solidity of the interpretation of sedimentary proxies.

As for sedimentary proxies, chironomids were used to reveal the changes in aquatic plants indirectly in this thesis. Further study on the macrofossil and pollen preserved in the sediments would give a direct glimpse of the variation in aquatic plants during ecosystem evolution. For the interpretation of isotopes in the sediment cores, catchment survey on aquatic plants, catchments plants were analysed in this thesis, whereas C/N ratios and $\delta^{13}C$ of algae were based on the work of Meyers and Teranes (2001). Future studies incorporating the isotopic signature of algae would make the explanation more reliable

9.5 Implications for water management

9.5.1 Nutrient loading control

Acting as one of the country's most important water resources, it is vital to scientifically and effectively protect and manage the water resources in the

Yangtze floodplain for sustainable development purposes (Yu et al., 2019). As reported in previous studies (Liu et al., 2016; Yu et al., 2019), palaeolimnological evidence from this thesis indicates that nutrients (mainly nitrogen and phosphorus) from human activities in the catchments were the primary causes of water quality and lake ecosystem degradation. In particular, pollutants from urban and industrial sources appears to cause the disproportional increase of P to N, and therefore blooms of toxic cyanobacteria in the lakes (Paerl et al., 2012). Therefore, it is important to control the nutrient loading from urban and industrial point sources (Edmondson, 1970; Heather et al., 2018). It has been reported that ~ 80% of environmental degradation was caused by small-scale enterprises which cannot afford wastewater treatment facilities and dispose of wastes directly into the environment in China (Wang, 1997), so an effective way is required to regulate these small-scale factories (Le et al., 2010). Building more wastewater treatment plants and promoting wastewater treatment efficiency are also ideal solutions to reduce the nutrient loading from urban and industrial sewage (Le et al., 2010; Yu et al., 2019). Nutrient loading from agriculturally diffuse sources is another trigger of water degradation in the middle Yangtze floodplain. Over application of synthetic fertilizers and low nutrient recycling rate are the main reason that nutrients are over saturated in soils (Yu et al., 2019). Therefore, it is important to reduce the application of synthetic fertilizers and to promote nutrient cycling efficiency to reduce nutrient loading from diffuse agricultural sources.

Apart from controlling external nutrient loading, measures to regulate internal nutrient loading from sediments are also necessary (Søndergaard et al., 2003). Except for those being flushed out, external P loading is retained and deposited in lakes (Vollenweider, 1976). In these severely eutrophic Yangtze floodplain lakes, large quantities of external nutrient loading are deposited in the lakes (Ding et al., 2019), which may be released and recycled in the water column with the influence of post depositional processes such as resuspension and redox (Søndergaard et al., 2003).

9.5.2 Free hydrological connection

Sedimentary evidence shows that free hydrological connection with the Yangtze main channel might conceal the side effects of increasing nutrient loading and alleviate the symptoms of eutrophication in the Yangtze floodplain lakes (Paerl et al., 2012). Currently, lakes in the middle Yangtze floodplain are over saturated with nutrients from human activities (Yang et al., 2008). Free hydrological connection with the Yangtze main channel can dilute the nutrient rich lake water with less eutrophic water from the Yangtze River (Paerl et al., 2012). Moreover, the high water flushing rates in hydrologically open lakes can consistently export nutrients and algae out of the lake to prevent bloom formation in the lakes. In Taihu Lake at the lower Yangtze floodplain, water has been transferred from the Yangtze River to alleviate eutrophication (Hu et al., 2010). Therefore, maintaining the free hydrological connection with the Yangtze main channel is a useful strategy to restore the water quality in floodplain lakes (Chen et al., 2016).

REFERENCES

Aldhous, P. (2003). The world's forgotten crisis. *Nature*, 422, 251-251.

Appleby, P.G., (2001). Chronostratigraphic Techniques in Recent Sediments. *In*: Last, W.M., Smol, J.P. (eds.), *Tracking Environmental Change Using Lake Sediments: Basin Analysis, Coring, and Chronological Techniques*. Dordrecht, Springer Netherlands, pp. 171-203.

Appleby, P.G., Oldfield, F. (1978). The calculation of lead-210 dates assuming a constant rate of supply of unsupported ^{210}Pb to the sediment. *CATENA*, 5, 1-8.

Armitage, P., (1997). The Chironomidae. Biology and ecology of non-biting midges. Reprinted. London: Chapman & Hall.

Attygalla, N.W., Baldwin, D.S., Silvester, E., Kappen, P., Whitworth, K.L. (2016). The severity of sediment desiccation affects the adsorption characteristics and speciation of phosphorus. *Environmental Science: Processes & Impacts*, 18, 64-71.

Barros, N., Cole, J.J., Tranvik, L.J., Prairie, Y.T., Bastviken, D., Huszar, V.L.M., del Giorgio, P., Roland, F. (2011). Carbon emission from hydroelectric reservoirs linked to reservoir age and latitude. *Nature Geoscience*, 4, 593-596.

Battarbee, R.W., Anderson, N.J., Bennion, H., Simpson, G.L. (2012). Combining limnological and palaeolimnological data to disentangle the effects of nutrient pollution and climate change on lake ecosystems: problems and potential. *Freshwater Biology*, 57, 2091-2106.

Battarbee, R.W., Jones, V.J., Flower, R.J., Cameron, N.G., Bennion, H., Carvalho, L., Juggins, S. (2001). Diatoms, in: Smol, J.P., Birks, H.J.B., Last, W.M., Bradley, R.S., Alverson, K. (Eds.), Tracking Environmental Change Using Lake Sediments: Terrestrial, Algal, and Siliceous Indicators. Springer Netherlands, Dordrecht, pp. 155-202.

Battarbee, R.W., Monteith, D.T., Juggins, S., Evans, C.D., Jenkins, A., Simpson, G.L. (2005). Reconstructing pre-acidification pH for an acidified Scottish loch: A comparison of palaeolimnological and modelling approaches. *Environmental Pollution*, 137, 135-149.

Bayley, P.B. (1995). Understanding Large River: Floodplain Ecosystems. *BioScience*, 45, 153-158.

Bell, B.A., Fletcher, W.J., Ryan, P., Seddon, A.W., Wogelius, R.A., Ilmen, R. (2018). UV-B-absorbing compounds in modern Cedrus atlantica pollen: The potential for a summer UV-B proxy for Northwest Africa. *The Holocene*, 28, 1382-1394.

Bennett, K.D. (1996). Determination of the number of zones in a biostratigraphical sequence. *New Phytologist*, 132, 155-170.

Bennion, H., Battarbee, R.W., Sayer, C.D., Simpson, G.L., Davidson, T.A. (2011). Defining reference conditions and restoration targets for lake ecosystems using palaeolimnology: a synthesis. *Journal of Paleolimnology*, 45, 533-544.

Bennion, H., Juggins, S., Anderson, N.J. (1996). Predicting epilimnetic phosphorus concentrations using an improved diatom-based transfer function and its application to lake eutrophication management. *Environmental Science & Technology*, 30, 2004-2007.

Birks, H.J.B. (1974). Numerical zonations of flandrian pollen data. *New Phytologist*, 73, 351-358.

Birks, H.J.B., Gordon, A.D. (1985). Numerical methods in Quaternary pollen analysis.

Blindow, I., Andersson, G., Hargeby, A., Johansson, S. (1993). Long-term pattern of alternative stable states in two shallow eutrophic lakes. *Freshwater Biology*, 30, 159-167.

Blokker, P., Yeloff, D., Boelen, P., Broekman, R.A., Rozema, J. (2005). Development of a Proxy for Past Surface UV-B Irradiation: A Thermally Assisted Hydrolysis and Methylation py-GC/MS Method for the Analysis of Pollen and Spores. *Analytical Chemistry*, 77, 6026-6031.

Blomqvist, P., Pettersson, A., Hyenstrand, P. (1994). Ammonium nitrogen - a key regulatory factor causing dominance of non-nitrogen-fixing cyanobacteria in aquatic systems. *Archiv für Hydrobiologie*, 132, 141-164.

Borcard, D., Gillet, F., Legendre, P. (2018). Numerical ecology with R. Springer.

Botrel, M., Gregory-Eaves, I., Maranger, R. (2014) Defining drivers of nitrogen stable isotopes ($\delta^{15}N$) of surface sediments in temperate lakes. *Journal of Paleolimnology*, 52, 419-433.

Brenner, M., Hodell, D.A., Leyden, B.W., Curtis, J.H., Kenney, W.F., Gu, B., Newman, J.M. (2006). Mechanisms for organic matter and phosphorus burial in sediments of a shallow, subtropical, macrophyte-dominated Lake. *Journal of Paleolimnology*, 35, 129-148.

Brodersen, K.P., Odgaard, B.V., Vestergaard, O., Anderson, N.J. (2001). Chironomid stratigraphy in the shallow and eutrophic Lake Søbygaard, Denmark: chironomid–macrophyte co-occurrence. *Freshwater Biology*, 46, 253-267.

Brodersen, K.P., Quinlan, R. (2006). Midges as palaeoindicators of lake productivity, eutrophication and hypolimnetic oxygen. *Quaternary Science Reviews*, 25, 1995-2012.

Brooks, S.J., Langdon, P.G., Heiri, O. (2007). *The identification and use of Palaearctic Chironomidae larvae in palaeoecology*. Quaternary Research Association.

Bryant, D.A., Frigaard, N.U. (2006). Prokaryotic photosynthesis and phototrophy illuminated. *Trends in Microbiology*, 14, 488-496.

Bucak, T., SaraoĞLu, E. C. E., LEVİ, E. E., Nihan Tavşanoğlu, Ü., Idil Çakiroğlu, A., Jeppesen, E., & BEKLİOĞLU, M. (2012). The influence of water level on macrophyte growth and trophic interactions in eutrophic Mediterranean shallow lakes: a mesocosm experiment with and without fish. *Freshwater Biology*, 57, 1631-1642.

Bunting, L., Leavitt, P.R., Gibson, C.E., McGee, E.J., Hall, V.A. (2007). Degradation of water quality in Lough Neagh, Northern Ireland, by diffuse nitrogen flux from a phosphorus-rich catchment. *Limnology and Oceanography*, 52, 354-369.

Bunting, L., Leavitt, P.R., Simpson, G.L., Wissel, B., Laird, K.R., Cumming, B.F., St. Amand, A., Engstrom, D.R. (2016). Increased variability and sudden ecosystem state change in Lake Winnipeg, Canada, caused by 20th century agriculture. *Limnology and Oceanography*, 61, 2090-2107.

Burden, E.T., McAndrews, J.H., Norris, G. (1986). Palynology of Indian and European forest clearance and farming in lake sediment cores from Awenda Provincial Park, Ontario. *Canadian Journal of Earth Sciences,* 23, 43-54.

Burger, D., Hamilton, D., Pilditch, C., Gibbs, M., (2007). Benthic nutrient fluxes in a eutrophic, polymictic lake, Shallow Lakes in a Changing World. Springer, pp. 13-25.

Burson, A., Stomp, M., Greenwell, E., Grosse, J., Huisman, J. (2018). Competition for nutrients and light: testing advances in resource competition with a natural phytoplankton community. *Ecology*, 99, 1108-1118.

Cantonati, M., Guella, G., Komárek, J., Spitale, D. (2014). Depth distribution of epilithic cyanobacteria and pigments in a mountain lake characterized by marked water-level fluctuations. *Freshwater Science*, 33, 537-547.

Cao, Y., Zhang, E., Cheng, G. (2014). A primary study on relationships between subfossil chironomids and the distribution of aquatic macrophytes in three lowland floodplain lakes, China. *Aquatic Ecology*, 48, 481-492.

Cao, Y., Zhang, E., Langdon, P.G., Liu, E., Shen, J. (2014). Chironomid-inferred environmental change over the past 1400 years in the shallow, eutrophic Taibai Lake (south-east China): Separating impacts of climate and human activity. *The Holocene*, 24, 581-590.

Capo, E., Debroas, D., Arnaud, F., Perga, M.-E., Chardon, C., Domaizon, I. (2017). Tracking a century of changes in microbial eukaryotic diversity in lakes driven by nutrient enrichment and climate warming. *Environmental Microbiology*, 19, 2873-2892.

Catalán, N., Marcé, R., Kothawala, D.N., Tranvik, L.J. (2016). Organic carbon decomposition rates controlled by water retention time across inland waters. *Nature Geoscience*, 9, 501.

Chatterjee, S., Hadi, A., Price, B. (2006). Simple linear regression. *In*: *Regression analysis by example*, 21-51.

Changjiang Water Resources Commission of the Ministry of Water Resources. (2006 – 2017). Bulletin of the Yangtze River sediments [Online]. Available: http://www.cjw.gov.cn/zwzc/bmgb/ [Accessed 2017].

Chen, N., Bianchi, T. S., Mckee, B. A. and Bland, J. M. (2001). Historical trends of hypoxia on the Louisiana shelf: application of pigments as biomarkers. *Organic Geochemistry*, 32, 543-561.

Chen, Q., Shi, W., Huisman, J., Maberly, S.C., Zhang, J., Yu, J., Chen, Y., Tonina, D., Yi, Q. (2020). Hydropower reservoirs on the upper Mekong River modify nutrient bioavailability downstream. *National Science Review*.

Chen, X., McGowan, S., Xu, L., Zeng, L., Yang, X. (2016). Effects of hydrological regulation and anthropogenic pollutants on Dongting Lake in the Yangtze floodplain. *Ecohydrology*, 9, 315-325.

Chen, X., McGowan, S., Zeng, L., Xu, L., Yang, X. (2017). Changes in carbon and nitrogen cycling in a floodplain lake over recent decades linked to littoral expansion, declining riverine influx, and eutrophication. *Hydrological Processes*, 31, 3110-3121.

Chen, X., Qiao, Q., McGowan, S., Zeng, L., Stevenson, M.A., Xu, L., Huang, C., Liang, J., Cao, Y. (2019). Determination of geochronology and sedimentation rates of shallow lakes in the middle Yangtze reaches using ^{210}Pb, ^{137}Cs and spheroidal carbonaceous particles. *CATENA*, 174, 546-556.

Chen, X., Yang, X., Dong, X., Liu, Q. (2011). Nutrient dynamics linked to hydrological condition and anthropogenic nutrient loading in Chaohu Lake (southeast China). *Hydrobiologia*, 661, 223-234.

Chen, Z., Li, J., Shen, H., Zhanghua, W. (2001). Yangtze River of China: historical analysis of discharge variability and sediment flux. *Geomorphology*, 41, 77-91.

Chislock, M.F., Doster, E., Zitomer, R.A., Wilson, A. (2013). Eutrophication: causes, consequences, and controls in aquatic ecosystems. *Nature Education Knowledge*, 4, 10.

Committee of Hubei Rural Statistical Yearbook. (2017). Hubei Rural Statistical Yearbook 2017. Beijing, China Statistics Press.

Conley, D.J., Paerl, H.W., Howarth, R.W., Boesch, D.F., Seitzinger, S.P., Havens, K.E., Lancelot, C., Likens, G.E. (2009). Controlling Eutrophication: Nitrogen and Phosphorus. *Science*, 323, 1014-1015.

Coops, H., Beklioglu, M., Crisman, T.L. (2003). The role of water-level fluctuations in shallow lake ecosystems-workshop conclusions. *Hydrobiologia*, 506, 23-27.

Cranston, P.S. (1995). The Chironomidae. The biology and ecology of non-biting midges. *Biogeography*, 62-84.

Cross, I.D., McGowan, S., Needham, T., Pointer, C.M. (2014). The effects of hydrological extremes on former gravel pit lake ecology: management implications. *Fundamental and Applied Limnology/Archiv für Hydrobiologie*, 185, 71-90.

Dai, S.B., Yang, S.-L., Zhu, J., Gao, A., Li, P. (2005). The role of Lake Dongting in regulating the sediment budget of the Yangtze River. *Hydrology and Earth System Sciences Discussions*, 9, 692-698.

Davidson, T.A., Bennion, H., Jeppesen, E., Clarke, G.H., Sayer, C.D., Morley, D., Odgaard, B.V., Rasmussen, P., Rawcliffe, R., Salgado, J., Simpson, G.L., Amsinck, S.L. (2011). The role of cladocerans in tracking long-term change in shallow lake trophic status. *Hydrobiologia*, 676, 299.

Dearing, J.A., Yang, X., Dong, X., Zhang, E., Chen, X., Langdon, P.G., Zhang, K., Zhang, W., Dawson, T.P. (2012). Extending the timescale and range of ecosystem services through paleoenvironmental analyses, exemplified in the lower Yangtze basin. *Proceedings of the National Academy of Sciences*, 109, E1111-E1120.

Deng, J., Cai, Y., Chen, Y., Zhang, L. (2010). Structure of phytoplankton community and its relationship with environment factors in Lake Honghu. *Journal of Lake Science*, 22, 70-78.

Desonie, D. Earth's Fresh Water. *In*: CK-12 Earth Science for High School [Online]. Available: https://www.ck12.org/book/ck-12-earth-science-concepts-for-high-school/section/16.6/ [Accessed 2020].

DeVore, G.R. (2017). Computing the Z score and centiles for cross-sectional analysis: a practical approach. *Journal of Ultrasound in Medicine*, 36, 459-473.

Ding, Y., Xu, H., Deng, J., Qin, B., He, Y. (2019). Impact of nutrient loading on phytoplankton: A mesocosm experiment in the eutrophic Lake Taihu, China. *Hydrobiologia*, 829, 167-187.

Dixit, A.S., Hall, R.I., Leavitt, P.R., Quinlan, R., Smol, J.P. (2000). Effects of sequential depositional basins on lake response to urban and agricultural pollution: a palaeoecological analysis of the Qu'Appelle Valley, Saskatchewan, Canada. *Freshwater Biology*, 43, 319-337.

Donald, D.B., Bogard, M.J., Finlay, K., Leavitt, P.R. (2011). Comparative effects of urea, ammonium, and nitrate on phytoplankton abundance, community composition, and toxicity in hypereutrophic freshwaters. *Limnology and Oceanography*, 56, 2161-2175.

Dong, X., Anderson, N.J., Yang, X., chen, X., Shen, J. (2012). Carbon burial by shallow lakes on the Yangtze floodplain and its relevance to regional carbon sequestration. *Global Change Biology*, 18, 2205-2217.

Dong, X., Bennion, H., Maberly, S.C., Sayer, C.D., Simpson, G.L., Battarbee, R.W. (2012). Nutrients exert a stronger control than climate on recent diatom communities in Esthwaite Water: evidence from monitoring and palaeolimnological records. *Freshwater Biology*, 57, 2044-2056.

Dong, X., Yang, X., Chen, X., Liu, Q., Yao, M., Wang, R., Xu, M. (2016). Using sedimentary diatoms to identify reference conditions and historical variability in shallow lake ecosystems in the Yangtze floodplain. *Marine and Freshwater Research*, 67, 803-815.

Downing, J.A., Cole, J.J., Middelburg, J.J., Striegl, R.G., Duarte, C.M., Kortelainen, P., Prairie, Y.T., Laube, K.A. (2008). Sediment organic carbon burial in agriculturally eutrophic impoundments over the last century. *Global Biogeochemical Cycles*, 22.

Downing, J.A., Watson, S.B., McCauley, E. (2001). Predicting Cyanobacteria dominance in lakes. *Canadian Journal of Fisheries and Aquatic Sciences*, 58, 1905-1908.

Du, Y., Cai, S., Zhang, X., Zhao, Y. (2001). Interpretation of the environmental change of Dongting Lake, middle reach of Yangtze River, China, by 210Pb measurement and satellite image analysis. *Geomorphology*, 41, 171-181.

Du, Y., Xue, H., Wu, S., Ling, F., Xiao, F., Wei, X. (2011). Lake area changes in the middle Yangtze region of China over the 20th century. *Journal of Environmental Management*, 92, 1248-1255.

Duan, S., Kaushal, S.S., Groffman, P.M., Band, L.E., Belt, K.T. (2012). Phosphorus export across an urban to rural gradient in the Chesapeake Bay watershed. *Journal of Geophysical Research: Biogeosciences*, 117.

Duong, T.T., Nguyen, H.Y., Le, T.P.Q., Nguyen, T.K., Tran, T.T.H., Le, N.D., Dang, D.K., Vu, T.N., Panizzo, V. (2019). Transitions in diatom assemblages and pigments through dry and wet season conditions in the Red River, Hanoi (Vietnam). *Plant Ecology and Evolution*, 152, 163-177.

Edmondson, W.T. (1970). Phosphorus, Nitrogen, and Algae in Lake Washington after Diversion of Sewage. *Science*, 169, 690-691.

Eggermont, H., Heiri, O. (2012). The chironomid-temperature relationship: expression in nature and palaeoenvironmental implications. *Biological Reviews*, 87, 430-456.

Ehleringer, J.R., Buchmann, N., Flanagan, L.B. (2000). Carbon isotope ratios in belowground carbon cycle processes. *Ecological Applications*, 10, 412-422.

Elliott, J.A. (2010). The seasonal sensitivity of Cyanobacteria and other phytoplankton to changes in flushing rate and water temperature. *Global Change Biology*, 16, 864-876.

Elser, J.J., Bracken, M.E.S., Cleland, E.E., Gruner, D.S., Harpole, W.S., Hillebrand, H., Ngai, J.T., Seabloom, E.W., Shurin, J.B., Smith, J.E. (2007). Global analysis of nitrogen and phosphorus limitation of primary producers in freshwater, marine and terrestrial ecosystems. *Ecology Letters*, 10, 1135-1142.

Engels, S., Cwynar, L.C. (2011). Changes in fossil chironomid remains along a depth gradient: evidence for common faunal thresholds within lakes. *Hydrobiologia*, 665, 15-38.

Engstrom, D.R., Fritz, S.C., Almendinger, J.E., Juggins, S. (2000). Chemical and biological trends during lake evolution in recently deglaciated terrain. *Nature*, 408, 161-166.

Entwistle, N.S., Heritage, G.L., Schofield, L.A., Williamson, R.J. (2019). Recent changes to floodplain character and functionality in England. *CATENA*, 174, 490-498.

Ersoy, Z., Scharfenberger, U., Baho, D.L., Bucak, T., Feldmann, T., Hejzlar, J., Levi, E.E., Mahdy, A., Nõges, T., Papastergiadou, E., Stefanidis, K., Šorf, M., Søndergaard, M., Trigal, C., Jeppesen, E., Beklioğlu, M. (2020). Impact of nutrients and water level changes on submerged macrophytes along a temperature gradient: a Pan-European mesocosm experiment. *Global Change Biology*, Published online.

Ezcurra, E., Barrios, E., Ezcurra, P., Ezcurra, A., Vanderplank, S., Vidal, O., Villanueva-Almanza, L., Aburto-Oropeza, O. (2019). A natural experiment reveals the impact of hydroelectric dams on the estuaries of tropical rivers. *Science Advances,* 5, eaau9875.

Falkowski, P., Scholes, R.J., Boyle, E., Canadell, J., Canfield, D., Elser, J., Gruber, N., Hibbard, K., Högberg, P., Linder, S., Mackenzie, F.T., Moore III, B., Pedersen, T., Rosenthal, Y., Seitzinger, S., Smetacek, V., Steffen, W. (2000). The Global Carbon Cycle: A Test of Our Knowledge of Earth as a System. *Science*, 290, 291-296.

Falkowski, P.G., Raven, J.A. (2013). Aquatic photosynthesis. Princeton University Press.

Fang, J., Wang, Z., Zhao, S., Li, Y., Tang, Z., Yu, D., Ni, L., Liu, H., Xie, P., Da, L., Li, Z., Zheng, C. (2006). Biodiversity changes in the lakes of the Central Yangtze. *Frontiers in Ecology and the Environment*, 4, 369-377.

Feng, L., Hu, C., Chen, X., Zhao, X. (2013). Dramatic Inundation Changes of China's Two Largest Freshwater Lakes Linked to the Three Gorges Dam. *Environmental Science & Technology*, 47, 9628-9634.

Fernandez, E., Galvan, A. (2007). Inorganic nitrogen assimilation in Chlamydomonas. *Journal of Experimental Botany*, 58, 2279-2287.

Foster, I., Greenwood, M.T. (2016). Linking the past to the present: the use of palaeoenvironmental data for establishing reference conditions for the Water Framework Directive, in: Gilvear, D. J., Greenwood, M. T., Thoms, M. C. and Wood, P. J. (Eds.), River Science: Research and Management for the 21st Century. Chichester: John Wiley. pp. 61-83.

Francis, D.R., Kane, T.C. (1995). Effect of Substrate on Colonization of Experimental Ponds by Chironomidae (Diptera). *Journal of Freshwater Ecology*, 10, 57-63.

Fritz, S., Juggins, S., Battarbee, R., Engstrom, D. (1991). Reconstruction of past changes in salinity and climate using a diatom-based transfer function. *Nature*, 352, 706.

Galloway, J.N., Townsend, A.R., Erisman, J.W., Bekunda, M., Cai, Z., Freney, J.R., Martinelli, L.A., Seitzinger, S.P., Sutton, M.A. (2008). Transformation of the Nitrogen Cycle: Recent Trends, Questions, and Potential Solutions. *Science*, 320, 889-892.

Gälman, V., Rydberg, J., de-Luna, S.S., Bindler, R., Renberg, I. (2008). Carbon and nitrogen loss rates during aging of lake sediment: Changes over 27 years studied in varved lake sediment. *Limnology and Oceanography*, 53, 1076-1082.

Gao, C., Zhang, T. (2010). Eutrophication in a Chinese Context: Understanding Various Physical and Socio-Economic Aspects. *AMBIO: A Journal of the Human Environment*, 39, 385-393.

Gao, J.H., Jia, J., Kettner, A.J., Xing, F., Wang, Y.P., Xu, X.N., Yang, Y., Zou, X.Q., Gao, S., Qi, S., Liao, F. (2014). Changes in water and sediment exchange between the Changjiang River and Poyang Lake under natural and anthropogenic conditions, China. *Science of the Total Environment*, 481, 542-553.

Gibbs, M., Özkundakci, D. (2011). Effects of a modified zeolite on P and N processes and fluxes across the lake sediment–water interface using core incubations. *Hydrobiologia*, 661, 21-35.

Gilbert, R.O. (1987). Statistical methods for environmental pollution monitoring. John Wiley & Sons.

Glibert, P.M., Harrison, J., Heil, C., Seitzinger, S. (2006). Escalating worldwide use of urea-a global change contributing to coastal eutrophication. *Biogeochemistry*, 77, 441-463.

Glibert, P.M., Wilkerson, F.P., Dugdale, R.C., Raven, J.A., Dupont, C.L., Leavitt, P.R., Parker, A.E., Burkholder, J.M., Kana, T.M. (2016). Pluses and minuses of ammonium and nitrate uptake and assimilation by phytoplankton and implications for productivity and community composition, with emphasis on nitrogen-enriched conditions. *Limnology and Oceanography*, 61, 165-197.

Goericke, R. (1994) Physiology of isotopic fractionation in algae and cyanobacteria. *In*: *Stable isotopes in ecology and environmental science*, 187-221.

Gong, G., Chang, J., Chiang, K., Hsiung, T., Hung, C., Duan, S., Codispoti, L.A. (2006). Reduction of primary production and changing of nutrient ratio in the East China Sea: Effect of the Three Gorges Dam? *Geophysical Research Letters*, 33.

Grimm, E.C. (1987). CONISS: a FORTRAN 77 program for stratigraphically constrained cluster analysis by the method of incremental sum of squares. *Computers & Geosciences*, 13, 13-35.

Guo, L. (2007). Doing battle with the green monster of Taihu Lake. *Science*, 317, 1166-1166.

Hall, R.I., Leavitt, P.R., Quinlan, R., Dixit, A.S., Smol, J.P. (1999). Effects of agriculture, urbanization, and climate on water quality in the northern Great Plains. *Limnology and Oceanography*, 44, 739-756.

Hannouche, A., Chebbo, G., Ruban, G., Tassin, B., Lemaire, B.J., Joannis, C. (2011). Relationship between turbidity and total suspended solids concentration within a combined sewer system. *Water Science and Technology*, 64, 2445-2452.

Harris, I., Jones, P.D., Osborn, T.J., Lister, D.H. (2014). Updated high-resolution grids of monthly climatic observations-the CRU TS3.10 Dataset. *International Journal of Climatology*, 34, 623-642.

Harris, J., (2017). Poyang Lake, Yangtze River Basin, China. *In*: Finlayson, C.M., Milton, G.R., Prentice, R.C., Davidson, N.C. (eds.), *The Wetland Book: II: Distribution, Description and Conservation*. Dordrecht, Springer Netherlands, pp. 1-9.

Harris, J., ZHUANG, H. (2010). An ecosystem approach to resolving conflicts among ecological and economic priorities for Poyang Lake wetlands. Gland, Switzerland: IUCN. Unpublished report.

Hassan, K.M., Swinehart, J.B., Spalding, R.F. (1997). Evidence for Holocene environmental change from C/N ratios, and $\delta^{13}C$ and $\delta^{15}N$ values in Swan Lake sediments, western Sand Hills, Nebraska. *Journal of Paleolimnology*, 18, 121-130.

Heathcote, A.J., Downing, J.A. (2012). Impacts of Eutrophication on Carbon Burial in Freshwater Lakes in an Intensively Agricultural Landscape. *Ecosystems*, 15, 60-70.

Heiler, G., Hein, T., Schiemer, F., Bornette, G. (1995). Hydrological connectivity and flood pulses as the central aspects for the integrity of a river-floodplain system. *Regulated Rivers: Research & Management*, 11, 351-361.

Heiri, O., Brooks, S.J., Birks, H.J.B., Lotter, A.F. (2011). A 274-lake calibration data-set and inference model for chironomid-based summer air temperature reconstruction in Europe. *Quaternary Science Reviews*, 30, 3445-3456.

Hobbie, S.E., Finlay, J.C., Janke, B.D., Nidzgorski, D.A., Millet, D.B., Baker, L.A. (2017). Contrasting nitrogen and phosphorus budgets in urban watersheds and implications for managing urban water pollution. *Proceedings of the National Academy of Sciences*, 114, 4177-4182.

Hu, L., Hu, W., Zhai, S., Wu, H. (2010). Effects on water quality following water transfer in Lake Taihu, China. *Ecological Engineering*, 36, 471-481.

Huang, D., Wan, Q., Li, L., Wang, T., Lu, S., Ou, F., Tian, Q. (2013). Changes of water quality and eutrophic state in recent 20 years of Dongting Lake. *Research of Environmental Sciences*, 26, 27-33.

Huang, W., Huang, Y., Lin, S., Chen, Z., Gao, B., Cui, S. (2018). Changing urban cement metabolism under rapid urbanization-a flow and stock perspective. *Journal of Cleaner Production*, 173, 197-206.

Hubei Provincial Bureau of Statistics. (2017). Huangshi Statistical Yearbook 2017[Online].Available:http://tjj.hubei.gov.cn/tjsj/sjkscx/tjnj/gsztj/hss/201911/P020200518337568896729.pdf [Accessed 2019].

Hubei Provincial Bureau of Statistics. (2017). Hubei Statistical Yearbook 2017 [Online].Available:http://tjj.hubei.gov.cn/tjsj/sjkscx/tjnj/qstjnj/201911/P020191104678605254106.zip [Accessed 2019].

Hubei Provincial Bureau of Statistics. (2017). Jingzhou Statistical Yearbook 2017[Online].Available:http://tjj.hubei.gov.cn/tjsj/sjkscx/tjnj/gsztj/jzs/201911/P020191209435294194941.pdf [Accessed 2019].

Hubei Wildlife Trust. (2005). Report of the biodiversity in Wanghu Lake.

Hunan Provincial Bureau of Statistics. (2017). Hunan Statistical Yearbook 2017 [Online]. Available: http://222.240.193.190/17tjnj/indexch.htm [Accessed 2019].

Ibáñez, C., Peñuelas, J. (2019). Changing nutrients, changing rivers. *Science*, 365, 637-638.

Jansson, M., Rune, A., Hans, B., Leonardson, L. (1994). Wetlands and Lakes as Nitrogen Traps. *Ambio*, 23, 320-325.

Jenny, J.-P., Normandeau, A., Francus, P., Taranu, Z.E., Gregory-Eaves, I., Lapointe, F., Jautzy, J., Ojala, A.E.K., Dorioz, J.-M., Schimmelmann, A., Zolitschka, B. (2016). Urban point sources of nutrients were the leading cause for the historical spread of hypoxia across European lakes. *Proceedings of the National Academy of Sciences*, 113, 12655-12660.

Jeppesen, E., Jensen, J.P., Jensen, C., Faafeng, B., Hessen, D.O., Søndergaard, M., Lauridsen, T., Brettum, P., Christoffersen, K. (2003). The Impact of Nutrient State and Lake Depth on Top-Down Control in the Pelagic Zone of Lakes: A

Study of 466 Lakes from the Temperate Zone to the Arctic. *Ecosystems*, 6, 313-325.

Jeppesen, E., Jensen, J.P., Lauridsen, T.L., Amsinck, S.L., Christoffersen, K., Søndergaard, M., Mitchell, S.F. (2003). Sub-fossils of cladocerans in the surface sediment of 135 lakes as proxies for community structure of zooplankton, fish abundance and lake temperature. *Hydrobiologia*, 491, 321-330.

Jeppesen, E., Peder Jensen, J., Søndergaard, M., Lauridsen, T., Junge Pedersen, L., Jensen, L., (1997). Top-down control in freshwater lakes: the role of nutrient state, submerged macrophytes and water depth. *In*: Kufel, L., Prejs, A., Rybak, J.I. (Eds.), *Shallow Lakes '95: Trophic Cascades in Shallow Freshwater and Brackish Lakes*. Dordrecht, Springer Netherlands, pp. 151-164.

Jeppesen, E., Søndergaard, M., Jensen, J.P., Kanstrup, E., Petersen, B., (1998). Macrophytes and Turbidity in Brackish Lakes with Special Emphasis on the Role of Top-Down Control. In: Jeppesen, E., Søndergaard, M., Søndergaard, M., Christoffersen, K. (eds.), *The Structuring Role of Submerged Macrophytes in Lakes*. New York, Springer New York, pp. 369-377.

Jiang, L., Wang, X., Li, E., Cai, X., Deng, F. (2012). Water quality change characteristics and driving factors of Honghu Lake before and after ecological restoration. *Wetland Science*, 10, 188-193.

Jiang, Y. (2009). China's water scarcity. *Journal of Environmental Management*, 90, 3185-3196.

Jiangxi Bureau of Statistics. (2017). Jiangxi Statistical Yearbook 2017 [Online]. Available: http://tjj.jiangxi.gov.cn/resource/nj/2017CD/indexch.htm [Accessed 2019].

Jiao, L. (2009). Scientists Line Up Against Dam That Would Alter Protected Wetlands. *Science*, 326, 508-509.

Jinglu, W., Chengmin, H., Haiao, Z., Schleser, G.H., Battarbee, R. (2007). Sedimentary evidence for recent eutrophication in the northern basin of Lake Taihu, China: human impacts on a large shallow lake. *Journal of Paleolimnology*, 38, 13-23.

Johnson, B.L., Richardson, W.B., Naimo, T.J. (1995). Past, Present, and Future Concepts in Large River Ecology. *BioScience*, 45, 134-141.

Johnson, K.A., Wing, O.E.J., Bates, P.D., Fargione, J., Kroeger, T., Larson, W.D., Sampson, C.C., Smith, A.M. (2020). A benefit–cost analysis of floodplain land acquisition for US flood damage reduction. *Nature Sustainability*, 3, 56-62.

Jones, J.I., Sayer, C.D. (2003). Does the Fish-Invertebrate-Periphyton Cascade Precipitate Plant Loss in Shallow Lakes? *Ecology*, 84, 2155-2167.

Juggins, S. (2017). rioja: Analysis of Quaternary Science Data, R package versi on (0.9-21). http://cran.r-project.org/package=rioja

Junk, W.J., Bayley, P.B., Sparks, R.E. (1989). The flood pulse concept in river-floodplain systems. *Canadian Special Publication of Fisheries and Aquatic Sciences*, 106, 110-127.

Karlsson, J., Byström, P., Ask, J., Ask, P., Persson, L., Jansson, M. (2009). Light limitation of nutrient-poor lake ecosystems. *Nature*, 460, 506.

Kaushal, S., Binford, M.W. (1999). Relationship between C: N ratios of lake sediments, organic matter sources, and historical deforestation in Lake Pleasant, Massachusetts, USA. *Journal of Paleolimnology*, 22, 439-442.

Ke, W., Chen, C., Ji, H. (2017). A loop-like relationship between water surface area of Lake Dongting and water level at Chenglingji, the Yangzi River. *Journal of Lake Sciences*, 29, 753-764.

Keeling, C.D. (1979). The Suess effect: ^{13}Carbon-^{14}Carbon interrelations. *Environment International*, 2, 229-300.

Kendall, C., Elliott, E.M., Wankel, S.D. (2007). Tracing anthropogenic inputs of nitrogen to ecosystems. *In*: *Stable Isotopes in Ecology and Environmental Science*, 2, 375-449.

Knowlton, M.F., Jones, J.R. (1997). Trophic status of Missouri River floodplanin lakes in relation to basin type and connectivity. *Wetlands*, 17, 468-475.

Krishnamurthy, R.V., Bhattacharya, S.K., Kusumgar, S. (1986). Palaeoclimatic changes deduced from 13C/12C and C/N ratios of Karewa lake sediments, India. *Nature*, 323, 150-152.

Krishnaswamy, S., Lal, D., Martin, J.M., Meybeck, M. (1971). Geochronology of lake sediments. *Earth and Planetary Science Letters*, 11, 407-414.

Lampert, W., Sommer, U. (2007). Limnoecology: the ecology of lakes and streams. Oxford university press.

Langdon, P.G., Ruiz, Z.O.E., Wynne, S., Sayer, C.D., Davidson, T.A. (2010). Ecological influences on larval chironomid communities in shallow lakes: implications for palaeolimnological interpretations. *Freshwater Biology*, 55, 531-545.

Leavitt, P.R., Brock, C.S., Ebel, C., Patoine, A. (2006). Landscape-scale effects of urban nitrogen on a chain of freshwater lakes in central North America. *Limnology and Oceanography*, 51, 2262-2277.

Leavitt, P.R., Fritz, S.C., Anderson, N.J., Baker, P.A., Blenckner, T., Bunting, L., Catalan, J., Conley, D.J., Hobbs, W.O., Jeppesen, E., Korhola, A., McGowan, S., RÜhland, K., Rusak, J.A., Simpson, G.L., Solovieva, N., Werne, J. (2009). Paleolimnological evidence of the effects on lakes of energy and mass transfer from climate and humans. *Limnology and Oceanography*, 54, 2330-2348.

Leavitt, P.R., Hodgson, D.A., (2001). Sedimentary Pigments. *In*: Smol, J.P., Birks, H.J.B., Last, W.M., Bradley, R.S., Alverson, K. (eds.), *Tracking Environmental Change Using Lake Sediments: Terrestrial, Algal, and Siliceous Indicators*. Dordrecht. Springer Netherlands, pp. 295-325.

Leavitt, P.R., Vinebrooke, R.D., Donald, D.B., Smol, J.P., Schindler, D.W. (1997). Past ultraviolet radiation environments in lakes derived from fossil pigments. *Nature*, 388, 457-459.

Legendre, P., Legendre, L.F. (2012). Numerical ecology. New York. Elsevier.

Leng, M.J. (2006). Isotopes in palaeoenvironmental research. Springer.

Liang, Y., Liu, X., Xiao, H., Gao, X., Li, W., Xiong, J. (2016). Impact of high water level fluctuations on stable isotopic signature of POM and source identification in a floodplain lake-Bang Lake (Poyang Lake). *Environmental Earth Sciences*, 75, 255.

Little, J.L., Smol, J.P. (2001). A chironomid-based model for inferring late-summer hypolimnetic oxygen in southeastern Ontario lakes. *Journal of Paleolimnology*, 26, 259-270.

Liu, E., Shen, J., Birch, G.F., Yang, X., Wu, Y., Xue, B. (2012). Human-induced change in sedimentary trace metals and phosphorus in Chaohu Lake, China, over the past half-millennium. *Journal of Paleolimnology*, 47, 677-691.

Liu, J., Yang, W. (2012). Water Sustainability for China and Beyond. *Science*, 337, 649-650.

Liu, X., Qian, K., Chen, Y., Gao, J. (2017). A comparison of factors influencing the summer phytoplankton biomass in China's three largest freshwater lakes: Poyang, Dongting, and Taihu. *Hydrobiologia*, 792, 283-302.

Liu, X., Sheng, H., Jiang, S., Yuan, Z., Zhang, C., Elser, J.J. (2016). Intensification of phosphorus cycling in China since the 1600s. *Proceedings of the National Academy of Sciences*, 113, 2609-2614.

Liu, Y., Wu, G., Guo, R., Wan, R. (2016). Changing landscapes by damming: the Three Gorges Dam causes downstream lake shrinkage and severe droughts. *Landscape Ecology*, 31, 1883-1890.

Long, T., Hunt, C.O., Taylor, D. (2016). Radiocarbon anomalies suggest late onset of agricultural intensification in the catchment of the southern part of the Yangtze Delta, China. *CATENA*, 147, 586-594.

Loos, J., Shader, E. (2016). Reconnecting rivers to floodplains: Returning natural functions to restore rivers and benefit communities. River Restoration Program. American Rivers.

Maavara, T., Chen, Q., Van Meter, K., Brown, L.E., Zhang, J., Ni, J., Zarfl, C. (2020). River dam impacts on biogeochemical cycling. *Nature Reviews Earth & Environment*, 1, 103-116.

Maavara, T., Dürr, H.H., Van Cappellen, P. (2014). Worldwide retention of nutrient silicon by river damming: From sparse data set to global estimate. *Global Biogeochemical Cycles*, 28, 842-855.

Maavara, T., Lauerwald, R., Regnier, P., Van Cappellen, P. (2017). Global perturbation of organic carbon cycling by river damming. *Nature Communications*, 8, 15347.

Maavara, T., Parsons, C.T., Ridenour, C., Stojanovic, S., Dürr, H.H., Powley, H.R., Van Cappellen, P. (2015). Global phosphorus retention by river damming. *Proceedings of the National Academy of Sciences*, 112, 15603-15608.

Mackey, A.P. (1977). Growth and Development of Larval Chironomidae. *Oikos*, 28, 270-275.

Maitland, P.S., PS, M. (1979). The distribution of zoobenthos and sediments in Loch Leven, Kinross, Scotland.

Mann, H.B. (1945). Nonparametric tests against trend. *Econometrica: Journal of the Econometric Society*, 245-259.

McCarthy, M.J., James, R.T., Chen, Y., East, T.L., Gardner, W.S. (2009). Nutrient ratios and phytoplankton community structure in the large, shallow, eutrophic, subtropical Lakes Okeechobee (Florida, USA) and Taihu (China). *Limnology*, 10, 215-227.

McGarrigle, M.L., (1980). The Distribution of Chironomid Communities and Controlling Sediment Parameters in L. Derravaragh, Ireland, *In*: Murray, D.A. (ed.), *Chironomidae*. Pergamon, pp. 275-282.

McGowan, S. (2007). *Pigments in sediments of aquatic environments. Encyclopedia of quaternary sciences*. Amsterdam. Elsevier.

McGowan, S., Anderson, N.J., Edwards, M.E., Hopla, E., Jones, V., Langdon, P.G., Law, A., Solovieva, N., Turner, S., van Hardenbroek, M., Whiteford, E.J., Wiik, E. (2018). Vegetation transitions drive the autotrophy–heterotrophy balance in Arctic lakes. *Limnology and Oceanography Letters*, 3, 246-255.

McGowan, S., Leavitt, P.R., Hall, R.I., Anderson, N.J., Jeppesen, E., Odgaard, B.V. (2005). Controls of algal abundance and community composition during ecosystem state change. *Ecology*, 86, 2200-2211.

McGowan, S., Leavitt, P.R., Hall, R.I., Wolfe, B.B., Edwards, T.W.D., Karst-Riddoch, T., Vardy, S.R. (2011). Interdecadal declines in flood frequency increase primary production in lakes of a northern river delta. *Global Change Biology*, 17, 1212-1224.

McGowan, S., Barker, P., Haworth, E.Y., Leavitt, P.R., Maberly, S.C., Pates, J. (2012). Humans and climate as drivers of algal community change in Windermere since 1850. *Freshwater Biology*, 57, 260-277.

McLeod, A.I. (2011). Kendall: Kendall rank correlation and Mann-Kendall trend test. R package version 2.2. https://CRAN.R-project.org/package=Kendall

Mei, X., Dai, Z., Du, J., Chen, J. (2015). Linkage between Three Gorges Dam impacts and the dramatic recessions in China's largest freshwater lake, Poyang Lake. *Scientific Reports*, 5, 18197.

Mendonça, R., Kosten, S., Sobek, S., Barros, N., Cole, J.J., Tranvik, L., Roland, F. (2012). Hydroelectric carbon sequestration. *Nature Geoscience*, 5, 838.

Meyers, P.A. (1997). Organic geochemical proxies of paleoceanographic, paleolimnologic, and paleoclimatic processes. *Organic Geochemistry*, 27, 213-250.

Meyers, P.A., Lallier-vergés, E. (1999). Lacustrine sedimentary organic matter records of late Quaternary paleoclimates. *Journal of Paleolimnology*, 21, 345-372.

Meyers, P.A., Teranes, J.L., (2002). Sediment organic matter *In*: *Tracking environmental change using lake sediments*. Dordrecht. Springer.

Miller, F., de le Rosa, E., Bohn, M. (2008). The challenge of moving from acknowledgement to action: A review of vulnerability to environmental stresses and natural hazards in PRSPs. Stockholm: SEI.

Miller Jr, R.G. (1997). Beyond ANOVA: basics of applied statistics. CRC press.

Milliman, J.D., Farnsworth, K.L. (2011). River Discharge to the Coastal Ocean: A Global Synthesis. Cambridge. Cambridge University Press.

Mitsch, W.J., Gosselink, J.G. (2000). Wetlands john wiley & sons. Inc., New York, New York.

Moorhouse, H.L., McGowan, S., Jones, M.D., Barker, P., Leavitt, P.R., Brayshaw, S.A., Haworth, E.Y. (2014). Contrasting effects of nutrients and climate on algal communities in two lakes in the Windermere catchment since the late 19th century. *Freshwater Biology*, 59, 2605-2620.

Moorhouse, H.L., McGowan, S., Taranu, Z.E., Gregory-Eaves, I., Leavitt, P.R., Jones, M.D., Barker, P., Brayshaw, S.A. (2018). Regional versus local drivers of water quality in the Windermere catchment, Lake District, United Kingdom: The dominant influence of wastewater pollution over the past 200 years. *Global Change Biology*, 24, 4009-4022.

Moran, E.F., Lopez, M.C., Moore, N., Müller, N., Hyndman, D.W. (2018). Sustainable hydropower in the 21st century. *Proceedings of the National Academy of Sciences*, 115, 11891-11898.

Morrison, W.M. (2013). China's economic rise: history, trends, challenges, and implications for the United States. Congressional research service Washington, DC.

Mulholland, P.J., Elwood, J.W. (1982). The role of lake and reservoir sediments as sinks in the perturbed global carbon cycle. *Tellus*, 34, 490-499.

Nakamura, K., Tockner, K., Amano, K. (2006). River and Wetland Restoration: Lessons from Japan. *BioScience*, 56, 419-429.

National Economy General Statistics Division of National Bureau of Statistics. (2010). *China compendium of statistics 1949–2008*.

Naumann, E. (1919). Några synpunkter angående limnoplanktons ökologi med särskild hänsyn till fytoplankton. *Svensk Botanisk Tidskrift*, 13, 129-163.

NBSC. National Bureau of Statistics of China [Online]. Available: http://data.stats.gov.cn/ [Accessed 2018].

Oksanen, J., Blanchet, F.G., Friendly, M., Kindt, R., Legendre, P., McGlinn, D., Minchin, P.R., O'Hara, R.B., Simpson, G.L., Solymos, P., Stevens, M.H.H., Szoecs, E., Wagner, Helene. (2019). vegan: Community Ecology Package. R package version 2.5-6. https://CRAN.R-project.org/package=vegan

Oldfield, F., Appleby, P.G., Battarbee, R.W. (1978). Alternative ^{210}Pb dating: results from the New Guinea Highlands and Lough Erne. *Nature*, 271, 339-342.

O'Leary, M.H. (1981). Carbon isotope fractionation in plants. *Phytochemistry*, 20, 553-567.

O'Leary, M.H. (1988). Carbon Isotopes in Photosynthesis. *BioScience*, 38, 328-336.

Oliver, D.R., Roussel, M.E. (1983). The insects and arachnids of Canada. *Part 11*: *The genera of larval midges of Canada. Diptera: Chironomidae*. Minister of Supply and Services.

Paerl, H.W., Paul, V.J. (2012). Climate change: Links to global expansion of harmful cyanobacteria. *Water Research*, 46, 1349-1363.

Paerl, H.W., Scott, J.T., McCarthy, M.J., Newell, S.E., Gardner, W.S., Havens, K.E., Hoffman, D.K., Wilhelm, S.W., Wurtsbaugh, W.A. (2016). It takes two to tango: when and where dual nutrient (N & P) reductions are needed to protect lakes and downstream ecosystems. *Environmental Science & Technology*, 50, 10805-10813.

Paerl, H.W., Xu, H., McCarthy, M.J., Zhu, G., Qin, B., Li, Y., Gardner, W.S. (2011). Controlling harmful cyanobacterial blooms in a hyper-eutrophic lake

(Lake Taihu, China): The need for a dual nutrient (N & P) management strategy. *Water Research*, 45, 1973-1983.

Palmer, M., Ruhi, A. (2019). Linkages between flow regime, biota, and ecosystem processes: Implications for river restoration. *Science*, 365, eaaw2087.

Papas, P. (2007). Effect of macrophytes on aquatic invertebrates: A literature review. *Arthur Rylah Institute for Environmental Research*.

Park, Y.S., Chang, J., Lek, S., Cao, W., Brosse, S. (2003). Conservation strategies for endemic fish species threatened by the Three Gorges Dam. *Conservation Biology*, 17, 1748-1758.

Pennington, W., Cambray, R.S., Eakins, J.D., Harkness, D.D. (1976). Radionuclide dating of the recent sediments of Blelham Tarn. *Freshwater Biology*, 6, 317-331.

Peršić, V., Horvatić, J. (2011). Spatial Distribution of Nutrient Limitation in the Danube River Floodplain in Relation to Hydrological Connectivity. *Wetlands*, 31, 933.

Peters, K.E., Sweeney, R.E., Kaplan, I.R. (1978). Correlation of carbon and nitrogen stable isotope ratios in sedimentary organic matter. *Limnology and Oceanography*, 23, 598-604.

Pierson, D.C., (2012). Light and Primary Production in Lakes, in: Bengtsson, L., Herschy, R.W., Fairbridge, R.W. (Eds.), Encyclopedia of Lakes and Reservoirs. Springer Netherlands, Dordrecht, pp. 485-492.

Pinder, L. (1986). Biology of freshwater Chironomidae. *Annual Review of Entomology*, 31, 1-23.

Pinder, L.C.V., (1980). Spatial distribution of chironomidae in an English chalk stream, in: Murray, D.A. (Ed.), Chironomidae. *Pergamon*, 153-161.

Qiu, J. (2010). China faces up to groundwater crisis. *Nature*, 466, 308-308.

Randsalu-Wendrup, L., Conley, D.J., Carstensen, J., Fritz, S.C. (2016). Paleolimnological records of regime shifts in lakes in response to climate change and anthropogenic activities. *Journal of Paleolimnology*, 56, 1-14.

R Core Team (2020). R: A language and environment for statistical computing R Foundation for Statistical Computing, Vienna, Austria. URL https://www.R-project.org/

Ramsar Convention (2020). The List of Wetlands of International Importance [Online].Available:https://www.ramsar.org/sites/default/files/documents/library/sitelist.pdf [Accessed 2020]

Rao, K., Zhang, X., Yi, X., Li, Z., Wang, P., Huang, G., Guo, X. (2018). Interactive effects of environmental factors on phytoplankton communities and benthic nutrient interactions in a shallow lake and adjoining rivers in China. *Science of the Total Environment*, 619-620, 1661-1672.

Resource and Environment Science and Data Center. Land use land cover change in China [Online]. Available: http://www.resdc.cn/data.aspx?dataid=99 [Accessed 2018].

Reynolds, C.S. (1998). What factors influence the species composition of phytoplankton in lakes of different trophic status? *Hydrobiologia*, 369, 11-26.

Rieradevall, M., Brooks, S.J. (2001). An identification guide to subfossil Tanypodinae larvae (Insecta: Diptera: Chrironomidae) based on cephalic setation. *Journal of Paleolimnology*, 25, 81-99.

Ritchie, J.C., McHenry, J.R. (1990). Application of Radioactive Fallout Cesium-137 for Measuring Soil Erosion and Sediment Accumulation Rates and Patterns: A Review. *Journal of Environmental Quality*, 19, 215-233.

Ritchie, J.C., McHenry, J.R., Gill, A.C. (1973). Dating recent reservoir sediments 1. *Limnology and Oceanography*, 18, 254-263.

Robbins, J.A., Edgington, D.N. (1975). Determination of recent sedimentation rates in Lake Michigan using Pb-210 and Cs-137. *Geochimica et Cosmochimica Acta*, 39, 285-304.

Rose, N.L., Boyle, J.F., Du, Y., Yi, C., Dai, X., Appleby, P.G., Bennion, H., Cai, S., Yu, L. (2004). Sedimentary evidence for changes in the pollution status of Taihu in the Jiangsu region of eastern China. *Journal of Paleolimnology*, 32, 41-51.

Rose, N.L., Morley, D., Appleby, P.G., Battarbee, R.W., Alliksaar, T., Guilizzoni, P., Jeppesen, E., Korhola, A., Punning, J.-M. (2011). Sediment accumulation rates in European lakes since AD 1850: trends, reference conditions and exceedence. *Journal of Paleolimnology*, 45, 447-468.

Saito, K., Tada, R., Zheng, H., Irino, T., Luo, C., He, M., Wang, K., Suzuki, Y. (2017). ESR signal intensity of quartz in the fine-silt fraction of riverbed sediments from the Yangtze River: a provenance tracer for suspended particulate matter. *Progress in Earth and Planetary Science*, 4, 4.

Sayer, C.D., Burgess, A.M.Y., Kari, K., Davidson, T.A., Peglar, S., Yang, H., Rose, N. (2010). Long-term dynamics of submerged macrophytes and algae in a small and shallow, eutrophic lake: implications for the stability of macrophyte-dominance. *Freshwater Biology*, 55, 565-583.

Sayer, C.D., Davidson, T.A., Jones, J.I., Langdon, P.G. (2010). Combining contemporary ecology and palaeolimnology to understand shallow lake ecosystem change. *Freshwater Biology*, 55, 487-499.

Scheffer, M. (1997). *Ecology of shallow lakes*. Springer Science & Business Media.

Scheffer, M., Carpenter, S., Foley, J.A., Folke, C., Walker, B. (2001). Catastrophic shifts in ecosystems. *Nature*, 413, 591-596.

Scheffer, M., Hosper, S.H., Meijer, M.L., Moss, B., Jeppesen, E. (1993). Alternative equilibria in shallow lakes. *Trends in Ecology & Evolution*, 8, 275-279.

Scheffer, M., van Nes, E.H. (2007). Shallow lakes theory revisited: various alternative regimes driven by climate, nutrients, depth and lake size. *Hydrobiologia*, 584, 455-466.

Schelske, C.L., Hodell, D.A. (1995). Using carbon isotopes of bulk sedimentary organic matter to reconstruct the history of nutrient loading and eutrophication in Lake Erie. *Limnology and Oceanography*, 40, 918-929.

Schindler, D.W. (1977). Evolution of Phosphorus Limitation in Lakes. *Science*, 195, 260-262.

Schindler, D.W. (2006). Recent advances in the understanding and management of eutrophication. *Limnology and Oceanography*, 51, 356-363.

Schindler, D.W., Hecky, R.E., Findlay, D.L., Stainton, M.P., Parker, B.R., Paterson, M.J., Beaty, K.G., Lyng, M., Kasian, S.E.M. (2008). Eutrophication of lakes cannot be controlled by reducing nitrogen input: Results of a 37-year whole-ecosystem experiment. *Proceedings of the National Academy of Sciences*, 105, 11254-11258.

Secor, D.H., Kerr, L.A. (2009). Lexicon of life cycle diversity in diadromous and other fishes. *American Fisheries Society Symposium*, 537-556.

Seddon, A.W.R., Froyd, C.A., Witkowski, A., Willis, K.J. (2014). A quantitative framework for analysis of regime shifts in a Galápagos coastal lagoon. *Ecology*, 95, 3046-3055.

Shankman, D., Liang, Q. (2003). Landscape Changes and Increasing Flood Frequency in China's Poyang Lake Region*. *The Professional Geographer*, 55, 434-445.

Shao, W., Li, Y., Yan, D., Liu, J., Yang, Z., Yang, Z., (2018). Analysis of the losses due to flood and waterlogging disasters in China during 2006 to 2017. *Multidisciplinary Digital Publishing Institute Proceedings*, p. 25.

Shen, J., Zhang, K., Liu, Z. (2020). Paleolimnological evidence of environmental change in Chinese lakes over the past two centuries. *Inland Waters*, 10, 1-10.

Shiklomanov, I., (1993). *World fresh water resources, water in crisis: A guide to the world's fresh water resources*. Oxford University Press, New York.

Shumway, R.H., Stoffer, D.S. (2017). *Time series analysis and its applications: with R examples*. Springer.

Simpson, G.L. (2018). Modelling palaeoecological time series using generalised additive models. *Frontiers in Ecology and Evolution*, 6.

Simpsona, G.L., Anderson, N.J. (2009). Deciphering the effect of climate change and separating the influence of confounding factors in sediment core records using additive models. *Limnology and Oceanography*, 54, 2529-2541.

Smith, B.N., Epstein, S. (1971). Two categories of $^{13}C/^{12}C$ ratios for higher plants. *Plant Physiology*, 47, 380-384.

Smith, V.H. (1983). Low nitrogen to phosphorus ratios favor dominance by blue-green algae in lake phytoplankton. *Science*, 221, 669-671.

Smith, V.H., Schindler, D.W. (2009). Eutrophication science: where do we go from here? *Trends in Ecology & Evolution*, 24, 201-207.

Smol, J.P., Birks, H.J.B., Lotter, A.F., Juggins, S., (2012). The march towards the quantitative analysis of palaeolimnological data *In: Tracking environmental change using lake sediments*. Dordrecht. Springer.

Sokal, M.A., Hall, R.I., Wolfe, B.B. (2008). Relationships between hydrological and limnological conditions in lakes of the Slave River Delta (NWT, Canada) and quantification of their roles on sedimentary diatom assemblages. *Journal of Paleolimnology*, 39, 533-550.

Sokal, M.A., Hall, R.I., Wolfe, B.B. (2010). The role of flooding on inter-annual and seasonal variability of lake water chemistry, phytoplankton diatom communities and macrophyte biomass in the Slave River Delta (Northwest Territories, Canada). *Ecohydrology*, 3, 41-54.

Sommer, U., Adrian, R., Domis, L.D.S., Elser, J.J., Gaedke, U., Ibelings, B., Jeppesen, E., Lürling, M., Molinero, J.C., Mooij, W.M., Donk, E.v., Winder, M. (2012). Beyond the plankton ecology group (PEG) model: mechanisms driving plankton succession. *Annual Review of Ecology, Evolution, and Systematics*, 43, 429-448.

Sommer, U., Gliwicz, Z.M., Lampert, W., Duncan, A. (1986). The PEG-model of seasonal succession of planktonic events in fresh waters. *Arch. Hydrobiol*, 106, 433-471.

Søndergaard, M. (2007). Nutrient Dynamics in Lakes: with emphasis on Phosphorus Sediment and Lake Restoration. NERI.

Song, X., Cai, X., Wang, Z., Li, E., Wang, X. (2016). Community change of dominant submerged macrophyte in Lake Honghu since 1950s. *Journal of Lake Sciences*, 28, 859-867.

Squires, M.M., Lesack, L.F.W. (2003). The relation between sediment nutrient content and macrophyte biomass and community structure along a water transparency gradient among lakes of the Mackenzie Delta. *Canadian Journal of Fisheries and Aquatic Sciences*, 60, 333-343.

Squires, M.M., Lesack, L.F.W., Huebert, D. (2002). The influence of water transparency on the distribution and abundance of macrophytes among lakes of the Mackenzie Delta, Western Canadian Arctic. *Freshwater Biology*, 47, 2123-2135.

Stone, R. (2016), Dam-building threatens Mekong fisheries. *Science*, 354, 1084-1085.

Swift, T.J., Perez-Losada, J., Schladow, S.G., Reuter, J.E., Jassby, A.D., Goldman, C.R. (2006), Water clarity modeling in Lake Tahoe: Linking suspended matter characteristics to Secchi depth. *Aquatic Sciences*, 68, 1-15.

Syvitski, J.P.M., Kettner, A.J., Overeem, I., Hutton, E.W.H., Hannon, M.T., Brakenridge, G.R., Day, J., Vörösmarty, C., Saito, Y., Giosan, L., Nicholls, R.J. (2009). Sinking deltas due to human activities. *Nature Geoscience*, 2, 681-686.

Syvitski, J.P.M., Vörösmarty, C.J., Kettner, A.J., Green, P. (2005). Impact of Humans on the Flux of Terrestrial Sediment to the Global Coastal Ocean. *Science*, 308, 376-380.

Taniguchi, H., Nakano, S., Tokeshi, M. (2003). Influences of habitat complexity on the diversity and abundance of epiphytic invertebrates on plants. *Freshwater Biology*, 48, 718-728.

Taranu, Z.E., Gregory-Eaves, I., Leavitt, P.R., Bunting, L., Buchaca, T., Catalan, J., Domaizon, I., Guilizzoni, P., Lami, A., McGowan, S., Moorhouse, H., Morabito, G., Pick, F.R., Stevenson, M.A., Thompson, P.L., Vinebrooke, R.D. (2015). Acceleration of cyanobacterial dominance in north temperate-subarctic lakes during the Anthropocene. *Ecology Letters*, 18, 375-384.

The Nature Conservancy. Benefits of Healthy Floodplains [Online]. Available: https://www.nature.org/en-us/what-we-do/our-priorities/protect-water-and-land/land-and-water-stories/benefits-of-healthy-floodplains/ [Accessed 2020].

Thicnemann, A., (1954). Chironomus. Leben, Verbreitung und Wirtschaftliche Bedeutung der Chironomiden. Die Binnengewasser, Vol. 20. E. Schweizerbart'sche Verlagsbuchhandlung, Stuttgart.

Thienemann, A. (1921). Seetypen. *Naturwissenschaften*, 9, 343-346.

Thienemann, A. (1918). Untersuchungen uber die Beziehungen zwischen dem Sauerstoffgehalt des Wassers und der Zusammensetzung der Fana in norddeutschen Seen. *Arch Hydrobiol*, 12, 1-65.

Tilman, D. (1985). The Resource-Ratio Hypothesis of Plant Succession. *The American Naturalist*, 125, 827-852.

Timpe, K., Kaplan, D. (2017). The changing hydrology of a dammed Amazon. *Science Advances*, 3, e1700611.

Tockner, K., Pennetzdorfer, D., Reiner, N., Schiemer, F., Ward, J.V. (1999). Hydrological connectivity, and the exchange of organic matter and nutrients in a dynamic river–floodplain system (Danube, Austria). *Freshwater Biology*, 41, 521-535.

Tockner, K., Pusch, M., Borchardt, D., Lorang, M.S. (2010). Multiple stressors in coupled river–floodplain ecosystems. *Freshwater Biology*, 55, 135-151.

Tockner, K., Stanford, J.A. (2002). Riverine flood plains: present state and future trends. *Environmental Conservation*, 29, 308-330.

Tundisi, J.G., Goldemberg, J., Matsumura-Tundisi, T., Saraiva, A.C.F. (2014). How many more dams in the Amazon? *Energy Policy*, 74, 703-708.

UN-Water, U., (2020). United Nations World Water Development Report 2020: Water and Climate Change. UNESCO: Paris, France.

Van den Brink, F.W. (1994). *Impact of hydrology on floodplain lake ecosystems along the lower Rhine and Meuse*. [Sl: sn].

Van den Brink, F.W.B., De Leeuw, J.P.H.M., Van Der Velde, G., Verheggen, G.M. (1992). Impact of hydrology on the chemistry and phytoplankton development in floodplain lakes along the Lower Rhine and Meuse. *Biogeochemistry*, 19, 103-128.

Van Drecht, G., Bouwman, A.F., Harrison, J., Knoop, J.M. (2009). Global nitrogen and phosphate in urban wastewater for the period 1970 to 2050. *Global Biogeochemical Cycles*, 23.

Vannote, R.L., Minshall, G.W., Cummins, K.W., Sedell, J.R., Cushing, C.E. (1980). The River Continuum Concept. *Canadian Journal of Fisheries and Aquatic Sciences*, 37, 130-137.

Vermaire, J.C., Greffard, M.-H., Saulnier-Talbot, É., Gregory-Eaves, I. (2013). Changes in submerged macrophyte abundance altered diatom and chironomid assemblages in a shallow lake. *Journal of Paleolimnology*, 50, 447-456.

Vidic, N.J., Montañez, I.P. (2004). Climatically driven glacial-interglacial variations in C3 and C4 plant proportions on the Chinese Loess Plateau. *Geology*, 32, 337-340.

Vincent, W.F., (2009). Cyanobacteria *In*: Likens, G.E. (ed.) *Encyclopedia of Inland Waters*. Oxford. Academic Press.

Walker, I.R., Smol, J.P., Engstrom, D.R., Birks, H.J.B. (1991). An assessment of chironomidae as quantitative indicators of past climatic change. *Canadian Journal of Fisheries and Aquatic Sciences*, 48, 975-987.

Walling, D.E., (2012). The role of dams in the global sediment budget. *Erosion and Sediment Yields in the Changing Environment, IAHS Publ*, 356: 3-11.

Wang, H., Liu, X., Wang, H., (2016). The Yangtze River floodplain: threats and rehabilitation. *American Fisheries Society Symposium*, 263-291.

Wang, H., Yang, Z., Wang, Y., Saito, Y., Liu, J.P. (2008). Reconstruction of sediment flux from the Changjiang (Yangtze River) to the sea since the 1860s. *Journal of Hydrology*, 349, 318-332.

Wang, M., Zhou, W., Ai, Y., (2011). The characteristics of nutrients and eutrophication status in Poyang Lake, China, 2011. *International Conference on Electric Technology and Civil Engineering (ICETCE)*, 1662-1665.

Wang, S.M., Dou, H.S. (1998). Lakes in China. Beijing. China Science Publishing.

Wang, Z., Shao, D., Westerhoff, P. (2017). Wastewater discharge impact on drinking water sources along the Yangtze River (China). *Science of the Total Environment*, 599, 1399-1407.

Ward, G.M., Cummins, K.W. (1979). Effects of food quality on growth of a stream detritivore, paratendipes Albimanus (Meigen) (Diptera: Chironomidae). Ecology, 60, 57-64.

Waters, C.N., Zalasiewicz, J., Summerhayes, C., Barnosky, A.D., Poirier, C., Gałuszka, A., Cearreta, A., Edgeworth, M., Ellis, E.C., Ellis, M., Jeandel, C., Leinfelder, R., McNeill, J.R., Richter, D.d., Steffen, W., Syvitski, J., Vidas, D., Wagreich, M., Williams, M., Zhisheng, A., Grinevald, J., Odada, E., Oreskes, N., Wolfe, A.P. (2016). The Anthropocene is functionally and stratigraphically distinct from the Holocene. *Science*, 351, aad2622.

Wayland, M., Hobson, K.A. (2001). Stable carbon, nitrogen, and sulfur isotope ratios in riparian food webs on rivers receiving sewage and pulp-mill effluents. *Canadian Journal of Zoology*, 79, 5-15.

Weber, K. (1907). Aufbau und vegetation der Moore Norddeutschlands.

Wiederholm, T. (1983). Chironomidae of the Holarctic region. Keys and diagnoses. *Part 1*: Larvae. *Entomologica scandinavica*. Supplementum.

Wiklund, J.A., (2012). Lakes of the Peace-Athabasca Delta: Controls on nutrients, chemistry, phytoplankton, epiphyton and deposition of polycyclic aromatic compounds (PACs). UWSpace.

Wolfe, B.B., Hall, R.I., Edwards, T.W.D., Johnston, J.W. (2012). Developing temporal hydroecological perspectives to inform stewardship of a northern floodplain landscape subject to multiple stressors: paleolimnological investigations of the Peace-Athabasca Delta. *Environmental Reviews*, 20, 191-210.

Wood, S.N. (2017). Generalized additive models: an introduction with R. Chapman and Hall/CRC.

Wood S.N., Pya, N., Saefken, B. (2016). Smoothing parameter and model selection for general smooth models (with discussion). *Journal of the American Statistical Association*, 111:1548-1575.

Woodward, C.A., Potito, A.P., Beilman, D.W. (2012). Carbon and nitrogen stable isotope ratios in surface sediments from lakes of western Ireland:

implications for inferring past lake productivity and nitrogen loading. *Journal of Paleolimnology*, 47, 167-184.

Wu, N., Schmalz, B., Fohrer, N. (2010). Distribution of phytoplankton in a German lowland river in relation to environmental factors. *Journal of Plankton Research*, 33, 807-820.

Wu, Y., Li, Y., Lv, J., Xi, B., Zhang, L., Yang, T., Li, G., Li, C., Liu, H. (2017). Influence of sediment DOM on environmental factors in shallow eutrophic lakes in the middle reaches of the Yangtze River in China. *Environmental Earth Sciences*, 76, 142.

Wuhan Bureau of Statistics. (1999). *Wuhand during the Last Fifty Years*. Beijing. China Statistics Press.

WWF. (2012). World Wide Fund for Nature. Yangtze Basin lakes shrinking as climate change, development takes its toll [online]. Available: https://wwf.panda.org/wwf_news/?203195/Yangtze-Basin-lakes-shrinking-as-climate-change-development-takes-its-toll [Accessed 2020].

Xiang, L., Lu, X.X., Higgitt, D.L., Wang, S.M. (2002). Recent lake sedimentation in the middle and lower Yangtze basin inferred from ^{137}Cs and ^{210}Pb measurements. *Journal of Asian Earth Sciences*, 21, 77-86.

Xie, C., Huang, X., Mu, H., Yin, W. (2017). Impacts of Land-Use Changes on the Lakes across the Yangtze Floodplain in China. *Environmental Science & Technology*, 51, 3669-3677.

Xie, Y., Yue, T., Chen, X., Feng, L., Deng, Z. (2015). The impact of Three Gorges Dam on the downstream eco-hydrological environment and vegetation distribution of East Dongting Lake. *Ecohydrology*, 8, 738-746.

Xu, H., Ai, L., Tan, L., An, Z. (2006). Stable isotopes in bulk carbonates and organic matter in recent sediments of Lake Qinghai and their climatic implications. *Chemical Geology*, 235, 262-275.

Xu, H., Paerl, H.W., Qin, B., Zhu, G., Gaoa, G. (2010). Nitrogen and phosphorus inputs control phytoplankton growth in eutrophic Lake Taihu, China. *Limnology and Oceanography*, 55, 420-432.

Xu, M., Dong, X., Yang, X., Chen, X., Zhang, Q., Liu, Q., Wang, R., Yao, M., Davidson, T.A., Jeppesen, E. (2017). Recent Sedimentation Rates of Shallow Lakes in the Middle and Lower Reaches of the Yangtze River: Patterns, Controlling Factors and Implications for Lake Management. *Water*, 9, 617.

Xu, M., Dong, X., Yang, X., Wang, R., Zhang, K., Zhao, Y., Davidson, T.A., Jeppesen, E. (2017). Using palaeolimnological data and historical records to assess long-term dynamics of ecosystem services in typical Yangtze shallow lakes (China). *Science of the Total Environment*, 584–585, 791-802.

Yan, Z., Han, W., Peñuelas, J., Sardans, J., Elser, J.J., Du, E., Reich, P.B., Fang, J. (2016). Phosphorus accumulates faster than nitrogen globally in freshwater ecosystems under anthropogenic impacts. *Ecology Letters*, 19, 1237-1246.

Yang, S.L., Milliman, J.D., Li, P., Xu, K. (2011). 50,000 dams later: Erosion of the Yangtze River and its delta. *Global and Planetary Change*, 75, 14-20.

Yang, S.L., Zhang, J., Xu, X.J. (2007). Influence of the Three Gorges Dam on downstream delivery of sediment and its environmental implications, Yangtze River. *Geophysical Research Letters*, 34.

Yang, X., Anderson, N.J., Dong, X., Shen, J.I. (2008). Surface sediment diatom assemblages and epilimnetic total phosphorus in large, shallow lakes of the Yangtze floodplain: their relationships and implications for assessing long-term eutrophication. *Freshwater Biology*, 53, 1273-1290.

Yang, X., Dong, X., Chen, X., Liu, Q. (2014). Damming-induced hydrological alternation hastened ecological regime shift in the Yangtze floodplain lakes. Australia-China Wetland Network Research Partnership, 36.

Yang, X., Lu, X. (2014). Drastic change in China's lakes and reservoirs over the past decades. *Scientific Reports*, 4,1-10.

Yang, X.J. (2013). China's Rapid Urbanization. *Science*, 342, 310-310.

Yu, C., Huang, X., Chen, H., Godfray, H.C.J., Wright, J.S., Hall, J.W., Gong, P., Ni, S., Qiao, S., Huang, G., Xiao, Y., Zhang, J., Feng, Z., Ju, X., Ciais, P., Stenseth, N.C., Hessen, D.O., Sun, Z., Yu, L., Cai, W., Fu, H., Huang, X., Zhang, C., Liu, H., Taylor, J. (2019). Managing nitrogen to restore water quality in China. *Nature*, 567, 516-520.

Zeng, L. (2016). *Study on the environmental change in Futou Lake and its driver over the past 200 years*. Thesis (MSc), China University of Geosciences (Wuhan).

Zeng, L., McGowan, S., Cao, Y., Chen, X. (2018). Effects of dam construction and increasing pollutants on the ecohydrological evolution of a shallow freshwater lake in the Yangtze floodplain. *Science of the Total Environment*, 621, 219-227.

Zhang, E., Bedford, A., Jones, R., Shen, J., Wang, S., Tang, H. (2006). A subfossil chironomid-total phosphorus inference model for lakes in the middle and lower reaches of the Yangtze River. *Chinese Science Bulletin*, 51, 2125-2132.

Zhang, E., Cao, Y., Langdon, P., Jones, R., Yang, X., Shen, J. (2012). Alternate trajectories in historic trophic change from two lakes in the same catchment, Huayang Basin, middle reach of Yangtze River, China. *Journal of Paleolimnology*, 48, 367-381.

Zhang, E., Chang, J., Cao, Y., Sun, W., Shulmeister, J., Tang, H., Langdon, P.G., Yang, X., Shen, J. (2017). Holocene high-resolution quantitative summer temperature reconstruction based on subfossil chironomids from the southeast margin of the Qinghai-Tibetan Plateau. *Quaternary Science Reviews*, 165, 1-12.

Zhang, K., Dong, X., Yang, X., Kattel, G., Zhao, Y., Wang, R. (2018). Ecological shift and resilience in China's lake systems during the last two centuries. *Global and Planetary Change*, 165, 147-159.

Zhang, L., Xie, L., Chen, H., Gao, C. (2005). Progress and prospects of seawater desalination in China. *Desalination*, 182, 13-18.

Zhao, S., Fang, J., Miao, S., Gu, B., Tao, S., Peng, C., Tang, Z. (2005). The 7-decade degradation of a large freshwater lake in central Yangtze River, China. *Environmental Science & Technology*, 39, 431-436.

Zhao, X., Zhou, Y., Min, J., Wang, S., Shi, W., Xing, G. (2012). Nitrogen runoff dominates water nitrogen pollution from rice-wheat rotation in the Taihu Lake region of China. *Agriculture, Ecosystems & Environment*, 156, 1-11.

Zheng, H. (2015). Birth of the Yangtze River: age and tectonic-geomorphic implications. *National Science Review*, 2, 438-453.

Zhu, Q., de Vries, W., Liu, X., Hao, T., Zeng, M., Shen, J., Zhang, F. (2018). Enhanced acidification in Chinese croplands as derived from element budgets in the period 1980–2010. *Science of the Total Environment*, 618, 1497-1505.

Zong, Y., Chen, X. (2000). The 1998 Flood on the Yangtze, China. *Natural Hazards*, 22, 165-184.

Zong, J. M., Wang, X. X., Zhong, Q. Y., Xiao, X. M., Ma, J., Zhao, B. (2019). Increasing Outbreak of Cyanobacterial Blooms in Large Lakes and Reservoirs under Pressures from Climate Change and Anthropogenic Interferences in the Middle–Lower Yangtze River Basin. *Remote Sensing*, 11, 1754.